

Thèse de Doctorat

Bahareh SADEGHIN

*Mémoire présenté en vue de l'obtention du
grade de Docteur de l'Université de Nantes
sous le sceau de l'Université Bretagne Loire*

École doctorale : *Sciences pour l'Ingénieur Géosciences, Architecture (SPIGA)*

Discipline : *Sciences pour l'ingénieur*

Spécialité : *Génie des Procédés*

Unité de recherche : *Laboratoire GEPEA, UMR-CNRS 6144*

Soutenue le 27 Septembre 2017

Effect of light supply on the hydrocarbon enriched microalga, *Botryococcus braunii* BOT-22.

JURY

Président du jury :	Mohammad-Ali FARAMARZI , Professeur, Faculté Pharmacie deTéhéran
Rapporteurs :	Soheila YAGHMAEI , Professeur, Université Technologie Sharif de Téhéran Carole MOLINA-JOUVE , Professeur, INSA de Toulouse
Autre membre :	Catherine DUPRÉ , Ingénieur de Recherche CNRS, Université de Nantes
Co-encadrant :	Dominique GRIZEAU , Maître de Conférences, Université de Nantes
Directeurs de thèse :	Mohammad-Hossein SARRAFZADEH , Co-directeur de thèse, Professeur assistant, Université de Téhéran Jack LEGRAND , Directeur de thèse, Professeur des Universités, Université de Nantes

Thèse de Doctorat

Bahareh SADEGHIN

Effect of light supply on the hydrocarbon enriched microalga, *Botryococcus braunii* BOT-22.

Effet des flux lumineux sur la productivité en hydrocarbures de la microalgue, *Botryococcus braunii* BOT-22.

Résumé

Botryococcus braunii Bot-22 a été cultivée dans un photobioréacteur plat dans des conditions photoautotrophiques continues. Deux densités de flux de photons (PFD) de 50 et 500 $\mu\text{mol quanta m}^{-2} \text{s}^{-1}$, deux taux de dilution de 0.178 et 0.357 d^{-1} , trois concentrations différentes d'oxygène dissous et deux périodes de exposition à la lumière ont été appliquées pour produire de différentes productions de biomasse et d'hydrocarbures et de profil d'acides gras. L'augmentation de dix fois du PAR-PFD appliqué sur la surface du photobioréacteur induit une augmentation transitoire du rEX, avant d'atteindre un nouvel état stationnaire correspondant à une productivité de la biomasse de 21.34 $\text{g m}^{-2} \text{d}^{-1}$, qui représente une augmentation de 360 % par rapport à la productivité obtenue sous 50 $\mu\text{mol quanta m}^{-2} \text{s}^{-1}$. En revanche, aucun changement apparent de rEX n'a été observé après avoir doublé le taux de dilution à PFD constant et cela malgré une double augmentation de la productivité de la biomasse jusqu'à 47.8 $\text{g m}^{-2} \text{d}^{-1}$. La productivité des hydrocarbures extracellulaires a suivi la même tendance que les celle de biomasse, atteignant une valeur maximale de 12.4 $\text{g m}^{-2} \text{d}^{-1}$ pour un rendement estimé de la biomasse sur l'apport lumineux de 1.1 $\text{g mol de photons}^{-1}$. La productivité d'hydrocarbures la plus élevée correspondait aux photons continus, une dilution de 0.357 d^{-1} , 500 $\mu\text{mol quanta m}^{-2} \text{s}^{-1}$ et à 4 % de la concentration d'oxygène dissous. Les principaux acides gras du «*B. braunii* race B strain BOT-22 fatty acids » étaient l'acide oléique, l'acide palmitique, l'acide α -linoléique, et l'acide stéarique.

Mots clés

microalgue, *Botryococcus braunii*, productivité en hydrocarbure, productivité en biomasse, cycles lumineux, photobioréacteur.

Abstract

Botryococcus braunii Bot-22 was cultivated in a flat-panel photobioreactor under continuous photoautotrophic conditions. Two photon flux densities (PFD) of 50 and 500 $\mu\text{mol photons m}^{-2} \text{s}^{-1}$, two dilution rates of 0.178 and 0.357 d^{-1} , three different dissolved oxygen concentration and two light periods were applied to provide different biomass and hydrocarbon production and fatty acids profile. The tenfold increase of the PAR-PFD applied on the photobioreactor surface induced a transient increase of rEX, before reaching a new steady state corresponding to a biomass productivity of 21.34 $\text{g m}^{-2} \text{d}^{-1}$, a 360 % increase as compared to the productivity obtained under 50 $\mu\text{mol photons m}^{-2} \text{s}^{-1}$. By contrast, no apparent change of rEX was observed after doubling the dilution rate at constant PFD, despite a twofold increase of the biomass productivity, up to 47.8 $\text{g m}^{-2} \text{d}^{-1}$. The extracellular hydrocarbons productivity followed the same trend as the biomass data, reaching a maximal value of 12.4 $\text{g m}^{-2} \text{d}^{-1}$ for an estimated biomass yield on light supply of 1.1 $\text{g mol photons}^{-1}$. The highest hydrocarbon productivity was corresponding to continuous light, dilution rate of 0.357 d^{-1} , 500 $\mu\text{mol photons m}^{-2} \text{s}^{-1}$ and 4 % of dissolved oxygen concentration. The main fatty acids of *B. braunii* race B strain BOT-22 fatty acids were, oleic acid, palmitic acid, α -linoleic acid, and stearic acid.

Key Words

microalgae, *Botryococcus braunii*, hydrocarbon productivity; biomass productivity, light/dark cycles, photobioreactor.

Acknowledgement

First, I would like to thank Luc Fillaudeau, who introduced me to the knowledgeable, kind and so supportive professor, Jack LEGRAND, and GEPEA laboratory. Then special thanks to Pr. Jack LEGRAND, my special supervisor, for giving me the opportunity of spending my PhD in GEPEA laboratory and trusting me during all ups and downs of my PhD and my bourse. Working with him is my honor. I would like to thank my Iranian supervisor, Dr Mohammad-Hossein Sarrafzadeh, specially because of his kind help during this time. I learned a lot from my co-director Dr GRIZEAU, a champion whose advices and suggestions helped me a lot to finish my PhD in a short time. He was always busy but during his busy schedule and lots of teaching hours, he was available for me even on week-ends, I'm so thankful of him and I'm so pleased of working with him. His stories make me never feel tired. Thanks to Catherine Dupre for being so friendly to me and her advices.

Special thanks to Jian Jin who supported me with his experience and knowledge. He helped me and supported me so kindly to continue his work.

Very special and big thanks to my Saint-Nazaire family: my lovely friends and technical staffs, in GEPEA who made this time in St-Nazaire so memorable for me. My deskmates: Alex, Remy, Lisa, Veladimir, Razmig, Eglantine, Marlene and my best friend and very special deskmate, Antoinette. My kind friends: Aumaya, Erika, Rossine, Charlène, Liliana, Meryam, Wenli, Jian, Jordan, Brioux, Remy, Jeremy, Arnaud, Sergio and Astrid. Special thanks to Armel, a clever internship and a new PhD student, who helped me a lot with my experiments and his good collaboration. The responsible, kind and skillful technical staffs: Delphine, Helen, Frank, Emanuel, Luarence, Guillaume, Jean-Luc not only for their help but also for their kindness and sympathy, their listening and understanding. Without all of you it was not possible to finish...

I also thank all the people with whom I shared good times with the CRTT, Laurette, Carole,... I would like to thank specially Pr. Javad Fouladgar, the Iranian Pr. in CRTT and his so kind wife. They thought me how to love, help and support unconditionally. Knowing them was my best experience in St-Nazaire.

I would also like to thank my family. I thank my parents for their love and unconditional support.

At the end I would like to thank France embassy for providing bourse to me.

Abstract

Botryococcus braunii Bot-22 was cultivated in a flat-panel photobioreactor under continuous photoautotrophic conditions using a sixfold N- and P-enriched AF6 culture medium. Two photon flux densities (PFD) 50 and 500 $\mu\text{mol photons m}^{-2} \text{s}^{-1}$, two dilution rates, 0.178 and 0.357 d^{-1} , three different dissolved oxygen concentration and two light periods were applied to provide different biomass and hydrocarbon production and fatty acids profile. The tenfold increase of the PAR-PFD applied on the photobioreactor surface induced a transient increase of r_{EX} , before reaching a new steady state corresponding to a biomass productivity of 21.34 $\text{g m}^{-2} \text{d}^{-1}$, a 360 % increase as compared to the productivity obtained under 50 $\mu\text{mol photons m}^{-2} \text{s}^{-1}$. By contrast, no apparent change of r_{EX} were observed after doubling the dilution rate at constant PFD, despite a twofold increase of the biomass productivity, up to 47.8 $\text{g m}^{-2} \text{d}^{-1}$. The extracellular hydrocarbons productivity followed the same trend as the biomass data, reaching a maximal value of 12.4 $\text{g m}^{-2} \text{d}^{-1}$ for an estimated biomass yield on light supply of 1.1 $\text{g moles photons}^{-1}$. The highest hydrocarbon productivity was correspond to discontinuous light, 0.357 d^{-1} , 500 $\mu\text{mol photons m}^{-2} \text{s}^{-1}$ and 4 % of dissolved oxygen concentration. The main fatty acids of *B. braunii* race B strain BOT-22, were oleic acid, palmitic acid, α -linoleic acid, and stearic acid.

Key Words

microalgae, *Botryococcus braunii*, hydrocarbon productivity; biomass productivity, light/dark cycles, photobioreactor.

Résumé

Botryococcus braunii Bot-22 a été cultivé dans un photobioréacteur plat dans des conditions photoautotrophiques continues. Deux densités de flux de photons (PFD) de 50 et 500 $\mu\text{mol quanta m}^{-2} \text{s}^{-1}$, deux taux de dilution de 0.178 et 0.357 d^{-1} , trois concentrations différentes d'oxygène dissous et deux périodes de exposition à la lumière ont été appliquées pour avoir différentes conditions de productions de biomasse et d'hydrocarbures et de profil d'acides gras. L'augmentation de dix fois du PAR-PFD appliquée sur la surface du photobioréacteur induit une augmentation transitoire du r_{EX} , avant d'atteindre un nouvel état stationnaire correspondant à une productivité de la biomasse de 21.34 $\text{g m}^{-2} \text{d}^{-1}$, qui représente une augmentation de 360 % par rapport à la productivité obtenue sous 50 $\mu\text{mol quanta m}^{-2} \text{s}^{-1}$. En revanche, aucun changement apparent de r_{EX} n'a été observé après avoir doublé le taux de dilution à PFD constant et cela malgré la double augmentation de la productivité de la biomasse jusqu'à 47.8 $\text{g m}^{-2} \text{d}^{-1}$. La productivité des hydrocarbures extracellulaires a suivi la même tendance que les celle de biomasse, atteignant une valeur maximale de 12.4 $\text{g m}^{-2} \text{d}^{-1}$ pour un rendement estimé de la biomasse sur l'apport lumineux de 1.1 $\text{g mol photons}^{-1}$. La productivité d'hydrocarbures la plus élevée correspondait à une dilution de 0.357 d^{-1} , 500 $\mu\text{mol quanta m}^{-2} \text{s}^{-1}$ et à 4 % de la concentration d'oxygène dissous. Les principaux acides gras du «*B. braunii* race B strain BOT-22 fatty acids» étaient l'acide oléique, l'acide palmitique, l'acide α -linoléique, et l'acide stéarique.

Mots clés

microalgue, *Botryococcus braunii*, productivité en hydrocarbure, productivité en biomasse, cycles lumineux, photobioréacteur.

Contents

Résumé en français de la thèse	1
Chapter 1: Literature review	15
1.1 Microalgae; scientific and industrial interests	15
1.2 Microalgae; biodiversity and chimiodiversity	16
1.3 The bio-hydrocarbon producers	17
1.4 Biofuel production	20
1.4.1 Biofuel production	20
1.4.2 Economy of biofuel production	21
1.5 Microalgae strains and culture systems	21
1.6 Effect of environmental factors	22
1.6.1 Temperature	22
1.6.2 Salinity	23
1.6.3 pH	24
1.6.4 Carbon source (Organic and Inorganic)	24
1.6.5 Dissolved oxygen concentrations	26
1.6.6 Nutrients (N, P and metals)	28
1.6.7 Photosynthetic active radiations (PAR)	28
1.6.7.1 Light intensity	30
1.6.7.2 Light and dark cycle	32
1.6.7.3 Light wavelength	34
1.6.7.4 Penetration depth	35
1.6.7.5 Photoinhibition	35
1.6.7.6 Photo-oxidation	36
1.7 Photosynthesis and photoaccimilation	37
1.8 Specific light supply rate (SLSR)	38
1.9 Pigments	39
1.10 Comparative efficiency of raceways and closed PBRs	42
1.11 Comparative efficiency of batch and continuous mode	44
1.12 High cell density and biomass productivity	44
1.13 Hydrocarbon content	46
1.14 Fatty acids	49
Chapter 2: Material and methods	52
2.1 Biological material	52

2.2 Strain and culture medium.....	52
2.3 Methods of culture.....	54
2.3.1 Batch cultures.....	54
2.3.2 Continuous culture	54
2.4 Analytical methods	58
2.4.1 Direct and indirect biomass determinations	58
2.4.2 Calculation of biomass productivity and biomass yield	59
2.4.3 Determination of pigments concentrations	60
2.4.4 Chromatographic analysis of carotenoids	60
2.4.5 Measurements of photosynthetic activities.....	60
2.4.6 Dissolved inorganic carbon determination.....	62
2.4.7 Ionic composition of the culture medium	63
2.4.8 Total lipids extract and hydrocarbon purification	64
2.4.9 GC-FID for hydrocarbons profiles analysis.....	68
2.4.10 GC-MS for hydrocarbons profiles analysis.....	68
2.4.11 GC-FID for total fatty acid analysis.....	69
2.4.12 Fluorescent microscopy observation.....	69
Statistical analysis.....	70
Chapter 3: Results and discussion	71
3.1 Biomass production in continuous cultures	71
3.1.2 Effect of continuous and discontinuous illumination on biomass production in continuous cultures under 21% of dissolved oxygen.....	Erreur ! Signet non défini.
3.1.3 Effect of continuous and discontinuous illumination under 4% of dissolved oxygen on biomass production in continuous cultures.....	76
3.1.4 Effect of dissolved oxygen concentrations under continuous illumination on biomass production in continuous cultures	77
3.1.5 Effect of dissolved oxygen concentrations under discontinuous illumination on biomass production in continuous cultures	78
3.2 Hydrocarbon production in continuous cultures	79
3.2.1 Effect of PFD and dilution rate on hydrocarbon production in continuous cultures.....	79
3.2.2 Effect of light period on hydrocarbon and intracellular lipid content in continuous cultures under 21% of dissolved oxygen concentration.....	Erreur ! Signet non défini.
3.2.3 Effect of dissolved oxygen concentration on hydrocarbon and intracellular lipid content in continuous cultures under continuous illumination	85
3.2.4 Effect of light period on hydrocarbon and intracellular lipid content in continuous cultures under 4% of dissolved oxygen concentration	86
3.2.5 Effect of dissolved oxygen concentration on hydrocarbon and intracellular lipid content in continuous cultures under discontinuous illumination	87
3.3 Fatty acids composition.....	88

3.3.1 Fatty acids components	88
3.3.2 Effect of light intensity on fatty acids composition.....	92
3.3.3 Effect of dilution rate on fatty acids composition	93
3.3.4 Effect of light period on fatty acids composition	93
3.3.5 Effect of dissolved oxygen concentration on fatty acids composition	94
3.4 Physiological characterization	95
3.4.1 Photosynthetic activity	95
3.4.1.1 Photosynthetic activity in continuous cultures at two incident light intensities ...	95
3.4.1.2 Photosynthetic activity in continuous cultures at two incident dilution rates	96
3.4.1.3 Photosynthetic activity in continuous cultures under continuous illumination and at the end of a dark period under 21 % of dissolved oxygen	97
3.4.1.4 Photosynthetic activity in continuous cultures under continuous illumination or at the end of a dark period under 4 % of dissolved oxygen	98
3.4.1.5 Photosynthetic activity in continuous cultures at the end of a 16 h dark period; in different dissolved oxygen concentrations.....	98
3.4.1.6 Photosynthetic activity in continuous cultures after a 16h dark period in different dissolved oxygen concentrations	99
3.4.2 Pigment composition	100
3.4.2.1 Pigment composition in continuous cultures at two incident light intensities....	100
3.4.2.2 Pigment composition in continuous cultures at two incident dilution rates	101
3.4.2.3 Pigment composition in continuous cultures under continuous illumination or after a 16h dark incubation under 21% of dissolved oxygen	102
3.4.2.4 Pigment composition in continuous cultures under continuous illumination or after a 16 h dark incubation under 4% of dissolved oxygen	103
3.4.2.5 Pigment composition in continuous cultures under continuous illumination; in different dissolved oxygen concentrations.....	104
3.4.2.6 Pigment composition in continuous cultures illumination and after a 16 h dark period in different dissolved oxygen concentrations	105
Chapter 4: Specific light supply rate and culture behavior	107
4.1 Evolution of r_{EX} and productivities during the transient phases.....	107
4.2 Evolution of r_{EX} and photosynthetic characteristics during the transient phases.....	110
4.3 Nutrient consumption	114
4.3.1 Dissolved inorganic carbon consumption	114
4.3.2 Nitrate and phosphate consumption	115
Conclusion– Perspectives.....	117
Nomenclature	120
List of figures	122
List of tables	125

References126

Résumé en français de la thèse

Les microalgues sont cultivées en conditions photo-autotrophiques avec du CO₂ comme source de carbone et des photons comme source d'énergie, en conditions hétérotrophiques où des sources de nutriments organiques servent à fournir le carbone et l'énergie ou en conditions photo-hétérotrophiques où le carbone est fourni par des nutriments organiques et l'énergie par les photons. Ces trois modes de culture correspondent à des applications industrielles, les premières essentiellement pour des applications en algues fourrage pour l'aquaculture et en biomasse pour la cosmétique et la nutraceutique, les deuxièmes pour des applications à hautes valeurs ajoutées, comme la production d'acides gras polyinsaturés à longues chaînes et les troisièmes pour des applications impliquant actuellement des productions d'ingrédients pour l'industrie chimique à partir de biomasses produites sur eaux résiduaires. En photo-autotrophie, le CO₂ provenant des gaz de combustion industriels et d'autres sources peut être absorbé par la culture des microalgues et être transformé en énergies renouvelables et respectueuses de l'environnement telles que les biocarburants, le diesel, l'éthanol, le méthane ou l'hydrogène (Singh et al. 2010). Un autre intérêt des microalgues est qu'elles n'ont pas besoin de terres arables pour leur croissance. Il semble qu'il soit possible d'obtenir une productivité plus élevée qu'avec les cultures terrestres (Singh et al. 2010).

Botryococcus braunii est une microalgue verte riche en hydrocarbures, connue pour sa capacité à produire une grande quantité d'hydrocarbures à longues chaînes (Metzger et Largeau, 2005). Ces hydrocarbures sont excrétés dans une matrice extracellulaire, qui sert à piéger les hydrocarbures et à maintenir les cellules sous forme de colonies pluricellulaires. Ces microalgues vivent généralement en eaux douces ou saumâtres, formant parfois des efflorescences denses dans les eaux subtropicales et tropicales (Aaronson et al. 1983 ; Metzger et Largeau, 2005 ; Townsend, 2001). En fonction de la nature des hydrocarbures, on distingue plusieurs races de *B. braunii* race A (alcadiène et alcatriène), race B (botryococcène) et race L (lycopadiène), S (alkane). Les souches de race B semblent les plus attrayantes depuis les études de Hillen et al. (1982). En effet, ces hydrocarbures pourraient être transformés en carburants sans oxygène comme les combustibles fossiles (Banerjee et al. 2002; Hillen et al. 1982). Par processus de craquage catalytique, les squalènes méthylés en C₃₁ à C₃₄ et les botryococcènes C₃₀ à C₃₇ peuvent être transformés en hydrocarbures de type combustible de chaînes plus courtes tels que, C₇H_n à C₁₁H_m pour de l'essence, C₁₂-C₁₅ pour kérosène ou C₁₆-C₁₈ pour diesel. La croissance et la composition des microalgues dépendent des apports en nutriments mais aussi pour les modes phototrophiques de l'apport de radiations actives pour la photosynthèse. La conception et le fonctionnement des photobioréacteurs (PBR) sont alors

essentiels pour optimiser les transferts de photons aux cultures cellulaires en limitant les processus d'auto-ombrage (self-shading) (Ogbonna et al. 2000). Dans ce mémoire, nous avons utilisé un PBR air lift pour étudier l'effet de différents paramètres opératoires sur le comportement de la souche *B. braunii* BOT-22 en vue de rechercher des conditions qui permettent de maximiser la productivité en hydrocarbures que ce soit en conditions stables ou en conditions fluctuantes. Ces dernières, étudiées en mini-PBR de laboratoire, doivent pouvoir représenter ce que les cultures devront subir lors du passage en PBR industriels en conditions naturelles. L'étude a plus particulièrement été focalisée sur les effets de modifications importantes des conditions d'illumination des cultures en tenant compte de l'impact de la concentration en biomasse dans le PBR. C'est pourquoi l'étude a porté sur des cultures en mode continu subissant des alternances lumière/obscurité, des modifications de l'intensité des flux lumineux et un accroissement du taux de dilution des cultures. Ces perturbations étant censées devoir impacter les teneurs en oxygène dissous des cultures, l'étude a intégré un contrôle de ces teneurs dans la phase gazeuse entrante en vue de vérifier si celles-ci devaient être prises en compte pour maîtriser les productivités des cultures. Cette étude cinétique a porté sur les critères de :

- production de biomasse
- production d'hydrocarbures
- composition en acides gras
- activités photosynthétiques
- composition en pigments

L'ensemble des données est analysée en fonction de l'évolution et caractéristique de la vitesse spécifique d'apport en lumière, r_{EX}

Les expérimentations ont été menées dans les conditions suivantes :

- température : 22 ± 2 ° C
- milieu de culture enrichi en nitrate et phosphate : 6N-6P-AF6, pH : $6,6 \pm 0,2$
- taux de CO₂ pour l'ajustement du pH : 3 mL min^{-1}
- taux d'aération : 60 mL min^{-1}

Ces conditions visaient à obtenir des cultures seulement limitées par les apports de lumière.

Ainsi, pour faire varier les transferts de lumière, les densités de flux lumineux en surface des PBR ont été fixés à 50 et $500 \mu\text{mol quanta m}^{-2} \text{ s}^{-1}$, le taux de dilution à 0.178 et 0.357 d^{-1} et la

concentration en oxygène dissous dans le flux gazeux alimentant le PBR à 4 % et 400 %, contre les 21 % de saturation correspondant aux conditions standard.

1- Influence des différents paramètres opératoires sur la production de biomasse

1-1 Effet de l'intensité lumineuse et du taux de dilution sur la production de biomasse

A un taux de dilution constant de $0,178 \text{ d}^{-1}$, l'augmentation du PFD de 50 à $500 \mu\text{mol quanta m}^{-2} \text{ s}^{-1}$ a entraîné une augmentation significative, d'environ 360 %, de la concentration de la biomasse, avec une productivité moyenne de $21,34 \pm 1,51 \text{ g m}^{-2} \text{ d}^{-1}$.

Le doublement du taux de dilution à $0,357 \text{ d}^{-1}$ a eu moins d'impact sur la concentration de biomasse (augmentation de 10 %). La valeur maximale de la concentration de biomasse en régime permanent était de $6,7 \text{ g L}^{-1}$, qui est parmi les valeurs les plus élevées obtenues pour les cultures cellulaires de *B. braunii*. Par conséquent, en doublant le taux de dilution, la valeur de la productivité de la biomasse a augmenté de plus de deux fois, atteignant $12,4 \pm 0,79 \text{ g m}^{-2} \text{ d}^{-1}$. A $50 \mu\text{mol quanta m}^{-2} \text{ s}^{-1}$, un taux de dilution de $0,357 \text{ d}^{-1}$ aboutit à l'élimination de la culture. L'absence apparente de carence nutritionnelle est confirmée par des concentrations résiduelles relativement élevées de nutriments principaux.

En augmentant la concentration de biomasse, en raison de l'auto-ombrage, il y avait une limitation de la diffusion de la lumière dans le PBR, ce qui pourrait entraîner une consommation plus faible que prévue de nutriments cellulaires en fonction de l'augmentation de la concentration de biomasse. En doublant le taux de dilution à $0,357 \text{ d}^{-1}$, la productivité de la biomasse a été augmentée plus de deux fois. Donc, un taux de dilution plus élevé augmente la disponibilité des nutriments pour les cellules. En augmentant la productivité de la biomasse, la consommation de nitrate et de phosphate a augmenté, ce qui pourrait être corrélé à l'augmentation du résidu de la concentration de carbone inorganique dissous.

La diminution de la valeur DIC à un taux de dilution plus élevé, peut suggérer que la consommation de nutriments a été ralentie. Cependant, le pH a été fixé à $6,6 \pm 0,2$, avec une injection de CO_2 . Comme le PBR a été alimenté en continu avec un milieu 6N-6P-AF6 frais non tamponné, la concentration élevée de nitrate dans les milieux de culture a légèrement augmenté l'alcalinité et donc une diminution de la concentration de DIC. Par conséquent, une valeur DIC inférieure peut être directement liée à une faible consommation d'éléments nutritifs.

En raison de la plus grande productivité de la biomasse, le taux de dilution de $0,357 \text{ d}^{-1}$ a été choisi pour les prochaines étapes.

1-2 Effet de la lumière continue et discontinue sous différents taux d'oxygène dissous sur la production de biomasse

Afin d'étudier l'effet de la période de lumière sur la production de *B. braunii*, deux périodes de lumière différentes ont été choisies : la lumière continue et le cycle de lumière et d'obscurité (8 heures de lumière et 16 heures d'obscurité). L'intensité de la lumière de $500 \mu\text{mol quanta m}^{-2} \text{ s}^{-1}$ et le taux de dilution de $0,357 \text{ d}^{-1}$ ont été maintenus constants.

Sous 21 % de la concentration en oxygène, la productivité de la biomasse à la lumière continue était de $2,39 \pm 0,15 \text{ g L}^{-1} \text{ d}^{-1}$ et pour le cycle lumière et à l'obscurité était de $2,25 \pm 0,19 \text{ g L}^{-1} \text{ d}^{-1}$, différence non significative. A 4 % d'oxygène dissous, la productivité de la biomasse à la lumière continue était de $3,07 \pm 0,2 \text{ g L}^{-1} \text{ d}^{-1}$ et pour le cycle lumière et obscurité était de $2,12 \pm 0,4 \text{ g L}^{-1} \text{ d}^{-1}$. Par conséquent il n'y a pas de croissance sur le cycle de l'obscurité. Cette réduction de la productivité de la biomasse était attendue.

La productivité de la biomasse au cycle lumière/obscurité avec 4 %, 21 % et 400 % de la concentration en oxygène dissous était de $2,12 \pm 0,4 \text{ g L}^{-1} \text{ d}^{-1}$, $2,25 \pm 0,19 \text{ g L}^{-1} \text{ d}^{-1}$, et $2,17 \pm 0,04 \text{ g L}^{-1} \text{ d}^{-1}$.

Avec 400 % saturation en oxygène dans la phase gazeuse alimentant le PBR, la consommation de nitrate et de phosphate a été augmentée, tandis que la concentration résiduelle en carbone inorganique dissous dans les milieux de culture a diminué et la concentration de biomasse dans les deux conditions a également diminuée légèrement.

L'évolution du PFD et du taux de dilution a eu des effets importants sur la concentration et la productivité de la biomasse. Ceux-ci pourraient également affecter la teneur et la productivité en hydrocarbures de *B. braunii*.

2- Influence des différents paramètres opératoires sur la production d'hydrocarbures

2-1 Effet du PFD et du taux de dilution sur la production d'hydrocarbures

La production d'hydrocarbures a été étudiée sous deux PFD (50 et $500 \mu\text{mol quanta m}^{-2} \text{ s}^{-1}$) et deux taux de dilution différents ($0,178 \text{ d}^{-1}$ et $0,357 \text{ d}^{-1}$).

À un taux de dilution constant, l'augmentation du PFD, de 50 à $500 \mu\text{mol quanta m}^{-2} \text{ s}^{-1}$, a induit une augmentation significative de la concentration en hydrocarbures, de 332 à 1249 mg L^{-1} . La même tendance s'est produite pour la concentration de biomasse. En effet, ces résultats confirment que la production d'hydrocarbures est corrélée à la croissance de biomasse. Au taux de dilution de $0,178 \text{ d}^{-1}$, il n'y avait pas de différence significative entre les teneurs en hydrocarbures à 50 et $500 \mu\text{mol quanta m}^{-2} \text{ s}^{-1}$ qui étaient ($20,24 \pm 1,67$) et ($20,51 \pm 1,39$) %.

Le contenu des lipides intracellulaires a été augmenté de $(21,47 \pm 0,72) \%$ à $(23,76 \pm 5,61) \%$. En effet, comme d'autres producteurs de lipides, *B. braunii* produit plus de lipides pendant le manque de l'azote (Venkatesan et al. 2013). La densité cellulaire élevée dans les milieux de culture combinée au niveau faible de la disponibilité des nitrates, peut être essentiellement la raison de l'augmentation de la teneur en lipides intracellulaires. La productivité des hydrocarbures à $50 \mu\text{mol quanta m}^{-2} \text{s}^{-1}$ était de $59,03 \pm 5,57 \text{ mg L}^{-1} \text{ d}^{-1}$ et à $500 \mu\text{mol quanta m}^{-2} \text{s}^{-1}$ était de $218,8 \pm 15,45 \text{ mg L}^{-1} \text{ d}^{-1}$.

En doublant le taux de dilution à $0,357 \text{ d}^{-1}$, il y a eu une augmentation du contenu total en lipides et en hydrocarbures. La teneur en hydrocarbures a été augmentée de $(20,51 \pm 1,39) \%$ à $(26,02 \pm 0,13) \%$ présentant une augmentation d'environ 27 %. De plus, en régime permanent, la productivité spécifique des hydrocarbures n'a pas été affectée par l'élévation du PFD, mais elle est passée de 36 à $93,4 \text{ mg g}^{-1} \text{ d}^{-1}$ après la hausse du taux de dilution. En outre, à un taux de dilution de $0,357 \text{ d}^{-1}$, le contenu en lipides intracellulaires a été augmenté d'environ 60 % et est devenu $(37,98 \pm 15,44) \%$. En doublant le taux de dilution et avec un PFD constant de $500 \mu\text{mol quanta m}^{-2} \text{s}^{-1}$, la concentration d'hydrocarbures a atteint 1742 mg L^{-1} . Cette valeur est supérieure à celle obtenue par Xu et al. (2012 b), Shimamura et al. (2012) et Yoshimura et al. (2013).

En effet, le doublement du taux de dilution réduit l'auto-ombrage à l'intérieur du PBR, de sorte que les microalgues ont été exposées à une forte irradiation lumineuse. Par conséquent, *B. braunii* produit éventuellement des hydrocarbures supplémentaires, et les accumule dans sa colonie afin de réduire l'exposition des cellules à une forte irradiation. En outre, l'augmentation de la production d'hydrocarbures pourrait être liée à deux facteurs : l'augmentation de la teneur en hydrocarbures et l'augmentation de la concentration de biomasse.

Au taux de dilution de $0,178 \text{ d}^{-1}$, la masse sèche était de $5,99 \pm 0,42 \text{ g L}^{-1}$, la productivité des hydrocarbures était de $218,8 \pm 15,45 \text{ mg L}^{-1} \text{ d}^{-1}$. A un taux de dilution de $0,357 \text{ d}^{-1}$ la masse sèche était de $6,7 \pm 0,43 \text{ g L}^{-1}$ et la productivité des hydrocarbures de $621,99 \pm 39,5 \text{ mg L}^{-1} \text{ d}^{-1}$ des hydrocarbures.

Parmi les trois conditions de changement de PFD et de taux de dilution, le maximum de productivité volumétrique et surfacique d'hydrocarbures était de $621,99 \pm 39,5 \text{ mg L}^{-1} \text{ d}^{-1}$ et $12,4 \pm 0,79 \text{ g m}^{-2} \text{ d}^{-1}$, correspondant à $500 \mu\text{mol quanta m}^{-2} \text{s}^{-1}$ et taux de dilution de $0,357 \text{ d}^{-1}$. Par conséquent, la conception du PBR pour des productions élevées de biomasse et d'hydrocarbures semble impliquer à la fois la disponibilité et un chemin court de la lumière,

un bon mélange, pas de zone de sédimentation et de fortes concentrations de nitrate et de phosphate, milieu de culture AF6 modifié pour les cultures de *B. braunii*. Dans ces conditions, la disponibilité de la lumière serait le principal facteur limitant.

2-2 Effet de la période de lumière sur les hydrocarbures et la teneur en lipides intracellulaires sous 21 % de la concentration d'oxygène dissous

La photopériode avec 21 % d'oxygène n'a aucun effet significatif sur la teneur en hydrocarbures. Dans les deux conditions, environ 26 % de la teneur en hydrocarbures a été acquise, mais la photopériode pourrait affecter les lipides intracellulaires. Sous la lumière continue, la concentration en lipides intracellulaires était de $37,98 \pm 15,44$ %, mais pour le cycle lumière/obscurité, la concentration a chuté à $17,11 \pm 1,47$ %. Cette tendance est en accord avec des études antérieures sur *B. braunii* confirmant que les hydrocarbures n'ont pas été consommés pendant la respiration dans le cycle lumière/obscurité (Sakamoto et al. 2012). La masse sèche à la lumière continue et discontinue était respectivement de $6,7 \pm 0,43$ et de $6,3 \pm 0,54$ g L⁻¹. Ainsi, la productivité des hydrocarbures à une lumière continue sous une concentration d'oxygène de 21 % était de $621,99 \pm 39,5$ mg L⁻¹ d⁻¹ tandis qu'avec la lumière discontinue était de $576,29 \pm 56,02$ mg L⁻¹ d⁻¹.

2-3 Effet de la concentration en oxygène dissous sur les hydrocarbures et la teneur en lipides intracellulaires sous éclairage continu et discontinue

Il existe une augmentation significative de la teneur en lipides intracellulaires sous la lumière continue avec différents niveaux de concentration d'oxygène. A 21 % d'oxygène dans l'air alimentant le PBR, la teneur en lipides intracellulaires obtenue est de $(37,98 \pm 15,44)$ %. L'augmentation des lipides totaux était principalement liée aux lipides intercellulaires alors que la teneur en hydrocarbures était d'environ 2 % de plus sous une lumière continue avec une concentration d'oxygène dissous de 4 % d'oxygène dans l'air alimentant le PBR. La productivité des hydrocarbures sous lumière continue avec une concentration d'oxygène dissous correspondant à 4 % et 21 % d'oxygène dans l'air alimentant le PBR était respectivement de $879,9 \pm 132,56$ et $621,99 \pm 39,5$ mg L⁻¹ d⁻¹.

La photopériode n'a pas d'effet significatif sur la teneur en hydrocarbures avec un taux de concentration en oxygène dissous inférieure à 4 %. La teneur en hydrocarbures était d'environ 29 et 28 % de la biomasse sèche sous une lumière continue et discontinue. Mais la photopériode pourrait affecter les lipides intracellulaires. La productivité des hydrocarbures à

la lumière continue sous une concentration d'oxygène de 4 % était de $879,9 \pm 132,56 \text{ mg L}^{-1} \text{ d}^{-1}$ et celle à la lumière discontinue était de $584,87 \pm 109,79 \text{ mg L}^{-1} \text{ d}^{-1}$.

Il n'y a pas d'augmentation significative avec la lumière discontinue sous différentes concentrations d'oxygène dissous, bien que la teneur la plus élevée en hydrocarbures et lipides ait été obtenue avec 4 % d'oxygène, soit environ 28 % et 50 % de la masse sèche. Il semble que l'oxygène ait un effet plus important sur les lipides intracellulaires. Avec une concentration de dissolution de moins de 4 %, 21 % et 400 % dans l'air alimentant le PBR, la productivité des hydrocarbures était respectivement de $584,87 \pm 109,79$, $576,29 \pm 56,02$ et $574,8 \pm 23,87 \text{ mg L}^{-1} \text{ d}^{-1}$.

3- Influence des différents paramètres opératoires sur la composition en acides gras

3-1 Composition en acides gras

Les principaux composants en acides gras de *B. braunii* BOT- 22 étaient l'acide oléique, l'acide palmitique, l'acide α -linoléique (ALA) et l'acide stéarique. Cheng et al. (2013) ont rapporté que pour *B. braunii* FACHB 357, les principaux acides gras étaient l'acide oléique, l'acide α -linoléique et l'acide palmitique, ce qui est similaire à cette étude. Pour *B. braunii* AP103, Ashokkumar et Rengasamy (2012) ont signalé l'acide oléique, l'acide α -linoléique et l'acide palmitique comme acides gras principaux. Wang et al. (2014) ont révélé un résultat similaire à celui de l'étude actuelle de *B. braunii*, c'est-à-dire des acides gras avec 16 et 18 atomes de carbone. Le profil d'acide gras pour *B. braunii* indique la présence de C16:0, C16:1, C18:0, C18:1, C18:2, C18:3, C20:0, C20:1, C20:3, C20:4, C20:5, C22:0, C22:1, C22:2, C22:6, C24:0 et C24:1.

3-2 Effet du PFD sur la composition en acides gras

A un taux de dilution constant de $0,178 \text{ d}^{-1}$, en augmentant le PFD de 50 à $500 \mu\text{mol quanta m}^{-2} \text{ s}^{-1}$, le pourcentage en poids d'acide oléique a augmenté tandis que celui de l'acide palmitique et de l'acide α -linoléique a diminué. En 2012, Wagenen et al. ont signalé que, pour *Nannochloropsis salina*, la teneur la plus élevée en acides gras se produisait dans des cultures à faible densité qui ont reçu de la lumière au-dessus du PFD saturant. Dans cette étude, la teneur en acide gras la plus élevée s'est produite dans des cultures de faible densité mais à faible PFD.

En augmentant le PFD à $500 \mu\text{mol quanta m}^{-2} \text{ s}^{-1}$, les acides gras polyinsaturés (AGPI) ont diminué de $(26,99 \pm 5,13) \%$ à $(22,06 \pm 3,79) \%$ selon Hu (2013) montrant que les AGPI sont

inversement liés au PFD. Dans cette étude, il a été démontré qu'en augmentant le PFD, l'acide palmitique et l'acide α -linoléique diminue alors que la teneur en acide oléique augmente.

Le pourcentage des lipides intracellulaires sur la masse sèche à 50 et 500 $\mu\text{mol quanta m}^{-2} \text{s}^{-1}$ était respectivement $(21,47 \pm 0,72) \%$ et $(23,76 \pm 5,61) \%$ tandis que la somme de C₁₆-C₁₈ était $(99,6 \pm 0,57) \%$ et $(97,17 \pm 2,29) \%$ des lipides intracellulaires.

3-3 Effet du taux de dilution sur la composition en acides gras

A un PFD constant de 500 $\mu\text{mol quanta m}^{-2} \text{s}^{-1}$, en doublant le taux de dilution, une augmentation de C16: 0 et C18: 0 a été observée. Ils passent respectivement de $(19,91 \pm 2,29) \%$ à $(27,75 \pm 3,52) \%$ et de $(1,07 \pm 0,16) \%$ à $(17,00 \pm 2,15) \%$, ce qui pourrait être un bon point pour la production de biodiesel. La composition des acides gras a montré des changements significatifs : l'acide béhénique, l'acide érucique et l'acide nervonique sont apparus dans la composition en acides gras. Le contenu de l'acide oléique et de l'acide α -linoléique a diminué nettement de $(53,09 \pm 7,17) \%$ à $(11,48 \pm 0,59) \%$ et de $(17,65 \pm 3,07) \%$ à $(9,18 \pm 2,35) \%$.

A 500 $\mu\text{mol quanta m}^{-2} \text{s}^{-1}$, le pourcentage de lipides intracellulaires par rapport à la masse sèche était pour le taux de dilution de 0,178 d⁻¹ $(23,76 \pm 5,61) \%$ et pour le taux de 0,357 d⁻¹ $(37,98 \pm 15,44) \%$ alors que la somme de C16-C18 était respectivement $(97,17 \pm 2,29) \%$ et $(66,84 \pm 8,95) \%$.

3-4 Effet de la photopériode sur la composition des acides gras

Pour le cycle lumière/obscurité avec 4 % de la concentration en oxygène dissous, à 500 $\mu\text{mol quanta m}^{-2} \text{s}^{-1}$ et un taux de dilution de 0,357 d⁻¹, la composition de l'acide palmitique, de l'acide oléique et de l'acide α -linoléique a augmenté par rapport à la lumière continue. Dans le cycle lumière/obscurité, il n'y avait pas d'acide stéarique, d'acide eicosapentaénoïque (EPA), d'acide béhénique, d'acide érucique, d'acide docosahexaénoïque (DHA), d'acide lignocérique et d'acide nervonique dans la composition en acides gras.

Dans le cycle lumière/obscurité avec 21 % de la concentration en oxygène dissous, à 500 $\mu\text{mol quanta m}^{-2} \text{s}^{-1}$ et un taux de dilution de 0,357 d⁻¹, la composition de l'acide érucique et de l'acide nerveux a été augmentée tandis que d'autres composants tels que l'acide palmitique, l'acide stéarique, l'acide oléique, l'acide α -linoléique, l'acide eicosapentaénoïque et l'acide béhénique ont été diminués par rapport à la lumière continue.

Le pourcentage de lipides intracellulaires par rapport à la masse sèche à 500 $\mu\text{mol quanta m}^{-2} \text{s}^{-1}$ sous lumière continue et discontinue avec une concentration d'oxygène dissous de 4 % était

respectivement de $(18,48 \pm 7,48)$ % et de $(22,83 \pm 2,63)$ % alors que la somme des C16-C18 étaient de $(54,27 \pm 1,65)$ % et de $(100 \pm 0,00)$ %. Le pourcentage de lipides intracellulaires à $500 \mu\text{mol quanta m}^{-2} \text{s}^{-1}$ sous une lumière continue et discontinue avec une concentration d'oxygène dissous de 21 % était $(37,98 \pm 15,44)$ % et $(17,11 \pm 1,47)$ % alors que la somme de C16-C18 était $(66,84 \pm 8,95)$ % et $(49,91 \pm 0,64)$ %.

4- Influences des différents paramètres opératoires sur les activités photosynthétiques.

4-1 Activité photosynthétique à deux PFD incidentes

En augmentant du PFD de 50 à $500 \mu\text{mol quanta m}^{-2} \text{s}^{-1}$, la valeur Fv/Fm a été diminuée de $0,79 \pm 0,01$ à $0,55 \pm 0,02$, cela montre qu'en augmentant le PFD, le stress augmente. Ce comportement s'explique par la photo-acclimatation cellulaire à $500 \mu\text{mol quanta m}^{-2} \text{s}^{-1}$ qui est également corrélée avec une modification du contenu pigmentaire. L'ETRm et α ont diminué.

4-2 Activité photosynthétique à deux taux de dilution

En doublant le taux de dilution de $0,178$ à $0,357 \text{ d}^{-1}$, la valeur Fv/Fm a été augmentée de $0,55 \pm 0,02$ à $0,64 \pm 0,03$, ce qui implique qu'en augmentant le taux de dilution, le stress diminue. Cela pourrait être dû à la disponibilité des éléments nutritifs pour les cellules et à la bonne adaptation des cellules à $500 \mu\text{mol quanta m}^{-2} \text{s}^{-1}$. L'ETRm reste à peu près le même $36,60 \pm 5,37$ et $36,63 \pm 2,68$, tandis que α passe de $0,14 \pm 0,01$ à $0,16 \pm 0,02$.

4-3 Activité photosynthétique sous lumière continue et discontinue sous différents taux d'oxygène dissous

En passant de la lumière continue à la lumière discontinue, la valeur Fv/Fm a été augmentée de $0,64 \pm 0,03$ à $0,714 \pm 0,05$, montrant que sous une lumière discontinue, le stress est moins important. L'ETRm et α ont également été augmentés.

En passant de la lumière continue à la lumière discontinue sous une concentration de 4 % d'oxygène dissous, la valeur de Fv/Fm a été augmentée de $0,65 \pm 0,02$ à $0,72 \pm 0,01$, montrant que sous une lumière discontinue, le stress est moins important (le même résultat atteint avec 21 % concentration d'oxygène dissous). L'ETR a été augmenté de $45,68 \pm 3,07$ à $64,26 \pm 9,71$, et α a également augmenté de $0,17 \pm 0,01$ à $0,24 \pm 0,02$. En comparaison de deux niveaux différents d'oxygène dissous (4 et 21 %) sous une lumière continue, la valeur Fv/Fm était

d'environ $0,65 \pm 0,02$ et $0,64 \pm 0,03$, montrant qu'avec une lumière continue, la contrainte est à peu près la même. L'ETRm et α ont également diminué.

En augmentant la concentration d'oxygène dissous de 4 % à 21 % et 400 % sous le cycle lumière/obscurité, la valeur Fv/Fm a légèrement diminué. Les valeurs de Fv / Fm pour 4 %, 21 % et 400 % ont changé de $0,72 \pm 0,01$ à $0,71 \pm 0,05$ et à $0,67 \pm 0,05$, ce qui montre qu'avec une lumière discontinue, une augmentation du taux d'oxygène dissous de 21 % à 400 %, augmente légèrement le stress. Le niveau presque équivalent de la valeur Fv/Fm dans 4 % et 21 % d'oxygène dissous sous aucune lumière, montre que les cellules étaient adaptées à l'obscurité.

5- Influence des paramètres opératoires sur la composition en pigments

5-1 Composition en pigments dans des cultures continues à deux PFD incidentes

La concentration en chlorophylle *a* et *b* à $50 \mu\text{mol quanta m}^{-2} \text{s}^{-1}$ et un taux de dilution de $0,178 \text{ d}^{-1}$ étaient respectivement de $15,63 \pm 0,15 \text{ mg L}^{-1}$ et $8,35 \pm 0,10 \text{ mg L}^{-1}$ qui ont légèrement diminués à $12,11 \pm 0,57 \text{ mg L}^{-1}$ et $6,20 \pm 0,38 \text{ mg L}^{-1}$, juste après avoir augmenté le PFD à $500 \mu\text{mol quanta m}^{-2} \text{s}^{-1}$. Il convient de mentionner que la concentration de caroténoïdes reste presque constante dans les deux PFD. Les caroténoïdes sont connus pour protéger l'appareil photosynthétique. Par conséquent, un niveau inchangé de caroténoïdes aux PFD élevés indique qu'il n'y avait pas de photo-inhibition juste après l'augmentation du PFD.

Au taux de dilution de $0,178 \text{ d}^{-1}$ sous un PFD de $50 \mu\text{mol quanta m}^{-2} \text{s}^{-1}$ et de $500 \mu\text{mol quanta m}^{-2} \text{s}^{-1}$, la moyenne de la teneur en Chl *a* était presque la même. Dans le même temps, la moyenne de la concentration de Chl *b* était aussi presque constante. Mais la moyenne de la teneur en caroténoïdes avec augmentation du taux de dilution a une augmentation significative de 95 % allant de $2,23 \pm 0,11$ à $4,47 \pm 0,26 \text{ mg L}^{-1}$. Le rapport Car / (Chl *a* + Chl *b*) a été augmenté de $0,13 \pm 0,01$ à $0,25 \pm 0,01$. De plus, en augmentant l'intensité lumineuse, la couleur de la culture dans PBR est passée de vert à jaune. La raison pourrait être une forte augmentation de la valeur des caroténoïdes. Ceci pourrait être dû à leur rôle de protection. Lorsqu'elles sont exposées à des flux de photons élevés, il existe une photo-acclimatation qui se traduit par une réduction de taille des antennes photosynthétiques qui entraîne une diminution du contenu en chlorophylles. Cette tendance a été rapportée dans une étude antérieure sur *B. braunii* (Sakamoto et al. 2012) et une autre souche *B. braunii* BOT-144 de race B (Baba et al. 2012).

5-2 Composition en pigments dans des cultures continues à deux taux de dilution

Le rapport Chl *a* / Chl *b* reste stable quel que soient les conditions appliquées. Par contre le rapport Car / (Chl *a* + Chl *b*) baisse de $0,25 \pm 0,01$ à $0,21 \pm 0,01$. Il semble qu'au taux de dilution de $0,178 \text{ d}^{-1}$, il y aurait une limitation nutritionnelle.

5-3 Composition pigmentaire sous lumière continue et discontinue sous 21 % d'oxygène dissous

En limitation lumineuse, l'organisme augmente sa pigmentation ce qui correspond soit à un accroissement du nombre d'unités photosynthétiques soit de la taille des complexes collecteur de la lumière (Masojidek et al. 2013).

Sous le cycle lumière/obscurité (8h L/ 16h D) par rapport à l'éclairage continu avec une concentration d'oxygène dissous de 21 %, plus de concentration de Chl *a* et plus de Chl *b* a été obtenue arrivant respectivement à $30,66 \pm 3,66$ et $16,61 \pm 2,12 \text{ mg L}^{-1}$, tandis que les teneurs en caroténoïdes ont une réduction d'environ 1 mg L^{-1} de $8,49 \pm 0,84$ à $7,50 \pm 1,01 \text{ mg L}^{-1}$. La couleur des cultures a été plus verte après la période d'obscurité. Dans l'incubation sombre, les microalgues ont produit plus de pigments pour compenser la faible disponibilité de la lumière. Le rapport Car / (Chl *a* + Chl *b*) a diminué de $0,21 \pm 0,01$ à $0,16 \pm 0,01$. Il semble que sous une lumière discontinue en raison de l'absence de lumière, les chlorophylles ont été augmentées et la couleur de la culture est devenue plus verte que sous une lumière continue.

Entre la lumière continue et discontinue avec une concentration d'oxygène dissous de 4 %, la teneur en Chl *a*, Chl *b* et caroténoïde a diminué respectivement de $30,82 \pm 0,98$, à $28,34 \pm 1,16$, de $16,80 \pm 0,76$ à $14,97 \pm 0,90$ et de $9,05 \pm 0,47$ à $7,53 \pm 0,49 \text{ mg L}^{-1}$, tandis qu'avec une concentration de 21 % d'oxygène dissous sous l'illumination discontinue, des résultats plus élevés de Chl *a*, Chl *b* et des caroténoïdes ont été obtenus par comparaison sous éclairage continu. Le rapport de Car / (Chl *a* + Chl *b*) a diminué de $0,19 \pm 0,01$ à $0,17 \pm 0,00$.

Sous une lumière continue avec une augmentation de la concentration d'oxygène dissous de 4% à 21 %, la teneur en Chl *a*, Chl *b* et caroténoïdes a diminué respectivement de $30,82 \pm 0,98$ à $26,27 \pm 1,86$, de $16,80 \pm 0,76$ à $14,68 \pm 1,05$ et de $9,05 \pm 0,47$, et $8,49 \pm 0,84$; Tandis qu'avec la lumière discontinue par rapport à différents niveaux d'oxygène, le maximum de Chl *a* et Chl *b* a été atteint à 21 % de la concentration d'oxygène. Le rapport Car / (Chl *a* + Chl *b*), en passant d'une concentration en oxygène dissous de 4 % à 21 % a augmenté de $0,19 \pm 0,01$ à $0,21 \pm 0,01$.

En comparant les trois concentrations différentes d'oxygène dissous (4 %, 21 % et 400 %) en lumière discontinue (8 h L/16 h D), la teneur en Chl *a* et Chl *b* a atteint la valeur la plus élevée

sous 21 % de la concentration d'oxygène dissous (Air) $30,66 \pm 3,66$ et $16,61 \pm 2,12$ mg L⁻¹. Alors que la plus forte concentration de caroténoïdes était sous saturation en oxygène. Il convient de mentionner que le contenu des caroténoïdes de moins de 4 % et de 21 % de la concentration en oxygène dissous est resté presque constant et une légère augmentation de la teneur en caroténoïdes à 400 % d'oxygène ($8,11 \pm 0,58$ mg L⁻¹). Le ratio Car / (Chl *a* + Chl *b*) en augmentant le taux d'oxygène dissous de 4 % à 21 % a diminué de $0,17 \pm 0,00$ à $0,16 \pm 0,01$, mais après avoir augmenté la concentration d'oxygène dissous de 21 % à 400 %. Le rapport Car / (Chl *a* + Chl *b*) a été augmenté de $0,16 \pm 0,01$ à $0,22 \pm 0,01$.

6- Evolution et caractéristiques du r_{EX}

6-1 Évolution du r_{EX} et des productivités pendant les phases transitoires

Le r_{EX} peut être évalué à partir des valeurs des concentrations de PFD et de biomasse incidentes (Cornet et Dussap 2009). En effet, dans cette étude, les concentrations de biomasse étaient supérieures à 1 g L⁻¹, ce qui correspond à l'absorption complète de la lumière dans laquelle le r_{EX} pourrait être calculé approximativement en tant que rapport du PFD incident sur la concentration de biomasse (Ogbonna et Tanaka 2000). L'augmentation du PFD au même taux de dilution ($0,178$ d⁻¹) a entraîné une augmentation de plus de trois fois de la productivité de la biomasse. Ainsi, la PFD incidente croissante a induit une augmentation transitoire du r_{EX} suivie d'une diminution asymptotique jusqu'à une valeur d'équilibre de $0,35$ mol photon g X⁻¹ d⁻¹. Cette valeur est environ deux fois celle observée pour la culture en régime permanent à 50 μ mol quanta m⁻² s⁻¹. La même tendance a été observée dans la production d'hydrocarbures.

La baisse du temps de séjour de 3,9 à 1,9 jours a été utilisée pour augmenter la disponibilité de la lumière en augmentant la dilution de la culture. En doublant le taux de dilution, tout en gardant le PFD à 500 μ mol quanta m⁻² s⁻¹, induit une double augmentation de la productivité de la biomasse. Cependant, après ce changement soudain du taux de dilution, le taux d'alimentation lumineuse spécifique n'a été réduit que de 28 %. Ce comportement pourrait être attribué à une cinétique rapide d'adaptation, contrairement à celle induite par l'augmentation soudaine de la PFD incidente. Comme la concentration de biomasse était relativement stable, on pouvait conclure que les cultures étaient en manque de lumière.

Une valeur de r_{EX} d'environ $0,28$ mol de photons g⁻¹ d⁻¹ semble optimale. Comme la production d'hydrocarbures était principalement associée à la croissance, la même valeur de r_{EX} a été trouvée pour les productions maximales d'hydrocarbures.

En utilisant le modèle Pirt basé sur des équations stœchiométriques pour la formation de biomasse, le rendement théorique en biomasse était de $1,5 \text{ g photons}^{-1}$ pour les cultures de microalgues sur le nitrate. Un rendement apparent en biomasse sur l'apport lumineux de $1,1 \text{ g photons}^{-1}$ a été déduit des valeurs les plus élevées de productivité de biomasse obtenues au cours de cette étude. Cette valeur semble relativement élevée, par rapport aux données publiées. Mais la présente étude portait sur une microalgue coloniale, qui produit des hydrocarbures extracellulaires. En tenant compte des 26 % d'hydrocarbures piégés dans la matrice des colonies, il en résulte un rendement cellulaire apparent sur l'apport lumineux de $0,8 \text{ g de photons}^{-1}$. Pour mieux comprendre le comportement physiologique des cultures de *B. braunii*, l'évolution de certaines caractéristiques photosynthétiques a été étudiée en fonction de l'apport lumineux spécifique.

6-2 Évolution des caractéristiques de la r_{EX} et de la photosynthèse pendant les phases transitoires

Dans nos conditions expérimentales, les cultures n'ont pas subi de dépigmentation. Seule une modification de la couleur de la culture, du vert au jaune a été observée après avoir augmenté l'intensité lumineuse. L'apparition d'un mécanisme de photo-acclimatation pourrait être supposée en fonction de l'évolution des teneurs en chlorophylles ou caroténoïdes en fonction de la fluctuation des densités de flux de photons. Sforza et al. (2015) ont indiqué que le contenu de chlorophylles (*a* et *b*) dans les cultures de *Nannochloropsis* a diminué en fonction de l'augmentation spécifique du taux de l'intensité lumineuse où, un rapport stable de 0.5 des caroténoïdes sur chlorophylles a été trouvé jusqu'à $0,5 \text{ mmol quanta g}^{-1} \text{ d}^{-1}$.

Dans nos conditions expérimentales, le rapport Chl *a*/Chl *b* est resté relativement stable. En revanche, l'augmentation du PFD de 50 à $500 \mu\text{mol quanta m}^{-2} \text{ s}^{-1}$ à taux de dilution constante de $0,178 \text{ d}^{-1}$ a entraîné une augmentation importante du rapport caroténoïdes sur la chlorophylles (*a + b*). Son apparition semble être liée à l'affaiblissement parallèle du r_{EX} . La modification de ce ratio de pigments semble être liée au rôle protecteur des caroténoïdes.

En revanche, le rapport caroténoïdes sur chlorophylles (*a + b*) semblait relativement peu affecté en doublant le taux de dilution jusqu'à $0,357 \text{ d}^{-1}$ au PFD de $500 \mu\text{mol quanta m}^{-2} \text{ s}^{-1}$. En effet, la concentration de biomasse, puis le processus d'auto-adhérence, était relativement constante pendant cette période.

L'augmentation du PFD de 50 à $500 \mu\text{mol quanta m}^{-2} \text{ s}^{-1}$ a entraîné une diminution rapide des activités PSII en fonction du rapport Fv/Fm. La nouvelle valeur Fv/Fm était relativement stable au cours des 17 jours de culture, du transitoire au nouvel régime permanent. Ensuite, on

observe aucune relation apparente entre le F_v/F_m et l'évolution asymptotique après une augmentation transitoire de r_{EX} . Dans l'étude rapportée par Sforza et al. (2015) sur *Nannochloropsis*, la valeur de F_v/F_m était également stable jusqu'à $0,5 \text{ mol photons g}^{-1} \text{ d}^{-1}$. Aux valeurs r_{EX} plus élevées, ces auteurs ont signalé une diminution de F_v/F_m . L'augmentation progressive de F_v/F_m observée après le doublement du taux de dilution n'a pas été associée à une évolution de la valeur de r_{EX} . Il n'y a pas d'augmentation de la concentration de biomasse pendant cette période transitoire, puis un processus d'auto-ombrage n'a pas pu expliquer la récupération partielle du F_v/F_m . Cela pourrait être lié à la double baisse du temps de séjour dans le PBR éclairé en continu.

L'analyse des données de la courbe de lumière obtenue avec le système Water-pam a confirmé qu'il n'y avait pas de processus photo-inhibiteur évident induit par les changements brusques du rayonnement ou de taux de dilution. En outre, les valeurs maximales du taux de transport d'électrons (ERT_{max}) et de l'efficacité de photosynthèse (α) semblent relativement stables sur la gamme des valeurs de r_{EX} appliquées aux cultures de *B. braunii*.

Chapter 1: Literature review

Chapter 1: Literature review

One of the challenges of the next future is to find efficient ways to replace petrochemicals products, including fuels, derived from fossil resources by bio-based products derived from renewable biomass. Current efforts are focused on biodiesel from oleaginous plant seeds and ethanol from sugarcane/corn, but also other compounds to be used by other industrial sectors, including food/feed, agriculture, plastic and cosmetic sectors for instance. However environmental and social concerns about plant derived resources are shifting the attention towards the development of next generation bio-resource (Williams 2007). For instance, biofuels produced from crops have become a major controversy due to food vs. fuel competition for arable area, water and fertilizers.

One of the other ways could be the culture of algae, which seem to be produced using poor quality waters on non-arable lands, then by this way not competing with food crops for arable land and water. Also, algal biomass productivities have been announced to be several folds higher than terrestrial crops (Singh et al. 2010).

For instance, biofuels, diesel, ethanol, methane or hydrogen, derived from algal biomass will be renewable and ecofriendly as these productions could be associated to water and gas remediations, through trapping nutrients and CO₂ from industrial, agricultural or urban wastewaters and gas effluents.

The recent increasing interest for potential applications of microalgae can be explained by some of the characteristics of these photosynthetic microorganisms. Some limitations have already been identified, justifying as well as the selection of special strains known as metabolites hyperproducers than the development of new photobioreactors configurations for improving the efficiency of metabolites production.

1.1 Microalgae; scientific and industrial interests

Microalgae are a group of unicellular or simple multicellular photosynthetic microorganisms that can fix CO₂ efficiently from different sources, including the atmosphere, industrial exhaust gases, and soluble carbonate salts (Wang et al. 2008).

Many reports have suggested using flue gas as carbon source for microalgal cultivation, which could combine biofuel production with current CO₂ mitigation strategies (Mashayekhi et al. 2017; Vunjak-Novakovic et al. 2005; Wang et al. 2008; Yoo et al. 2010).

Benefits arising from the utilization of aquatic over terrestrial biomass include: (1) higher photosynthesis efficiency (about 5% vs. 1.5%) (Posten and Schaub 2009), (2) utilization of marginal areas (e.g. desert and coastal regions), (3) possible coupling with other activities (e.g. wastewater treatment, CO₂ sequestration), (4) minor dependence on climatic conditions, (5) availability of a larger number of species and (6) easier genetic manipulation to modify chemical composition (e.g. lipid content) (An et al. 2003; Chisti 2007, 2008 a, b; Rosenberg et al. 2008; Shen et al. 2008).

1.2 Microalgae; biodiversity and chimiodiversity

The microalgae are photosynthetic microorganisms of prokaryotic (cyanobacteria) and eukaryotic nature. With respect to diversity they include 11 divisions and 28 classes (Hoeket al. 1995). Algal diversity may also be measured in terms of biochemical pathways, ecological roles, endosymbiotic genomes, morphology, reproductive strategies, and so forth. For example, the nontraditional, unusual, and even unique biochemical pathways. The recent discovery of cryptic endosymbiotic genomes is significant; for example, predominately green algal genes in diatoms (Moustafa et al. 2009).

The carbohydrate storage product in many algae is starch or a starch-like product (e.g., green and red algae, cryptophytes, dinoflagellates). These starches have a primary α -1, 4-linked glucan molecular backbone, and typically the backbone chain has α -1,6-linked side chains (Ball et al. 2011; Viola et al. 2001). Another group of algae utilize a β -1,3-linked glucan backbone (e.g., heterokont algae, haptophytes, euglenoids).

The diversity of algal lipids is also extensive (Wood 1984) and the cellular lipid composition can be manipulated (Hu et al. 2008; Wang et al. 2009), that is, under low nitrogen conditions (e.g., in the stationary phase), cells carry out photosynthesis and produce lipids from photosynthetically fixed carbon (e.g., 3-phosphoglycerate). *Nannochloropsis* accumulates significant amounts of membrane-bound eicosapentaenoic acid (EPA) (KhozinGoldberg and Iskandarov, 2011). The heterokont algae (e.g., *Chaetoceros*, *Nannochloropsis*, *Pinguicoccus*) and the haptophytes (e.g., *Pavlova*, *Isochrysis*) typically use oil droplets as a storage product, especially when their carbohydrate storage is chrysolaminarin like. The *Pinguiphyceae* store EPA in large quantities (Kawachi et al. 2002), and DHA is stored in many haptophyte algae (Guschina and Harwood 2006; Khozin-Goldberg and Iskandarov 2011) and considerable number of chlorophyte green algae (e.g., *Scenedesmus*, *Chlorella*) store oils under stress (Guschina and Harwood 2006).

Cyanobacteria have peptidoglycan cell walls and, therefore, are an excellent source of proteins, that is, 40–60 % of the dry weight is protein (e.g., *Arthrospira (Spirulina)*, *Synechococcus*) (Becker 2007). Green algae are also good sources (e.g., *Chlorella*, *Scenedesmus*); *Euglena gracilis* as well as *Porphyridium* produce up to 30–60 % protein of the dry weight.

Among this huge diversity of species (about 40,000) (Hu et al. 2008), the green algae *Botryococcus braunii* is a notable one that secreting hydrocarbons under different conditions (Metzger and Largeau 2005). It can produce hydrocarbons which could be converted to oxygen-free fuels like fossil fuels (Banerjee et al. 2002; Hillen et al. 1982). Indeed, these last years, hydrocarbons from *B. braunii* were among the most well-known products for potential industrial applications (e.g., biofuels production) (Cardozo et al. 2007; Mata et al. 2010; Pulz and Gross 2004; Ranga Rao et al. 2006; Yen et al. 2013). This microalga also produces exopolysaccharides (EPS) (Kenny et al. 2014).

Botryococcus braunii is usually found in fresh and brackish water environments, and it sometimes forms a dense bloom in subtropical and tropical regions (Aaronson et al. 1983; Baldwin et al. 2003; Chiang et al. 2004; Metzger and Largeau 2005; Townsend 2001; Wake and Hillen 1980). *Botryococcus braunii* because of its ability to accumulate large amounts of long-chain hydrocarbons, attracted particular interest according to some special characteristics, which differentiate it from other organisms, as well as plants or bacteria. Indeed, the same species includes strains producing a high chimiodiversity of hydrocarbons, strains therefore classified into four races (Jin et al. 2016 b) which will be discussed in this chapter.

1.3 The bio-hydrocarbon producers

Hydrocarbons are widely distributed in all organisms, including animals, plants, bacteria, and fungi. The share of hydrocarbons in the body of an organism is generally less than 3% of the dry weight (Gołębiowski et al. 2011; Huang et al. 2011; Jones 1969; Kunst and Samuels 2009; Ladygina et al. 2006).

Hydrocarbon oils are the most readily available source for converting bio-oils into gasoline, diesel, and jet fuel. However, apart from a squalene-accumulating strain of the heterotrophic alga *Aurantiochytrium*, which has recently been isolated from a mangrove area on the southern coast of Japan (Kaya et al. 2011; Nakazawa et al. 2012), only *Botryococcus* has been known to produce a high amount of hydrocarbons (Watanabe and Tanabe 2013).

Large quantities of hydrocarbons can be accumulated in *Botryococcus braunii*. The oil-rich green alga, *Botryococcus braunii*, known to produce a high amount of hydrocarbons. This pyramid shaped planktonic unicellular microalgae are held together as colonies by lipid biofilms (Metzger and Largeau 2005). Colonies of *B. braunii* typically have a morphology resembling a “botryoid” organization of individual grape-seed-like or pyriform-shaped cells with amorphous three-dimensional structures, held together by a thick hydrocarbon matrix. The matrix surrounding individual cells forms an outer cell wall which stores the bulk of *B. braunii* hydrocarbons (Largeau et al. 1980).

Most examined microalgae store lipid bodies in their cytoplasm while in *Botryococcus braunii* most of lipids storage is in the extracellular place (Largeau et al. 1980; Dote et al. 1994). Indeed, even if the biosynthesis and initial segregation of botryococcene hydrocarbons take place in vesicles within the cells, large quantities of liquid hydrocarbons are excreted and trapped within a thick matrix composed of very long chains hydrocarbons (Largeau et al. 1980; Wolf et al. 1985 a). An exceptional value of 86 % of its dry cell weight was reported for an algal sample, which was harvested from a natural bloom (Brown et al. 1969; Casadevall et al. 1985; Maxwell et al. 1968). These contents are generally lower, from 10 to about 50 %, being more abundant in race B strains than in race A strains (Jin et al. 2016 a).

Hence, intracellular hydrocarbons are only a small fraction of the total hydrocarbon content (Largeau et al. 1980). Based on the types of hydrocarbons synthesized, *B. braunii* was initially classified into 4 races, A, B, S and L, (Kawachi et al. 2012; Metzger et al. 1985; Metzger et al. 1990) in range from 0.4 % (Metzger and Largeau 1999) to 61.0 % of their dry cell weight (Metzger et al. 1985). Race A is characterized by n-alkadiene and/or n-trienes and their derivatives with odd carbon number (C_{23} – C_{33}) (Metzger et al. 1985; Metzger et al. 1989). Race B strains produces specific C_nH_{2n-10} triterpenes, known as botryococcenes (C_{30} – C_{37}) (Metzger et al. 1985), and methylated squalenes (C_{31} – C_{34}) (Achitouv et al. 2004; Huang and Poulter 1989 a). Their hydrocarbon contents are in the range of 30 % to 64 % dry cell weight (Metzger et al. 1985; Xu et al. 2012 b), even if lower levels down to 9 % have also been reported (Okada et al. 1995). The exceptionally high level of 86 % of botryococcenes noticed by Brown et al. (1969) with algae in the resting phase of growth, probably due to partial lysis or degradation of cell content, has not been observed again. Race S strain produces C_{20} saturated n-alkane (Kawachi et al. 2012). Race L strains synthesizes a tetraterpenoid known as lycopadiene ($C_{40}H_{78}$) it constitutes up to 0.1–8 % of the dry biomass. The B race produces polyunsaturated and branched C_{30} – C_{37} terpenoid hydrocarbons known as polymethylated botryococcenes. These products are attracting sources of renewable energy because of their

high accumulation levels (26–86 % on dry cell weight of the algae) (Achitouv et al. 2004; Brown et al. 1969; Metzger et al. 1985; Metzger et al. 1987; Metzger et al. 1997; Metzger et al. 2005).

In both races A and B, the biosynthetic pathways to these hydrocarbons have been clarified, and some of the enzymes involved in the synthetic activity have been characterized (Dennis et al. 1991; Dennis and Kolattukudy 1992; Matsushima et al. 2012; Niehaus et al. 2011; Okada et al. 2000; Okada et al. 2004; Wang and Kolattukudy 1995). Races B and L are more closely related to each other than either is to race A, Senousy et al. (2004) predicted a possible correlation between phylogeny and chemistry and hypothesized that the hydrocarbons of races B and L would be biosynthetically related and the same was suggested by Weiss et al. at 2010.

Two researches by Metzger et al. showed that in algae of the race L the range of hydrocarbon content was from a value less than 0.1% in two Indian strains up to 8.0% for a Thai strain (Metzger and Casadevall 1987; Metzger et al. 1997).

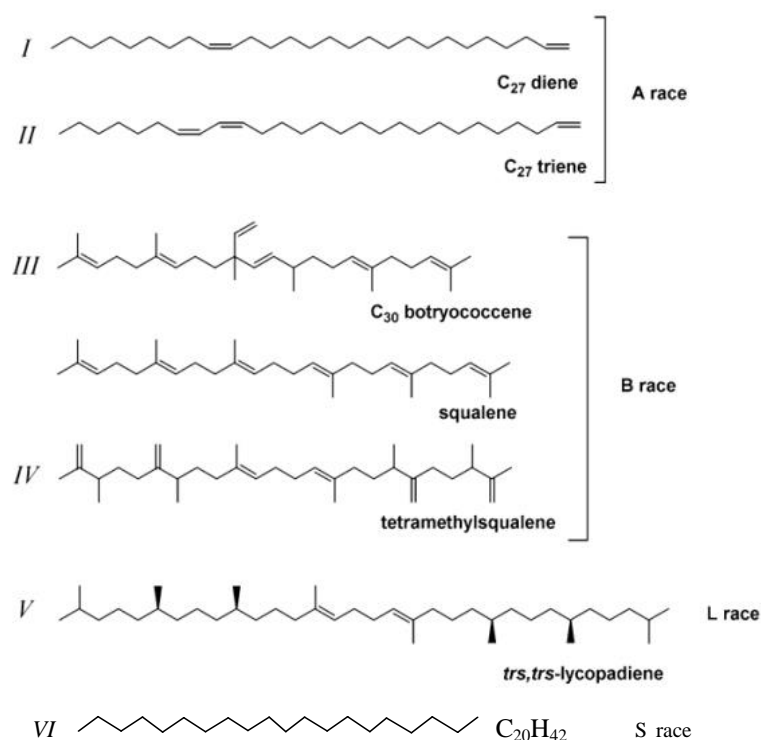


Figure 1-1: Types of hydrocarbons produced by four races of *B. barunii*.

The Figure 1-1, shows different types of hydrocarbons produced by races A, B, L and S (I: Knights et al. 1970, II: Villarreal-Rosales et al. 1992, III: Metzger and Casadevall 1983, IV: Huang and Poulter 1989 b, V: Metzger and Casadevall 1987, VI: Kawachi et al. 2012).

The race B strains seem the most attractive since the suggestion of Hillen et al. (1982) to convert C_{31} – C_{34} methylated squalenes and heavier C_{30} – C_{37} botryococcenes into shorter-length fuel-type hydrocarbons, such as C_7H_n to $C_{11}H_m$ for gasoline, C_{12} – C_{15} for kerosene (jet fuel), or C_{16} – C_{18} for diesel by catalytic cracking processes.

The hydrocarbon productivities of the A, B and L races of *B. braunii* were shown to be optimal during the exponential phase of growth (Largeau et al. 1980; Metzger et al. 1985, 1990) suggesting the production of hydrocarbons is growth associated in *B. braunii* cultures. In media with deficiency of nitrogen and phosphorous, hydrocarbon synthesis does not occur (Brenckman et al. 1985; Casadevall et al. 1985; Wolf et al. 1985 b).

A-race cells, unlike their B-race counterparts, break easily upon mechanical dispersion of the micro-colonies, releasing photosynthetic pigments, which are then mixed with the diene hydrocarbons in the medium. A-race strains, are more easily subject to cell rupture and pigment release, compared to their B-race counterparts (Eroglu et al. 2011).

1.4 Biofuel production

1.4.1 Biofuel production

While the total content of lipids and hydrocarbons of race A is the highest, race B produce more hydrocarbons fraction than race A (Suzuki et al. 2013), therefore race B become much more interesting for hydrocarbons production (Moheimani et al. 2014).

Microalgae have been studied widely for fuel production. Algae biomass can be processed into biofuel such as bioethanol, biodiesel, and biohydrogen, using thermochemical and biochemical conversion (Brennan and Owende, 2010 ; Karimi Alavijeh and Yaghmaei 2016). Recent efforts to produce bioethanol focused on microalgae as a feedstock rich in carbohydrates and fibers that can be hydrolyzed and used as carbon sources for fermentation process. *Chlorococum* sp. have been investigated as a substrate for bioethanol production (Lam and Lee 2015). There are many species of oleaginous microalgae (*Botryococcus*, *Nannochloropsis*, *Schizochytrium*, *Chlorella*, *Nitzschia*) which shown a strong capacity to produce high contents of lipids (triglycerides and fatty acids), that can be converted into biodiesel by transesterification (Abinandan and Shanthakumar 2015; Prabandono and Amin 2015). One of the most studied microalgae in that purpose is green microalgae *Botryococcus*

braunii which has the special particularity to produce more than 50% DCW of lipids and hydrocarbon that can be easily converted into biofuel (Al-Hothaly et al. 2015; Watanabe et al. 2015). Hydrogen fuel is also a clean energy which exhibits the advantages of high-energy yields with H₂O as the only major by-product when burned with oxygen. It is used for the spacecraft propulsion and researches are undergo to potentially produce and commercialized it for cars and aircrafts in the coming years (Oncel 2015; Prabandono and Amin 2015). Microalgae *C. reinhardtii*, is known as one of the best hydrogen producers (Oncel 2015).

1.4.2 Economy of biofuel production

A business assessment of *B. braunii* oil production system has already been to evaluate the cost of installations and operations at large scale. The *B. braunii* oils price estimated 230 € per barrel (0, 89 € per liter) which is about 4 times of the current price of the crude oil (Shiho et al. 2012).

Economical and technical constraints remain the main factors which restrict the mass production of *B. braunii* for biofuel and other purpose (Watanabe and Tanabe 2013). Using wastewater and low-cost medium could reduce the cost of biofuel production from *B. braunii*.

1.5 Microalgae strains and culture systems

Similar to other photosynthetic microalgae, *B. braunii* requires CO₂, photosynthetically active radiations, inorganic nutrients, and water for its growth. Studies on the effects of various factors on the production of biomass and hydrocarbon have been mostly conducted in the laboratory with small-scale culture systems. The important factors that affect the production of biomass and hydrocarbons were temperature (Lupi et al. 1991; Qin 2005), salinity (Qin 2005; Vázquez-Duhalt and Arredondo-Vega 1991; Ranga Rao et al. 2007 a), photoperiod and light intensity (Kojima et al. 1999; Lupi et al. 1994; Qin 2005), CO₂ concentration (Ge et al. 2011; Ranga Rao et al. 2007 a; Wolf et al. 1985 a; Yoo et al. 2010), nitrogen concentration (Lupi et al. 1994; Singh and Kumar 1991; Yang et al. 2004), and the presence of organic carbon compounds such as glucose and acetate (Tanoi et al. 2011; Weetall 1985).

A number of culture media have been used for the cultivation of *B. braunii*. These include Chu-13, modified Chu-13, AF-6, and BG11 media. Of these, modified Chu-13 is the most commonly used medium (Banerjee et al. 2002) because this medium can achieve the maximum growth rate for *B. braunii* (Largeau et al. 1980). Cultures were grown autotrophically in bold basal (BBM) (Kanz and Bold 1969) and modified BBM, BG11 (Richmond 1986), Chu13 and modified Chu13 media (Largeau et al. 1980) and also AF-6

(Kasai et al. 2004). Although the composition of each medium is different, all media include the essential components for algal growth, that is, nitrogen, phosphorus, and metals. AF-6 medium is often used instead of modified Chu-13 medium to preserve *B. braunii* strains in algal culture collections as well as those in private stock. This is because the long-term effects of vitamin deficiency on *B. braunii* are poorly understood; it is possible that *B. braunii* may reduce or lose its growth potential, as has been demonstrated in earlier experiments. Of note, *B. braunii*'s vitamin requirements remain unclear, despite the fact that *B. braunii* can grow in a vitamin-free medium such as modified Chu-13 (Watanabe and Tanabe 2013).

AF-6 includes NaNO₃ (140), NH₄NO₃ (22), KH₂PO₄ (10), K₂HPO₄ (5), MgSO₄·7H₂O (30), CaCl₂·2H₂O (10), ferric citrate (2), citric acid (2), biotin (0.002), thiamine HCl (0.01), vitamin B₆ (0.001), vitamin B₁₂ (0.001), and trace metals mg L⁻¹ (Kasai et al. 2004).

Generally, microalgae grow in the presence of bacteria which can stimulate their growth by releasing substances such as vitamins or nitrogen derivatives. Several bacteria (as *Pseudomonas* sp. and *Rhizobium* sp.) have been identified in microalgae cultures (Tanabe et al. 2012). Some of them can be beneficial to microalgae growth other are antagonistic (Rivas et al. 2010). Such effects were strongly dependent on the species involved as well as culture conditions (Tanabe et al. 2012).

A recent study on axenic culture of *Botryococcus* strain Bot-22 has identified and describe a new ectosymbiotic bacteria called BOTRYCO-2 (Candidatus Phycosocius bacilliformis') that promote the growth yields and hydrocarbon production of *B. braunii* (Tanabe et al. 2012 ; Tanabe et al. 2015). This uncultivated bacterium belongs to the *Alphaproteobacteria* lineage and the microscopic observation did not allow localizing precisely whether BOTRYCO-2 was present inside or attached to the matrix (Tanabe et al. 2015).

1.6 Effect of environmental factors

1.6.1 Temperature

Most strains showed the fastest growth rate at approximately 25–28°C (Li and Qin 2005; Lupi et al. 1991; Murakami and Ikenouchi 1997). Some strains grow equally at a broad range of temperatures (20–30°C). This type of strain is a good candidate for open-air cultivation systems, especially in temperate regions where seasonal variation in temperatures can be significant. However, some strains have been shown to yield a smaller biomass at higher temperatures in which the growth rate remains near the optimal value (Li and Qin, 2005). One *B. braunii* strain cannot grow at 33°C (Lupi et al. 1991), whereas another strain can grow at 35°C but produces approximately half the biomass produced at the optimal temperature (25°C)

(Murakami and Ikenouchi 1997). The latter reported that *B. braunii* can grow slowly at 15°C, which is the lowest temperature reported till date. Of note, *B. braunii* can significantly decrease its lipid content at higher temperatures at which maximum biomass was obtained (Kalacheva et al. 2002). The optimal temperature should be determined on the basis of lipid productivity, or more specifically hydrocarbon productivity rather than biomass productivity (Watanabe and Tanabe 2013).

The temperature was set at 23°C for the present study, value used by previous studies at the laboratory (Jin, 2016 a).

1.6.2 Salinity

Increase in salinity may result in slightly increased total lipid content of algae, as observed in cultures of *Monodus subterraneus* (Iwamoto and Sato, 1986), *Dunaliella* sp. (Borowitzka M.A. and Borowitzka L.J. 1988; Takagi et al. 2006), *Nannochloropsis* sp. (Pal et al. 2011), and *Chlamydomonas nivalis* (Lu et al. 2012). But results for several *B. braunii* strains were opposite (Yeesang and Cheirsilp 2011).

However, some strains can grow equally well or even better at low salinity levels. Ben-Amotz et al., at 1985 found that the lipid content of *B. braunii* in salt concentration was higher than that without salt or (Qin and Li 2006) demonstrated that one *B. braunii* strain can grow better in media with 0.15 M NaCl than in media without NaCl. The maximum salinity at which *B. braunii* has been shown to survive is 3 M NaCl (Vazquez-Duhalt and Arredondo-Vega, 1991).

Several researchers demonstrated that lipid content decreases with increasing salinity (Li and Qin 2005), whereas others demonstrated that lipid content is similar between cultures with and without NaCl (Ben-Amotz et al. 1985; Vazquez-Duhalt and Arredondo-Vega 1991). Recent reports indicated that the amount of TAGs increases at low salinity levels (Zhila et al. 2011). However, the advantages expected from increased salinity are not balanced by its impact on the effect of salts when the culture medium has to be recycled in order to reduce the water footprint of microalgae production (Hadj-Romdhane et al. 2013). Then for the present work, the parameter salinity was not studied.

It is not known whether the effect of salinity on lipid synthesis is species-specific or salt concentration dependent (Hu 2013); While high salinity media are less contaminated.

1.6.3 pH

Culture media are usually adjusted to pH 7.5 and pH 6.6 for Chu-13 and AF-6 media, respectively, and *B. braunii* can grow equally well in both media. Some studies have investigated the influence of pH on *B. braunii* cultivation (Ge et al. 2011; Dayananda et al. 2006; Dayananda et al. 2007 b; Hifney and Abdel-Basset 2014; Yoshimura et al. 2013). Consistent with this observation, it was demonstrated that both biomass and hydrocarbon contents are similar in media with pH ranging from 6.0 to 8.5 (Dayananda et al. 2007 b). Also it has been reported that maximum production of both biomass and hydrocarbon could be achieved at pH about 6.3 (Ge et al. 2011) or at pH 7.5 (Dayananda et al. 2007 b), while in other study showed that higher biomass could be achieved at pH 6.0 but hydrocarbon content showed little response to in the pH range of 6.0 to 8.5 (Dayananda et al. 2006). In the media pH is strongly related to its CO₂ concentration (Ge et al. 2011).

Jin et al. (2016 a) have shown that maximal biomass and hydrocarbon productivities are obtained at pH 6.5, with a direct correlation between the inorganic carbon speciation and the hydrocarbon productivity in cultures of the *B. braunii* race-A strain SAG 7081.

For the present PhD work, the pH was regulated at 6.5, usual pH value for cultures of the *B. braunii* BOT-22 strain (Yoshimura et al. 2013).

1.6.4 Carbon source (Organic and Inorganic)

Although *B. braunii* is a green alga that can grow photoautotrophically, addition of organic carbons promotes its growth. This mixotrophic mode of growth was first investigated by Weetall (1985), who demonstrated that several organic carbon sources (fructose, glucose, mannose, galactose, and lactic acid) can promote the growth of *B. braunii*. Weetall (1985) also indicated that mannose has the most significant growth-promoting effect on *B. braunii*. But Zhang et al. (2011) demonstrated that all organic carbon sources tested (maltose, glucose, saccharose, lactose, glycerol, and starch) promoted the growth of *B. braunii* at 2- to 4-fold compared to the control culture without organic carbons and that glucose is the most significant growth promoter. Tanoi et al. (2011) demonstrated that glucose and mannose can equally promote the growth of *B. braunii*. They also demonstrated that the significantly higher biomass observed in the presence of glucose is related to larger colony size. Weetall (1985) demonstrated that there are no differences in oil content between mixotrophic and photoautotrophic cultures of *B. braunii*, whereas Tanoi et al. (2011) showed increased oil lipid contents both in mixotrophy and heterotrophy.

Addition of organic carbon sources to the media does promote the growth of not only *B. braunii* but also bacteria, which makes the open-air culture of *B. braunii* virtually impossible, because the mixotrophic growth of *B. braunii* is still much slower than that of the contaminating bacteria. Another problem may be the cost of glucose implementation, which cannot be overlooked especially in mass cultivation systems (Watanabe and Tanabe 2013).

Microalgae are sunlight-driven cell factories that convert carbon dioxide to potential biofuels, foods, feeds and high-value bioactives (Akkerman et al. 2002; Banerjee et al. 2002; Borowitzka 1999 a; Ghirardi et al. 2000; Kay 1991; Lorenz and Cysewski 2003; Melis 2002; Metting and Pyne 1986; Metzger and Largeau 2005; Schwartz 1990; Shimizu 1996, 2003; Singh et al. 2005; Spolaore et al. 2006).

Green algae are eukaryotic organisms that can perform photosynthesis. Just like plants, they use water as their electron source, sunlight as their energy source, and CO₂ as their carbon source. In turn they produce oxygen and carbohydrates, protein, and lipids contained within the cells. They are typically more efficient than higher plant at converting solar energy into biomass because of the simple cellular structure and the readily available supply of CO₂ and various nutrients dissolved in water. Thus, microalgae can produce 30 times more oil than terrestrial oilseed crops for a given surface area (Sheehan et al. 1998).

Microalgae could be grown on dissociated type (HCO₃⁻, CO₃²⁻) and undissociated type (CO₂, H₂CO₃) of inorganic carbon sources (Lee and Palsson 1994).

Optimal CO₂ conditions differ among strains (Table 1-1). Strain Showa has been cultured in 0.3–2 % CO₂ in previous studies (Okada et al. 1995; Wolf et al. 1985 a), confirmed as an appropriate CO₂ conditions by the present result. Ranga Rao et al. (2007 b) reported that strain LB-572 (A race) showed optimal growth and hydrocarbon content in 2 % among 0–2 % CO₂ enriched air, while strain 765 showed uniform growth among the 2–20 % CO₂ range examined (Ge et al. 2011). These results show that optimum CO₂ concentrations for the growth and tolerance to high levels of CO₂ are strain specific.

Under high CO₂ concentrations, *B. braunii* produced hydrocarbons with carbon numbers of C₃₀–C₃₂, instead of hydrocarbons with C₃₃–C₃₄ produced under ambient air conditions (Wolf et al. 1985 b).

Table 1-1

CO₂ concentration for growing *B. braunii* race B and specific growth rate in different studies.

Strain	Race	CO ₂ enrichment of air (%)	Specific growth rate (d ⁻¹)	References
Showa	B	1	0.50	Yoshimura et al. (2013)
Showa	B	1-10	0.19-0.44	Yoshimura et al. (2013)
Showa	B	0	0.12	Wolf et al. (1985 a)
Showa	B	0.3	0.42	Wolf et al. (1985 a)
Showa	B	2	No data	Okada et al. (1995)
Yayoi	B	2	0.20	Okada et al. (1997)
FACHB 357	B	1	0.22	Cheng et al. (2013)
BOT-22	B	1	0.033	Shimamura et al. (2012)

The present PhD was limited to oxygenic photoautotrophic culture conditions, where only inorganic nutrients, except vitamins, are provided. Then the light supply was a crucial nutrient factor.

1.6.5 Dissolved oxygen concentrations

The effect of light intensity has been studied in greatest details in connection with photosynthesis, and is usually measured as O₂ evolved or as CO₂ consumed (Rabinowitch 1945).

The apparent oxygen production rate (OPR) will decrease after the cell concentration reaches a certain density (Lee and Palsson 1994).

Photosynthesis generates oxygen. Under high irradiance, the maximum rate of oxygen generation in a typical tubular photobioreactor may be as high as 10 g O₂ m⁻³ min⁻¹. Dissolved oxygen levels much greater than the air saturation values inhibit photosynthesis (Molina Grima et al. 2001).

Oxygen concentration above air saturation is known to inhibit the growth of microalgae. Some studies have indicated that up to 400 % of air saturation causes a reduction in growth rate of *Spirulina platensis* to 36 % (Marquez et al. 1995). Molina Grima et al. (2001) achieved that in an outdoor tubular photobioreactor, accumulation of oxygen causes extremely lower productivity during hours of peak irradiance, however, photosynthetic activity of the cells recovered after a few hours, when the algae were exposed to lower light intensity. The synergetic effects of light and oxygen on algal growth have been extensively reported (Ugwu et al. 2007; Vonshak et al. 1996 b). Very few studies have been published on the effect of

oxygen at low light intensity, and these indicated that the algal growth rate significantly decreased due to photorespiration effects (Kliphus et al. 2011; Sousa et al. 2011). Photorespiration is related to oxygen production that occurs during the dark reaction. The high concentration of the medium causes high ratio concentration of O₂ versus CO₂ within the chloroplast where Rubisco enzyme is located. At these high oxygen conditions, Rubisco not only fixes carbon dioxide through photosynthesis but also catalyzes the reaction with oxygen in photorespiration.

Growth is seldom exponential since increased biomass concentrations result in self-shading and decreased specific growth rates (Eriksen et al. 1996), and increased competition for light will often cause phototrophic microalgae to increase the contents of their pigment (Richardson et al. 1983) therefore their composition will change. The ratio between O₂ evolution rate and CO₂ uptake rate (the photosynthetic quotient, PQ) depends on the composition of the produced biomass and the substrates that are utilized. Especially oxidized nitrogen sources, which must be reduced before they are incorporated into the biomass, affect the PQ. When biomass composition equals the Redfield ratio, CH₂ O (NH₃)_{0.15} (Redfield et al. 1963), and NO₃⁻ is the nitrogen source



a PQ of 1.3 will be expected. With the lesser reduced NO₂⁻ as nitrogen source, the expected PQ is 1.2. Growth on NH₄⁺,



When no organic products are secreted from the cells, not the case of *B. braunii* colonies, all CO₂ taken up is incorporated into the biomass, and the PQ is equal to y_{O2}/x :

$$\text{PQ} = y_{\text{O}_2}/x = \gamma_x / -\gamma_{\text{O}_2} = \gamma_x / 4$$

According to Henry's law the maximum solubility of oxygen in water for the temperature influence: 100 % air saturation equals a dissolved oxygen concentration of 258 μmol L⁻¹ at 25°C. The biomass-specific (per gram dry weight) oxygen production rate (PO₂; μmolO₂ g⁻¹ s⁻¹) is the slope of dissolved oxygen concentration versus time divided by the biomass (dry weight) concentration (cx, g L⁻¹). There is a dependency of maintenance respiration on dissolved oxygen concentration. Maintenance respiration is a part of respiratory activity during photosynthesis in the light. The oxygen yield on absorbed light energy in continuous light is influenced by maintenance respiration. For *Chlamydomonas reinhardtii* as Vejrazka et al. 2013 achieved, the highest net oxygen yield in continuous light was observed between a PFD of 100 μmol m⁻² s⁻¹ and 200 μmol m⁻² s⁻¹. At a PFD below 100 μmol m⁻² s⁻¹, the yield decreased due to a relative increase in maintenance (absolute maintenance is constant) to

support cell metabolism. This range of PFDs is surprising because photosynthesis starts to become saturated already at $200 \mu\text{mol m}^{-2} \text{s}^{-1}$, which was confirmed by a decrease in gross yield at a PFD of $200 \mu\text{mol m}^{-2} \text{s}^{-1}$ (Vejrazka et al. 2013).

As photosynthetic oxygen can be accumulated in closed photobioreactor, but can also decrease as a consequence under light incubation of an efficient gas stripping, consumption by bacterial contaminations or, under dark incubation, of high respiratory activities, the present work includes a comparative study on the effect of low and high oxygen supply to continuous cultures in photobioreactors.

1.6.6 Nutrients (N, P and metals)

Botryococcus braunii is a photosynthetic green alga, and as such, it requires nitrogen, phosphorus, and metals for its growth. Of the three basic inorganic nitrogen sources (NO_3^- , NO_2^- , and NH_4^+), *B. braunii* prefers NO_3^- (Yang et al. 2004).

Lack of nitrogen limits protein synthesis and thus increases lipid (Converti et al. 2009) or sometimes, carbohydrate accumulation (Hu 2013).

Phosphorus was one of the most important limitation elements in eutrophication, whose most objectionable symptom was the appearance of floating algal blooms (Schindler 1977).

K_2HPO_4 used as phosphorus source in AF6, BG11 and modified Chu 13. In AF6, KH_2PO_4 is used as the other phosphorus source.

Hu (2013) reported that iron deficiency reduced growth and biomass of algae, but that excess iron elicits an oxidative stress leading to a physiological changes (Hu 2013) and negative effects on growth (Yeesang and Cheirsilp 2011).

1.6.7 Photosynthetic active radiations (PAR)

According to species, microalgae have different trophic behavior, from photoautotrophy to strict heterotrophy, but also photoheterotrophy. In this manuscript, Microalgae have evolved to absorb more light than needed for their photosynthetic requirements. The excess light energy is dissipated as heat and fluorescence (Wang et al. 2003):



According to Eq. when photon utilization increases in microalgae, light conversion efficiency increases, and the ability of CO_2 fixation increases as well (Melis 2009). Energy requirement in the form of 9.5 mol photons (hv) for the conversion of 1 mol CO_2 into 30 g biomass equivalent (CH_2O) (Bjorkman and Demmig 1987; Ley and Mauzerall 1982). There is a losses of 10 % of the primary biomass in the course of the day due to cellular respiration

(respiration/photosynthesis ratio = 0.1:1) (Melis 2009), and also losses of an additional 20 % of the primary biomass due to photorespiration and other cellular metabolic activity (Bolton and Hall 1991).

Carvalho et al. 2011, studied light requirements in microalgal photoreactors. They noticed that cultivating microalgae in photobioreactors (PBRs) should be provided with appropriate light duration, intensity and wavelength. Insufficient light may lead to growth limiting or photo-oxidation and inhibition.

For example Yeh et al. (2010) achieved that for *Chlorella vulgaris* ESP-31 fluorescent lamps were more effective light sources for microalgae growth than tungsten lamp. Pigments in *Chlorella* sp. are mainly chlorophyll and carotenoids, which mainly capture the light with wavelengths of 400–500, and 650–700 nm (Ravelonandro et al. 2008). The fluorescent lamp covered similar light distribution to the adsorption spectrum of *C. vulgaris* ESP-31 over the range of 450–650 nm, thereby providing needed light wavelengths for the growth of the microalga. In contrast, the light distribution of tungsten lamp was primarily between 700 and 850 nm; this seems to explain why the fluorescent lamp was better light source for the growth of *C. vulgaris* ESP-31 (Yeh et al. 2010).

Zemke et al. (2010) the use of sunlight to produce biodiesel using microalgae can only be expected to operate with efficiencies of at most 9 %, and likely much less. As much as 90 % of the inefficiencies can be attributed to biological limits to the efficiency at which sunlight can be used. They achieved, the most significant improvements can be made by minimizing optical losses (maximizing the solar energy received by the algae) and minimizing light over-saturation of the microalgae.

Growth and composition of microalgae depends on light supply (type of light source and light intensity) (Ogbonna et al. 2000) so that design and operation of PBRs are critical for light availability.

Sunlight and artificial light have been used via outer surface exposure as well as inner volume exposure, through the placement of lighting devices (e.g. LEDs or optical fibers) inside the reactor itself (Suh and Lee 2003). The photosynthetically active radiance is normally assumed to be 43–45% in the wavelength range of 400–700 nm (Laws et al. 1986).

Outdoor sunlight is not easily controllable because in different geographical regions and different times of a day the magnitude and the amplitude of solar radiation is not the same and will change during time, microalgae are usually studied under artificial lights. Different varieties of lamps such as tungsten, fluorescent, LED (Light Emitting Diode), ... are used as artificial illumination.

As it shown in Table 1-2, in most of the previous studies, cool white florescent lamps were used as a light source. In this study LED (Light Emitting Diode) were used as a light source for the experiments.

Table 1-2

PAR, photoperiod and light source for *B. braunii* races in different studies.

Strain	Race	PAR ($\mu\text{mol m}^{-2} \text{s}^{-1}$)	Photoperiod in a day	Light source	References
Showa	B	850	14 h	cool white florescent light	Yoshimura et al. (2013)
Showa	B	85-398	14 h	cool white florescent light	Yoshimura et al. (2013)
Showa	B	250	24 h	cool white florescent light	Wolf et al. (1985 a)
Showa	B	250	24 h	cool white florescent light	Wolf et al. (1985 a)
Showa	B	240	12 h	cool white fluorescent light	Okada et al. (1995)
IPE 001	B	35	16 h	N d	Xu et al. (2012 b)
Yayoi	B	240	12 h	cool white fluorescent light	Okada et al. (1997)
FACHB 357	B	60	24 h	cold white fluorescent lamps	Cheng et al. (2013)
BOT-22	B	100-200	(N d)	cool white florescent light	Shimamura et al. (2012)
Yamanaka	A	240	12 h	cool white fluorescent light	Okada et al. (1995)
765	N d	150	24 h	cool white florescent light	Ge et al. (2011)
CHN 357	N d	60	12 h	cool fluorescent lamps	Li and Qin (2005)
KMILT 2	N d	200	24 h	fluorescent tube lamps	Ruangsomboon (2012)
NIES-836	N d	60	12 h	cool fluorescent lamps	Li and Qin (2005)
UK 807-2	N d	60	12 h	cool fluorescent lamps	Li and Qin (2005)
AP103	N d	30	16 h	N d	Ashokkumar and Rengasami (2012)
UC 58	N d	250	24 h	cool white florescent light	Lupi et al. (1991)

1.6.7.1 Light intensity

Sunlight is the main source of energy for microalgae. Although light intensity requirements of typical microalgal cells are relatively low compared to those of higher plants, microalgal metabolic activity rates usually increases with increasing light intensity up to $400 \text{ mmol m}^{-2} \text{ s}^{-1}$ (Munoz and Guieysse 2006). The saturating light intensity of *Chlorella* and *Scenedesmus* sp. is $200 \mu\text{mol m}^{-2} \text{ s}^{-1}$ (Kumar et al. 2010). The thermophilic *Chlorogleopsis* sp. Exhibits high light adaptability, growing successfully under both high light intensity ($246.1 \text{ mmol m}^{-2} \text{ s}^{-1}$) and low light intensity ($36.9 \text{ mmol m}^{-2} \text{ s}^{-1}$) with the optimum light intensity $200 \text{ mmol m}^{-2} \text{ s}^{-1}$ (Ono and Cuello 2007). Under low light conditions, many microalgal species switch from phototrophic to heterotrophic growth, and some can even grow mixotrophically. The optimum intensity of microalgae could be modified genetically and altering the size of the chlorophyll antenna (Zeng et al. 2011).

In general, light intensity has effect on photoautotrophic growth of photosynthetic cells. When the light intensity increases from zero to higher values, the effect of light intensity on microalgal growth could be classified as four phases, including 1) lag phase, 2) light limitation, 3) light saturation, and 4) light inhibition(Ogbonna et al. 2000). At very high light intensities, photoinhibition becomes a very important problem (Tschiersch and Ohmann 1993; Vonshak et al. 1996 a).

Photon absorption is affected by many factors, such as pigmentation in the algae cells, density of the culture, and the specific position of the cell (Richmond 2004).

Low light intensity causes a reduction in dry weight while high intensity causes biochemical damage to the photosynthetic machinery (photoinhibition) (Scott et al. 2010). To achieving the high photosynthetic efficiency, the light intensity received by the algal cells should equal or lower than LSP (Light Saturation Point) (Chisti 2007). This high efficiency should be attributed to the structure of type of bioreactor, through which the high light was diluted into an appropriate level (between the light saturation and light compensation point) (Liu et al. 2013) to support algal growth on larger surface than incident surface by light with less light inhibition.

An overdose of excitation energy can lead to production of toxic species (for example singlet oxygen) and to photosystem damage (Barber 1994; Vacha 1995). Carotenoids are capable of scavenging toxic photoproducts (Edge et al. 1997; Vacha 1995). More important, they can prevent formation of these products because an overdose of excitation energy can be dissipated as heat by carotenoids in the antenna complex (Casper-Lindley and Bjorkman 1998; Demming-Adams et al. 1995; Gilmore 1997; Masojidek 1999; Niyogi et al. 1997). Also carotenoids (for example astaxanthin) can accumulate and possibly act as a “sun- shade” during high light exposure in combination with other stress factors (Masojidek et al. 2000).

Production of excessive photoassimilates can be stored in the form of lipid, probably as a means to convert excess light to chemical energy in order to avoid photooxidative damage (Solovchenko et al. 2008).

For *Chlorella vulgaris* ESP-31, Yeh et al. (2010) achieved that from 5 to 18 W m⁻² of light intensity, the specific growth rate increased and from 18 to 42 W m⁻² of light intensity, it decreased; while the percentage of carbon utilization from 9 to 42 W m⁻² of light intensity are about the same.

The control and optimization of light quality and quantity is one of the most important parameters for the mass culture of a photosynthetic microorganism (Ugwu et al. 2008). The

rate of extracellular polysaccharide production in race B strains of *B. braunii* decreases under low light intensity (Zhang and Kojima 1998). Growth is also affected by changes in light intensity in the range of 3–10 klx but hydrocarbon production is not (Zhang and Kojima 1998).

Cheng et al. (2013) reported that for the *B. braunii* FACHB 357 (B race), the light intensity of 60 $\mu\text{mol photons m}^{-2} \text{s}^{-1}$ could be considered as the light saturation point (LSP). The LSP is critical reference for determining the light dilution rate (R L) of a multiple-plates photobioreactors. However these authors, didn't mention the culture concentration and the self-shading.

Also for *B. braunii* BOT-22 Sakamoto et al. (2012) reported the half-saturating light intensity for photosynthesis and the saturated light intensity for hydrocarbon production were the same (200 $\mu\text{mol m}^{-2} \text{s}^{-1}$). These data indicate that an increase in photosynthetic activity above 200 $\mu\text{mol m}^{-2} \text{s}^{-1}$ does not stimulate hydrocarbon productivity per unit of chlorophyll in wild-type *B. braunii* BOT-22. These authors also didn't take the culture concentration and the self-shading in account.

In this study the specific light supply rate will be investigated to find how SLSR could affect the biomass and hydrocarbon productivity.

1.6.7.2 Light and dark cycle

In order to optimize the efficiency of the light use in PBRs by controlling the total irradiance, several methods have been proposed. These methods follow two main strategies: (1) control of the exposure time or, (2) control of the irradiance supplied to the cultures. A combination of both strategies is commonly used in most systems. The control of light/dark periods to increase microalgal productivity has been explored for many years (Gutierrez-Wing et al. 2014).

Light conditions affect directly the growing and photosynthesis of microalgae (Duration and intensity). Microalgae needs a light/dark regime for productive photosynthesis, it needs light for a photochemical phase to produce (ATP) Adenosine triphosphate (NADPH) Nicotinamide adenine dinucleotide phosphate-oxidase) and also needs dark for biochemical phase synthesize essential molecules for growth (Cheirsilp and Torpee 2012).

A high biomass concentration results in an illuminated zone with net photosynthesis and a dark zone with possible respiration. As a result of mixing, algae experience flashing light or light/ dark (L/D) cycles. These mixing-induced L/D cycles are suggested to enhance PBR efficiency (Degen et al. 2001; Hu and Richmond 1996; Richmond 1996). The major influence

of L/D cycles on photosynthetic rate was found with oversaturation, incident PFDs during the flash (Vejrazka et al. 2011; Xue et al. 2011).

Under full light integration, algae do not respond to the actual PFD during the flash of an L/D cycle but to the lower, time-averaged PFD of the whole cycle (flash + dark time). In other words, biomass yield will be comparable with cultivation under continuous and limiting PFD. Opposite to full light integration; algae can respond directly to the PFD during the flash and respire during the dark part of the L/D cycle. This behavior can be called growth integration and is not favorable because it leads to low biomass yields (Vejrazka et al. 2013).

The existence of a longer dark period between the short flashes of the light can increase photosynthetic efficiency, especially for high intensity illumination (Kok 1953; Kok 1956; Park et al. 2000; Phillips and Myers 1954; Weller and Franck 1941). Thus, by using a flashing light, algae can assimilate the same amount of light as they can by using the same average intensity of steady light. A flashing light has advantages over a steady light of same net intensity, since the total amount of photosynthesis will be the same in either case (Park and Lee 2000) The efficiency with which light is utilized by the algae tends to be greater in intermittent light than it is in steady light of intensity equal to that of the light flashes (Fredrickson and Tsuchiya 1970).

One parameter which characterizes and influences the amount of light integration is the duty cycle: it determines the time fraction algae spend in the light during one full L/D cycle. In a PBR, the duty cycle is dependent on the biomass concentration. An increase in biomass concentration will lead to an increase in a dark zone and thus a decrease in duty cycle, which might affect algae growth and productivity (Vejrazka et al. 2013).

The characteristics of the light/dark cycle exhibited a strong effect on microalgal growth in the airlift bioreactors. Generally, the dark time in the light/dark cycle is considered to reduce photoinhibition resulting from long exposure to high-intensity light and the dark zone allows for reparation of photo-induced damage (Barbosa et al. 2003). In the case of *B. braunii*, high intensity light has been demonstrated to be adverse to the cell growth due to a decrease in chlorophyll content, but it is beneficial for metabolite accumulation in cells (Sakamoto et al. 2012). Thus, the regulation of light/dark cycle in the airlift reactor could be an efficient method to achieve both increased biomass production and a higher metabolite content, which could result in the improvement of hydrocarbon production by *B. braunii* (Xu et al. 2012 a).

The ratio of light to dark (or low-intensity light) periods in a cycle is crucial for microalgal productivity (Munoz and Guieysse 2006). Similar overall numbers of moles of photons do not necessarily produce equal growth rates of (or CO₂ assimilation by) microalgae. When the

light/dark cycle period approaches the photosynthetic unit turnover time (equal to the dark reaction time, estimated to lie within 1–15 ms), maximum photosynthetic efficiencies can be achieved (Richmond et al. 2003).

Ruangsomboon (2012) achieved *Botryococcus braunii* KMITL 2 under a 24:0 light cycle achieved a biomass four times than under 12:12 light/dark cycles. The highest lipid content and lipid yield was obtained under 16:8 light conditions.

Sakamoto (2012) achieved the production of lipids and hydrocarbons were not directly supported by an increase in photosynthetic activity. The length of the dark period did not affect hydrocarbon production or the efficiency of light energy utilization for hydrocarbon production by *B. braunii* (Sakamoto et al. 2012).

But the effect of the light and dark cycle on the production of hydrocarbon which could be very important for increasing the hydrocarbon production was not studied yet and there is a need to pay attention to this fact.

1.6.7.3 Light wavelength

Photosynthetic microorganisms (microalgae and cyanobacteria) contain three major pigment groups, chlorophylls, carotenoids, and phycobilins. Each pigment has a characteristic light absorption range. The chlorophylls, the most abundant of the pigment groups have two major absorption ranges. The first one is in the range of the blue light (450–475 nm) and the second and most significant is in the red light range (630–675 nm). The carotenoids, which include α -carotenes and β -carotenes and xanthophylls including lutein, violaxanthin, zeaxanthin, and fucoxanthin, among others. Carotenoids have an absorption range from 400 to 550 nm (Masojidek et al. 2007). Low irradiances result in light limitation and impaired growth and high irradiances can induce photoinhibition and in severe cases photobleaching, that can be irreversible and result in the destruction of the photosynthetic pigments. In terrestrial plants, the highest growth rates have been observed by some authors using red and blue lights, matching the absorbance peaks of the chlorophylls. Similarly, experiments conducted using LED lights have found that microalgal growth is higher in many species using red light (Carvalho et al. 2011; Chen et al. 2010; Yeh and Chung 2009).

The wavelength distribution of the light in the PBRs affects the photosynthetic efficiency and modifies the bioproducts that can be obtained from the microalgal cultures.

Under blue light *B. braunii* Bot-144 achieved a higher cell density than in green and red light but for the hydrocarbon composition, under red and blue light the composition are about the

same but higher than in green light but the important fact is all of three lights are not totally different for the hydrocarbon composition (Baba et al. 2012).

Growth, pigment composition, colony shape, and the rate of photosynthetic CO₂ fixation in *B. braunii* Bot-144 were regulated by changes in light quality, whereas the photosystem machinery and metabolic pathways for hydrocarbon production was not (Baba et al. 2012).

The control of wavelength distribution can be done through monochromatic lights such as narrow range LEDs (Fu et al. 2013; Gordon and Polle 2007; Katsuda et al. 2004). Also, filters can be used to restrict the input of undesirable wavelengths (Mohsenpour et al. 2012). But for large-scale PBRs, these strategies can be very cost effective and the possibility of controlling the output of valuable bioproducts may offset the costs.

There is no single wavelength that will be useful for all species and all bioproducts (Gutierrez-Wing et al. 2014).

1.6.7.4 Penetration depth

In dense culture, the gradient of light varies along the radius of the PBR because of light attenuation (Molina Grima et al. 1994). The attenuation of light intensity is dependent on its wave length, cell concentration, geometry of PBR, and the penetration distance of light (Fernandes et al. 2010).

Penetration depth is defined as the distance from the illumination surface at which the light intensity reaches the compensation intensity per cell. Beer-Lambert's law can be used to determine light penetration depth in *C.kessleri* culture (Lee 1999).

For high-density microalgal cultures, which absorb incident light efficiently, performance is determined by light distribution and penetration rather than light intensity (Kim and Lee 2001).

Comparing the light penetration in bubble and airlift PBRs, the light penetration path is wider for bubble columns than airlift PBRs, because of the longer path to the center of the bubble column, and because of the cloud effect caused by chaotic rising bubbles in the column (Oncel and Sukan 2008).

1.6.7.5 Photoinhibition

Above a certain value of light intensity, a further increase in light level actually reduces the biomass growth rate. This phenomenon is known as photoinhibition. Microalgae become photoinhibited at light intensities only slightly greater than the light level at which the specific

growth rate peaks. Photoinhibition results from generally reversible damage to the photosynthetic apparatus, as a consequence of excessive light (Camacho Rubio et al. 2003).

The photoinhibition can be controlled by (1) reducing the total irradiance input, increasing the cycling of the microbes between the light and dark zones of the culture either by aeration, mixing, flow, or the use of intermittent light pulses reduction of the light source power or increasing the distance to the culture, (2) increasing the depth of the cultures to provide longer dark periods and areas with lower irradiance levels, and (3) using filters to exclude unnecessary light wavelengths, thus reducing the total light energy to the system. Photolimitation can be controlled by increased total irradiance input and decrease of culture depth. Although nonusable wavelength can increase the effect of photoinhibition and the risk of heat damage, increasing the light in those spectrums will not reduce the photolimitation effectively (Gutierrez-Wing et al. 2014).

Photoinhibition occurs during prolonged exposure to high irradiance (Tedesco and Duerr 2006). Light is found to be a major limiting factor of productivity and growth when nutrition and temperature are satisfied (Richmond 1999). Optimizing light utilization through design and operations is critical.

1.6.7.6 Photo-oxidation

In high light conditions an excessive amount of electrons is generated at Photosystem II and these electrons react with photosynthetically produced oxygen, forming oxygen radicals (Murata et al. 2007). These oxygen radicals are usually dealt with in the water-water cycle, but when too many electrons are generated, the enzymes in the water-water cycle are no longer capable of dealing with the surplus of electrons and oxygen radicals and other reactive oxygen species (ROS) such as H_2O_2 are accumulating and this has a destructive effect on biological systems (Asada 2006; Asada 1999; Endo and Asada 2008). The formation of singlet oxygen is bound to occur at high light intensities. This highly reactive compound is produced photochemically, via photoactivation (Triantaphylides et al. 2008). The singlet oxygen can attack photosynthetic pigments in PSII, causing photo-oxidative damage.

Both photoinhibition and low light stress of photosynthesis causes decrease in biomass production (Vonshak et al. 1994). Tredici achieved if algae are grown under light-limiting conditions, then photosynthetic efficiency is high (Tredici 2009).

1.7 Photosynthesis and photoacclimation

A common trend characterizes the mechanism of photoacclimation, is, an increase in chlorophyll *a*, and in other light-harvesting pigments, as growth irradiance decreases. The increase in pigment content during acclimation to low light, results in a decrease in the optical cross-sectional*($m^2 \text{ mg}^{-1} \text{ Chl } a$), thus reducing the gain in light harvesting. Indeed, in a microalgal culture, a doubling of cellular chlorophyll does not bring about a doubling in the rate of light absorption (Dubinsky et al. 1995).

Many species of phytoplankton, both algae and cyanobacteria, acclimate to a broad range of light irradiances in a relatively short period of time. The photoacclimation process is characterized by changes at the optical, biophysical, biochemical, ultrastructural, physiological, and molecular levels (Escoubas et al. 1995; Falkowski and LaRoche 1991; Falkowski 1992; Richardson et al. 1983).

Photoinactivation is manifested as an exponential (single-order) decline of variable fluorescence F_v (F_0 remains constant), paralleled by a decline of the Hill reaction (Setlik et al, 1990) (Figure 1-2). The inactivation of a part of the units caused by excess irradiance does not necessarily reduce the overall rates of electron transfer. At saturating light intensities, the rate of photosynthesis usually depends on the CO_2 fixation rate, and a moderate reduction in the number of active PS II units might not have any effect (Behrenfeld et al. 1998).

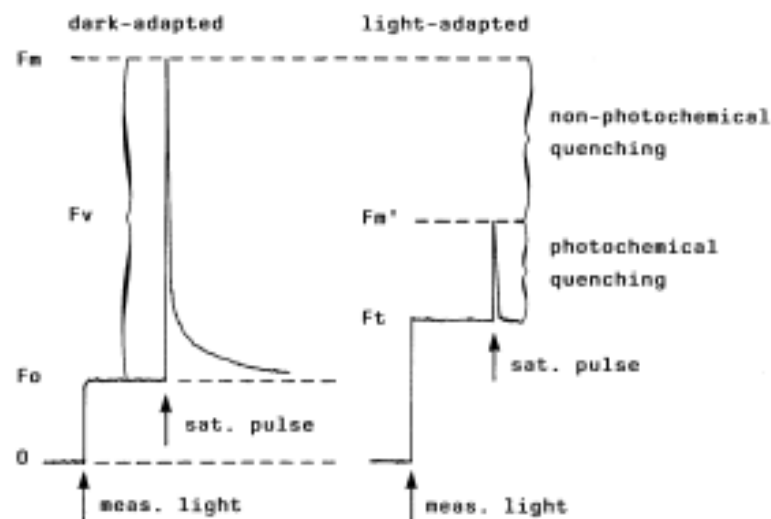


Figure 1-2: Principle of saturation pulse quenching analysis.

In recent years, evidence from a number of research groups has shown that the overall quantum yield of photochemical energy conversion can be assessed by the simple expression:

$$\text{YIELD} = (F_m' - F) / F_m' = \Delta F / F_m$$

This expression, which was introduced by Genty et al. (1989) is identical to the YIELD-parameter measured by PAM-Fluorometers.

1.8 Specific light supply rate (SLSR)

The yield of biomass on light energy is best investigated in chemostat cultivations where the organisms are acclimated to the conditions in the bioreactor with no biomass accumulation. In this case, the biomass yield can be directly related to a specific light availability (Zijffers et al. 2010).

For designing of photobioreactors, a relatively high specific light supply rate should be maintained. A process with high cell densities and high yields at high light intensities can only be obtained in short light path photobioreactors. Specific light supply rate is a parameter which is dependent to cell density, light intensity and the pathway of light (Lee et al. 2014; Ogbonna et al. 1995; Rochatte et al. 2016; Zijffers et al. 2010).

Sforza et al. (2015) observed that, for *Nannochloropsis salina*, the biomass production kinetic, the cell physiology and the stability of the continuous culture system can be related to the specific light supply rate. It was mentioned that light supply rate can be expressed as a linear function of the growth rate, and cells are indeed exposed to different light supply rate depending on the residence time. For the pigments it was reported by Sforza et al. (2015) that the Chl *a* content linearly decreased with the specific light supply rate while the Car/Chl ratio was found constant up to about 500 mmol photons per gramme per day and for Fv/Fm, up to about 500 mmol photons per gramme per day was found to be stable and then decreased with the light supply rate.

All these data were determined, thanks to the dynamic behavior of chemostat cultures, at successive steady states. Yet, transient growth dynamics could show how microalgae respond to environmental changes, before reaching new steady states. Whether the colonial state could affect the light availability is about of more than academic interest, considering the implications for an optimal design of photobioreactor for industrial production.

The photon flux entering the panel photobioreactor was divided by the amount of biomass present in the reactor (Zijffers et al. 2010).

$$r_{E,x} = \frac{\text{PFD}_m \times A}{C_x \times V} \quad (\mu\text{mol photons g}^{-1} \text{s}^{-1})$$

It was reported by Zijffers et al. (2010) that the strong decrease of biomass yield on light energy observed at low specific light supply rates, for example, low specific growth rates and high biomass densities, in the panel reactors, however, does not correlate to the change in light regime, for example, the decrease in size of the photic zone. The yield decrease, on the other hand, can be explained assuming that a significant fraction of the available light energy is not used for biomass formation but it is used for basic physiological maintenance, which includes processes such as osmoregulation, cell motility, defense mechanisms, and proofreading and internal turnover of macromolecular compounds (Van Bodegom 2007).

1.9 Pigments

All photosynthetic organisms contain organic pigments for harvesting light energy. There are three major classes of pigments: chlorophylls, carotenoids, and phycobilins. The various types of chlorophyll molecules designated *a*, *b*, *c*, and *d* differs in their side-group substituents on the tetrapyrrole ring. All chlorophylls have two major absorption bands: blue or blue-green (450–475 nm) and red (630–675 nm), which results in their characteristic green color. Chl *a* is present in all oxygenic photoautotrophs as a part of the core and reaction centre pigment–protein complexes, and in light-harvesting antennae it is accompanied by Chl *b* or Chl *c*. The so-called accessory (antennae) pigments Chl *b*, *c*, and *d* extend the range of light absorption. Carotenoids represent a large group of biological chromophores with an absorption range between 400 and 550nm, resulting in their yellow-orange color (Masojidek et al. 2013).

Assessment of the photosynthetic pigments (chlorophyll *a*, chlorophyll *b* and carotenoids) is a reliable indicator of the physiological state of microalgae. Quantitative change in the pigment composition can provide a lot of information on the photosynthetic metabolism or can be a useful stress indicator (Gomes et al. 2014; Netto et al. 2005).

In order to quantify chlorophylls and carotenoids the pigments are extracted in organic solvents (methanol, ethanol, acetone, etc.): the absorbance of the extract is determined spectrophotometrically and the pigment content is calculated using mathematical formulae (Lichtenthaler and Wellburn, 1983).

In previous studies were mentioned that in *B. braunii* with increasing the light intensity from low light to high light, the color of the colonies changed from green to yellowish. Also it was reported that spectroscopic pigment analysis showed that this change was due to an increase in the ratio of carotenoids/chlorophyll (Baba et al. 2012; Sakamoto et al. 2012; Wolf et al. 1985 a).

In the Figure 1-3, the structure of chlorophyll *a* and *b* and carotenoids are shown. The difference of Chl *a* and *b* is in the R group. Carotenoids are conjugated isoprenes with cyclic 6-carbon side groups.

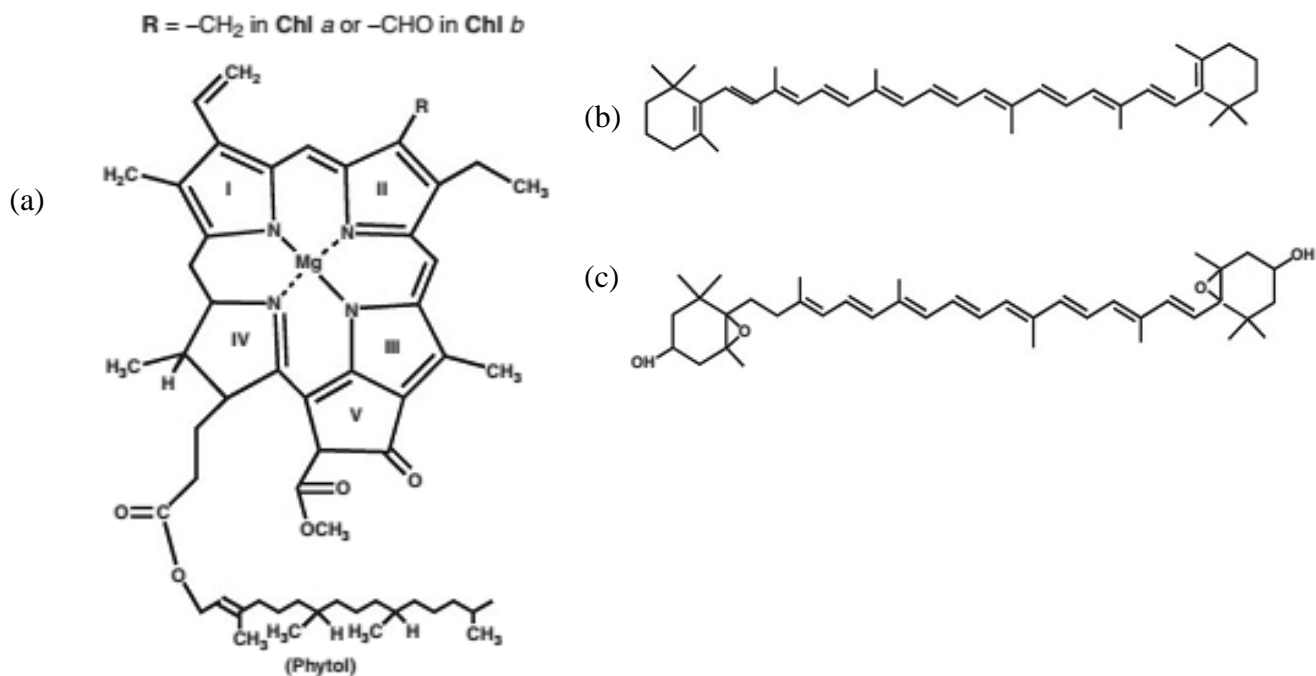


Figure 1-3: Structure of chlorophyll *a* and *b* (a), carotenoids (β -carotene (b) and violaxanthin (c)).

Table 1-3

Chl *a*/ Chl *b*, total carotenoids, Car/ Chl for *B. braunii* in different studies.

Strain	Chl <i>a</i> / Chl <i>b</i> (mol:mol)	Total carotenoids	Car / Chl (w:w)	References
<i>B. braunii</i> Showa	2.2:1	0.25 (% of DCW)	0.5	Eroglu and Melis (2010)
<i>B. braunii</i> var. Showa	2.2	0.21 (% of DCW)	0.43	Eroglu et al. (2011)
<i>B. braunii</i> Kawaguchi-1	2.3	0.54 (% of DCW)	0.63	Eroglu et al. (2011)
<i>B. braunii</i> Yamanaka	2.0	0.1 (% of DCW)	0.26	Eroglu et al. (2011)
<i>B. braunii</i> UTEX 2441	2.5	0.19 (% of DCW)	0.50	Eroglu et al. (2011)
<i>B. braunii</i> UTEX LB572	2.1	0.13 (% of DCW)	0.20	Eroglu et al. (2011)
<i>B. sudeticus</i> UTEX 2629	2.9	0.42 (% of DCW)	0.26	Eroglu et al. (2011)
<i>C. reinhardtii</i> CC503	2.2	0.37 (% of DCW)	0.18	Eroglu et al. (2011)
<i>B. braunii</i> (Nitrogen sufficient)	N d	0.48 (% of DCW)	0.29	Thomas et al. (1984)
<i>B. braunii</i> (Nitrogen depletion)	N d	0.26 (% of DCW)	0.56	Thomas et al. (1984)
<i>B. braunii</i> (Nitrogen sufficient)	N d	0.22 (% of DCW)	0.32	Thomas et al. (1984)
<i>B. braunii</i>	N d	1.42 mg L ⁻¹		Sirakov et al. (2013)
<i>S. dimorphus</i>	N d	1.47 mg L ⁻¹		Sirakov et al. (2013)

For *B. braunii*, from the fourteen separated carotenoids, twelve can be considered valuable biomarkers: α -carotene, β -carotene are the two carotenes and ten xanthophylls (violaxanthin, 5,6-epoxy-lutein, anteraxanthin, lactucaxanthin, lutein, zeaxanthin, α -criptoxanthin, β -criptoxanthin, echinenone and 5,6-epoxy- β -carotene) (Muntean et al. 2008).

Ranga Rao et al. (2007 a) reported that the HPLC analysis of carotenoid extract from *B. braunii* revealed that lutein was the major carotenoid followed by β -carotene and low levels of violoxanthin, astaxanthin and zeaxanthin were identified against authentic standards.

It was reported that the constituents of the resistant biopolymers in races A and L have similar structures to the hydrocarbons they produce; while those in the race B are thought to be

related to linear hydrocarbons rather than botryococcenes (Berkaloff et al. 1983; Derenne et al. 1990; Laureillard et al. 1988; Templier et al. 1992).

1.10 Comparative efficiency of raceways and closed PBRs

Nowadays, the research on designing of photobioreactors to cultivate photosynthetic cells of microalgae is extensively investigated. Photobioreactor gives a better control on most of parameters compared to open pond systems (Chisti 2007).

Algae cultivation in open pond production systems has been used since the 1950s (Borowitzka 1999 b). These systems can be categorized into natural waters (lakes, lagoons, and ponds) and artificial ponds or containers. Raceway ponds are the most commonly used artificial system (Jiménez et al. 2003).

Compared to closed photobioreactors, open pond is the cheaper method of large-scale algal biomass production (Brennan and Owende 2010). Open ponds have lower energy input requirement (Rodolfi et al. 2008), and regular maintenance and cleaning are easier (Ugwu et al. 2008), and therefore may have the potential to return large net energy production (Rodolfi et al. 2008).

Due to the lack of control involved with open systems, the pond becomes a function of the local climate, thus the location significantly contributes to the success of the cultivation (Masojidek and Torzillo 2008).

In raceways, any cooling is achieved only by evaporation. Temperature fluctuates within a diurnal cycle and seasonally. Evaporative water loss can be significant. Because of significant losses to atmosphere, raceways use carbon dioxide much less efficiently than photobioreactors. Productivity is affected by contamination with unwanted algae and microorganisms that feed on algae (Terry and Raymond 1985). A long production period causes bacterial and other biological contaminants (Becker 1994). The biomass concentration remains low because raceways are poorly mixed and cannot sustain an optically dark zone (Terry and Raymond 1985).

Currently, photoautotrophic production is the only method which is technically and economically feasible for large-scale production of algae biomass for non-energy production (Borowitzka 1997). Two systems that have been deployed are based on open pond and closed photobioreactor technologies (Borowitzka 1999 b).

Because of the limitation of open pond systems, enclosed photobioreactors (PBR) have evolved in the last 50 years. Two major types of enclosed PBR are tubular and plate types.

Due to enclosed structure and relative controllable environment, enclosed PBR can reach high cell density and easy to maintain monoculture (Lee 2001; Ugwu et al. 2008).

There is application of tubular photobioreactors in culturing microalgae: vertical (Babcock et al. 2002), horizontal (Richmond et al. 1993), and helical (Hall et al. 2003), also flat-plate photobioreactor is broadly in use due to narrow light path, which helps maintaining higher cell densities by more than an order of magnitude compared to other photobioreactors (Hu et al. 1996).

Flat-plate photobioreactors are suitable for mass cultures of algae due to low accumulation of dissolved oxygen and the high photosynthetic efficiency achieved when compared to tubular versions (Richmond 2000). Flat plate PBRs are generally more efficient at sunlight utilization than tubular PBRs because they have a wider surface area (Tredici and Zittelli 1998). In Flat-plate photobioreactors although there is a large illumination surface area but there are difficulties with scale-up and temperature control. Also small degree of hydrodynamic stress and some degree of wall growth are the limitations that were observed before (Brennan and Owende 2010). On the other hand, flat-plate photobioreactor is broadly in use due to narrow light path, which helps maintaining higher cell densities by more than an order of magnitude compared to other photobioreactors (Hu et al. 1996). The appropriate reactor design is required to obtain the maximal cell mass. Various designs of flat-plate photobioreactors to cultivate microalgae have been constructed: glass types (Qiang et al. 1998), thick transparent PVC materials (Ramos de Ortega and Roux 1986), V-shaped (Iqbal et al. 1993) and inclined (Hu et al. 1996).

The tubular array captures sunlight and can be aligned horizontally (Molina Grima et al. 2001), vertically (Sanchez Miron et al. 1999), inclined (Ugwu et al. 2002) or as a helix (Watanabe and Saiki 1997). Tubular photobioreactors have design limitations on length of the tubes, which is dependent on potential O₂ accumulation, CO₂ depletion, and pH variation in the systems (Eriksen 2008). The major difference between the configurations is that the vertical design allows greater mass transfer and a decrease in energy usage, while the horizontal reactor is more scaleable, but requires a large area of land (Ugwu et al. 2008).

Column photobioreactors offer the most efficient mixing, the highest volumetric mass transfer rates and the best controllable growth conditions. They are low-cost, compact and easy to operate. The vertical columns are aerated from the bottom, and illuminated through transparent walls (Eriksen 2008), or internally (Suh and Lee 2003). Their performance compares favorably with tubular photobioreactors (Sanchez Miron et al. 2002).

1.11 Comparative efficiency of batch and continuous mode

Batch mode cultivation has invariably been used by researchers for optimizing culture conditions, but, it has many disadvantages, such as low productivity and high harvesting costs (Fernandes et al. 2015). Moreover, the irradiance and nutrients become limited over time with an increase in the cell density (Tang et al. 2011). In contrast, continuous mode cultivation in a chemostat offers many advantages for accurately investigating the microalgal physiological characteristics under specific culture conditions (Cho et al. 2016). Furthermore, a high biomass concentration can be produced around an optimum cell density under stable conditions, which results in maximal biomass productivity (Richmond 2013). Moreover, continuous mode cultivation in a chemostat provides higher degree of control compared to batch cultivation, as the growth rate can be regulated for an extended time period and the biomass concentration controlled by varying the dilution rate (Mata et al. 2010).

1.12 High cell density and biomass productivity

‘High-cell-density culture’ (HCD) is generally applied to those values of biomass concentration that fall within the range of the highest values published for photoautotrophic or heterotrophic processes. For a photoautotrophic system, the highest biomass concentration achieved to date is 40 g L⁻¹ of dry cell weight (DCW) with thin-layer cultures with *Chlorella* sp. (Doucha and Lívanský 2006). In Table 1-4 there is a comparison between different cultivation systems according to cell densities and it seems that thickness is playing an effective role on cell density and it is obvious in thin layer photobioreactors cell density. The lower penetration depth could be one of the reasons which causes high cell densities in thin layer photobioreactors.

Table 1-4

Cultivation system, cell density and biomass productivity for *B. braunii* and some other strains in different studies.

Strain	Cultivation system	Cell density (g L ⁻¹)	Biomass productivity (g L ⁻¹ d ⁻¹)	References
<i>Anabaena</i> sp.	Open pond	0.23 ± 0.02	0.235 ± 0.037	Moreno et al. (2003)
<i>Spirulina platensis</i>	Open pond	1.6	0.32 ± 0.01	Pushparaj et al. (1997)
<i>Botryococcus braunii</i> TN101	Open pond	1.5**	0.194 ± 0.003	Ashokkumar et al. (2014)
<i>Haematococcus pluvialis</i>	Open pond	0.202	0.261*	Huntley and Redalje (2007)
<i>Haematococcus pluvialis</i>	Bubble column	1.4	0.55	García-Malea López et al. (2006)
<i>Haematococcus pluvialis</i>	Tublar	7	0.41*	García-Malea López et al. (2006)
<i>Chlorella</i> sp.	Thin-layer	10	–	Setlik et al. (1970)
<i>Chlorella</i> sp.	Thin-layer	40	3	Doucha and Lívanský (2006)
<i>Botryococcus braunii</i> 765	Airlift	2.31	–	Ge et al. (2011)
<i>Botryococcus braunii</i> SAG 30.81	–	2	–	Dayananda et al. (2007 a)
<i>Botryococcus braunii</i> LB-572	–	2.8	–	Dayananda et al. (2007 a)
<i>Botryococcus braunii</i> BOT-22	Test tubes	1.7 **	0.17 **	Tanabe et al. (2014)
<i>Botryococcus braunii</i> SAG 30.81	Airlift	1.115	0.223	Jin et al. (2016 a)
<i>Botryococcus braunii</i> 2441	Tublar	4.963±0.34	0.1733±0.168	Pérez-Mora et al. (2016)
<i>Botryococcus braunii</i> 2441	Tublar	3.857±0.192	0.2156±0.011	Pérez-Mora et al. (2016)
<i>Botryococcus braunii</i> 2441	Tublar	3.987±0.307	0.2233 ± 0.018	Pérez-Mora et al. (2016)
<i>Botryococcus braunii</i> 2441	Tublar	3.254±0.15	0.1816 ± 0.021	Pérez-Mora et al. (2016)
<i>Botryococcus braunii</i> AP103	Open pond	1.7 ± 0.12	0.114	Ashokkumar and Rengasami (2012)
<i>Botryococcus braunii</i> BOT-22 (nitrogen depletion)	polycarbonate bottles	2.86	–	Shimamura et al. (2012)
<i>Botryococcus braunii</i> BOT-22 (nitrogen sufficient)	polycarbonate bottles	1.06	–	Shimamura et al. (2012)
<i>Botryococcus braunii</i> Showa	Test tubes	3.3	1.65*	Yoshimura et al. (2013)
<i>Botryococcus braunii</i> KMILT 2	flasks	1.91±0.24	–	Ruangsomboon (2012)
<i>Botryococcus braunii</i> IPE 001	Airlift	2.87	–	Xu et al. (2012 b)
<i>Botryococcus braunii</i> Yayoi	flasks	1.9	–	Okada et al. (1997)
<i>Botryococcus braunii</i>	CSTR	8.57	–	Ramaraj et al. (2016)
<i>Botryococcus braunii</i> Gottingen 807/1	Airlift	5.45	–	Casadevall et al. (1985)

*calculated from published data / **calculated from published graph

1.13 Hydrocarbon content

B. braunii forms colonies by embedding individual cells into the biopolymers called extracellular matrix and a large part of hydrocarbons is accumulated in the matrix (Berkaloff et al. 1984; Largeau et al. 1980; Metzger et al. 1987). Under microscopy observation, the size of the colonies varies between 90 to 340 μm (Jin et al. 2016 b), depending on the culture conditions. The colonies organization of *B. braunii* exhibits a botryoid form containing 50 to 100 individual pyriform-shaped cells tightened together into smaller cluster and enclosed in a polymerized hydrocarbon extracellular matrix (h-ECM) (Weiss et al. 2012). Each cell contains intracellular lipid bodies associated with the chloroplast and endoplasmic reticulum (ER) which forms a continuous subcortical system directly linked to the cell membrane (Weiss et al. 2012). The bulk of *B. braunii* hydrocarbons are stored in outer walls (Largeau et al. 1980). Only a few amounts of liquid hydrocarbons are released out of the colony, in the *B. braunii* culture medium (in the range of 1 % of the total hydrocarbons produced) (Griehl et al. 2014). Wolf et al. (1985 a), estimated that only about 7 % of the botryococenes are intracellular, with the majority of these hydrocarbons forming the extracellular colonial matrix. Likewise, Largeau et al. (1980) reported that 95% of the botryococenes are located in the extracellular pool of hydrocarbons. These observations raise the question of the mechanism by which such substantial amounts of long-chain hydrocarbons, synthesized and segregated in the form of globules intracellularly, are eventually excreted into the extracellular space.

As mentioned in previous studies, *B. braunii* BOT-22 is producing $\text{C}_{34}\text{H}_{58}$ with 466 molecular weight (Kawachi et al. 2012).

The size and the number of lipid bodies vary during the cell life cycle and the hydrocarbons production seems to be growth associated (Suzuki et al. 2013). So, the highest content and productivity of lipids and hydrocarbons are closely linked to the optimal growth conditions (Kawachi et al. 2012).

Many cultivation parameters including light intensity and quality, photoperiod, nutrient availability, temperature, salinity, pH, CO_2 supplied, dilution rate, and presence of contaminants can affect biomass and lipids/hydrocarbons content and productivity of *B. braunii* (Jin et al. 2016 a; Talukdar et al. 2014; Watanabe and Tanabe 2013).

The advantage of *B. braunii* race B is that its hydrocarbon can be directly hydrocracked into shorter chains to acquire a distillate fraction containing 67 % gasoline, 15 % kerosene, 15 % diesel fuel, and 3 % residual oil, with interesting physical and calorific properties (Eroglu et al. 2011; Jin et al. 2016 a; Watanabe et al. 2015). In fact, the heating value of *B. braunii*

hydrocarbon is in the range of 32.9–54.7 MJ kg⁻¹, about two times higher in comparison to other microalgae (like *Chlorella* sp., *Nannochloropsis*, *Spirulina* sp.) (Jin et al. 2016 b; Moheimani et al. 2014; Watanabe et al. 2015). Furthermore, this high heating value is almost similar to that of fossil oil (42 MJ kg⁻¹) (Moheimani et al. 2014). Figure 1-4 demonstrates the main biosynthetic pathway of hydrocarbon of race B (Watanabe and Tanabe 2013).

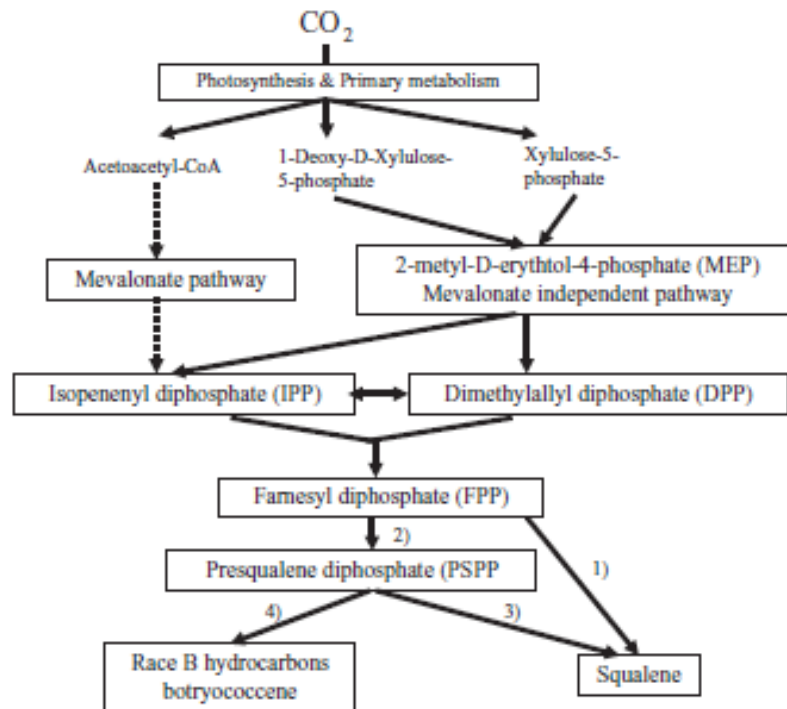


Figure 1-4: Main biosynthetic pathway of hydrocarbon of race B. 1) squalene synthase gene, BBS; 2) squalene synthase-like gene, SSL-1; 3) squalene synthase-like gene, SSL-2; 4) squalene synthase-like gene SSL-3 (Watanabe and Tanabe 2013).

In the Table 1-5 some hydrocarbon contents of different species of *B. braunii* is mentioned.

Table 1-5
Hydrocarbon contents (%) and hydrocarbon culture concentration of identified *B. braunii* specious.

Strain	Race	Hydrocarbon content (%)	Hydrocarbon concentration (mg L ⁻¹)	References
Showa	B	39.2	1293.6*	Yoshimura et al. (2013)
Showa	B	24-29	250*	Wolf et al. (1985 a)
Showa	B	37.9	N d	Okada et al. (1995)
IPE 001	B	64.3	1150.97*	Xu et al. (2012 b)
Yayoi	B	40.5	769.5*	Okada et al. (1997)
FACHB 357	B	34.3	–	Cheng et al. (2013)
BOT-22 (nitrogen depletion)	B	44.9	475.9*	Shimamura et al. (2012)
BOT-22 (nitrogen sufficient)	B	40.6	1161.16*	Shimamura et al. (2012)
Yamanaka	A	16.1	N d	Okada et al. (1995)
Gottingen 807/1	A	23.3	1269.8*	Casadevall et al. (1985)
Gottingen 807/1	A	44.2	959*	Casadevall et al. (1985)
LB 572	A	28	504**	Ranga Rao et al. (2007 b)
LB 572	A	33	924*	Dayananda et al. (2007 a)
SAG 30.81	A	46	920*	Dayananda et al. (2007 a)
SAG 30.81	A	5.7	62.5*	Jin et al. (2016 a)
TN101	No data	22.6	399*	Ashokkumar et al. (2014)
AP103	No data	13 ± 0.62	221*	Ashokkumar and Rengasami (2012)
CFTRI-Bb1	No data	13-18	129*	Dayananda et al. (2007 b)
<i>Botryococcus braunii</i>	No data	35.32	3026.9*	Ramaraj et al. (2016)
765	No data	24.45	564.8*	Ge et al. (2011)

*calculated from published data / **calculated from published graph

Table 1-6

Major hydrocarbons detected from isolated strains of *B. braunii* is shown on the table (Kawachi et al. 2012).

Molecular formula of major hydrocarbons with molecular weight	Race	Strains
C ₃₁ H ₅₈ (430)	A	Bot88-2
C ₃₃ H ₆₄ (460)	A	Bot45, 97-2
C ₃₂ H ₅₄ (438)	B	Bot25
C ₃₃ H ₅₆ (452)	B	Bot23, 34, 38, 61, 72
C ₃₄ H ₅₈ (466)	B	Bot12, 22, 24, 26, 27, 28, 30-1, 30-2, 60, 70, 76, 81, 90
C ₄₀ H ₇₈ (558)	L	Bot80, 84
C ₄₀ H ₇₆ (556)	L	Bot52
C ₄₁ H ₈₄ (576)		
C ₁₈ H ₃₆ O (268)	S	Bot16, 20, 21, 36, 39
C ₂₀ H ₄₂ (282)	S	Bot15

As it shown on the Table 1-6 *Botryococcus braunii* BOT-22 is producing C₃₄H₅₈.

1.14 Fatty acids

Numerous studies with microalgae of various classes suggest that the cellular content of lipids is proportional to light intensity, that is, the higher the light intensity, the greater the total lipid content in the cells. However, polyunsaturated fatty acids (PUFAs), including eicosapentaenoic acid (EPA, 20:5 ω 3), are inversely related to light intensity (Hu 2013). Sukenik et al. (1989) reported that *Nannochloropsis* cells were characterized by low lipid contents and high proportions of EPA under light-limiting conditions, whereas 16:0 and 16:1 species, predominate as light intensity increased to or above saturated level. These saturated and monounsaturated fatty acids are present mainly in a form of triacylglycerol stored in cytosolic lipid bodies (Hu et al. 2008). Since PUFAs are the major constituents of the thylakoid membranes, low light increases thylakoid membranes and thus the PUFA content to augment photosynthesis (Burner et al. 1989; Catarina et al. 2010). There are some exceptions. High light intensity was observed to increase the PUFA level in the diatom *Phaeodactylum tricornutum* (Molina Grima et al. 1999) and the green microalga *Parietochloris incisa* (Solovchenko et al. 2008). In *Parietochloris* cells, PUFAs were accumulated mainly in triacylglycerol stored in cytosolic lipid bodies (Khozin-Goldberg et al. 2002).

The highest fatty acid content occurred in low-density (exponentially growing) cultures, which received light above the saturating light intensity. The increased fatty acid content corresponded to increases in the proportion of palmitic and palmitoleic acids (Wagenen et al. 2012).

Sukenik 1993 demonstrated, the C16 fatty acids are the main components of triacylglycerols (TAGs) of *Nannochloropsis* sp. and TAGs are known to increase and become richer in C16 fatty acids with high light.

Wang et al. (2014) reported for *Botryococcus braunii*, fatty acids with 16 and 18 carbon atoms, were the major components and account for more than 97 % of the total fatty acid content. In addition, there were nine detectable fatty acids with stearic acid (18:0), oleic acid (18:1), and linolenic acid (18:3) as the most abundant components. Nearly half of the fatty acids were polyunsaturated fatty acids (PUFAs).

Fatty acids with 16 and 18 carbon atoms are ideal components for biodiesel (Xu et al. 2006).

For *B. braunii* race A strain, a percentage of free fatty acids of 0.6 % on a dry cell weight basis was achieved (according to data of Yamaguchi et al. 1987). For *B. braunii* race A, Samorì et al. 2010 reported that oleic, palmitic, linoleic and stearic acids are the main fatty acids. Ranga Rao et al. (2007 a) reported the fatty acid profile for *Botryococcus braunii* race A indicated the presence of C16:0, C16:1, C18:0, C18:1, C18:2, C22:0, C22:1 and C24:0 fatty acids. Also they mentioned stearic and linoleic acids were in higher proportion in modified Chu 13 medium while palmitoleic and oleic acids were the major fatty acids in 34mM and 85mM salinity which were added to modified Chu 13 medium.

Ashokkumar and Rengasamy (2012) reported oleic (25.7 %), linolenic (34.26 %) and palmitic (9.42 %) acids were the major fatty acids present in the lipids extracted from *Botryococcus braunii* AP103 while the fatty acid composition of the isolate AP103 revealed the presence of lauric, myristic, palmitic, stearic, oleic, linolenic, and arachidic acid. Dayananda et al. (2007 a) reported that the fat content of the *Botryococcus braunii* was found to be 22 % (w/w) while palmitic and oleic acids as the major fatty acids constituting 40.6% and 22.3 %, respectively. Also Laureillard et al. (1988) reported that oleic acid could involve in the formation of very long chain fatty acid derivatives through chain elongation. For *B. braunii* FACHB 357 which is a B race, under sufficient nitrogen it was reported by Cheng et al. (2013) that oleic acid (C18:1, 52.25 %), linolenic acid (C18:3, 15.81 %) and palmitic (C16:0, 11.32 %) were the main fatty acids. Also they reported the nitrogen concentration in culture medium significantly affected the content of oleic acid (18:1) and linolenic acid (C18:3). Under nitrogen deficient condition, the content for oleic acid (18:1) increased and linolenic acid (18:3) decreased. Kalacheva et al. (2000) reported that *Botryococcus* contained more than 12 % free fatty acids (FFA) dominated by C16: 0 (60–80 % of the total FFA) and C18: 0 (5–15 % of the total FFA) acids.

This study aimed at questioning whether the production and accumulation of hydrocarbon in or out of *Botryococcus braunii* colonies could be impacted by

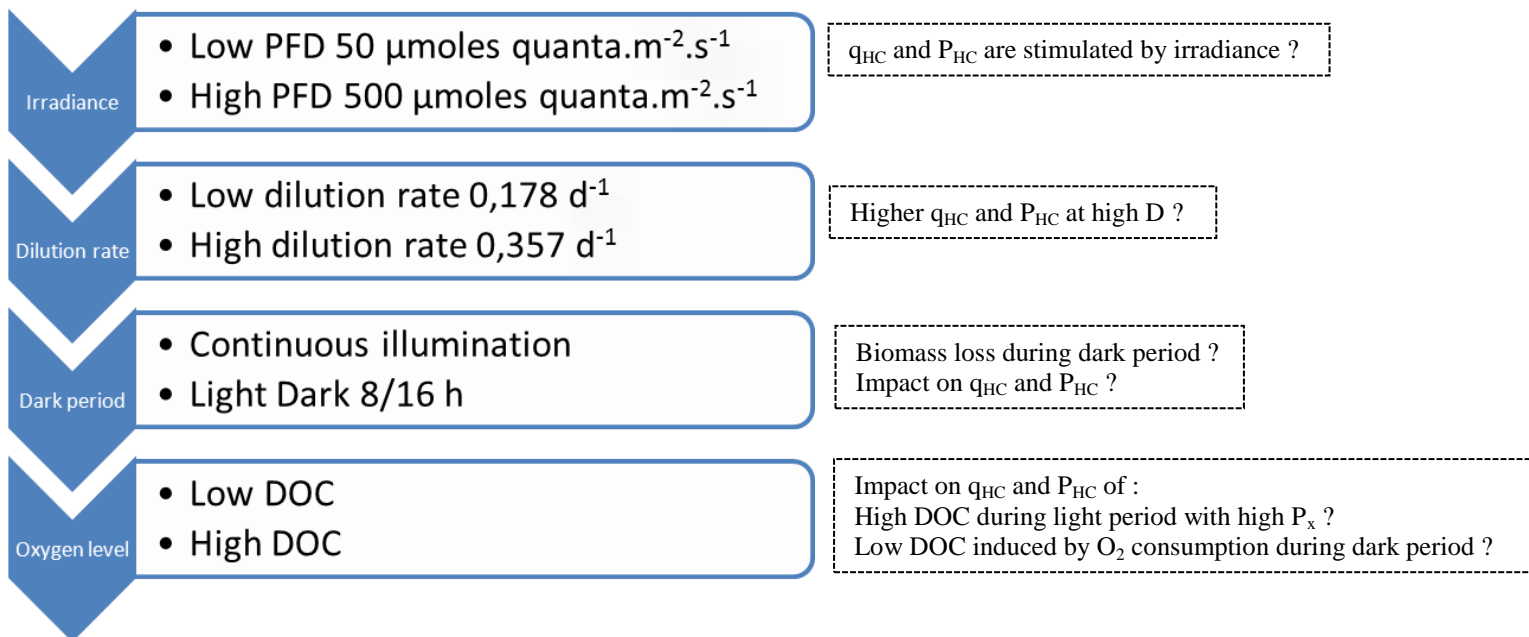
- the photon flux density
- the dilution rate
- the level of dissolved oxygen in the culture medium
- a light/dark transition

not only during the steady state phase but also during the transient phase.

According to the previous specific light supply on the photobioreactor.

PARAMETERS

WORKING HYPOTHESIS



Chapter 2: Material and methods

Chapter 2: Material and methods

2.1 Biological material

B. braunii race B strain BOT-22 was provided by the team of the Pr M.M. Watanabe from Tsukuba University, Japan (Figure 2-1). This strain is mainly known to produce the botryococcene $C_{34}H_{58}$. It was sub-cultured on buffered AF-6 in 300 mL column. The subcultures were regularly checked for absence of bacteria and fungi by control on Plate Count Agar (Fluka).

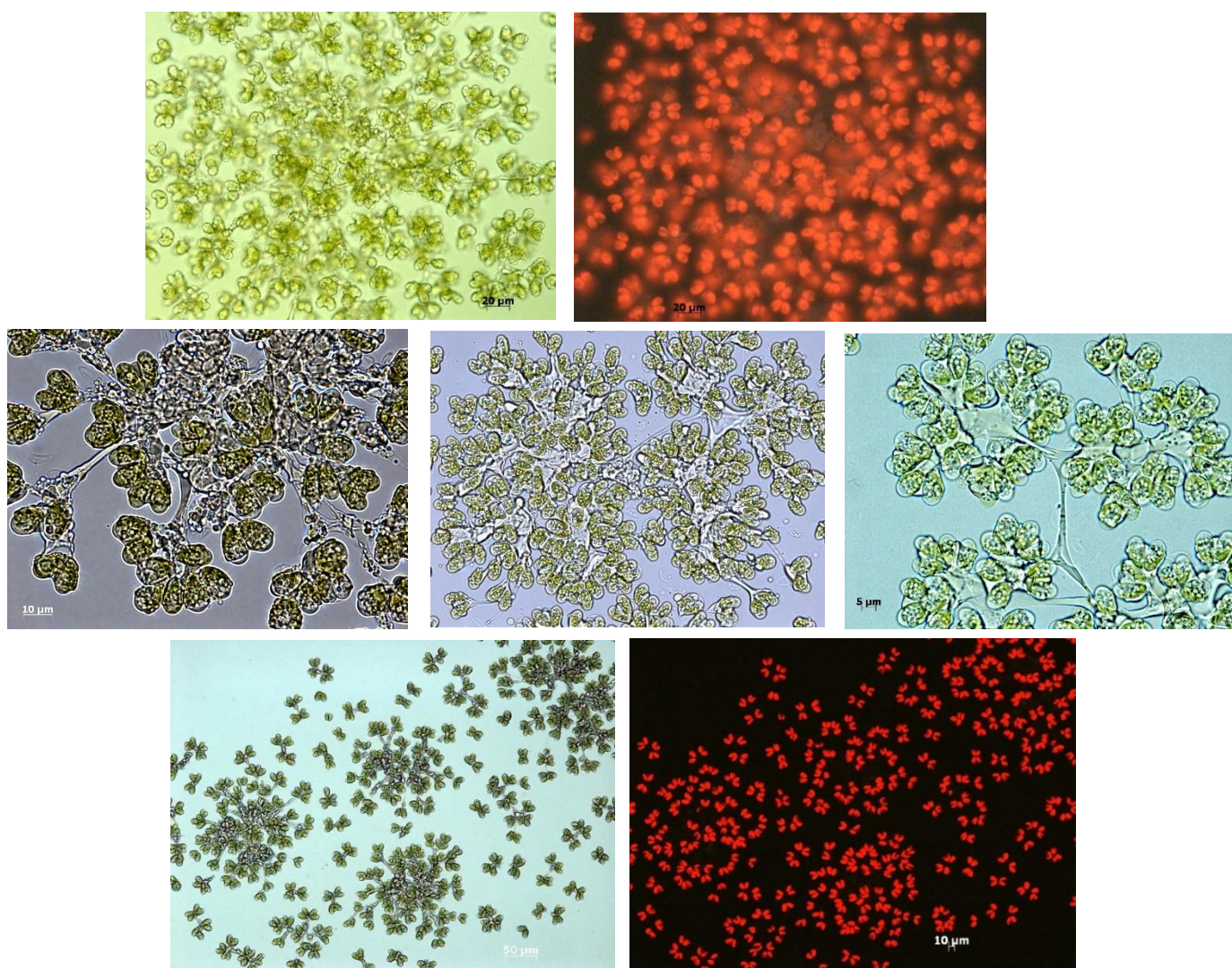


Figure 2-1: *B. braunii* race B strain BOT-22.

2.2 Strain and culture medium

The AF-6 medium buffered with 2-(N-morpholino) ethanesulfonic acid (MES, 2 mmol L^{-1}) at pH 6.5 was used for batch cultivations. The final concentration of AF-6 medium contains

NaNO₃ 140 mg L⁻¹, NH₄NO₃ 22 mg L⁻¹, MgSO₄·7H₂O 30 mg L⁻¹, KH₂PO₄ 10 mg L⁻¹, K₂HPO₄ 5 mg L⁻¹, CaCl₂·2H₂O 10 mg L⁻¹, FeCl₃·6H₂O 1 mg L⁻¹, Fe-citrate 2 mg L⁻¹, citric acid 2 mg L⁻¹, Na₂EDTA·2H₂O 8 mg L⁻¹, microelements (MnCl₂·4H₂O 200 µg L⁻¹, ZnSO₄·7H₂O 40 µg L⁻¹, CoCl₂·6H₂O 8 µg L⁻¹, Na₂MoO₄·2H₂O 20 µg L⁻¹, NH₄VO₃ 1 µg L⁻¹, H₂SeO₃ 5µg L⁻¹) and Vitamins (biotin 2 µg L⁻¹, thiamine HCl 10 µg L⁻¹, vitamin B₆ 0.1µg L⁻¹, vitamin B₁₂ 1µg L⁻¹). pH was adjusted to 6.6 by using KOH before steam sterilization (121°C, 20 min).

A modified culture medium was used for the continuous cultures. Indeed a 6 times sodium nitrate and 6 times phosphate concentrations enriched medium (6N 6P-AF-6) was used in order to avoid nutrient limitation for biomass production, taking into account the early results obtained by Jin et al. (2016 a). The feeding medium for continuous cultures was devoided of the MES pH buffer, as pH was automatically controlled by the PBR system. The final concentrations of this mineral medium is presented in Table 2-1.

Table 2-1
Final concentrations of modified AF6 mineral medium.

Elements	concentration
NaNO ₃	840 mg L ⁻¹
NH ₄ NO ₃	22 mg L ⁻¹
MgSO ₄ ·7H ₂ O	30 mg L ⁻¹
KH ₂ PO ₄	60 mg L ⁻¹
K ₂ HPO ₄	30 mg L ⁻¹
CaCl ₂ ·2H ₂ O	10 mg L ⁻¹
FeCl ₃ ·6H ₂ O	1 mg L ⁻¹
Fe-citrate	2 mg L ⁻¹
citric acid	2 mg L ⁻¹
Na ₂ EDTA·2H ₂ O	8 mg L ⁻¹
MnCl ₂ ·4H ₂ O	200 µg L ⁻¹
ZnSO ₄ ·7H ₂ O	40 µg L ⁻¹
CoCl ₂ ·6H ₂ O	8 µg L ⁻¹
Na ₂ MoO ₄ ·2H ₂ O	20 µg L ⁻¹
NH ₄ VO ₃	1 µg L ⁻¹
H ₂ SeO ₃	5µg L ⁻¹
biotin	2 µg L ⁻¹
thiamine HCl	10 µg L ⁻¹
vitamin B ₆	0.1µg L ⁻¹
vitamin B ₁₂	1µg L ⁻¹

2.3 Methods of culture

2.3.1 Batch cultures

Batch culture experiments were conducted in 300 mL bubble columns. Aeration was provided by injecting 0.2 µm-filtered air at the bottom of the columns at a rate of 0.1 vvm (volume per volume per minute). Batch cultures were maintained at 22 ± 2 °C. A continuous illumination was provided on the surface of the cultures at a photon flux density (PFD) of $150 \mu\text{mol photons m}^{-2} \text{ s}^{-1}$, corresponding to photosynthetically active radiations (PAR), by cool-white fluorescent lamps (Philips, Master TLD 18W). Measurements were performed at the surface of the columns using a Li-Cor light meter (LI-250A).

2.3.2 Continuous culture

Two identical flat-panel photobioreactors (PBR) with a beveled shape (Figure 2-2, Figure 2-3), were designed for preventing sedimentation. The optical surface was the front of the PBR which made of transparent material (polycarbonate), the rest being made of stainless steel (type 316 L). The working volume (V) was 0.269 L with light incident area (A) of 134.5 cm^2 and then A/V ratio of 50 m^{-1} .

A light-emitting diode (LED) panel composed of white light LEDs was used to provide controlled photon flux density the PBR from the front. Photosynthetically active radiations (PAR; 400–700 nm) were provided on the PBR surface by light-emitting diodes (LEDs) panels. The PAR were measured using a plane cosine quantum sensor Li-Cor light meter (LI-250A). The mean value was the average of measurements made at 5 different locations on the reactor front. The soft allowed to program light/dark alternance.

To take into account the effect of biomass concentration and for full light absorption, the specific light supply rate was calculated according to the relation:

$$r_{\text{EX}} = \text{specific light supply rate} = \frac{\text{PFD}}{X}. (\text{mol photon g X}^{-1} \text{ d}^{-1})$$

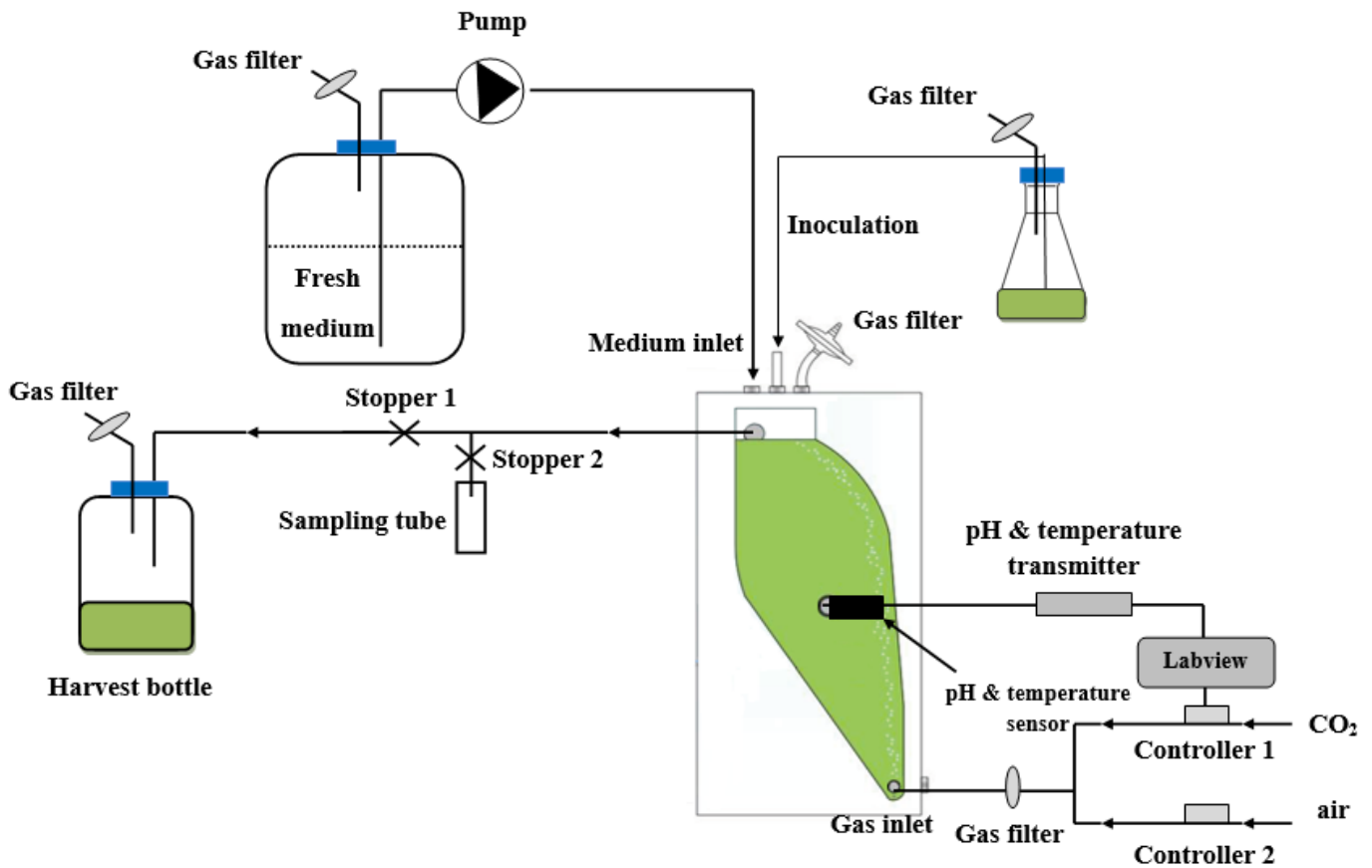


Figure 2-2: Experimental setup of the continuous culture of *Botryococcus braunii*; 269 mL flat-vertical photobioreactor designed to maximize the hydrodynamic conditions and, then, to prevent cell sedimentation; computer-controlled pH, temperature, inlet air and CO₂ flows, were computer-controlled through sensors and gas-flowmeters; culture overflow for collecting samples or accumulating biomass in a harvest tank.

System description: At sampling, stopper 1 is open and stopper 2 is closed. At other times, stopper 1 is closed and stopper 2 is open. Sampling tube and harvest bottle were autoclaved (121 °C, 25 min) before being connected. Controller 1 (CO₂ flow controller) will be open when the pH value detected online is higher than the set point pH value, or closed when the pH value is lower than set point pH. Controller 2 (airflow controller) is open all the time at a constant airflow rate (60 mL min⁻¹), with culture pH controlled at the set point pH 6.6 ± 0.2 pH unit.

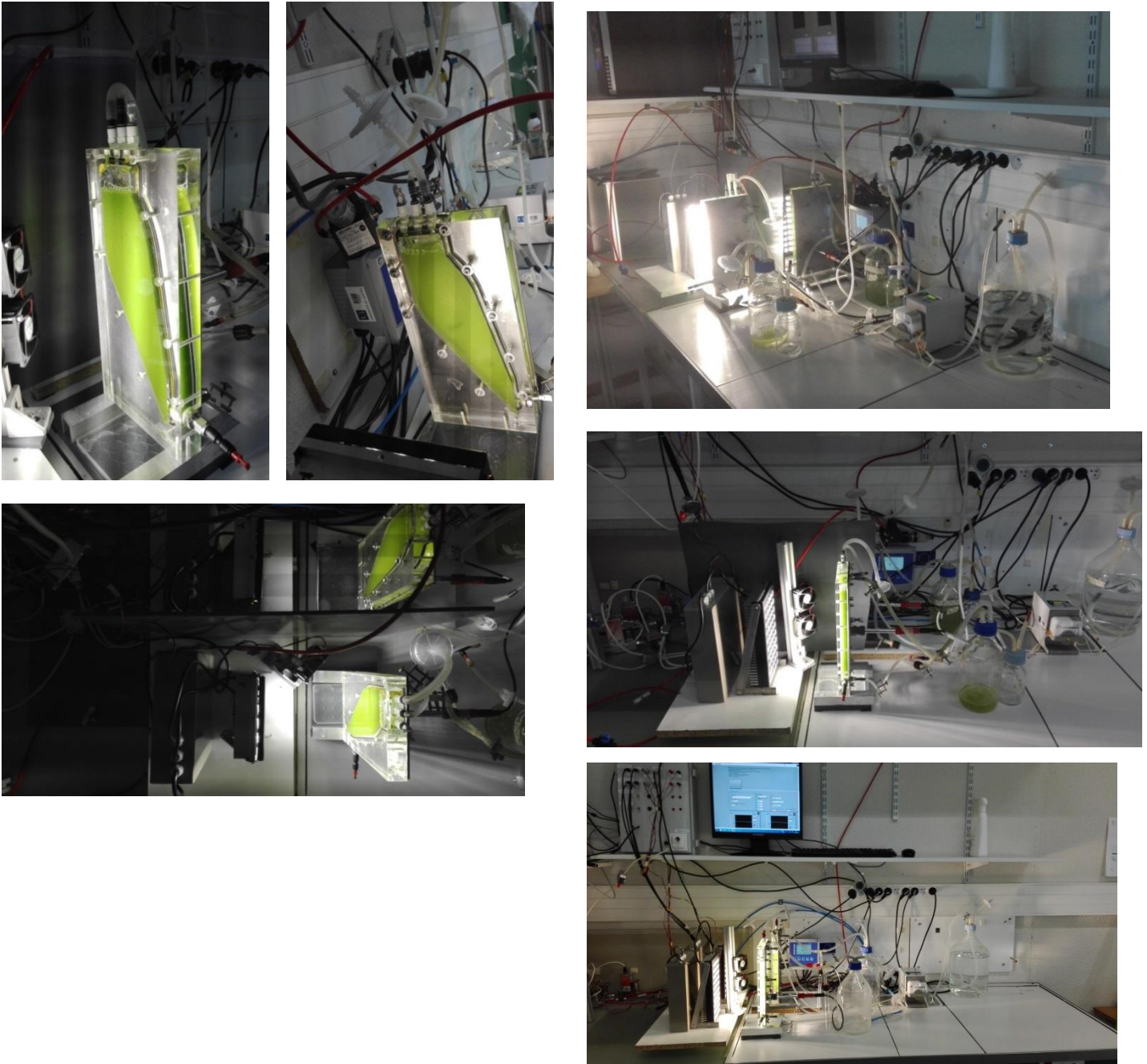


Figure 2-3: Pictures of the two PBRs system.

The photobioreactor was illuminated at two photons flux densities, 50 and 500 $\mu\text{mol photon m}^{-2} \text{ s}^{-1}$, in the 400–700 nm wavebands. The continuous cultures were fed with 6P-6N-AF6 medium at flow rates of (F) of 0.048 or 0.096 L d^{-1} , corresponding to a dilution rate $D=F/V$ of 0.178 d^{-1} or 0.357 d^{-1} .

The PBR was sterilized by a peracetic acid treatment 0.5 % for 2 hours, followed by rinsing with sterilized distilled water before inoculation.

Temperature was controlled at $22 \pm 2 \text{ }^\circ\text{C}$. Gas flow rate was 60 mL min^{-1} corresponding to an aeration rate of 0.223 vvm. The pH was regulated at 6.6 through an automatic CO_2 injection (pH-controller Mettler Toledo M200) for set values with the flow rate of 3 mL min^{-1} .

The setup for continuous cultures included a sampling tube and harvest bottle autoclaved ($121 \text{ }^\circ\text{C}$, 25 min) before connection to the PBR. The fresh medium was injected using a peristaltic pump (ISMATEC pump, ISM 597 D), and harvesting was by overflowing into a flask by gas pressure, by this way the reactor volume was kept constant and there was no more problem of clogging of the event filters. Dilution rate (D, d^{-1}) was calculated by the relation:

$$D = \frac{F}{V}$$

Where, F is the flow rate (L d^{-1}). In continuous culture, the biomass concentration in photobioreactor, the specific growth rate (μ) of microalga and the dilution rate are related to the equation as flows:

$$\frac{dX}{dt} = \mu \cdot X - D \cdot X$$

Then, at steady state,

$$\mu = D$$

Curve of the gas hold up of the PBR

In all of experiments the rate of aeration was 60 mL min^{-1} and at this point the ϵ is equal to 0.0025 which is very negligible (Figure 2-4).

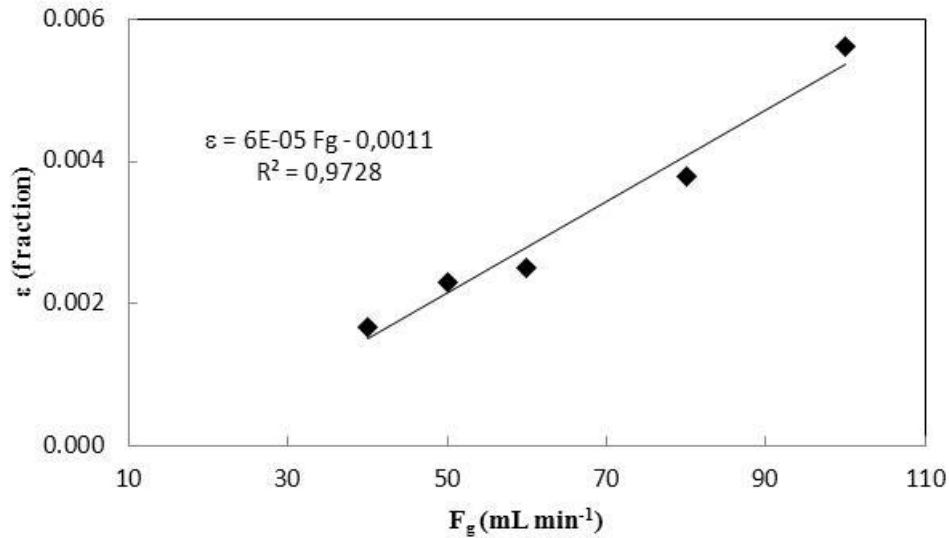


Figure 2-4: Curve of the gas hold up of the PBR.

2.4 Analytical methods

2.4.1 Direct and indirect biomass determinations

2.4.1.1. Biomass related determinations

Biomass concentration (X , g L⁻¹ or g m⁻²) was determined by dry cell weight (DCW) measurement (Ruangsomboon 2012; Sarrafzadeh et al. 2015). A sample volume was filtered over pre-weighed glass fiber filters (Whatman GF/F) (M1) and washed with distilled water. The dry cell weight was calculated from the weight of the filters dried at 105 °C for 24 h, cooled down in a desiccator and weighted to give M2. These values were correlated to optical density measurements at 750 nm (Spectrophotometer, Perkin Elmer Lambda 2S). The dry weight was calculated as:

$$\frac{(M2-M1)}{V} \text{ g.L}^{-1} \text{ DCW} \quad (\text{with } M1 \text{ and } M2 \text{ in mg and } V \text{ in mL})$$

The relation between cell density (OD₇₅₀) and dry cell weight was plotted, as shown in Fig. One unit of absorbance is equal to 1.4121 g.L⁻¹ DCW (Figure 2-5).

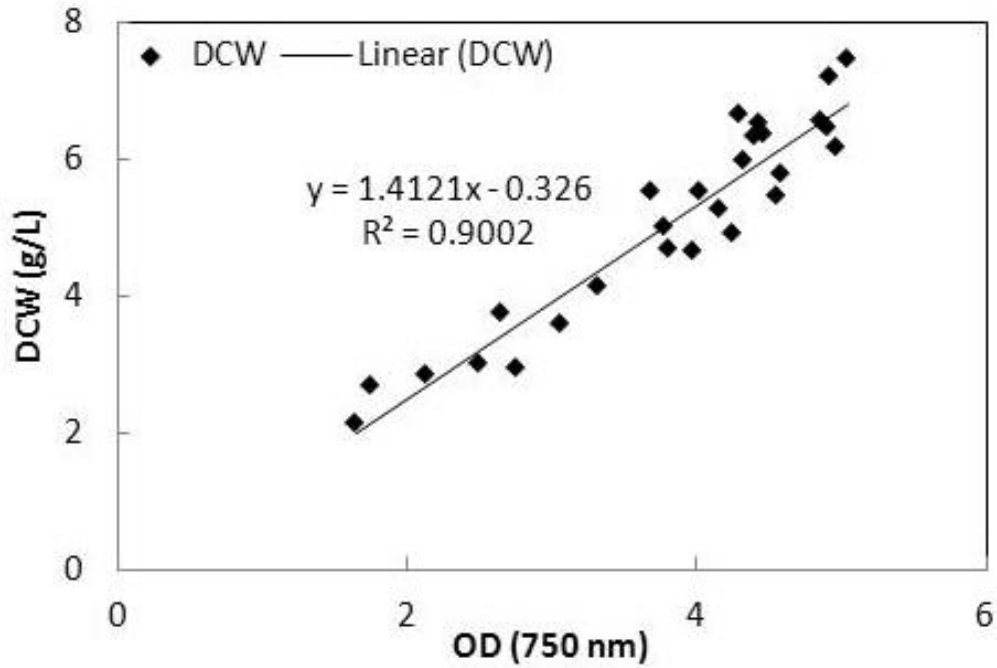


Figure 2-5: Graph of the (OD_{750}) and dry cell weight (DCW).

2.4.2 Calculation of biomass productivity and biomass yield

The biomass productivity P_x ($g L^{-1} d^{-1}$ or $g m^{-2} d^{-1}$) was calculated as:

$$P_x = D \cdot X, (g L^{-1} d^{-1} \text{ or } g m^{-2} d^{-1})$$

The apparent biomass yield on light supply Y_x ($g \text{ mol photons}^{-1}$) was calculated according to Zijffers et al. (2010) as:

$$Y_{xEobs} = \frac{X \times D \times a}{PFD \times 24 \times 3600 \times 10^{-6}} (g \text{ mol photons}^{-1})$$

This yield was not corrected for unused photons passing through the panel photobioreactor (Zijffers et al. 2010). The study addressed corrections are considered necessary only at low biomass concentrations.

2.4.3 Determination of pigments concentrations

Cells harvested by filtration through glass fiber filters (Whatman GF/F) were suspended in 2 mL methanol-water solution (90 % v/v). The extraction was done by sonication and vortexing (18000 rpm), followed by a dark incubation during 2 h. The supernatant was clarified by centrifugation (12100 g, 10 min) and the optical densities were read at 470 nm, 652.4 nm, 665.2 nm and 750 nm (Perkin Elmer Lambda 2S spectrophotometer). Then the chlorophylls (Chl, including chlorophyll *a*, Chl *a* and chlorophyll *b*, Chl *b*) and carotenoids (Car) concentrations were determined according to the next spectrophotometric equations adapted from Lichtenthaler and Buschmann (2001) :

$$\text{Chl } a = (OD_{665.2nm} - OD_{750nm}) \cdot 16.82 - (OD_{652.4nm} - OD_{750nm}) \cdot 9.28, (\text{mg L}^{-1})$$

$$\text{Chl } b = (OD_{652.4nm} - OD_{750nm}) \cdot 36.92 - (OD_{665.2nm} - OD_{750nm}) \cdot 16.54, (\text{mg L}^{-1})$$

$$\text{Car} = \frac{1000 \cdot (OD_{470nm} - OD_{750nm}) - 1.91 \cdot \text{Chl } a - 95.15 \cdot \text{Chl } b}{225}, (\text{mg L}^{-1})$$

The total chlorophyll content ([Chl]_x, % DCW) and Car content ([Car]_x, % DCW) were calculated as the following relations:

$$[\text{Chl}]_x = \frac{\text{Chl } a + \text{Chl } b}{x} \cdot 100\%, (\% \text{ DCW})$$

$$[\text{Car}]_x = \frac{\text{Car}}{x} \cdot 100\%, (\% \text{ DCW})$$

2.4.4 Chromatographic analysis of carotenoids

Sampling extraction saponification HPLC DAD standards

2.4.5 Measurements of photosynthetic activities

A Water-PAM (Walz GmbH, Germany) was used to measure *in vivo* chlorophyll fluorescence of photosystem II (PSII). Samples from continuous cultures were dark adapted for 20 min for F_0 determination.

A saturating pulse (800 ms; irradiance of about 2400 $\mu\text{mol photon m}^{-2} \text{ s}^{-1}$) was applied for F_m measurement. The photochemical efficiency (F_v/F_m), calculated by the software Wincontrol

(Walz GmbH). The Fv/Fm is an indicator of the physiological state of the cells, as it represents the level of the PSII activity (Figure 2-6).

For photosynthesis-irradiance (P/I) curve determinations, samples of microalgal cells were exposed to eight incremental levels of irradiance (0, 75, 109, 165, 245, 346, 479, 773 and 1127 $\mu\text{mol photon m}^{-2} \text{s}^{-1}$). To obtain a relative high ETR_{max} value, the duration of light adaptation of each step was 3 mins (Cosgrove and Borowitzka 2006). The WinControl-3 gave access to the Light Curves (LC), i.e. the Photosynthesis/Irradiance (P/I) curves as the electron transport rates (ETR) vs photosynthetic active radiations (PAR) values were fitted according to the Platt's equation:

$$\text{ETR} = \text{PAR} \cdot \text{Factor}_{\text{ETR}} \cdot \frac{P_{\text{PS2}}}{P_{\text{PPS}}} \cdot Y(\text{II})$$

$$Y(\text{II}) = \frac{F_{m'} - F_0}{F_{m'}}$$

Where:

- PAR photon flux density of photosynthetic active radiations ($\mu\text{mol photon m}^{-2} \text{s}^{-1}$).
- Values of $\text{Factor}_{\text{ETR}}$ and $\frac{P_{\text{PS2}}}{P_{\text{PPS}}}$ are 0.84 and 0.5, respectively.
- $F_{m'}$; maximum fluorescence level of illuminated sample as induced by saturating pulses which temporarily close all PS II reactions centers.
- F_0 ; Minimum fluorescence level excited by very low intensity of measuring light to keep PS II reaction centers open.

The light curve was fit as Platt's equation (1980), i.e.:

$$\text{ETR} = \text{ETR}_{\text{mPot}} \cdot \left(1 - e^{-\frac{\alpha \cdot \text{PAR}}{\text{ETR}_{\text{mPot}}}}\right) \cdot e^{-\frac{\beta \cdot \text{PAR}}{\text{ETR}_{\text{mPot}}}}$$

Where α is initial slope of LC which is related to quantum efficiency of photosynthesis (electrons/photon) and β is photo-inhibition parameter.

The values of α , β and ETR_{mPot} are estimated by the fitting procedure.

The maximum electron transport rate (ETR_{max} , $\mu\text{mol electrons m}^{-2} \text{s}^{-1}$) is determined by the following equation:

$$\text{ETR}_{\text{max}} = \text{ETR}_{\text{mPot}} \cdot \left(\frac{\alpha}{\alpha + \beta}\right) \cdot \left(\frac{\beta}{\alpha + \beta}\right)^{\frac{\beta}{\alpha}}$$

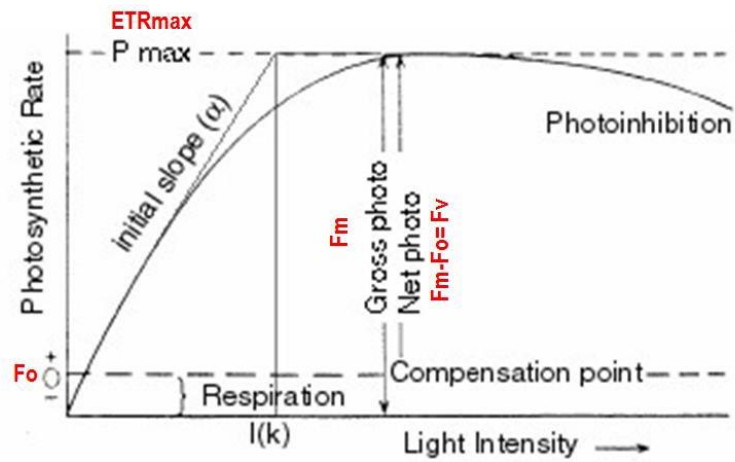


Figure 2-6: Light response curve (P/I).

2.4.6 Dissolved inorganic carbon determination

Dissolved inorganic carbon (DIC) was determined using a TOC Analyzer (Shimadzu TOC-5000A). NaHCO_3 and Na_2CO_3 were used as the standard for the calibration (Figure 2-7). Samples of the cultures were immediately centrifuged (12100 g, 10°C, 10 min) or filtered through glass fiber filters (Whatman GF/F) to separate the cells from culture medium. The last supernatant was injected into the TOC analyzer. Total DIC value was determined by its reaction with 25% phosphoric acid to transform all the inorganic carbon forms present (CO_2 , H_2CO_3 , HCO_3^- and CO_3^{2-}) into gaseous CO_2 . Then, CO_2 was quantified by an infrared analyzer.

Calibration curve of the DIC concentration measurement

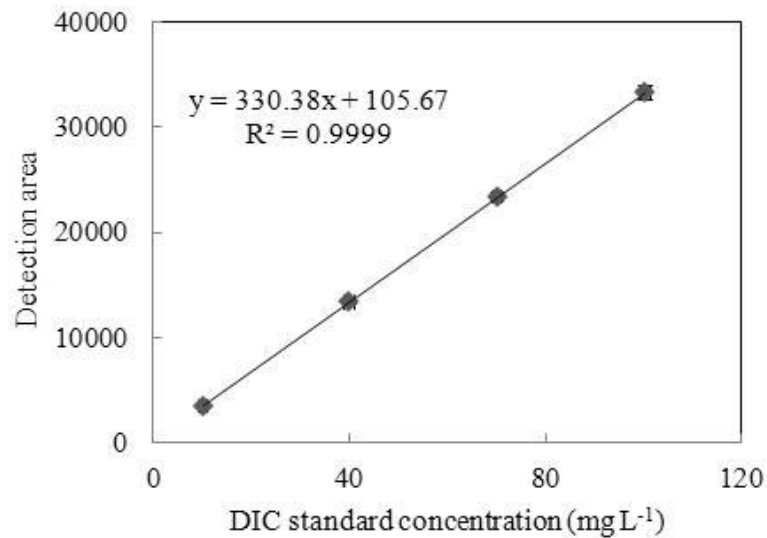


Figure 2-7: Calibration curve of the dissolved inorganic carbon concentration measurement.

From the DIC and the pH values at each steady state with the equations derived from the following reactions, the relative concentrations of all DIC species, dissolved $\text{CO}_{2(\text{aq})}$, H_2CO_3 , HCO_3^- , and CO_3^{2-} in the culture, were calculated:

$$[\text{DIC}] = [\text{CO}_{2(\text{aq})}] + [\text{H}_2\text{CO}_3] + [\text{HCO}_3^-] + [\text{CO}_3^{2-}]$$

2.4.7 Ionic composition of the culture medium

The microalgae were cultivated under photoautotrophic conditions. The changes in the concentration of the major mineral nutrients were followed by ionic chromatography. Nitrogen (N- NO_3^-) and phosphorus (P- PO_4^{3-}) concentrations were determined using an ionic chromatograph (Dionex-ICS 900-IonPac) equipped with a guard column (AG9-HC) and a separation column (AS9HC) and an external AMMS (Anion-ICE MicroMembrane Suppressor 300, Dionex) supplied with sulfuric acid (H_2SO_4 , 25 mmol L⁻¹, 1.8 mL min⁻¹). Detection and quantitation were done thanks to conductimetry detection and data processing with the software program Chromeleon (Dionex). Calibrations were done using ions as standard.

2.4.8 Total lipids extract and hydrocarbon purification

The first step was to extract the total lipid fraction, including intracellular lipids and extracellular liquid hydrocarbons. The second step was to separate, from the lipid fraction, the hydrocarbon sub-fraction according to the method described by Ishimatsu et al. (2012).

Determination of total lipid content

A precise mass of freeze dried microalgae was mixed vigorously in the presence of 6 mL of chloroform: methanol (2:1 [v/v]). This suspension was disrupted by sonic disintegration for 1 min using an Ultrasonic Disruptor. Then the suspension was shook for 6 hours at room temperature, before adding 1.5 mL of 0.9 % NaCl and vigorous mixing. The suspension was centrifuged (3700g for 5 min) at 5 °C and the bottom layer was recovered in a pre-weighed glass vial. The solvent was evaporated and dried under gentle flow of nitrogen gas. Total lipids content ($[TL]_x$, % DCW) was determined gravimetrically and expressed as percent of biomass dry cell weight.

Purification of the liquid hydrocarbon fraction

This method aims at determining the content of liquid hydrocarbons in the total lipid fraction and not that of the polymerized hydrocarbons (hydrocarbons with more than 80 carbons), which are part of the matrix composition. The residual oil obtained for total lipids determination was dissolved in n-hexane and subjected to a silica gel column chromatography with four bed volumes of n-hexane as mobile phase (Figure 2-8, Figure 2-9). All the fractions before the elution of the first color band of pigments were collected, evaporated and dried under mild nitrogen flow gas. The purity of the extracted hydrocarbons was confirmed by thin layer chromatography (TLC). The hydrocarbon content ($[HC]_x$, % DCW) determined gravimetrically.

Hydrocarbon concentration and productivity

The hydrocarbon concentration (HC, $g L^{-1}$ or $g m^{-2}$) and hydrocarbon productivity (P_{HC} , $g L^{-1} d^{-1}$ or $g m^{-2} d^{-1}$) were calculated according the next relations:

$$HC = X \cdot [HC]_x, (g L^{-1} \text{ or } g m^{-2})$$

$$P_{HC} = P_x \cdot [HC]_x, (g L^{-1} d^{-1} \text{ or } g m^{-2} d^{-1})$$

The specific rate of hydrocarbon production was determined by:

$$q_{\text{HC}} = \frac{P_{\text{HC}}}{X}, (\text{gHC gX}^{-1}\text{d}^{-1})$$

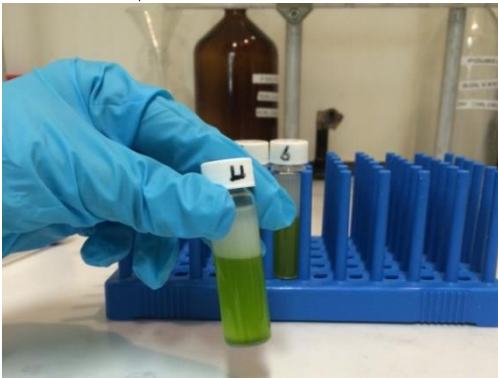
The content of intracellular lipids ($[\text{IL}]_x$, % DCW) was estimated according to the following relation:

$$[\text{IL}]_x = [\text{TL}]_x - [\text{HC}]_x, (\% \text{ DCW})$$

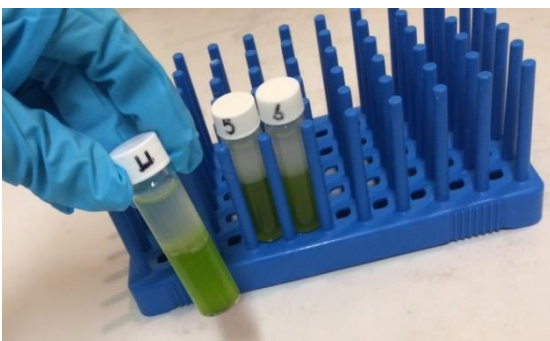
Shaking over night after adding 6 mL
chloroform: methanol (2:1 [v/v])



Adding 1.5 mL of 0.9% NaCl



Centrifuged (3700g for 5 min) at 20 °C



Transferred to a pre-weighed glass vial
evaporated and dried under flow of nitrogen gas

Measuring the weight of
total lipid



Evaporated and dried under
flow of nitrogen gas



Figure 2-8: Total lipid extraction.

Measuring the weight of hydrocarbon



Residual oil obtained for total lipids determination dissolved in n-hexane



Evaporated and dried under flow of nitrogen gas



Silica gel column chromatography with four bed volumes of n-hexane as mobile phase

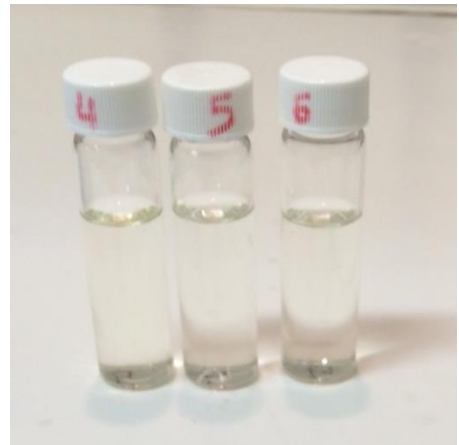


Figure 2-9: Hydrocarbon extraction.

2.4.9 GC-FID for hydrocarbons profiles analysis

Purified hydrocarbon extracts were analyzed by gas chromatography coupled to a flame ionization detector (GC-FID). A specified amount of sample was dissolved in n-hexane as well as of a n-alkane standard mixture (C₁₀–C₄₀, all even). They were analyzed with a 7820A gas chromatograph (Agilent Technologies, Santa-Clara, CA, USA) equipped with a split injector (injected quantity: 2 µL, split set at 1/10–10 mL min⁻¹), an HP-5 capillary column (apolar phase 5% phenyl methylpolysiloxane, internal diameter 0.32 mm, film thickness 0.25 µm, length 30 m, Agilent Technologies, Santa-Clara, CA, USA) and a flame ionization detector. The flow rate of carrier gas (hydrogen) during the analysis was constant at 2.0 mL·min⁻¹; the gas was produced using a hydrogen generator (WM-H2, F-DGSi, Evry, France). The chromatograph temperature program was: injector temperature 280 °C, FID 340 °C, oven 75 °C for 3 min, then ramped at 10 °C min⁻¹ to 300 °C for 15 min. Chromatographic data were recorded and identified by comparison of the retention times of the eluting hydrocarbons to the even-number C₁₀–C₄₀ standard mark.

2.4.10 GC-MS for hydrocarbons profiles analysis

To determine the hydrocarbon formula, the purified hydrocarbon extract further analyzed by GC-MS. The analytical device used was a Trace GC Ultra (Thermo Fisher Scientific, Boston, MA, USA) coupled to a Trace ISQ single quadrupole mass spectrometer (Thermo Fisher Scientific, Boston, MA, USA). The optimized separation conditions for the measurement of the molecules of interest (HCs and FAMES) were set up as follows: 2 µL of sample was injected onto a TG-5HT column (apolar phase 5% phenyl methylpolysiloxane, internal diameter 30 m × 250 µm, film thickness 0.25 µm; Thermo Scientific, Waltham, MA, USA) using programmed temperature vaporization (PTV), injection set at constant temperature (CT) mode at 280 °C, with a split mode of 1/10 (10 mL min⁻¹). The flow rate of carrier gas (hydrogen produced by a generator; WM-H2, F-DGSi, Evry, France) during the analysis was 1.5 mL·min⁻¹. The oven temperature gradient for the separation of the mixture of hydrocarbons was 75 °C for 3 min, ramped at 10 °C min⁻¹ to 300 °C for 1 min, and finally at 100 °C min⁻¹ to 340 °C for 4 min for cleaning. The temperature of the transfer line to the MS was 300 °C, and the ion source was set at 320 °C. Electron ionization was conducted at 70 eV. The mass resolution was 1 mass unit throughout the mass range of 50–600 amu. The total GC–MS analysis time was 30 min. Data were post-processed and analyzed using the Xcalibur 2.1 software (Thermo Fisher Scientific, Waltham, MA, USA Thermo-Fisher).

2.4.11 GC-FID for total fatty acid analysis

A specified mass of freeze dried microalgae was rehydrated by distilled water in glass vial. After adding Butylated hydroxytoluene (BHT, 20g L⁻¹) as antioxidant, cells were re-suspended in 6 mL of a chloroform/methanol mixture (2:1, v/v). To ensure a complete total fatty acid extraction, vials were sonicated in a water bath and maintained 6 h under agitation. The total lipids extracts were transesterified before the GC-FID analysis. The transesterification reaction was performed on a 100 µL aliquot of the total lipid extract to which 10 µg of glyceryl triheptadecanoate (TAG 17:0) was added as an internal standard. After evaporation to dryness under nitrogen and addition of 1mL of boron trifluoride (BF₃), the fractions were heated for 10 min at 100 °C. After cooling and adding 1 mL of hexane, the organic phase containing the fatty acid methyl esters (FAMES) was washed three times with 1.5 mL of water saturated hexane. FAMES were then recovered.

The quantity and the quality of total fatty acids were analyzed by gas chromatography coupled to a flame ionization detector (GCFID) with a 7820A gas chromatograph (Agilent Technologies, Santa-Clara, CA, USA) equipped with a split injector (injected quantity 2 µL, split set at 1/10–10 mL min⁻¹), a TR-FAME capillary column (polar phase 70% cyanopropyl polysilphenylene-siloxane, internal diameter 0.25 mm, thickness 0.25 µm film, length 30 m, Thermo Fisher Scientific, Waltham, MA, USA) and a flame ionization detector. The flow rate of carrier gas (hydrogen) during the analysis was constant at 1.0 mL·min⁻¹; the gas was produced using a hydrogen generator (WM-H2, F-DGSi, Evry, France). The chromatograph temperature program was: injector temperature 250 °C, FID 280 °C, oven at 80 °C for 1 min, then ramped at 5 °C min⁻¹ to 145 °C for 12 min, then at 1 °C min⁻¹ to 155 °C for 5 min and finally at 5 °C min⁻¹ to 200 °C for 5min. The FAMES were identified from their retention times compared with known standard mixtures. The FAME quantities were determined from their respective peak areas relative to that of the TAG 17:0 internal standard mark. Integration and calculation were performed using the Agilent software Chemstation v. 0.1.0.4. The absolute quantities of the TL were first expressed in µg of TL-FAs in the analyzed sample and in % DCW relative to the biomass concentration of the test sample.

2.4.12 Fluorescent microscopy observation

A bright field microscope and a fluorescence microscope were used for microscopic observations (ZEISS, AXIO scope.A1). Cells were incubated in medium with Nile red stock solution prepared in DMSO for 5 min at room temperature (final concentration of Nile red is 1µg mL⁻¹, DMSO is 10 %). Fluorescence was observed under a microscope with the No.20 HE filter (λ_{excitation}, 540-552 nm; λ_{emission}, 567-647 nm) as the Nile red channel and the

No. 5 filter ($\lambda_{\text{excitation}}$, 395-440 nm; $\lambda_{\text{emission}}$, 470 nm) as the merge channel of Nile red and chlorophyll auto-fluorescence (Figure 2-10).

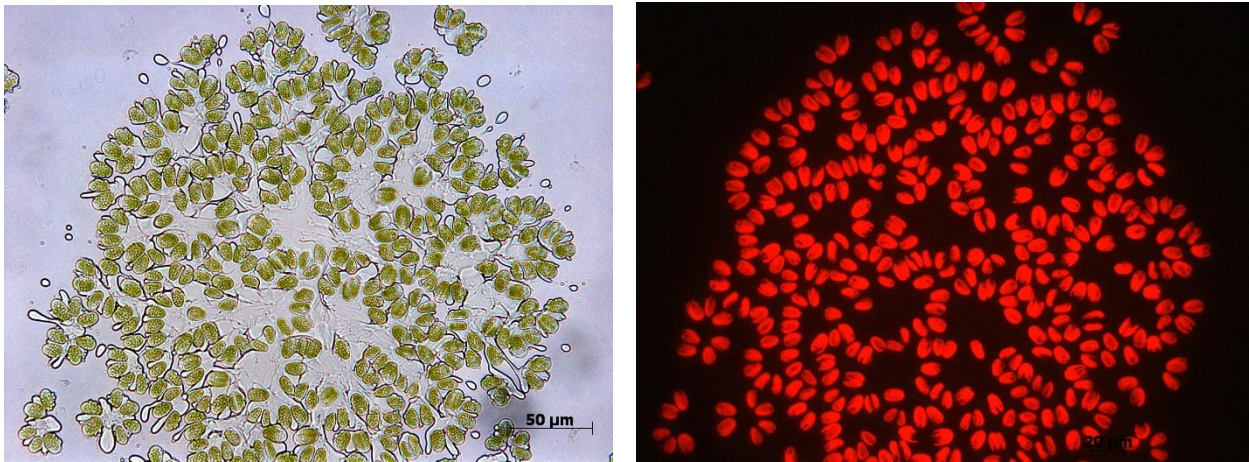


Figure 2-10: *B. braunii* BOT-22.

Statistical analysis

Results were expressed as the mean \pm standard deviation (SD). In order to test the homogeneity of variance, the data were treated by R software (<http://www.r-project.org>) by using levene Test (Car package). Differences between the groups were statistically analyzed by using one-way analysis of variance (ANOVA) and Tukey's 'Honest Significant Difference' method (TukeyHSD) with 95 % family-wise confidence level.

Chapter 3: Results and discussion

Chapter 3: Results and discussion

The production of biomass was studied as a function of two incident photon flux densities, two different dilution rates, two different light periods and different dissolved oxygen concentrations. Initially, the two identical photobioreactors were continuously illuminated while the dilution rate was the same for both. The aim was to determine the relation between global light availability, hydrocarbon content, intracellular lipids, biomass and hydrocarbon productivities, photosynthetic parameters, nutrients consumption and specific rate of hydrocarbon production. In the next step a change in the dilution rate was applied in order to characterize the impact of specific light supply on the biomass and hydrocarbon production.

3.1 Biomass production in continuous cultures

The effect of high and low light intensities (50 and $500 \mu\text{mol photon m}^{-2} \text{s}^{-1}$) was compared to find how light intensity could affect biomass and hydrocarbon productivity. Moreover, the effect of dilution rate on biomass production of *B. braunii* BOT-22 was investigated at two different dilution rates of 0.178 d^{-1} (2 mL h^{-1}) and 0.357 d^{-1} (4 mL h^{-1}). During the experiments the following conditions were kept constant: temperature was $22 \pm 2 \text{ }^\circ\text{C}$, continuous light, culture medium was 6N-6P-AF6, pH was 6.6 ± 0.2 , rate of CO_2 for pH adjustment was 3 mL min^{-1} , and aeration rate was 60 mL min^{-1} and dissolved oxygen concentration was 21 % (air).

The results obtained at three steady state culture conditions are presented in Table 3-1. These conditions are specified as A, B and C, where A and B corresponded to the same dilution rate, but in two different PFD and where B and C corresponded to the same PFD, but to two different dilution rates.

At constant dilution rate of 0.178 d^{-1} , increasing light intensity at the surface of the photobioreactor from $50 \mu\text{mol photon m}^{-2} \text{s}^{-1}$ to $500 \mu\text{mol photon m}^{-2} \text{s}^{-1}$, resulted in a significant increase, about 360 %, of the biomass concentration. Consequently, as shown in table 3-1, the mean surface biomass productivity were 5.83 ± 0.33 and $21.34 \pm 1.51 \text{ g m}^{-2} \text{d}^{-1}$ at 50 and $500 \mu\text{mol photon m}^{-2} \text{s}^{-1}$, respectively. Then in our experimental conditions, at $50 \mu\text{mol photon m}^{-2} \text{s}^{-1}$, the *B. braunii* cultures were light limited.

In contrast, doubling the dilution rate from 0.178 d^{-1} to 0.357 d^{-1} had less impact on the biomass concentration, with only a 10 % increase. The maximal value of the steady state

biomass concentration was 6.7 g L^{-1} . Consequently, by doubling the dilution rate, the value of biomass productivity increased more than twice, reaching $12.4 \pm 0.79 \text{ g m}^{-2} \text{ d}^{-1}$. It should be mentioned that at $50 \text{ } \mu\text{mol photon m}^{-2} \text{ s}^{-1}$ light intensity a dilution rate of 0.357 d^{-1} induced wash out of the culture (data not shown). This last observation confirmed that cultures were light limited at such PFD. The residual concentrations shown in Table 3-1 confirmed that there was no C, N or P limitation in these steady state cultures. The apparent absence of nutritional deficiency is confirmed by the relatively high residual concentrations of the main nutrients.

The maximal value of steady state biomass concentration, 6.7 g L^{-1} , is among the highest value obtained for *Botryococcus braunii* cell cultures, except the high cell density of 20 g L^{-1} , in continuous culture of *Botryococcus braunii* Showa by using a trickle-film photobioreactor, which provides a small thickness thin film (Khatri et al. 2014). The DIC (dissolved inorganic carbon) value in the culture media is related to pH and the nutrient consumption of microalgae (Talukdar et al. 2012). Growth of microalgae at high DIC concentrations increases the nutrients consumption, while low level of DIC value leads to slow consumption (Huertas et al. 2000; Nguyen and Rittmann 2015). As shown in Table 3-1, by increasing light intensity from low light to high light and therefore increase of biomass productivity, the nitrate and phosphate consumption increased. This increase could be correlated to increase of residual of dissolved inorganic carbon concentration in culture media. By increasing the biomass concentration, due to self-shading, there was limitation of light diffusion inside the PBR which could causes lower cellular nutrients consumption than it was expected according to increase of biomass concentration. By doubling the dilution rate, from 0.178 to 0.357 d^{-1} , the values of biomass productivity were increased more than twice. So higher dilution rate increases the nutrients availability for cells to growth. The volumetric biomass productivity at $500 \text{ } \mu\text{mol photons m}^{-2} \text{ s}^{-1}$ and 0.357 d^{-1} dilution rate, was $2.39 \pm 0.15 \text{ g L}^{-1} \text{ d}^{-1}$ which shows changing dilution rate from 0.178 to 0.357 d^{-1} at constant light intensity of $500 \text{ } \mu\text{mol photon m}^{-2} \text{ s}^{-1}$, could have a significant effect on biomass productivity.

Decrease in DIC value at higher dilution rate, suggested that the nutrients consumption was slowed. However, this study was carrying out with a monitored pH fixed at 6.6 ± 0.2 , only with CO_2 injection. As PBR was continuously feed with a non-buffered fresh 6P6N-AF-6 media, high nitrate concentration in the culture media slightly increased the alkalinity, and consequently decreased the DIC concentration. Therefore, lower DIC value can not be related to low nutrient consumption directly.

Table 3-1

Biomass concentration and productivity (volumetric and surface), in steady state cultures of *Botryococcus braunii* BOT-22 race B strain at two incident light intensities on the photobioreactor surface (50 and 500 $\mu\text{mol photons m}^{-2} \text{s}^{-1}$) and two dilution rates 0.178 and 0.357 d^{-1} .

D (d^{-1})	0.178		0.357
PFD ($\mu\text{mol photons m}^{-2} \text{s}^{-1}$)	50	500	500
Condition	A	B	C
X (g L^{-1})	1.64 \pm 0.09	5.99 \pm 0.42	6.7 \pm 0.43
Volumetric biomass productivity ($\text{g L}^{-1} \text{d}^{-1}$)	0.29 \pm 0.02	1.07 \pm 0.08	2.39 \pm 0.15
Surface biomass productivity ($\text{g m}^{-2} \text{d}^{-1}$)	5.83 \pm 0.33	21.34 \pm 1.51	47.81 \pm 3.04
Residual NO_3 (mg L^{-1})	142.36 \pm 21.11	100.89 \pm 22.18	273.81 \pm 49.57
Residual PO_4 (mg L^{-1})	38.4 \pm 5.1	8.5 \pm 0.5	17.1 \pm 2.9
Residual dissolved inorganic carbon (mg L^{-1})	40.01 \pm 3.55	90.03 \pm 5.55	61.71 \pm 3.66

As shown in Table 3-2, the biomass concentration reached under condition C is among the highest values obtained with cell suspension cultures of *B. braunii*. Indeed Pérez-Mora et al. at 2016 achieved a 4.69 g L^{-1} biomass of *B. braunii* 2441 (race A) in a 2L tubular photobioreactor and Ramaraj et al. at 2016, 8.57 g L^{-1} of not specified *Botryococcus braunii* in a 4L flask, both studied carried out according to a fed-batch operating mode, i.e. without steady state. There is an exception with higher biomass concentration, as high as 20 g L^{-1} , but with 1.5 $\text{g L}^{-1} \text{d}^{-1}$ biomass productivity reached in a continuous culture of *B. braunii* Showa within a trickle-film photobioreactor (Khatri et al. 2014). Table 3-2 shows the comparison of biomass concentration, biomass productivity of different *B. braunii* strains with this study. In comparison with previous studies for *B. braunii* the biomass productivity in open ponds was less than 0.194 $\text{g L}^{-1} \text{d}^{-1}$ (Table1-4).

Table 3-2

The maximum values of biomass concentration and productivity obtained in cultures of different *Botryococcus braunii* race B. strains in the literature and in this study.

Strain	Biomass concentration (g L ⁻¹)	Biomass productivity (g L ⁻¹ d ⁻¹)	References
Showa	3.3	1.65*	Yoshimura et al. 2013
IPE 001	2.87	NA	Xu et al. 2012 b
Yayoi	1.9	NA	Okada et al. 1997
BOT-22 (nitrogen depletion)	1.06	NA	Shimamura et al. 2012
BOT-22 (nitrogen sufficient)	2.86	NA	Shimamura et al. 2012
Showa	20	1.5	Khatri et al. 2014
BOT-22	1.7 **	0.17 **	Tanabe et al. 2014
BOT-22	6.7	2.39	This study (C condition)

*calculated from published data / **calculated from published graph

According to this observation, the growth of the cell culture in our experimental conditions appeared to adapt the cell population to the available light, confirming its role of growth-limiting factor.

Due to the higher biomass productivity, the dilution rate of 0.357 d⁻¹ (4 mL h⁻¹) was chosen for the next steps.

3.1.2 Effect of a dark period on biomass production in continuous cultures under 21% of dissolved oxygen

In order to investigate the effect of a darkt period on biomass production of *B. braunii* BOT-22, a dark cycle (16 hours dark) was applied to the continuous culture. During the experiments these conditions were kept constant: temperature was 22 ± 2 °C, PFD was 500 μ mole photons m⁻² s⁻¹ before and after the dark period, the culture medium was 6N-6P-AF6, pH was 6.6 ± 0.2, dilution rate was 0.357 d⁻¹, rate of CO₂ for pH adjustment was 3 mL min⁻¹, aeration rate was 60 mL min⁻¹ and concentration of dissolved oxygen was 21% (air).

The biomass productivity at continuous light under 21% of oxygen concentration was 2.39 ± 0.15 g L⁻¹ d⁻¹. It should be mentioned that the growth under light and dark cycle was more than what was eIt was shown that there was no biomass loss during the dark period, the

decrease in biomass concentration was only the result of the dilution rate (the graph is not shown here).

On the other hand, when compare the residual concentrations of nitrate and phosphate in the dark to their level in 6N6P-AF-6 media; it interestingly appears that the cells were still consuming the nutrients in the dark. This is probably because they need nitrate and phosphate to maintain their cellular integrity, but also to biosynthesize essential metabolites to survive and protect themselves from light starvation (Table 3-3).

During the dark incubation, the DIC concentrations was about at the same level of continuous light $61.71 \pm 3.66 \text{ mg L}^{-1}$ and $63.93 \pm 10.62 \text{ mg L}^{-1}$. This is mainly due to the high residual concentration of nitrate in the culture media, but also to the slow uptake of nutrients as the light become the nutrient-limiting factor.

Table 3-3

Biomass concentration and productivity (volumetric and surface) of *B. braunii* BOT-22 race B strain at 500 $\mu\text{mol photons m}^{-2} \text{s}^{-1}$ and 0.357 d^{-1} dilution rates under continuous light and after a 16h dark period with 21 % of dissolved oxygen concentration.

Light period	Continuous light	16 hrs darkness
X (g L⁻¹)	6.7 ± 0.43	6.3 ± 0.54
Volumetric productivity (g L⁻¹d⁻¹)	2.39 ± 0.15	2.25 ± 0.19
Surface productivity (g m⁻²d⁻¹)	47.81 ± 3.04	44.98 ± 3.86
Residual NO₃ PO₄ (mg L⁻¹)	273.81 ± 49.57	406.3 ± 60.24
Residual PO₄ (mg L⁻¹)	17.09 ± 2.95	22.5 ± 4.93
Residual dissolved inorganic carbon (mg L⁻¹)	61.71 ± 3.66	63.93 ± 10.62

3.1.3 Effect of continuous and discontinuous illumination under 4% of dissolved oxygen on biomass production in continuous cultures

The effect of light and dark cycle at steady states conditions on biomass production of *B. braunii* BOT-22 was measured at two different light periods: continuous light and light and dark cycle (8 hours light and 16 hours dark) to find if under 4 % concentration of dissolved oxygen, light period could have any effects on biomass productivity (Table 3-4). During the experiments these conditions were kept constant: temperature was 22 ± 2 °C, PFD was 500 $\mu\text{mole photons m}^{-2} \text{s}^{-1}$ (using light & dark cycle and continuous light), culture medium was 6N-6P-AF6, pH was 6.6 ± 0.2, rate of CO₂ for pH adjustment was 3 mL min⁻¹, dilution rate was 0.357 d^{-1} , aeration rate was 60 mL min⁻¹ and oxygen level was 4 % (using nitrogen).

The biomass productivity at continuous light with 4 % of oxygen concentration was 3.07 ± 0.2 g L⁻¹ d⁻¹ and on light & dark cycle (8 hours of light and 16 hours of dark) was 2.12 ± 0.4 g L⁻¹ d⁻¹. According there is no growth on dark cycle, this reduction on biomass productivity was expected.

Table 3-4

Biomass concentration and productivity (volumetric and surface) of *B. braunii* BOT-22 race B strain at $500 \mu\text{mol photons m}^{-2} \text{s}^{-1}$ and 0.357d^{-1} dilution rates under continuous light and after a 16h dark period with 4 % of dissolved oxygen concentration.

Light period	Continuous light	16 hrs darkness
X (g L^{-1})	8.6 ± 0.56	5.94 ± 1.21
Volumetric productivity ($\text{g L}^{-1}\text{d}^{-1}$)	3.07 ± 0.2	2.12 ± 0.4
Surface productivity ($\text{g m}^{-2}\text{d}^{-1}$)	61.4 ± 3.98	42.41 ± 8
Residual NO_3 (mg L^{-1})	213.5 ± 47.66	324.14 ± 112.72
Residual PO_4 (mg L^{-1})	7.38 ± 4.16	16.54 ± 4.6
Residual dissolved inorganic carbon (mg L^{-1})	73.8 ± 12.58	47.28 ± 7.11

3.1.4 Effect of dissolved oxygen concentrations under continuous illumination on biomass production in continuous cultures

The effect of dissolved oxygen concentration on continuous light at steady states conditions on biomass production of *B. braunii* BOT-22 was studied with 4 % and 21 % dissolved oxygen concentrations (Table 3-5). During the experiments these conditions were kept constant: temperature was $22 \pm 2 \text{ }^\circ\text{C}$, PFD was $500 \mu\text{mol photons m}^{-2} \text{s}^{-1}$, culture medium was 6N-6P-AF6, pH was adjusted at 6.6 ± 0.2 , rate of CO_2 for pH adjustment was 3 mL min^{-1} , dilution rate was 0.357d^{-1} , aeration rate was 60 mL min^{-1} and oxygen level was 4 % (using nitrogen) and 21 % (air).

The biomass productivity at continuous light with 4 % of oxygen was $3.07 \pm 0.2 \text{ g L}^{-1} \text{d}^{-1}$ and with 21 % of oxygen (air) 2.39 ± 0.15 was $\text{g L}^{-1} \text{d}^{-1}$.

Table 3-5

Biomass concentration and productivity (volumetric and surface) of *B. braunii* BOT-22 race B strain at 500 $\mu\text{mol photons m}^{-2} \text{s}^{-1}$ and 0.357 d^{-1} dilution rates under continuous light and with 4 % and 21 % of dissolved oxygen concentration.

Dissolved oxygen concentrations	4 %	21 %
X (g L^{-1})	8.6 \pm 0.56	6.7 \pm 0.43
Volumetric productivity ($\text{g L}^{-1} \text{d}^{-1}$)	3.07 \pm 0.2	2.39 \pm 0.15
Surface productivity ($\text{g m}^{-2} \text{d}^{-1}$)	61.4 \pm 3.98	47.81 \pm 3.04
Residual NO_3 (mg L^{-1})	213.5 \pm 47.66	273.81 \pm 49.57
Residual PO_4 (mg L^{-1})	7.38 \pm 4.16	17.09 \pm 2.95
Residual dissolved inorganic carbon (mg L^{-1})	73.8 \pm 12.58	61.71 \pm 3.66

3.1.5 Effect of dissolved oxygen concentrations under discontinuous illumination on biomass production in continuous cultures

During photosynthesis reactions, microalgae produce oxygen. The effect of dissolved oxygen level on light and dark cycle at steady states conditions on biomass production of *B. braunii* BOT-22 was investigated at three concentrations: 4 %, 21 % and 400 %; to find if it could have any effect; specially inhibitory effects; on biomass productivity. During the experiments these conditions were kept constant: temperature was 22 \pm 2 $^{\circ}\text{C}$, PFD was 500 $\mu\text{mol photons m}^{-2} \text{s}^{-1}$ (using light & dark cycle), culture medium was 6N-6P-AF6, pH was 6.6 \pm 0.2, rate of CO_2 for pH adjustment was 3 mL min^{-1} , dilution rate was 0.357 d^{-1} , aeration rate was 60 mL min^{-1} and oxygen level was 4 % (using nitrogen), 21 % (air) and oxygen saturation.

In oxygen limitation and saturation the consumption of nitrate and phosphate were increased which could be because of limitation and saturation of oxygen while the residual of dissolved inorganic carbon concentration in culture media was decreased and the biomass concentration in both condition also was decreased slightly. As PBR was continuously feed with fresh 6P6N-AF-6 media (non-buffered), high nitrate concentration in the culture media slightly increased the alkalinity, and consequently decreased the DIC concentration. Therefore, lower DIC level cannot be related to low nutrient consumption directly.

3.2 Hydrocarbon production in continuous cultures

Changing photon flux density and dilution rate had significant effects on biomass concentration and productivity. These parameters could also affect the hydrocarbon content and hydrocarbon productivity of *Botryococcus braunii* BOT-22.

3.2.1 Effect of PFD and dilution rate on hydrocarbon production in continuous cultures

The production of hydrocarbon was studied under two different light intensities (50 and 500 $\mu\text{mol photons m}^{-2} \text{s}^{-1}$) and two different dilution rates of 0.178 d^{-1} (2 mL h^{-1}) and 0.357 d^{-1} (4 mL h^{-1}).

During the experiments these conditions were kept constant: temperature was 22 ± 2 °C, continuous light, culture medium was 6N-6P-AF6, pH was 6.6 ± 0.2 , rate of CO_2 for pH adjustment was 3 mL min^{-1} , rate of aeration was 60 mL min^{-1} and dissolved oxygen level was 21% (air).

At constant dilution rate, increasing light intensity, from 50 $\mu\text{mol photons m}^{-2} \text{s}^{-1}$ to 500 $\mu\text{mol photons m}^{-2} \text{s}^{-1}$, induced a significant increase of the hydrocarbon concentration, from 332 to 1249 mg L^{-1} . This increase is in the same order than that observed for biomass concentration. Indeed these culture conditions, confirm that the hydrocarbon production was growth associated. By contrast, the hydrocarbon content was not impacted by the tenfold increase in PFD.

By doubling the dilution rate from 0.178 d^{-1} to 0.357 d^{-1} at a constant PFD of 500 $\mu\text{mol photons m}^{-2} \text{s}^{-1}$, the concentration of hydrocarbon reached 1742 mg L^{-1} , i.e. about 40% increase. This value is higher than those obtained by Xu et al. (2012 b), Shimamura et al. (2012) and Yoshimura et al. (2013), but, for race B strains higher hydrocarbon contents between 40 and 64 % DCW was reported (Table 3-8).

It should be mentioned that increasing the dilution rate from 0.178 d^{-1} to 0.357 d^{-1} , under a constant PFD of 500 $\mu\text{mol photons m}^{-2} \text{s}^{-1}$, induced a 27 % increase in the hydrocarbon content. Moreover, at steady state, the specific hydrocarbon productivity was not affected by the PFD rise, but it is changed from 36 to 93.4 $\text{mg g}^{-1} \text{d}^{-1}$ after the rise in dilution rate (Table 3-6).

Among the three conditions, the maximum of volumetric hydrocarbon productivity was $621.99 \pm 39.5 \text{ mg L}^{-1} \text{d}^{-1}$ and the maximum of surface hydrocarbon productivity was $12.4 \pm 0.79 \text{ g m}^{-2} \text{d}^{-1}$, which correspond to 500 $\mu\text{mol photons m}^{-2} \text{s}^{-1}$ and dilution rate of 0.357 d^{-1} . The apparent absence of nutritional deficiency is confirmed by the relatively high residual concentrations of the main nutrients in Table 3-7. Consequently, high biomass and

hydrocarbon productivities seem to involve together the PBR design for its light availability, short light path, a good mixing, no sedimentation zone and high nitrate and phosphate concentrations, modified AF6 culture medium, for *Botryococcus braunii* BOT-22 cultures where light availability would be the main limiting factor. Specific light supply rate is another important parameter for improving biomass and hydrocarbon productivity that is discussed in next chapter.

Table 3-6

Hydrocarbon concentration, hydrocarbon productivity (volumetric and surface) and hydrocarbon content in steady state cultures of *Botryococcus braunii* BOT-22 race B strain at two incident light intensities on the photobioreactor surface (50 and 500 $\mu\text{mol photons m}^{-2} \text{s}^{-1}$) and two dilution rates of 0.178 and 0.357 d^{-1} .

D (d^{-1})	0.178		0.357
PFD ($\mu\text{mol photons m}^{-2} \text{s}^{-1}$)	50	500	500
Condition	A	B	C
HC (mg L^{-1})	332 \pm 31.27	1249 \pm 120.17	1742 \pm 110.64
HC content (%)	20.24 \pm 1.67	20.51 \pm 1.39	26.02 \pm 0.13
Volumetric HC productivity ($\text{mg L}^{-1} \text{d}^{-1}$)	59.03 \pm 5.57	218.8 \pm 15.45	621.99 \pm 39.5
Surface HC productivity ($\text{g m}^{-2} \text{d}^{-1}$)	1.18 \pm 0.11	4.38 \pm 0.31	12.4 \pm 0.79
Specific HC productivity ($\text{mg g}^{-1} \text{d}^{-1}$)	35.8	36.6	93.4
Residual NO_3 (mg L^{-1})	142.36 \pm 21.11	100.89 \pm 22.18	273.81 \pm 49.57
Residual PO_4 (mg L^{-1})	38.4 \pm 5.1	8.5 \pm 0.5	17.1 \pm 2.9
Residual dissolved inorganic carbon (mg L^{-1})	40.0 \pm 3.5	90.0 \pm 5.5	61.7 \pm 3.7

Table 3-7

The maximum values of hydrocarbon contents (%) and hydrocarbon concentration obtained in cultures of different *Botryococcus braunii* race B. strains in the literature and in this study.

Strain	Hydrocarbon content (%)	Hydrocarbon concentration (mg L ⁻¹)	References
Showa	39.2	1293.6*	Yoshimura et al. 2013
Showa	24-29	250*	Wolf et al. 1985 a
Showa	37.9	NA	Okada et al. 1995
IPE 001	64.3	1150.97*	Xu et al. 2012 b
Yayoi	40.5	769.5*	Okada et al. 1997
BOT-22 (nitrogen depletion)	44.9	475.9*	Shimamura et al. 2012
BOT-22 (nitrogen sufficient)	40.6	1161.16*	Shimamura et al. 2012
Showa	18-23	4533	Khatri et al. 2014
BOT-22	26.02	1742	This study (C condition)

*calculated from published data

Figure 3-1 demonstrate that with dilution rate of 0.178 d⁻¹, there was no significant difference among of hydrocarbons contents at 50 μmol photons m⁻² s⁻¹ and 500 μmol photons m⁻² s⁻¹ which was (20.24 ± 1.67) and (20.51 ± 1.39) %, respectively. One of the reasons could be the lower consumption of nitrate and phosphate due to self-shading at high light intensity (500 μmol photons m⁻² s⁻¹) which could causes light limitation. However, the content of intracellular lipid was increased from (21.47 ± 0.72) % to (23.76 ± 5.61) % (about 11 % increases) which seems it was especially due to increase of intracellular lipids. Moreover, like the other lipids producers, *B. braunii* is known to produce more lipids during nitrogen starvation (Venkatesan et al. 2013). The high cell density in the culture media combined to the lower level of nitrate availability, can substantially be the reason of increase in intracellular lipids content.

The hydrocarbon productivity at 50 μmol photons m⁻² s⁻¹ was 59.03 ± 5.57 mg L⁻¹ d⁻¹ while the dry weight was 1.64 ± 0.09 g L⁻¹ and at 500 μmol photons m⁻² s⁻¹ was 218.8 ± 15.45 mg L⁻¹ d⁻¹ with the dry weight of 5.99 ± 0.42 g L⁻¹, respectively.

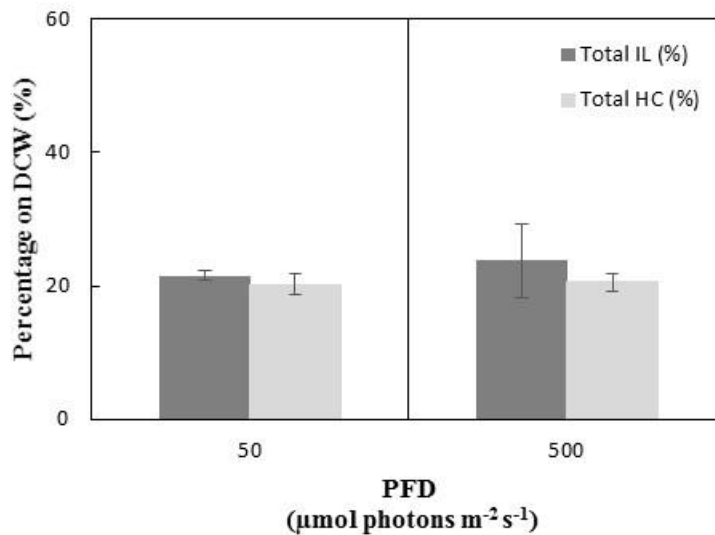


Figure 3-1: Total hydrocarbon and intracellular lipids content percentage on dry cell weight (% total HC and % IL) of *B. braunii* race B strain BOT-22 at two incident PFD 50 and 500 $\mu\text{mol photons m}^{-2} \text{s}^{-1}$.

Figure 3-2 shows that with doubling the dilution rate from 0.178 d^{-1} to 0.357 d^{-1} there was an increase in both total lipid and hydrocarbons contents. Hydrocarbon content was increased from $(20.51 \pm 1.39) \%$ to $(26.02 \pm 0.13) \%$, respectively; about 27 % increases was achieved. Also the content of intracellular lipid was increased about 60% which was $(23.76 \pm 5.61) \%$ at dilution rate of 0.178 d^{-1} and became $(37.98 \pm 15.44) \%$ at dilution rate of 0.357 d^{-1} ; it seems that it was due to increase of intracellular and extracellular lipids.

In fact, doubling the dilution rate reduces the self-shading inside the PBR, so that the microalgae were exposed to the high light irradiance. Therefore, *B. braunii* BOT-22 possibly produces supplementary hydrocarbons, and accumulate them in its colony in order to reduce the cells exposition to high irradiance. Indeed, the colonial growing state of *B. braunii* has been hypothesized as a shielding organization to protect the cells against the environmental stress conditions (Weiss et al. 2012). Furthermore, the increase of hydrocarbons production is related to two factors: the increase of hydrocarbon content and the increase in biomass concentration.

At dilution rate of 0.178 d^{-1} the dry weight was $5.99 \pm 0.42 \text{ g L}^{-1}$ and the hydrocarbon productivity was $218.8 \pm 15.45 \text{ mg L}^{-1} \text{ d}^{-1}$ and at dilution rate of 0.357 d^{-1} with $6.7 \pm 0.43 \text{ g L}^{-1}$ dry weight, $621.99 \pm 39.5 \text{ mg L}^{-1} \text{ d}^{-1}$ hydrocarbon productivity was achieved. The increase of hydrocarbon could be because of the increasing of dilution rate which could cause a decrease in self-shading, availability of nutrients and also it could affect the stress conditions.

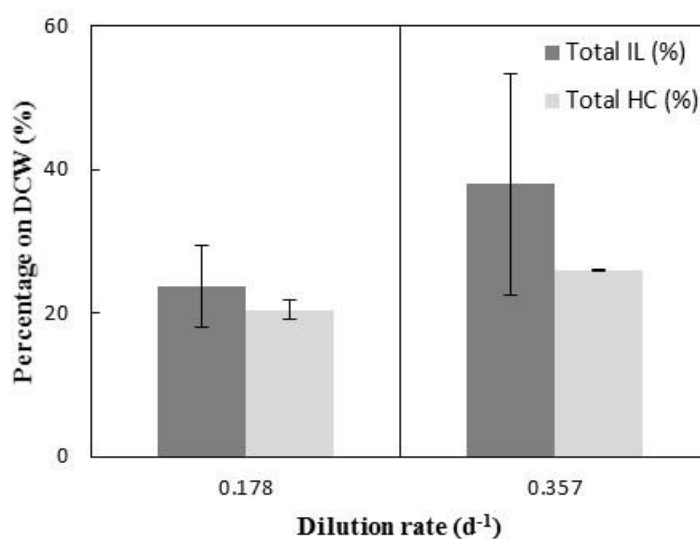


Figure 3-2: Total hydrocarbon and intracellular lipids content percentage on dry cell weight (% total HC and %IL) of *B. braunii* race B strain BOT-22 at two incident dilution rates 0.178 and 0.357 d⁻¹.

3.2.2 Effect of a dark period on hydrocarbon and intracellular lipid content in continuous cultures under 21% of dissolved oxygen concentration

During the dark period, there was not active growth and the culture was diluted by the continuous feeding. So a decrease in biomass and also hydrocarbon productivity was observed as expected.

Figure 3-3 demonstrates that at the end of the dark period with 21% of oxygen does not have any significant effect on hydrocarbon content and in both conditions, about 26% of hydrocarbon content was gained but photo period could affect the intracellular lipids. In continuous light, intracellular lipid was (37.98 ± 15.44) %, but in light and dark cycle the intracellular lipid became (17.11 ± 1.47) %, i.e. a significant decrease was observed.

This trend agreed with a previous observation in *B. braunii* Bot-22 confirming that the hydrocarbons in *B. braunii* were not consumed during the dark respiration in the light dark cycle (Sakamoto et al. 2012).

A simulation (data not shown) with an experimental rate of decreasing has been made to verify whether the cells were still growing during the dark period or not. The results

demonstrated that the cells still grew a little during the dark period. This simulation seems to confirm that during dark incubation there is no biomass decrease as a consequence of respiration and consumption of carbons reserves.

The MEP (Methylerythritol 4-phosphate), or/and the DOXP (1-Deoxy-D-xylulose-5-phosphate) are the main pathway for the biosynthesis of chloroplastic isoprenoids, such as carotenoids, phytol (a side chain of chlorophylls), but also the botryococenes in *B. braunii* Bot-22 (Ishimatsu et al. 2012 ; Paniagua-Michel et al. 2012; Sakamoto et al. 2012). This relation between the biosynthetic pathways could certainly be the reason why the level of hydrocarbon content was also increase or remained stable during the dark period.

The dry weight at continuous and discontinuous light was 6.7 ± 0.43 and 6.3 ± 0.54 g L⁻¹, respectively; so the hydrocarbon productivity at continuous light under 21 % concentration of oxygen was 621.99 ± 39.5 mg L⁻¹ d⁻¹ while at discontinuous light was 576.29 ± 56.02 mg L⁻¹ d⁻¹ (Figure 3-3).

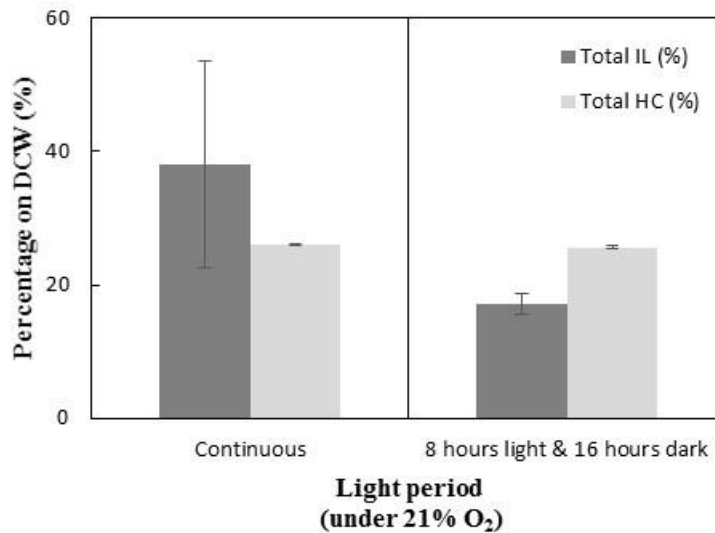


Figure 3-3: Total hydrocarbon and intracellular lipids content percentage on dry cell weight (% total HC and %IL) of *B. braunii* race B strain BOT-22 under continuous light and after a 16 hours dark period with 21% dissolved oxygen concentration.

3.2.3 Effect of dissolved oxygen concentration on hydrocarbon and intracellular lipid content in continuous cultures under continuous illumination

Figure 3-4 shows that there is a significant increase on intracellular lipid content under continuous light and different levels of oxygen concentration. (37.98 ± 15.44) % of intracellular lipid was obtained under continuous light and 21 % of oxygen. The increase of total lipid was mostly related to intercellular lipids while the hydrocarbons content was about 2 % more under continuous light with 4 % concentration of oxygen.

The hydrocarbon productivity under continuous light with 4 % and 21 % concentration of dissolved oxygen were 879.9 ± 132.56 and 621.99 ± 39.5 mg L⁻¹ d⁻¹ where the dry weight was 8.6 ± 0.56 and 6.7 ± 0.43 g L⁻¹, respectively.

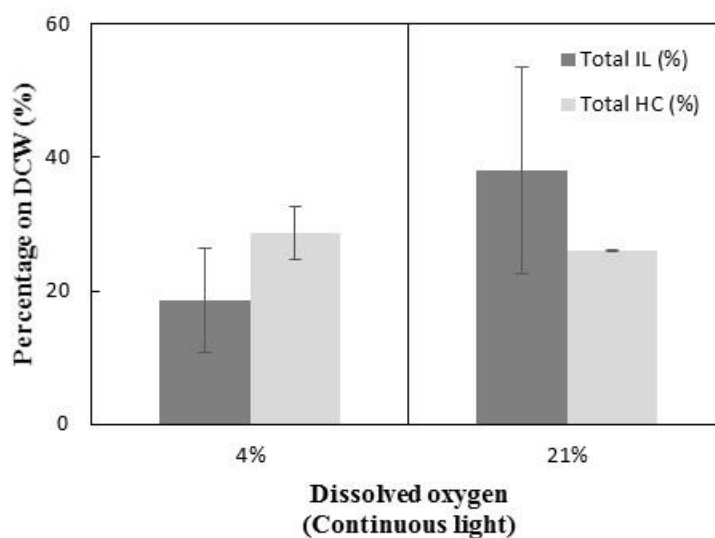


Figure 3-4: Total hydrocarbon and intracellular lipids content percentage on dry cell weight (% total HC and %IL) of *B. braunii* race B strain BOT-22 under continuous light with 4 % and 21 % of dissolved oxygen concentration.

3.2.4 Effect of a dark period on hydrocarbon and intracellular lipid content in continuous cultures under 4% of dissolved oxygen concentration

Figure 3-5, shows that photo period under 4% of dissolved oxygen concentration does not have any significant effect on hydrocarbon content and it was about 29 and 28% of hydrocarbon content under continuous light or at the end of a 16h dark period.

The hydrocarbon productivity at continuous light under 4% concentration of oxygen where the dry weight was $8.6 \pm 0.56 \text{ g L}^{-1}$, was $879.9 \pm 132.56 \text{ mg L}^{-1} \text{ d}^{-1}$.

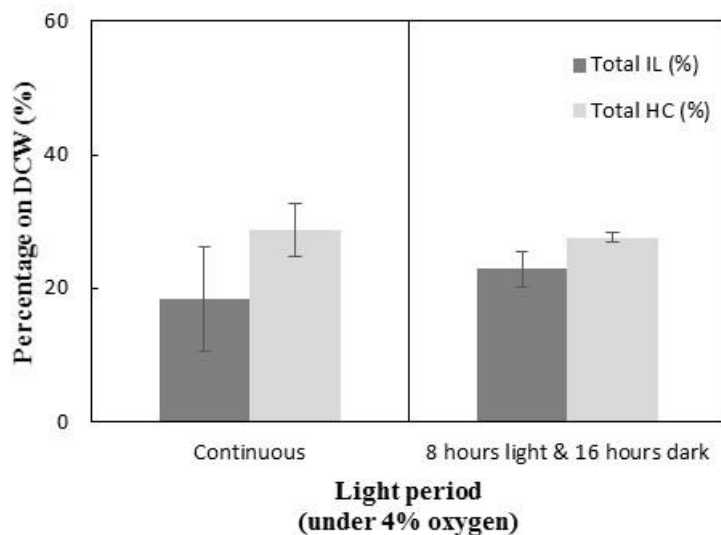


Figure 3-5: Total hydrocarbon and intracellular lipids content percentage on dry cell weight (% total HC and %IL) of *B. braunii* race B strain BOT-22 under continuous light or after a 16 hours of dark with 4% dissolved oxygen concentration.

3.2.5 Effect of dissolved oxygen concentration on hydrocarbon and intracellular lipid content in continuous cultures under discontinuous illumination

Figure 3-6 shows that there is no significant increase in discontinuous light under 3 different dissolved oxygen concentration although the highest hydrocarbon content achieved with 4 % of oxygen which was about 28 %. Also the highest value of total lipid content was achieved at 4 % of oxygen which was about 50 %. It seems that oxygen has larger effect on intracellular lipids.

The dry weight under 4 %, 21 % and 400 % concentration of dissolved oxygen was 5.94 ± 1.21 , 6.3 ± 0.54 and 6.08 ± 0.12 g L⁻¹, therefore the hydrocarbon productivity was 584.87 ± 109.79 , 576.29 ± 56.02 and 574.8 ± 23.87 mg L⁻¹ d⁻¹, respectively.

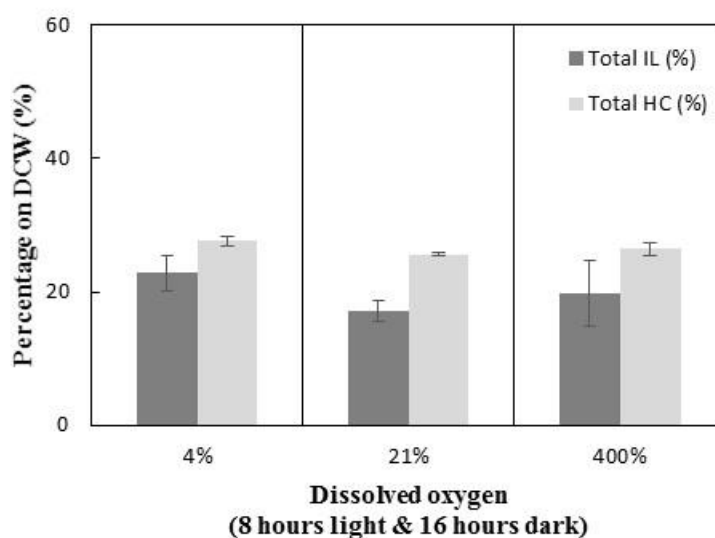


Figure 3-6: Total hydrocarbon and intracellular lipids content percentage on dry cell weight (% total HC and % IL) of *B. braunii* race B strain BOT-22 after a 16 hours of dark with 4 %, 21 % and 400 % of dissolved oxygen concentration.

3.3 Fatty acids composition

3.3.1 Fatty acids components

As shown in figure 3-7, the main fatty acid components of *B. braunii* race B strain BOT-22 fatty acids, were oleic acid, palmitic acid, α -linoleic acid, erucic acid and stearic acid. Cheng et al. (2013) reported that for *B. braunii* FACHB 357 (race B), the main fatty acid components were oleic acid, linoleic acid and palmitic acid which is similar to this study. For *B. braunii* AP103 Ashokkumar and Rengasamy (2012) reported oleic acid, linoleic acid and palmitic acid as the main fatty acids. For *B. braunii* race A, Samorì et al. 2010 reported that oleic, palmitic, linoleic and stearic acids are the main fatty acids. Wang et al. (2014) reported for *B. braunii*, stearic acid (18:0), oleic acid (18:1), and linolenic acid (18:3) were the most abundant components. Wang et al. (2014) reported a similar result as the current study for *B. braunii*, i.e. fatty acids with 16 and 18 carbon atoms, were the major components.

It should be mentioned that in all of the experimental conditions in this study oleic acid, palmitic acid and α -linoleic acid were the dominant components.

The fatty acid profile for *B. braunii* BOT-22 race B indicated the presence of C16:0, C16:1, C18:0, C18:1, C18:2, C18:3, C20:0, C20:1, C20:3, C20:4, C22:0, C22:1, C22:2, C22:6, C24:0 and C24:1 fatty acids. Ranga Rao et al. (2007 a) reported the fatty acid profile for *B. braunii* race A indicated the presence of C16:0, C16:1, C18:0, C18:1, C18:2, C22:0, C22:1 and C24:0 fatty acids.

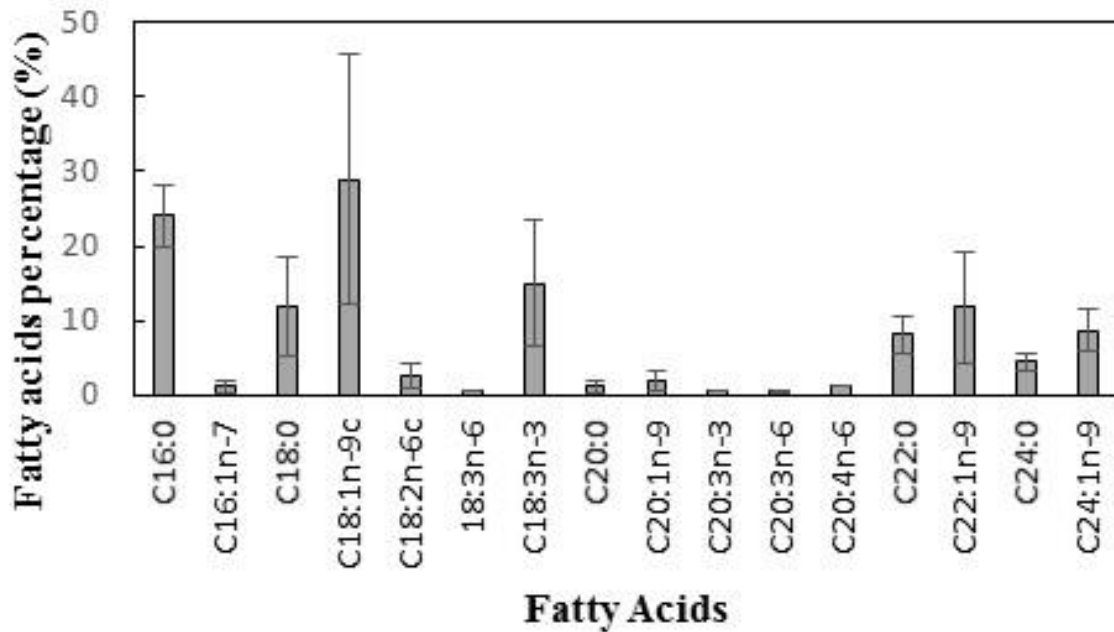


Figure 3-7: Fatty acids profile of *B. braunii* race B strain BOT-22 under different conditions; (A) Continuous light, 0.178 d^{-1} , light intensity $50 \mu\text{mol photons m}^{-2} \text{ s}^{-1}$ and 21% dissolved oxygen concentration; (B) Continuous light, 0.178 d^{-1} , light intensity $500 \mu\text{mol photons m}^{-2} \text{ s}^{-1}$ and 21% dissolved oxygen concentration; (C) Continuous light, 0.357 d^{-1} , light intensity $500 \mu\text{mol photons m}^{-2} \text{ s}^{-1}$ and 21% dissolved oxygen concentration; (D) Continuous light, 0.357 d^{-1} , light intensity $500 \mu\text{mol photons m}^{-2} \text{ s}^{-1}$ and 4% dissolved oxygen concentration; (E) End of a 16 hours dark period, 0.357 d^{-1} , light intensity $500 \mu\text{mol photons m}^{-2} \text{ s}^{-1}$ and 4% dissolved oxygen concentration; (F) End of a 16 hours dark period, 0.357 d^{-1} , light intensity $500 \mu\text{mol photons m}^{-2} \text{ s}^{-1}$ and 21% dissolved oxygen concentration; (G) End of a 16 hours dark period, 0.357 d^{-1} , light intensity $500 \mu\text{mol photons m}^{-2} \text{ s}^{-1}$ and 400% dissolved oxygen concentration.

Table 3-8

Biomass concentration (g L^{-1}), PUFAs content (%), C16-C18 content (%), hydrocarbon and intracellular content (%) on DCW of *Botryococcus braunii* BOT 22 race B strain at two incident light intensities (50 and 500 $\mu\text{mol photons m}^{-2} \text{s}^{-1}$) on the photobioreactor surface, two dilution rates (0.178 and 0.357 d^{-1}), two light periods (continuous light and light and dark cycle) and different dissolved

Condition	A	B	C	D	E	F	G
LI ($\mu\text{mol photons m}^{-2} \text{s}^{-1}$)	50	500	500	500	500	500	500
LP	CL	CL	CL	CL	LD	LD	LD
DO (%)	21%	21%	21%	4%	4%	21%	400%
DR (d^{-1})	0.178	0.178	0.357	0.357	0.357	0.357	0.357
DCW (g L^{-1})	1.64 \pm 0.09	5.99 \pm 0.42	6.7 \pm 0.43	8.6 \pm 0.56	5.94 \pm 1.21	6.3 \pm 0.54	6.08 \pm 0.12
PUFAs content (%)	26.99 \pm 5.13	22.06 \pm 3.79	21.09 \pm 1.33	29.26 \pm 2.65	33.46 \pm 1.55	18.5 \pm 0.89	25.60 \pm 8.26
HC content (%)	20.24 \pm 1.67	20.51 \pm 1.39	26.02 \pm 0.13	28.67 \pm 3.90	27.6 \pm 0.72	25.61 \pm 0.31	26.47 \pm 0.97
IL content (%)	21.47 \pm 0.72	23.76 \pm 5.61	37.98 \pm 15.44	18.48 \pm 7.84	22.83 \pm 2.63	17.11 \pm 1.47	19.86 \pm 4.94
C16-C18 content (%)	99.6 \pm 0.57	97.17 \pm 2.29	66.84 \pm 8.95	54.27 \pm 1.65	100 \pm 0.00	49.91 \pm 0.64	46.01 \pm 2.47

oxygen concentrations (4 %, 21 % and 400 %).

Table 3-9

Biomass concentration (g L^{-1}), C16-C18 content (%), hydrocarbon and intracellular content (%) on DCW obtained in cultures of different *Botryococcus braunii* strains in the literature and in this study.

Strain	C16-C18 content (Wt% (%))	IL content (%)	HC content (%)	DCW (g L^{-1})		Reference
AP103	–	17 ± 0.87	13 ± 0.62	1.7 ± 0.12	Laboratory	Ashokkumar and Rengasamy 2012
AP103	73.21	19 ± 0.98	11 ± 0.56	1.8 ± 0.13	Open raceway	Ashokkumar and Rengasamy 2012
IPE 001 (Race B)	97	6.13 ± 0.26	40.37 ± 1.26	1.23	airlift bioreactor	Wang et al. 2014
LB 572 (Race A) control	89.44*	20**	19**	1**	Flasks	Ranga Rao et al. 2007
LB 572 (Race A) 34mM NaCl	90.75*	24-28**	20**	1.4**	Flasks	Ranga Rao et al. 2007
LB 572 (Race A) 85mM NaCl	81.43*	24-28**	15**	1.3**	Flasks	Ranga Rao et al. 2007
FACHB 357 (Race B) Nitrogen sufficient	93.47*	23.2**	19.4	20.66*	Single layer	Cheng et al. 2013
FACHB 357 (Race B) Nitrogen deficient	94.15*	17.3**	34.3	10**	Single layer	Cheng et al. 2013
BOT-22 (Race B)	66.84 ± 8.95	37.98 ± 15.44	26.02 ± 0.13	6.7 ± 0.43	airlift bioreactor	This study

*calculated from published data / **calculated from published graph

3.3.2 Effect of light intensity on fatty acids composition

As shown in Figure 3-8, at constant dilution rate of 0.178 d^{-1} , by increasing the light intensity from 50 to $500 \mu\text{mol photons m}^{-2} \text{ s}^{-1}$, weight percentage of oleic acid increased from $(44.52 \pm 8.89) \%$ to $(53.09 \pm 7.17) \%$ while that of palmitic acid and α -linoleic acid decreased from $(28.09 \pm 4.33) \%$ to $(19.91 \pm 2.29) \%$ and from $(22.11 \pm 4.32) \%$ to $(17.65 \pm 3.07) \%$, respectively. Wagenen et al., at 2012 reported that for *Nannochloropsis salina* the highest fatty acid content occurred in low-density cultures which received light above the saturating light intensity. In this study also the highest fatty acid content occurred at low-density cultures but at the low light intensity which could show that fatty acid content could occurred in low-density cultures.

By increasing the light intensity from 50 to $500 \mu\text{mol photons m}^{-2} \text{ s}^{-1}$, the PUFAs decreased from $(26.99 \pm 5.13) \%$ to $(22.06 \pm 3.79) \%$ as it was reported by Hu (2013) that polyunsaturated fatty acids (PUFAs), are inversely light intensity related. In this study it was shown that by increasing light intensity, palmitic acid and α -linoleic acid content was decreased while oleic acid content was increased. For diatom *Phaeodactylum tricornutum*, Molina Grima et al. (1999) reported high light intensity was increased the PUFA level. For green microalga *Parietochloris incise*, Solovchenko et al. (2008) reported the same trend.

As shown in Table 3-9, the intracellular lipid percentage on DCW at 50 and $500 \mu\text{mol photons m}^{-2} \text{ s}^{-1}$ were $(21.47 \pm 0.72) \%$ and $(23.76 \pm 5.61) \%$ while the sum of the C16 and C18 were $(99.6 \pm 0.57) \%$ and $(97.17 \pm 2.29) \%$, respectively. Although according to intracellular lipid percentage on DCW and the sum of the C16 and C18, this dilution rate could be suitable for biodiesel production but the biomass concentration is not good in the dilution rate of 0.178 d^{-1} .

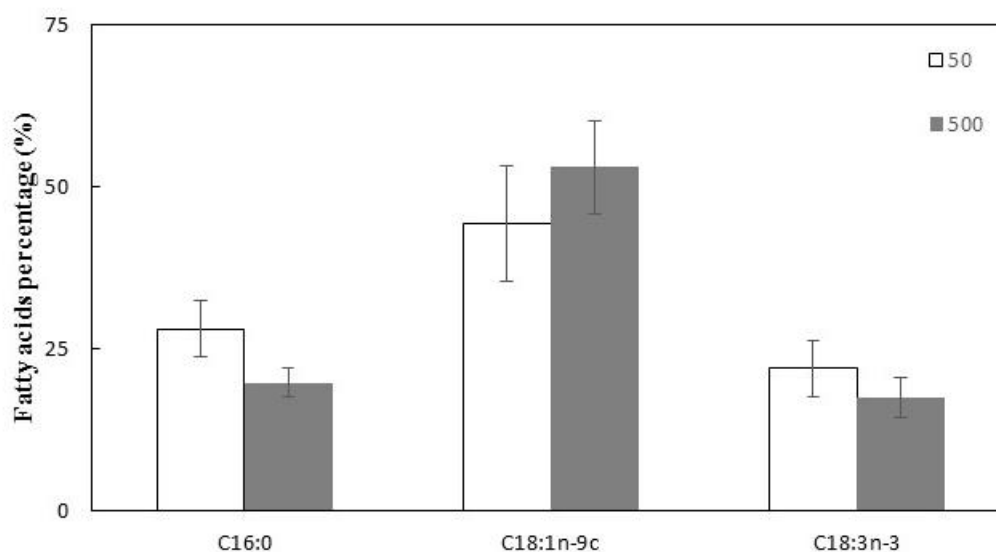


Figure 3-8: Comparison of main fatty acids compositions of *B. braunii* race B strain BOT-22 at two different light intensities (50 and 500 $\mu\text{mol photons m}^{-2} \text{s}^{-1}$). Other common parameters were: continuous light, dilution rate of 0.178 d^{-1} and 21 % dissolved oxygen concentration.

3.3.3 Effect of dilution rate on fatty acids composition

As shown in Figure 3-9, at constant light intensity of $500 \mu\text{mol photons m}^{-2} \text{s}^{-1}$, by doubling the dilution rate an increase in C16:0 and C18:0 was observed from $(19.91 \pm 2.29) \%$ to $(27.75 \pm 3.52) \%$ and $(1.07 \pm 0.16) \%$ to $(17.00 \pm 2.15) \%$, respectively, which could be a good point for biodiesel production. On the other hand the composition of fatty acids showed significant changes; behenic acid, erucic acid and nervonic acid appeared in the fatty acids components. The composition of oleic acid and α -linolenic acid (ALA) decreased sharply from $(53.09 \pm 7.17) \%$ to $(11.48 \pm 0.59) \%$ and $(17.65 \pm 3.07) \%$ to $(9.18 \pm 2.35) \%$, respectively. It seems in dilution rate of 0.178 d^{-1} , there was lack of nutrients for synthesis long chain fatty acids with more than 18 carbons in comparison of dilution rate of 0.357 d^{-1} .

As shown in Table 3-9, at $500 \mu\text{mol photons m}^{-2} \text{s}^{-1}$, the intracellular lipid percentage on DCW were at dilution rate of 0.178 d^{-1} and 0.357 d^{-1} were $(23.76 \pm 5.61) \%$ and $(37.98 \pm 15.44) \%$ while the sum of the C16 and C18 were $(97.17 \pm 2.29) \%$ and $(66.84 \pm 8.95) \%$, respectively.

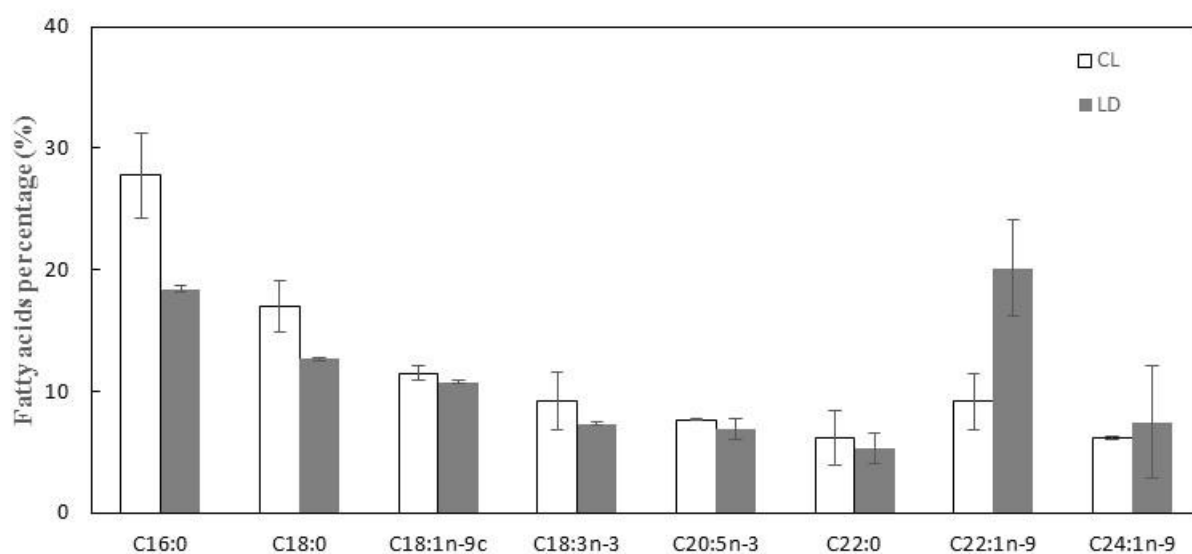


Figure 3-9: Comparison of main fatty acids compositions of *B. braunii* race B strain BOT-22 at two different light periods (continuous light and end of dark period. Other common parameters were: light intensity $500 \mu\text{mol photons m}^{-2} \text{s}^{-1}$, dilution rate of 0.357 d^{-1} and 21 % dissolved oxygen concentration.

3.3.5 Effect of dissolved oxygen concentration on fatty acids composition

Figure 3-10, shows in comparison of different dissolved oxygen concentrations (4 % and 21 %) at $500 \mu\text{mol photons m}^{-2} \text{s}^{-1}$, dilution rate of 0.357 d^{-1} and under continuous light, with 21 % of dissolved oxygen concentrations palmitic acid and stearic acid were increased to $(27.75 \pm 3.52) \%$ and $(17.00 \pm 2.15) \%$, respectively. The maximum of α -linoleic acid achieved at $500 \mu\text{mol photons m}^{-2} \text{s}^{-1}$, 4 % dissolved oxygen concentration, discontinuous light and dilution rate of 0.357 d^{-1} ($29.64 \pm 2.22) \%$ on dry cell weight). Under light and dark cycle (8 hours of light and 16 hours of dark), 0.357 d^{-1} , light intensity $500 \mu\text{mol photons m}^{-2} \text{s}^{-1}$ and 4% dissolved oxygen concentration, the main fatty acids composition was palmitic acid, oleic acid and α -linolenic acid (ALA) with a big difference among 21 % and 400 % dissolved oxygen concentration. According to figures 3-12 and 3-13, it seems 4 % of dissolved oxygen concentration in both continuous and discontinuous light period with dilution rate of 0.357 d^{-1} , is suitable for production of α -linolenic acid (ALA).

The intracellular lipid percentage on DCW at $500 \mu\text{mol photons m}^{-2} \text{s}^{-1}$ under continuous light with 4 % and 21 % dissolved oxygen concentrations, were $(18.48 \pm 7.84) \%$ and $(37.98 \pm 15.44) \%$ while the sum of the C16 and C18 were $(54.27 \pm 1.65) \%$ and $(66.84 \pm 8.95) \%$, respectively. The intracellular lipid percentage on DCW at $500 \mu\text{mol photons m}^{-2} \text{s}^{-1}$ under

discontinuous light with 4 %, 21 % and 400 % dissolved oxygen concentrations, were (22.83 ± 2.63) %, (17.11 ± 1.47) % and (19.86 ± 4.94) % while the sum of the C16 and C18 were (100 ± 0.00) %, (49.91 ± 0.64) % and (46.01 ± 2.47) %, respectively.

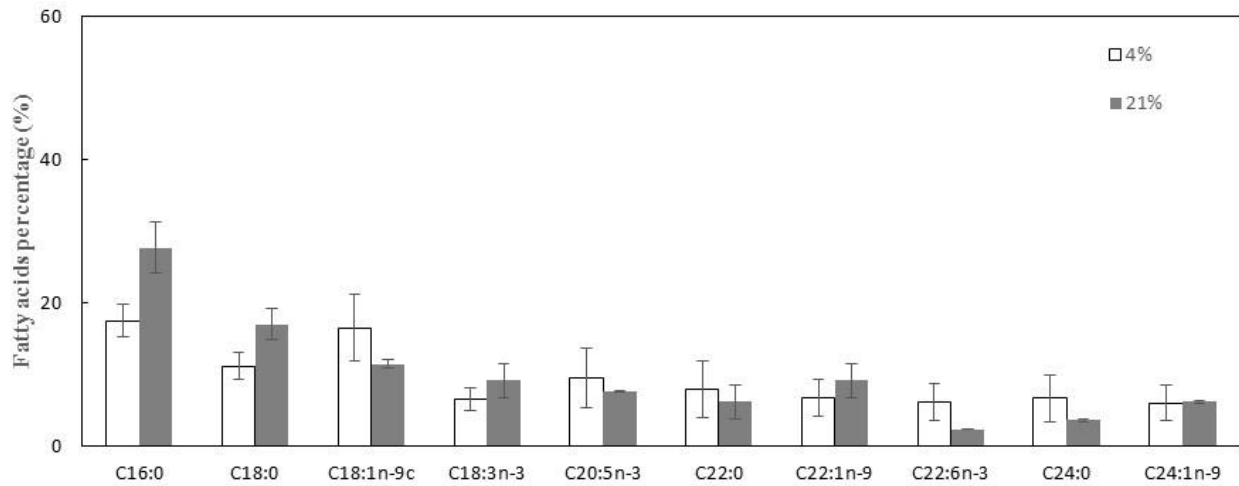


Figure 3-10: Comparison of main fatty acids compositions of *B. braunii* race B strain BOT-22 at two different dissolved oxygen concentrations (4 % and 21 %). Other common parameters were: continuous light, light intensity $500 \mu\text{mol photons m}^{-2} \text{s}^{-1}$ and dilution rate of 0.357 d^{-1} .

3.4 Physiological characterization

3.4.1 Photosynthetic activity

3.4.1.1 Photosynthetic activity in continuous cultures at two incident light intensities
 F_v/F_m value indicate stress in microalgae. It could be diagnose the integrity of the photosynthetic system and therefore the cellular metabolism. As Figure 3-11 shows, by increasing the light intensity from 50 to $500 \mu\text{mol photons m}^{-2} \text{s}^{-1}$, F_v/F_m value, was decreased from 0.79 ± 0.01 to 0.55 ± 0.02 which shows by increasing the light intensity the stress was increased. This behavior could be explained by cellular photoacclimation at $500 \mu\text{mol photons m}^{-2} \text{s}^{-1}$ which is also correlated with a change in pigment contents. The ETR_m was decreased from 55.52 ± 5.00 to 36.60 ± 5.37 and α was decreased from 0.25 ± 0.02 to 0.14 ± 0.01 , respectively, like other photosynthetic parameters.

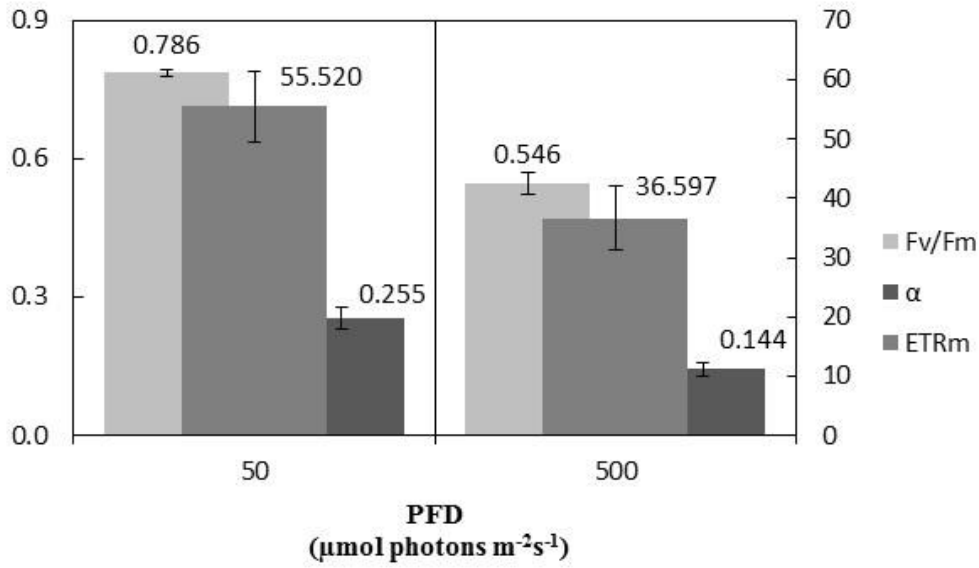


Figure 3-11: Photosynthetic factors (Fv/Fm, α and ETRm) of *B. braunii* race B strain BOT-22 at two incident PFDs 50 and 500 $\mu\text{mol photons m}^{-2}\text{s}^{-1}$.

3.4.1.2 Photosynthetic activity in continuous cultures at two incident dilution rates

Figure 3-12 demonstrates that by changing the dilution rate from 0.178 to 0.357 d^{-1} , the Fv/Fm value, was increased from 0.55 ± 0.02 to 0.64 ± 0.03 which implies by increasing the dilution rate the stress decreased. This could be a result of nutrient availability for the cells and well adaption of the cells to 500 $\mu\text{mol photons m}^{-2}\text{s}^{-1}$ light intensity. The ETRm remains about the same 36.60 ± 5.369 and 36.63 ± 2.68 , respectively while α was 0.14 ± 0.01 and 0.16 ± 0.02 , respectively.

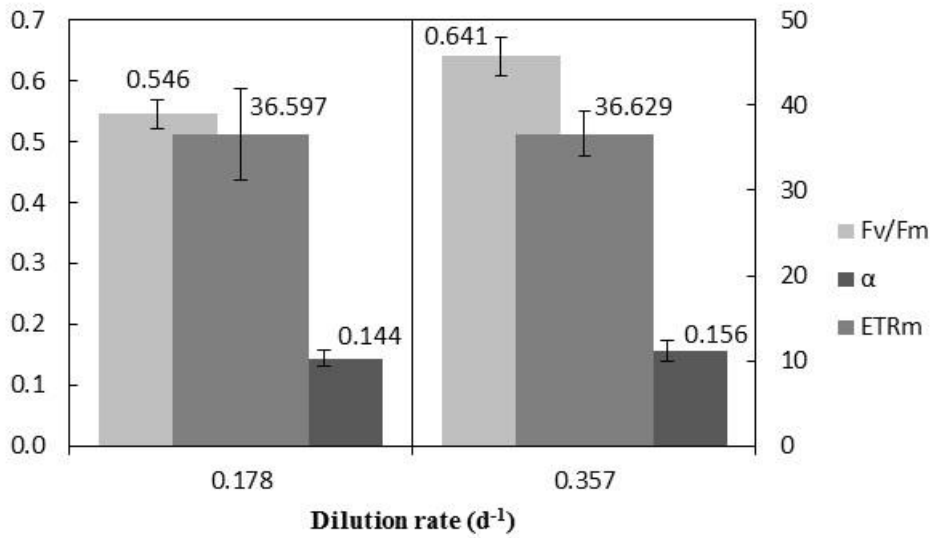


Figure 3-12: Photosynthetic factors (Fv/Fm, α and ETRm) of *B. braunii* race B strain BOT-22 at two incident dilution rates 0.178 and 0.357 d⁻¹.

3.4.1.3 Photosynthetic activity in continuous cultures under continuous illumination and at the end of a dark period under 21 % of dissolved oxygen

As Figure 3-13 shows, by changing the light period from continuous light to a prolonged dark period, Fv/Fm value, was increased from 0.64 ± 0.03 to 0.714 ± 0.05 which shows that after a dark period the stress is less. The ETRm was increased from 36.63 ± 2.68 to 48.93 ± 9.65 , respectively and α is also was increased from 0.16 ± 0.02 to 0.22 ± 0.05 .

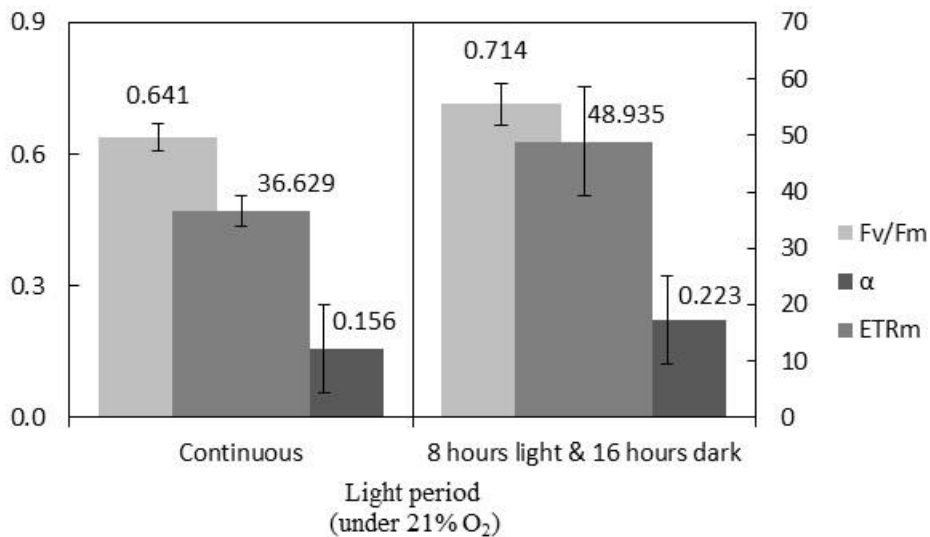


Figure 3-13: Photosynthetic factors (Fv/Fm, α and ETRm) of *B. braunii* race B strain BOT-22 under continuous light and light and at the end of a dark period with 21 % dissolved oxygen concentration.

3.4.1.4 Photosynthetic activity in continuous cultures under continuous illumination or at the end of a dark period under 4% of dissolved oxygen

Figure 3-14 demonstrates that in comparison of continuous light and at the end of a dark period under 4 % concentration of dissolved oxygen, Fv/Fm value, was increased from 0.65 ± 0.02 to 0.72 ± 0.01 which shows under discontinuous light the stress is less (the same result achieved under 21 % concentration of dissolved oxygen). The ETRm was increased from 45.68 ± 3.07 to 64.26 ± 9.71 , respectively and α was also increased from 0.17 ± 0.01 to 0.24 ± 0.02 .

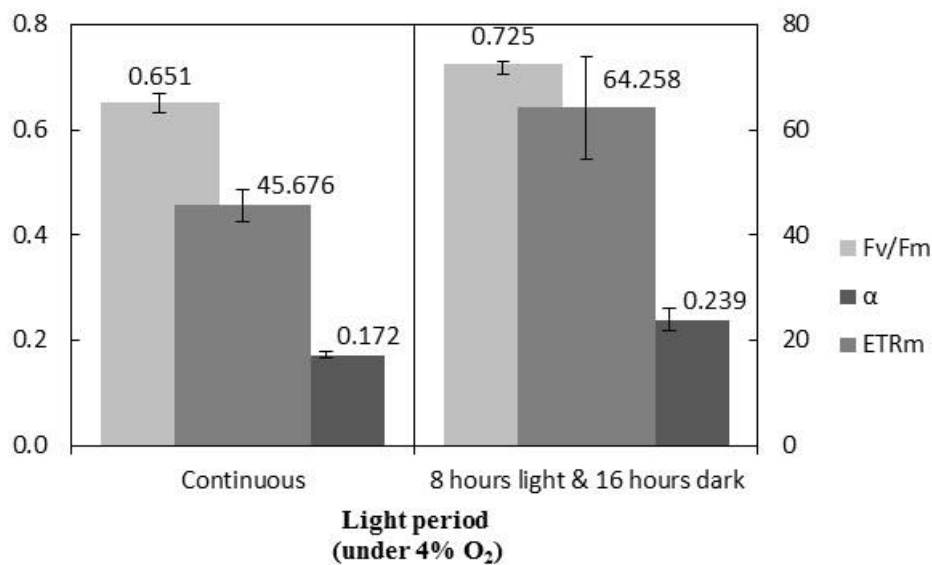


Figure 3-14: Photosynthetic factors (Fv/Fm, α and ETRm) of *B. braunii* race B strain BOT-22 under continuous light and at the end of a 16h dark period with 4 % dissolved oxygen concentration.

3.4.1.5 Photosynthetic activity in continuous cultures at the end of a 16 h dark period; in different dissolved oxygen concentrations

Figure 3-15 demonstrates that in comparison of two different level of dissolved oxygen (4 % and 21 %) under continuous light, Fv/Fm value, was about the same 0.65 ± 0.02 and 0.64 ± 0.03 which shows under 21 % of dissolved oxygen concentration the stress is more. The ETRm was decreased from 45.68 ± 3.07 to 36.63 ± 2.68 , respectively and α was also decreased from 0.17 ± 0.01 to 0.16 ± 0.02 .

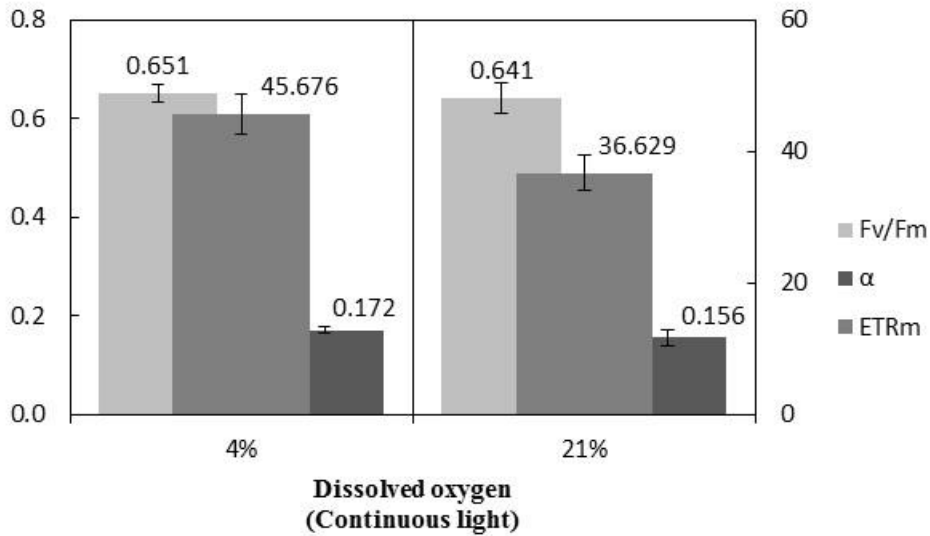


Figure 3-15: Photosynthetic factors (Fv/Fm, α and ETRm) of *B. braunii* race B strain BOT 22 under continuous light with 4 % and 21 % of dissolved oxygen concentration.

3.4.1.6 Photosynthetic activity in continuous cultures after a 16 h dark period ; in different dissolved oxygen concentrations

As Figure 3-16 demonstrates that by increasing the concentration of dissolved oxygen from 4 % to 21 % and 400 % under light and after a 16h dark period, Fv/Fm value, was decreased slightly. The values of Fv/Fm for 4 %, 21 % and 400 % changed from 0.72 ± 0.01 to 0.71 ± 0.05 and to 0.67 ± 0.05 which shows under discontinuous light by increasing the dissolved oxygen level from 21 % to 400 % the stress becomes more slightly. About the same level of Fv/Fm value in 4 % and 21 % of dissolved oxygen under no light in both cases, shows that cells were dark-adapted. The high Fv/Fm value, shows that the photosynthesis was almost inactive, and the Fv/Fm became dependent on the dark respiration pathway and the slight decrease of Fv/Fm demonstrates that the dark respiration is dropped during oxygen limitation. The ETRm was decreased from 64.26 ± 9.71 to 48.93 ± 9.65 and to 44.92 ± 11.34 , respectively and α was also decreased from 0.24 ± 0.02 to 0.22 ± 0.05 and to 0.18 ± 0.03 .

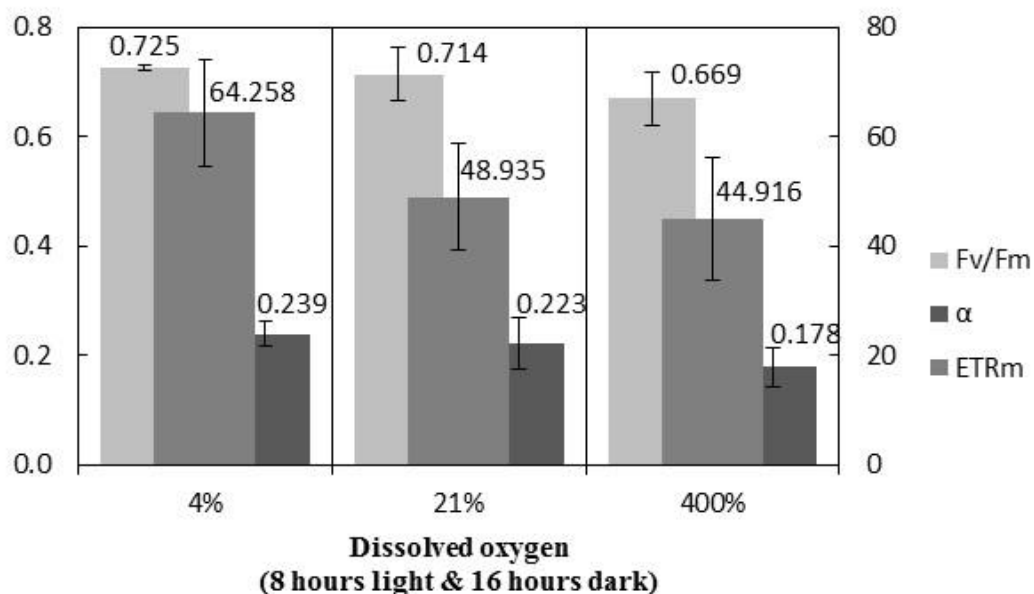


Figure 3-16: Photosynthetic factors (Fv/Fm, α and ETRm) of *B. braunii* race B strain BOT-22 under light and after a 16h dark incubation with 4 %, 21 % and 400 % of dissolved oxygen concentration.

3.4.2 Pigment composition

3.4.2.1 Pigment composition in continuous cultures at two incident light intensities
 The concentration of chlorophyll *a* and *b* at 50 $\mu\text{mol photons m}^{-2} \text{s}^{-1}$ and dilution rate of 0.178 d^{-1} , were $15.63 \pm 0.15 \text{ mg L}^{-1}$ and $8.35 \pm 0.10 \text{ mg L}^{-1}$ which were slightly decreased to $12.11 \pm 0.57 \text{ mg L}^{-1}$ and $6.20 \pm 0.38 \text{ mg L}^{-1}$, just after increasing the PFD from 50 to 500 $\mu\text{mol photons m}^{-2} \text{s}^{-1}$. It should be mentioned that the concentration of carotenoids remains almost constant in both conditions. Carotenoids are known to act as a protector of the photosynthetic device; therefore, the unchanged level of carotenoids at high PFDs indicates that there was no photoinhibition just after increasing the PFD.

Figure 3-17 shows at dilution rate of 0.178 day^{-1} under light intensity of 50 $\mu\text{mol photons m}^{-2} \text{s}^{-1}$ and 500 $\mu\text{mol photons m}^{-2} \text{s}^{-1}$, the mean of Chl *a* content was 11.18 ± 0.46 and $11.56 \pm 0.60 \text{ mg L}^{-1}$, respectively which were almost the same. At the same time the mean of Chl *b* concentration was also almost constant at 6.23 ± 0.30 and $6.50 \pm 0.37 \text{ mg L}^{-1}$. But the mean of carotenoids content with increase in light intensity from 50 to 500 $\mu\text{mol photons m}^{-2} \text{s}^{-1}$ has a

significant increase from 2.23 ± 0.11 and 4.47 ± 0.26 mg L⁻¹; i.e. about 95 % increase was observed. The ratio of Car / (Chl a + Chl b) was increased from 0.13 ± 0.01 to 0.25 ± 0.01 . Also by changing light intensity from 50 $\mu\text{mol photons m}^{-2} \text{s}^{-1}$ to 500 $\mu\text{mol photons m}^{-2} \text{s}^{-1}$, the color of the culture in PBR was changed from green to yellowish; the reason could be high increase of carotenoids value. The increase of carotenoids could be because of the protection role of carotenoids. In high photon fluxes there is photoacclimation for adopting cells photosynthetic antenna which causes a decrease on chlorophylls contents. This trend has been reported in a previous study on *B. braunii* BOT-22 (Sakamoto et al. 2012) and in another study of *B. braunii* BOT-144 race B strain (Baba et al. 2012).

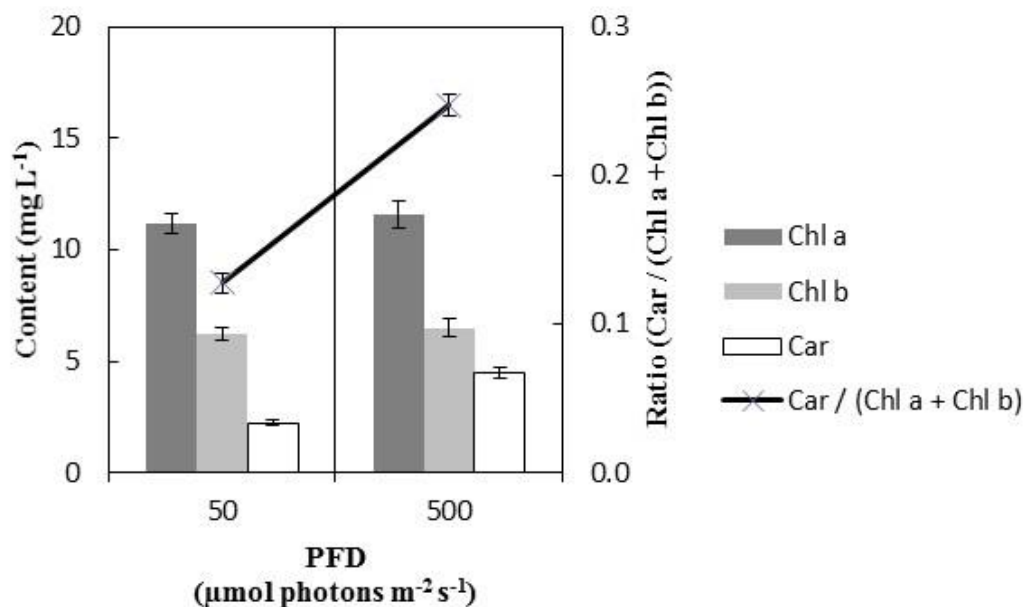


Figure 3-17: Pigment analysis (chlorophyll *a*, *b* and carotenoids) and ratio of carotenoids over total chlorophylls of *B. braunii* race B strain BOT-22 at two incident PFD 50 and 500 $\mu\text{mol photons m}^{-2} \text{s}^{-1}$.

3.4.2.2 Pigment composition in continuous cultures at two incident dilution rates

The concentration of Chl *a*, Chl *b* and carotenoids remained stable just after doubling the dilution rate which could be because that cells were already photoacclimated to 500 $\mu\text{mol photons m}^{-2} \text{s}^{-1}$ which was applied before changing the dilution rate.

Figure 3-18 demonstrates that with increasing dilution rate from 0.178 d⁻¹ to 0.357 d⁻¹ at constant light intensity (500 $\mu\text{mol photons m}^{-2} \text{s}^{-1}$), a large increase in mean value of Chl *a*, Chl *b* and carotenoid was observed. Chl *a* increased from 11.56 ± 0.60 to 26.27 ± 1.86 mg L⁻¹,

Chl *b* was increased from 6.50 ± 0.37 to 14.68 ± 1.05 mg L⁻¹ and carotenoid was increased from 4.47 ± 0.26 to 8.49 ± 0.84 mg L⁻¹, respectively. The ratio of Car / (Chl *a* + Chl *b*) was decreased from 0.25 ± 0.01 to 0.21 ± 0.01 . It seems that maybe at the dilution rate of 0.178 d⁻¹ there was lack of nutrients for cells. Also with ionic chromatography high rate of nitrate consumption was observed which prove the lack of nutrients (Table 3-1).

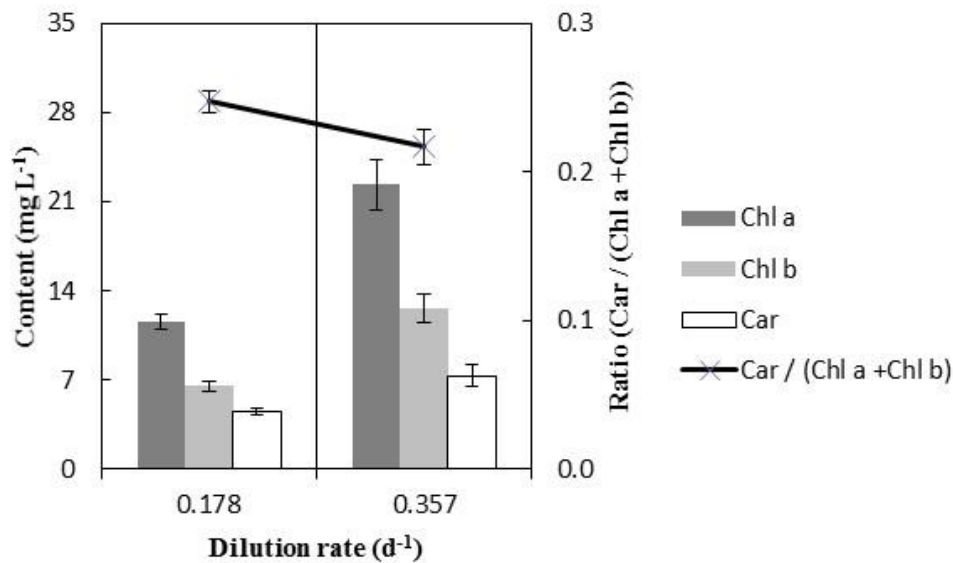


Figure 3-18: Pigment analysis (chlorophyll *a*, *b* and carotenoids) and ratio of carotenoids over total chlorophylls of *B. braunii* race B strain BOT-22 at two incident dilution rate 0.178 and 0.357 d⁻¹.

3.4.2.3 Pigment composition in continuous cultures under continuous illumination or after a 16h dark incubation under 21% of dissolved oxygen

In light-limiting conditions, the organism increases pigmentation, that is, increases the number of photosynthetic units and/or the size of light-harvesting complexes. Under supra-optimal irradiance, the pigmentation is reduced (Masojidek et al. 2013).

As Figure 3-19 shows, after a 16 h dark incubation in comparison with continuous illumination with 21% dissolved oxygen concentration, more concentration of Chl *a* and more Chl *b* was achieved; i.e. 30.66 ± 3.66 and 16.61 ± 2.12 mg L⁻¹, respectively while the carotenoid contents has about 1 mg L⁻¹ reduction from 8.49 ± 0.84 to 7.50 ± 1.01 mg L⁻¹. The color of culture media turned greener after the dark period. In dark incubation, the microalgae produced more pigments to compensate low light availability.

The ratio of Car / (Chl *a* + Chl *b*) was decreased from 0.21 ± 0.01 to 0.16 ± 0.01 . It seems that, after a prolonged dark period, due to having no light the chlorophylls were increased and also the color of the culture became greener than under continuous light.

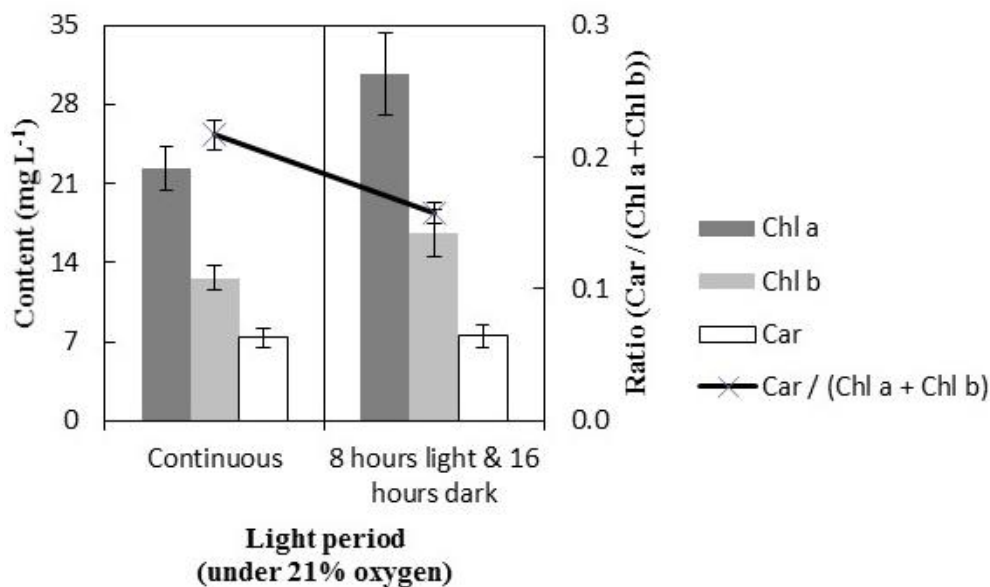


Figure 3-19: Pigment analysis (chlorophyll *a*, *b* and carotenoids) and ratio of carotenoids over total chlorophylls of *B. braunii* race B strain BOT-22 under continuous light and light and after a 16 h dark incubation with 21 % dissolved oxygen concentration.

3.4.2.4 Pigment composition in continuous cultures under continuous illumination or after a 16 h dark incubation under 4% of dissolved oxygen

Figure 3-20 shows between continuous and discontinuous light with 4 % concentration of dissolved oxygen, the content of Chl *a*, Chl *b* and carotenoid was decreased from 30.82 ± 0.98 , 16.80 ± 0.76 and 9.05 ± 0.47 to 28.34 ± 1.16 , 14.97 ± 0.90 and 7.53 ± 0.49 mg L⁻¹, respectively; while with 21% concentration of dissolved oxygen under discontinuous illumination higher contents of Chl *a*, Chl *b* and carotenoids were achieved in comparison of under continuous illumination. The ratio of Car / (Chl *a* + Chl *b*) was decreased from 0.19 ± 0.01 to 0.17 ± 0.00 .

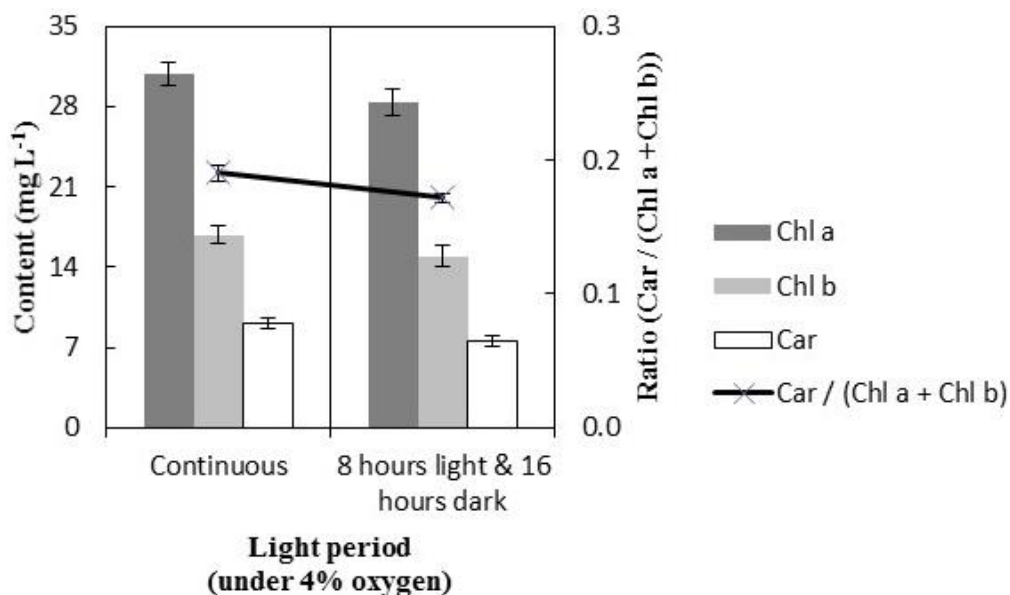


Figure 3-20: Pigment analysis (chlorophyll *a*, *b* and carotenoids) and ratio of carotenoids over total chlorophylls of *B. braunii* race B strain BOT-22 under continuous light and after a 16 h dark period with 4% dissolved oxygen concentration.

3.4.2.5 Pigment composition in continuous cultures under continuous illumination; in different dissolved oxygen concentrations

Figure 3-21 shows that under continuous light with increasing the level of dissolved oxygen from 4 % to 21 %, the content of Chl *a*, Chl *b* and carotenoids was decreased from 30.82 ± 0.98 , 16.80 ± 0.76 and 9.05 ± 0.47 to 26.27 ± 1.86 , 14.68 ± 1.05 and 8.49 ± 0.84 ; while on discontinuous light in comparison of different levels of oxygen, the highest Chl *a* and Chl *b* was achieved at 21 % of oxygen concentration. The ratio of Car / (Chl *a* + Chl *b*) had an increase after increasing the dissolved oxygen concentration from 4% to 21% from 0.19 ± 0.01 to 0.21 ± 0.01 , respectively.

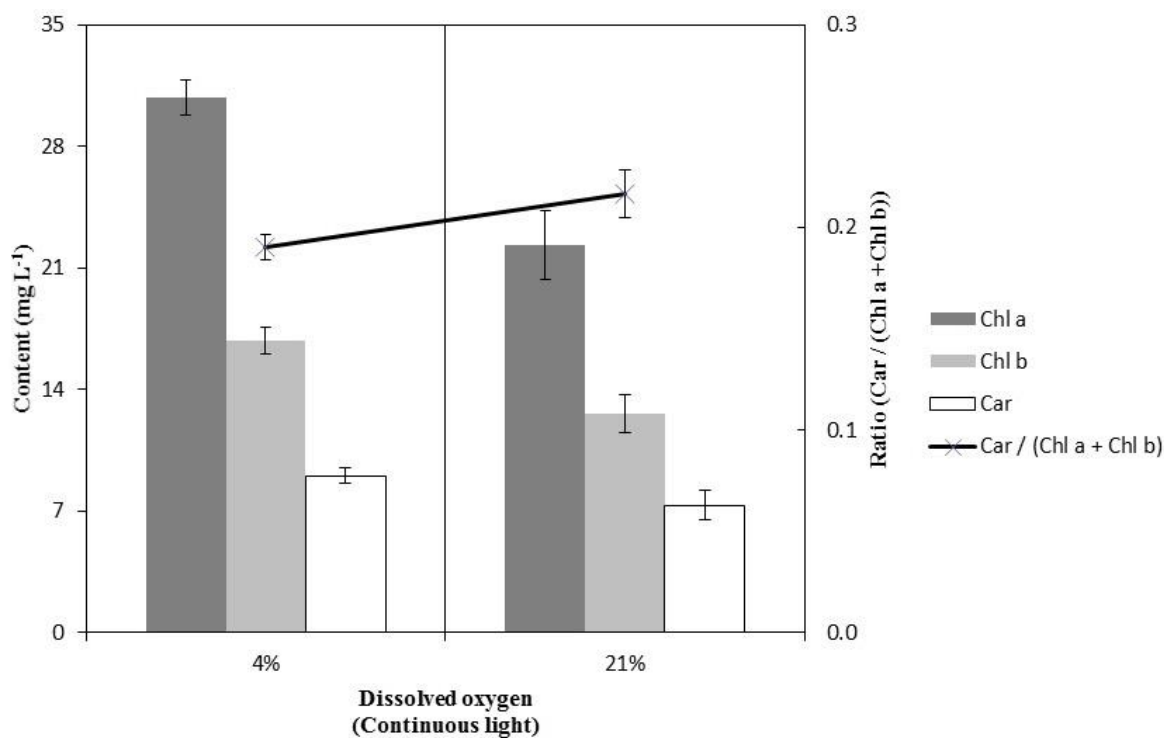


Figure 3-21: Pigment analysis (chlorophyll *a*, *b* and carotenoids) and ratio of carotenoids over total chlorophylls of *B. braunii* race B strain BOT-22 under continuous light with 4 % and 21 % of dissolved oxygen concentration.

3.4.2.6 Pigment composition in continuous cultures illumination and after a 16 h dark period in different dissolved oxygen concentrations

As Figure 3-22 demonstrates, comparing the three different concentrations of dissolved oxygen (4 %, 21 % and 400 %) after a 16 h dark period, the content of Chl *a* and Chl *b* achieved the highest value under 21 % of dissolved oxygen concentration (air) 30.66 ± 3.66 and 16.61 ± 2.12 mg L⁻¹, respectively; while the highest concentration of carotenoids was under oxygen saturation. It should be mentioned that the content of carotenoids under 4 % and 21 % of dissolved oxygen concentration remained almost constant (7.50 ± 1.01 mg L⁻¹) and there was a slight increase on the content of carotenoids at 400 % of oxygen (8.11 ± 0.58 mg L⁻¹). The ratio of Car / (Chl *a* + Chl *b*) by increasing the level of dissolved oxygen from 4 % to 21 % was decreased from 0.17 ± 0.00 to 0.16 ± 0.01 but after increasing the concentration

of dissolved oxygen from 21 % to 400 % the ratio of Car / (Chl *a* + Chl *b*) was increased from 0.16 ± 0.01 to 0.22 ± 0.01 .

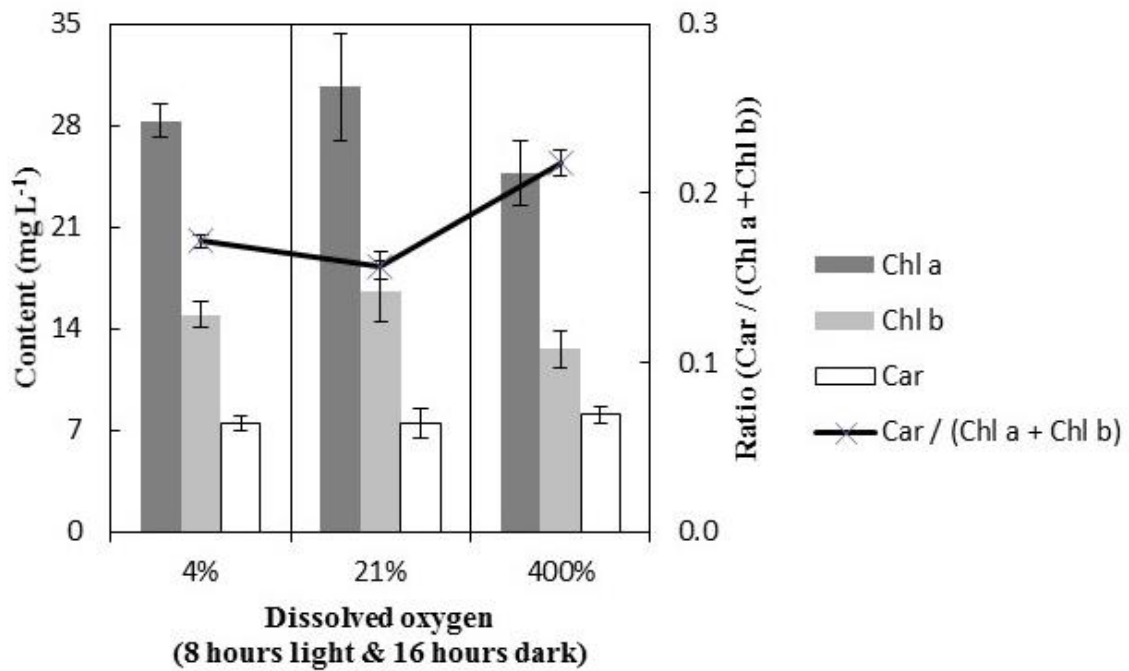


Figure 3-22: Pigment analysis (chlorophyll *a*, *b* and carotenoid) and ratio of carotenoids over total chlorophylls of *B. braunii* race B strain BOT-22 at the end of a 16 h dark period with 4%, 21% and 400% of dissolved oxygen concentration.

Chapter 4: Specific light supply rate and culture behavior

Chapter 4: Specific light supply rate and culture behavior

To investigate the effect of light supply to the *B. braunii* BOT-22 microalgae, the kinetics of biomass and hydrocarbon productions were studied after a PAR-PFD transition from 50 to 500 $\mu\text{mol photons m}^{-2} \text{s}^{-1}$ and a dilution rate transition from 0.178 to 0.357 d^{-1} . The analysis included both transient and steady states responses to such changes in culture conditions.

4.1 Evolution of r_{EX} and productivities during the transient phases

In various studies different light intensities were used for growth of *Botryococcus braunii* BOT-22 and the range of the light intensities which were mainly used was up to 300 $\mu\text{mol photons m}^{-2} \text{s}^{-1}$. The available information on photosynthetic activity for continuous cultures of *B. braunii* in PBRs is little while it could affect the biomass productivity and physiology of cells.

To investigate the effect of light supply to the microalgae colonies, the production of biomass and hydrocarbon and photosynthetic parameters of *Botryococcus braunii* BOT-22 was studied at two PAR-PFD, 50 and 500 $\mu\text{mol photons m}^{-2} \text{s}^{-1}$, and two dilution rates, 0.178 and 0.357 d^{-1} . These culture conditions are specified as A, B and C (Table 3-1). The study took into account both transient and steady states.

Culture medium was 6N-6P-AF6, pH was 6.6 ± 0.2 , rate of CO_2 for pH adjustment was 3 mL min^{-1} , rate of aeration was 60 mL min^{-1} and dissolved oxygen concentration was 21 % (air).

The r_{EX} can be approximated from the values of the incident PFD on the surface of the photobioreactors and the biomass concentrations (Cornet and Dussap 2009). Indeed, in our experimental conditions, the biomass concentrations were higher than 1 g L^{-1} , corresponding to full light absorption in which r_{EX} calculations could be approximate as the ratio of incident PFD on biomass concentration (Ogbonna and Tanaka 2000). As reported in Figure 4-1, increasing light intensity at the same dilution rate of 0.178 d^{-1} induced an increase of the biomass and hydrocarbon productivities up to more than three times. Then increasing the incident PFD induced a transient increase of the r_{EX} followed by an asymptotic decrease up to a steady state value of 0.35 $\text{mol photon g X}^{-1} \text{d}^{-1}$ (Figure 4-1). This value is about twice that observed for the steady state culture at 50 $\mu\text{mol photons m}^{-2} \text{s}^{-1}$. The same trend was observed

in hydrocarbon production, i.e. increase of the hydrocarbon productivity related to a r_{EX} decrease.

The drop of the residence time from 3.9 to 1.9 days was used as a way to increase the light availability through increasing the dilution of the culture. The Figure 4-1 shows that doubling the dilution rate at a constant light intensity of $500 \mu\text{mol photons m}^{-2} \text{s}^{-1}$ induced a twofold increase in the biomass productivity. However after this sudden shift-up in dilution rate, the specific light supply rate was only reduced by 28 %. This behavior could be attributed to a fast kinetic of adaptation, by contrast with that induced by the sudden increase of the incident photon flux density. As the biomass concentration was relatively stable, it could be concluded that, in our experimental conditions, the cultures were light limited.

The changes in light availability seem characterized by a transient response not so complex as that observed in microalgae cultures, such as *Chlorella vulgaris*, exposed to changes in nitrogen availability (Massie et al. 2013). However, the small oscillations in the biomass concentration observed during the two weeks following the change in dilution rate have to be confirmed and analyzed in a larger photobioreactor, as an impact of the small sample size from a 269 mL continuous culture on the accuracy of the data cannot be excluded.

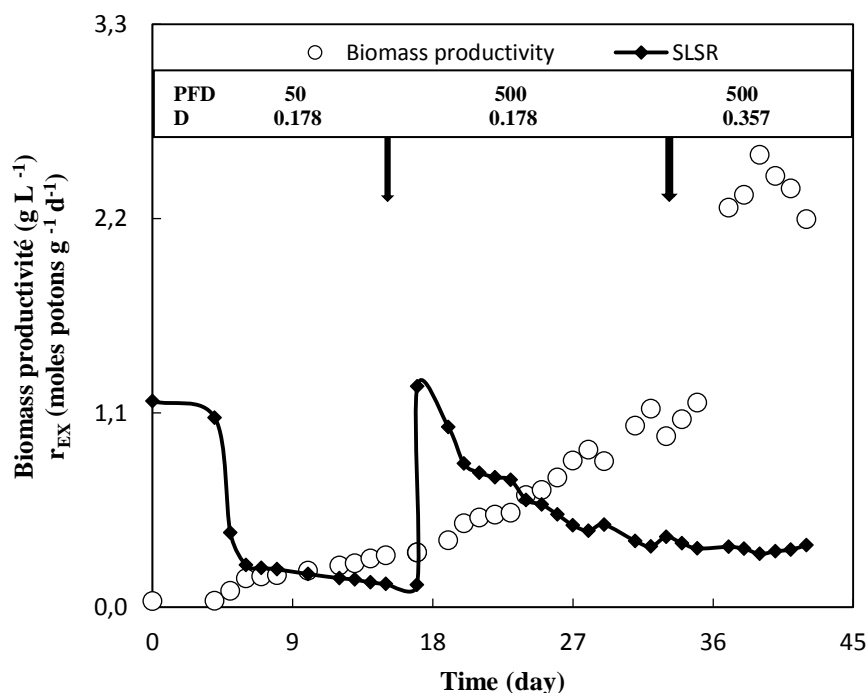


Figure 4-1: Evolution of r_{EX} (specific light supply rate) and biomass productivity of a *B. braunii* culture after changing the incident PFD on surface of the photobioreactor, from 50 to $500 \mu\text{mol photons m}^{-2} \text{s}^{-1}$ and the dilution rate from 0.178 d^{-1} to 0.357 d^{-1} . Conditions A, B and C as described in Table 3-1.

The Figure 4-2 shows the relation between r_{EX} and biomass productivity. A r_{EX} value of about 0.28 mole photons $gX^{-1} d^{-1}$ seems optimal. As hydrocarbon production was mainly growth associated, the same r_{EX} value was found for maximal hydrocarbon productivities.

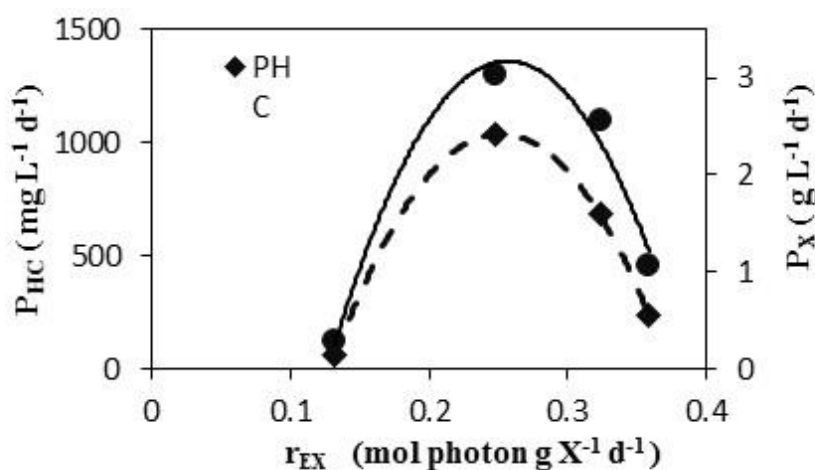
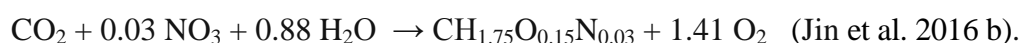


Figure 4-2: Biomass productivity of *B. braunii* in continuous cultures as a function of the r_{EX} (specific light supply rate) value in continuous cultures.

Using the Pirt model (Pirt et al. 1980) based on the stoichiometric reaction equations for the formation of biomass, authors generally agree for a theoretical biomass yield of 1.5 g mol photons⁻¹ for microalgae cultures on nitrate. Based on the previously determined elemental composition of *Botryococcus braunii* (Watanabe et al. 2014), a stoichiometric equation for the global biomass was calculated as :



Usual measured values of the quantum yield are about 0.1 mol oxygen per mol photons, when a maximal theoretical value of 1.25 based on the requirement of 8 moles of photons for reduction of 1 mole of CO_2 , in absence of photo- or chloro-respiration (Cournac et al. 2002). The C-mol molecular weight of *B. braunii* biomass is 16.6 $gmol^{-1}$ highly different from the values obtained for other green microalgae, such as *Chlorella* (Zijffers et al. 2010). Then 14.1 moles photons are theoretically used for 1 mole of biomass, so a biomass yield of 1.18 g mol photons⁻¹ based on the stoichiometric reaction.

An apparent biomass yield on light supply Y_{xEobs} of 1.1 g mol photons⁻¹ was deduced from the highest values of biomass productivity obtained during this study, close to the value predicted by the stoichiometric equation. This value seems relatively high, when compared to published data. Indeed, values of 0.78 and 0.75 g mol photons⁻¹ were observed for *D.*

tertiolecta and *C. sorokiniana* cultures, respectively (Cuaresma et al. 2009; Zijffers et al. 2010). But the present study addressed a colonial microalga, with an extracellular accumulation of the product, the liquid hydrocarbons mainly composed of C₃₄H₅₈ (Watanabe et al. 2014). Taking into account the 26 % hydrocarbons was trapped within the colony matrix leads to an apparent cellular yield on light supply of 0.8 g mol photons⁻¹, closer to data obtained with other green microalgae (Zijffers et al. 2010). The relatively high biomass and hydrocarbon yields on light energy seem to compensate the high residence time, 2.8 d of this oily microalga.

To bring more insight on the physiological behavior of the *B. braunii* cultures, the evolution of some photosynthetic characteristics were investigated as a function of the specific light supply rate.

4.2 Evolution of r_{EX} and photosynthetic characteristics during the transient phases

In our experimental conditions, the cultures were not bleached, except a change in the culture color, from green to yellowish, after increasing the light intensity. The occurrence of a photo-acclimation mechanism could be assumed based on changes in chlorophyll or carotenoid contents as a function of fluctuation in the photon flux densities. Sforza et al. (2015) reported that the Chl *a* content in *Nannochloropsis* cultures decreased according the specific increase of the light supply rate, when the ratio carotenoid over chlorophyll was found stable up to 0.5 mmol photons g⁻¹ d⁻¹.

Figure 4-3 shows that, in our experimental conditions, the ratio of Chl *a*/Chl *b* remained relatively stable. By contrast, increasing the light intensity from 50 μmol photons m⁻² s⁻¹ to 500 μmol photons m⁻² s⁻¹ at a constant dilution rate of 0.178 d⁻¹, induced a huge increase of the ratio carotenoid over chlorophyll *a+b* was increased (Figure 4-4). Its rise seems to be related to the parallel decay of the r_{EX} . The change in this pigment ratio seems to be related to the protective role of carotenoids.

By contrast, the ratio of carotenoid over chlorophyll *a+b* seemed relatively unaffected by the twofold rise of the dilution rate up to 0.357 d⁻¹ at constant light intensity of 500 μmol photons m⁻² s⁻¹. Indeed, the biomass concentration, then the self-shading process, was relatively constant during this period.

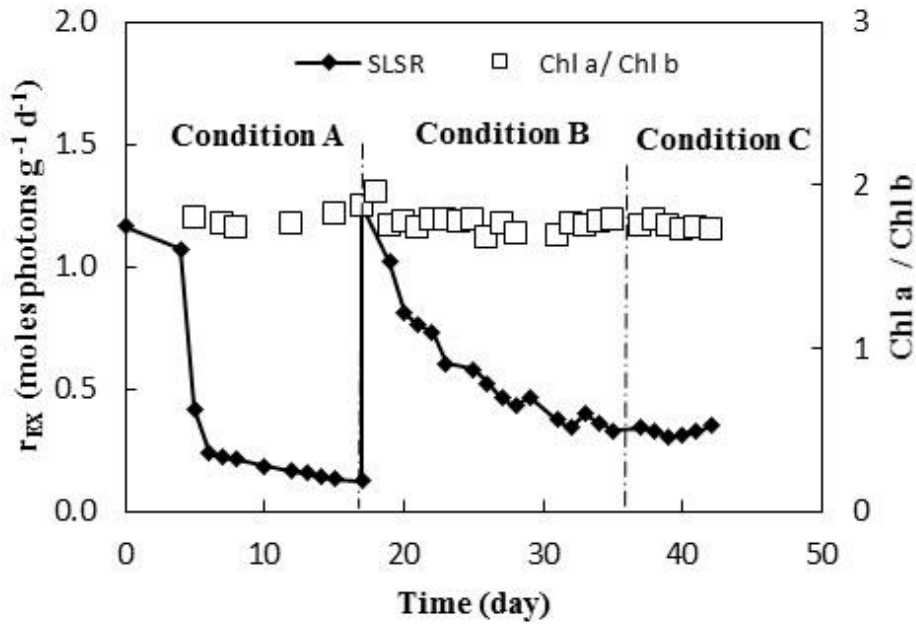


Figure 4-3: Evolution of r_{EX} (specific light supply rate) and photosynthetic pigment composition: ratio of Chl *a* over Chl *b* (w:w) of *B. braunii* race culture after changing the incident PFD on surface of the photobioreactor, from 50 to 500 $\mu\text{mol photons m}^{-2} \text{s}^{-1}$ and the dilution rate from 0.178 d^{-1} to 0.357 d^{-1} .

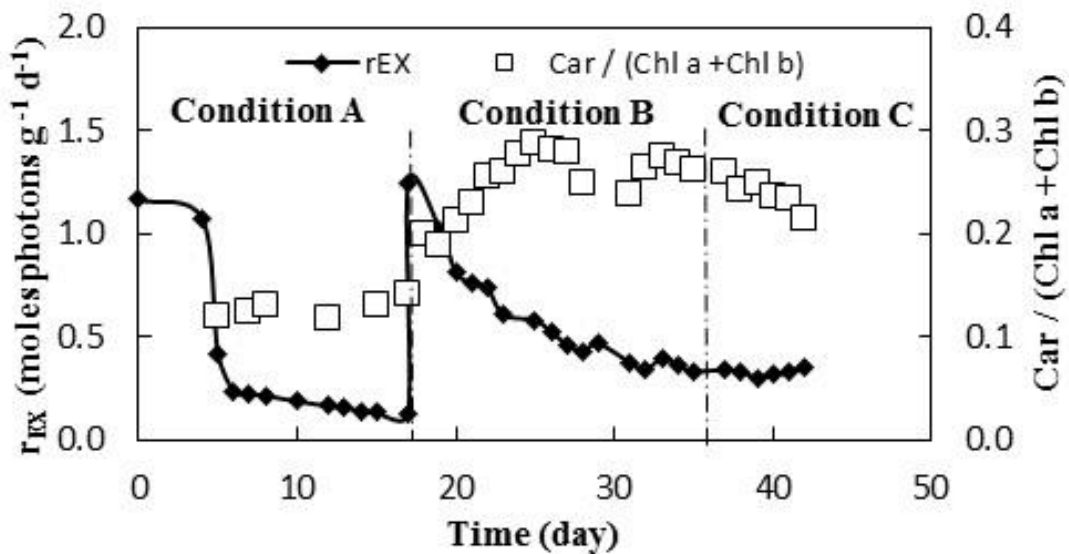


Figure 4-4: Evolution of r_{EX} (specific light supply rate) and photosynthetic pigment composition: ratio of carotenoids over total chlorophylls (w:w) of *B. braunii* race culture after changing the incident PFD on surface of the photobioreactor, from 50 to 500 $\mu\text{mol photons m}^{-2} \text{s}^{-1}$ and the dilution rate from 0.178 d^{-1} to 0.357 d^{-1} .

It should be mentioned that by increasing the light intensity from 50 $\mu\text{mol photons m}^{-2} \text{s}^{-1}$ to 500 $\mu\text{mol photons m}^{-2} \text{s}^{-1}$ the mean of carotenoid content has a significant increased (about 95

% increasing was observed from 2.229 ± 0.113 and 4.471 ± 0.263 mg L⁻¹). By increasing the light intensity the color of the culture in PBR was changed from green to yellowish; the reason could be high increase of carotenoid value. The increase of carotenoids could be because of the protection role of carotenoids. Carotenoid content of this strain is considerable even in comparison with the well-known source of carotenoid producers such as *Dunaliella salina* (Pour Hosseini et al. 2017). In high photon fluxes there is photoacclimation for adopting cells photosynthetic antenna which causes a decrease on chlorophylls contents. The mean of chlorophyll content (*a* and *b*) was about the same by changing light intensity. Mean of Chl *a* was 11.184 ± 0.465 and 11.565 ± 0.604 mg L⁻¹, respectively; which was about the same; at the same time mean of Chl *b* content also was at the same level which was 6.232 ± 0.296 and 6.504 ± 0.37 mg L⁻¹, respectively.

A Fv/Fm decrease of the maximum quantum yield, Fv/Fm, is generally considered as an indication of a cellular stress in photosynthetic cells. As shown in Figure 4-5, increasing the light intensity from 50 to 500 $\mu\text{mol photons m}^{-2} \text{s}^{-1}$, induced a fast decrease of the PSII activities based on the ratio of Fv/Fm. The new Fv/Fm value was relatively stable over the 17 days of the culture from the transient to the new steady state. Then no apparent relation between the Fv/Fm and the asymptotic evolution after a transient increase of r_{EX} . In the study reported by Sforza et al. (2015) on *Nannochloropsis*, the value of Fv/Fm was also stable up to 0.5 mol photons g⁻¹ d⁻¹. At higher r_{EX} values, these authors reported a decrease of Fv/Fm. The progressive increase of Fv/Fm observed after the twofold increase of the dilution rate was not associated with an evolution of r_{EX} value. There is no increase in biomass concentration during this transient period and then a self-shading process could not explain the partial recovery of the Fv/Fm. It could be related to the twofold drop in the residence time in the continuously illuminated photobioreactor.

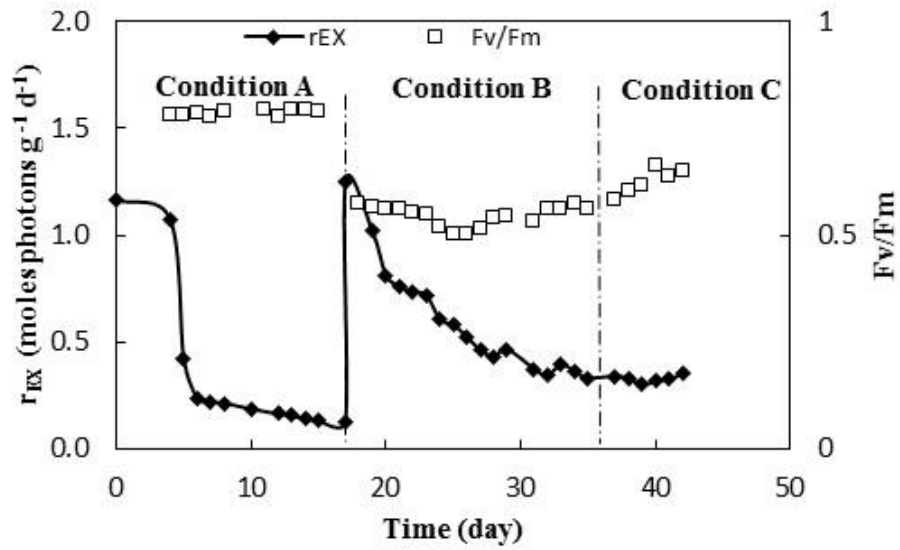


Figure 4-5: Evolution of r_{EX} (specific light supply rate) and photosynthetic activities (F_v/F_m) of *B. braunii* BOT-22 culture after changing the incident PFD on surface of the photobioreactor, from 50 to 500 $\mu\text{mol photons m}^{-2} \text{s}^{-1}$ and the dilution rate from 0.178 d^{-1} to 0.357 d^{-1} . Conditions A, B and C as described in Table 3-1.

The analysis of light-curve data obtained with the water-pam system confirmed that there was no obvious photo-inhibitory process induced by the sudden changes in irradiance or dilution rate. Moreover, the maximal values of electron transport rate (ERT_{max}) and photosynthesis efficiency (α) seem relatively stable on the range of the r_{EX} values applied to the *B. braunii* cultures (Figure 4-6).

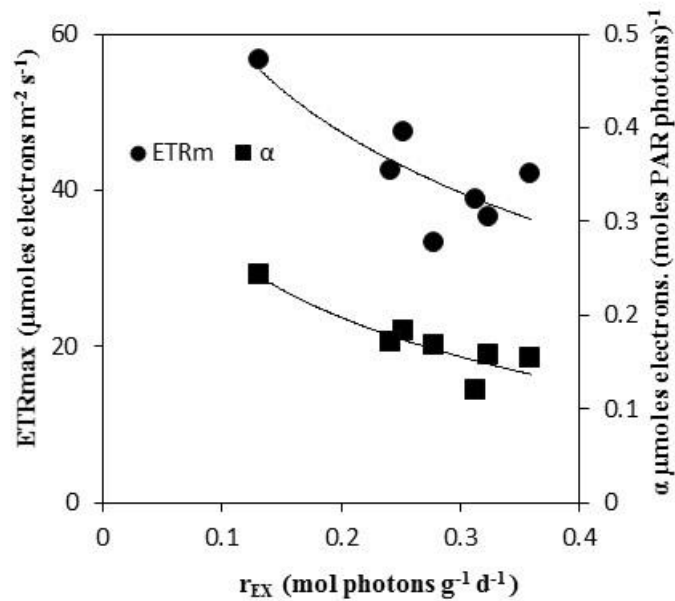


Figure 4-6: Photosynthetic characteristics of a *B. braunii* culture as a function of the r_{EX} (specific light supply rate) value in the continuous cultures.

This preliminary study of the transient phase suggests that the response of *B. braunii* continuous cultures, in nutrient-sufficient conditions, to changing incident PFD on the surface of the photobioreactor or changing the dilution rate could be an adaptation of its cell population and pigmentation in order to get a stable value in a narrow range of specific light rate supply (Figure 4-2). This study confirms the interest of chemostat for understanding the physiological adaptation of microalgae cultures, through the analysis not only of successive steady states, but also of the transients between them.

4.3 Nutrient consumption

4.3.1 Dissolved inorganic carbon consumption

The mean of residual dissolved inorganic carbon concentration under 50 and 500 $\mu\text{mol photons } m^{-2} s^{-1}$ at dilution rate of 0.178 d^{-1} was $40.0 \pm 3.5 \text{ mg } L^{-1}$ and $90.0 \pm 5.5 \text{ mg } L^{-1}$, respectively. The mean of residual inorganic carbon concentration at 500 $\mu\text{mol photons } m^{-2} s^{-1}$ and dilution rate of 0.357 d^{-1} was $61.7 \pm 3.7 \text{ mg } L^{-1}$ which confirms there was enough inorganic carbon in the culture medium for cells to be used. Growth under high level of

inorganic carbon concentration may causes increasing in nitrate, nitrogen, phosphate and phosphorus consumption by microalgae.

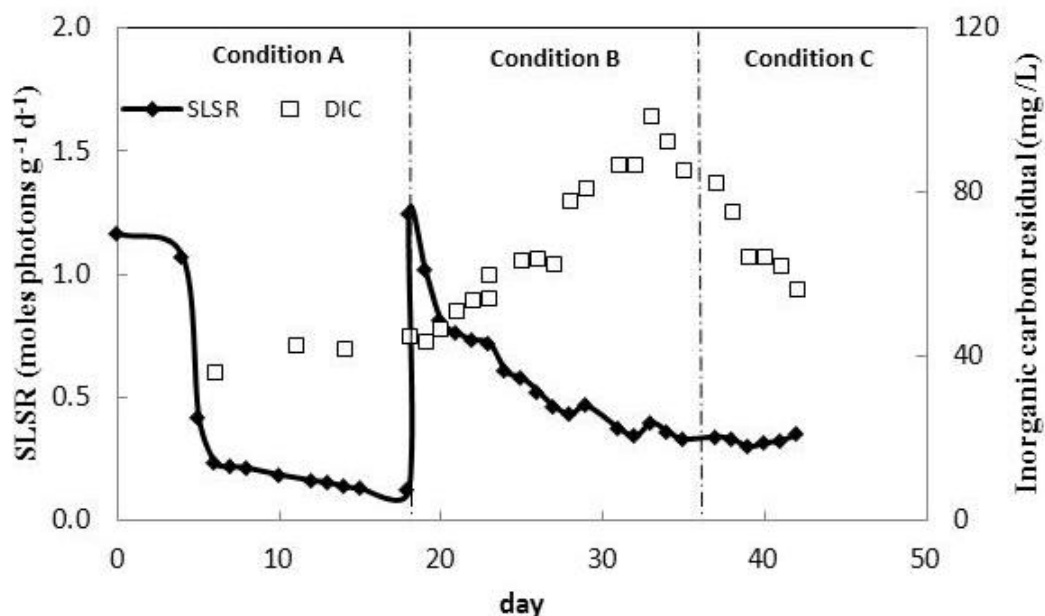


Figure 4-7: r_{EX} (specific light supply rate) and residual inorganic carbon concentration (mg L^{-1}) inside the PBR for cultivating *B. braunii* race B strain BOT-22 at two incidents PFD 50 and 500 $\mu\text{mol photons m}^{-2} \text{s}^{-1}$.

4.3.2 Nitrate and phosphate consumption

As shown in Figures 4-8 and 4-9, by increasing the light intensity from 50 to 500 $\mu\text{mol photons m}^{-2} \text{s}^{-1}$ at dilution rate of 0.178 d^{-1} , while the mean of dry weight increased from $1.64 \pm 0.09 \text{ g L}^{-1}$ to $5.99 \pm 0.42 \text{ g L}^{-1}$, respectively, the rate of nitrogen and phosphorus consumption increased. Where the inlet of nitrate and phosphate in culture medium was 629.83 and 58.23 mg L^{-1} , respectively, in the out let of the PBR under 50 $\mu\text{mol photons m}^{-2} \text{s}^{-1}$ light intensity the mean concentration of nitrate and phosphate was 142.36 ± 21.11 and $38.4 \pm 5.1 \text{ mg L}^{-1}$ and under 500 $\mu\text{mol photons m}^{-2} \text{s}^{-1}$ light intensity was 100.89 ± 22.18 and $8.5 \pm 0.5 \text{ mg L}^{-1}$, respectively. According to the high rate of nitrate and phosphate consumption under the light intensity of 500 $\mu\text{mol photons m}^{-2} \text{s}^{-1}$ (as shown with results), the dilution rate increased up to twice (changing condition B to C).

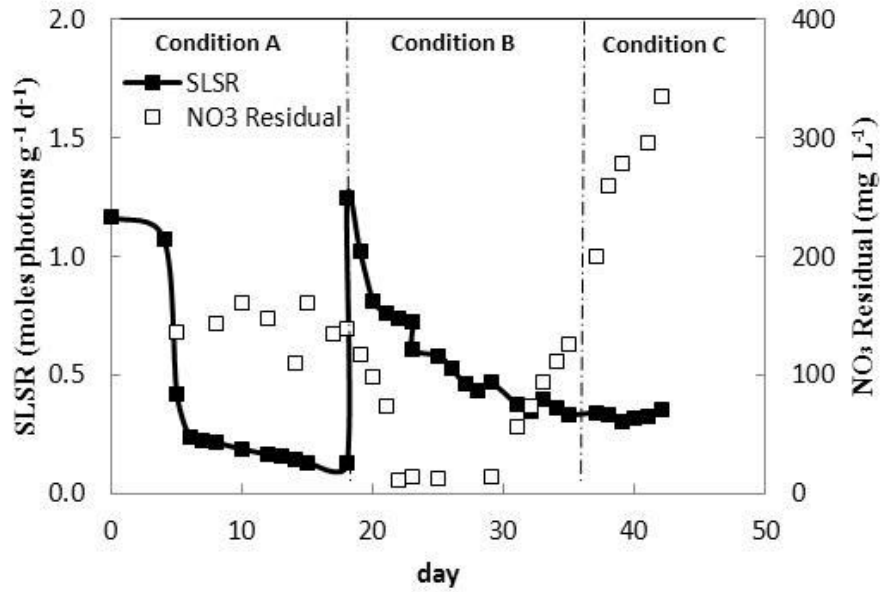


Figure 4-8: r_{EX} (specific light supply rate) and residual nitrate concentration (mg L^{-1}) inside the PBR for cultivating *B. braunii* race B strain BOT-22 at two incidents PFD 50 and $500 \mu\text{mol photons m}^{-2} \text{s}^{-1}$.

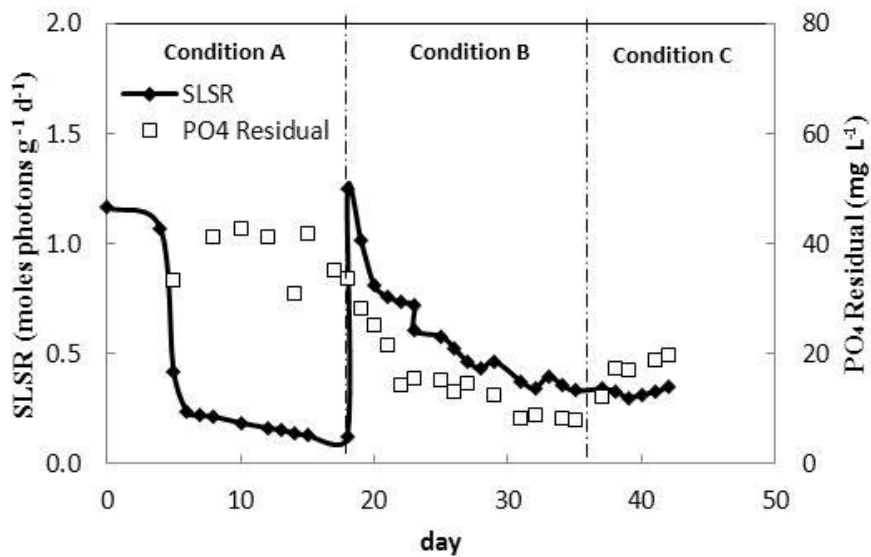


Figure 4-9: r_{EX} (specific light supply rate) and residual phosphate concentration (mg L^{-1}) inside the PBR for cultivating *B. braunii* race B strain BOT-22 at two incidents PFD 50 and $500 \mu\text{mol photons m}^{-2} \text{s}^{-1}$.

Conclusion– Perspectives

High hydrocarbon productivities were obtained with *B. braunii* cultures in small flat panel photobioreactors. Choosing appropriate criteria in irradiation, photo period, dilution rate, dissolved oxygen concentration of photoautotrophic continuous cultures of *Botryococcus braunii* strain BOT-22 (Race B) on biomass and hydrocarbons production and fatty acids compositions in a controlled photobioreactor can facilitate the interpretation of different related results.

The continuous cultures were investigated at chemostat mode and two different dilution rates of 0.178 d⁻¹ and 0.356 d⁻¹, under continuous irradiation at two different light intensities, 50 and 500 μmol photons m⁻² s⁻¹. According to photoperiod, the effect of continuous light condition was compared with light and dark cycle (8h light and 16h dark). The effect of dissolved oxygen concentrations during continuous and discontinuous illumination were also investigated. Light intensity is a common factor for comparing different works. The usefulness of r_{EX} as a function of light intensity, penetration depth and biomass concentration was also evaluated in this study.

Results demonstrated linear relation between the biomass and the hydrocarbon productivity of *B. braunii* BOT-22, under continuous light while light intensity has a significant effect on biomass production, more than on hydrocarbon content. By the increase of biomass concentration, hydrocarbon productivity enhanced. Moreover, the dilution rate is the main parameter of growing *B. braunii* BOT-22 in continuous culture. Therefore, determining the right dilution rate is very important for controlling and boosting biomass growth, hydrocarbons production and fatty acids compositions.

A prolonged dark period (16 hours duration) did not have any effect on the hydrocarbon content, but negatively affected the biomass concentration and therefore, hydrocarbons productivity. More unexpectedly, the dark period contributes to the maximum level of hydrocarbon content (27% reported in the present work).

During the dark period, *B. braunii* BOT-22 consume oxygen slowly to grow relatively. Furthermore, oxygen limitation during dark period without affecting hydrocarbon content, is detrimental to the biomass concentration.

High light intensity along with the higher dilution rate (500 μmol photons m⁻² s⁻¹, 0.357 d⁻¹ and 21 % dissolved oxygen concentration) led to overproduction of hydrocarbon more than 10 times in comparison with the initial condition (50 μmol photons m⁻² s⁻¹, 0.178 d⁻¹ and 21 % dissolved oxygen concentration).

Additionally, in this study, the maximum biomass volumetric productivity of *B. braunii* BOT-22 obtained was $3.07 \pm 0.2 \text{ g L}^{-1} \text{ d}^{-1}$ with a corresponding hydrocarbons productivity of $879.9 \pm 132.56 \text{ mg L}^{-1} \text{ d}^{-1}$. This is more than three times of the maximum amount reported till date on *B. braunii* species, cultivated in photobioreactor.

It should be mentioned that the unbalance between available nutrients such as light, nitrate, phosphate and dissolved inorganic carbon, seems to be a noticeably limiting factor that could be taken into consideration for optimizing biomass concentration and hydrocarbons production of *B. braunii*. Insufficient nutrients globally slowed the uptake of nutrients.

The main fatty acids of *B. braunii* race B strain BOT-22, were oleic acid, palmitic acid, α -linoleic acid, euric acid and stearic acid.

Under nutrient sufficient conditions, the light supply was shown to be the limiting factor. A tenfold increase in the PFD on the surface of the photobioreactor resulted in a twofold increase in the specific light supply rate (r_{EX}). A twofold increase in the dilution rate induced an increase in the hydrocarbon content and productivity, but without impact on the r_{EX} . Further studies are necessary for elucidating the effect of the radiative properties on the transient responses in *B. braunii* continuous cultures. In steady-state continuous photoautotrophic cultures of *Botryococcus braunii* Bot-22, hydrocarbon and biomass yields are dependent to r_{EX} , light intensity, light period, dilution rate and dissolved oxygen concentration.

There are several improvement and a wide field of perspectives that could be undertaken from the basis of this work. The first will be the development of analytical methodology of hydrocarbons estimation instead of gravimetric quantification, in order to minimize the errors of overestimation in the results. Additionally, improvement of the experimental set-up appears to be another step for establishing an efficient system of investigation and a scalable process of production.

The development of a biological system modelling for biomass and hydrocarbon production for *B. braunii* BOT-22 is also an interesting approach.

Development of a stress induced production of hydrocarbon which is interesting for mass-production could be followed for further investigations.

Oxygen limitation could be a useful strategy for optimization of hydrocarbon productivity of *B. braunii* in a two-step production: first growth up to high cell density, and then decrease the light and oxygen to increase the hydrocarbon production.

Physiological understanding is the key step to control and overcome the restrictions of a cost-effective mass-production of *B. braunii*.

Further studies on puls light and matrix of *Botryococcus braunii* race-B strains cultivated at different dissolved oxygen level are needed to bring more clarification on how hydrocarbon and biomass productivity are co-related.

Nomenclature

Greek letters

μ	specific growth rate (d^{-1})
μ_{max}	
λ	maximal specific growth rate (d^{-1}) wavelength (nm)

Nomenclature

Chl <i>b</i>	chlorophyll <i>b</i> concentration (mg L^{-1})
Car	carotenoids concentration (mg L^{-1})
[Car] _x	carotenoids content in biomass (% DCW)
D	dilution rate (d^{-1})
ETR	electron transport rate ($\mu\text{mol electrons m}^{-2} \text{s}^{-1}$)
ETR _{max}	maximal electron transport rate ($\mu\text{mol electrons m}^{-2} \text{s}^{-1}$)
F	flow rate of feeding medium (L d^{-1})
F _v /F _m	maximum photochemical quantum yield of PS II
HC	hydrocarbon concentration (g L^{-1} or g m^{-2})
[HC] _x	hydrocarbon content in biomass (% DCW)
IL	intracellular lipid concentration (g L^{-1} or g m^{-2})
[IL] _x	intracellular lipid content in biomass (% DCW)
PFD	photon flux density ($\mu \text{mol photon m}^{-2} \text{s}^{-1}$ or $\mu \text{mol photon m}^{-2} \text{s}^{-1}$)
P _x	biomass productivity ($\text{g L}^{-1} \text{d}^{-1}$ or $\text{g m}^{-2} \text{d}^{-1}$)
P _{HC}	hydrocarbon productivity ($\text{g L}^{-1} \text{d}^{-1}$ or $\text{g m}^{-2} \text{d}^{-1}$)
r _{EX}	specific light supply rate (mole photon $\text{gX}^{-1} \text{d}^{-1}$)
SLSR	specific light supply rate ($\text{mg S gX}^{-1} \text{d}^{-1}$)
T	temperature ($^{\circ}\text{C}$)
[TL] _x	total lipids content in biomass (% DCW)
V	volume (L)
X	biomass concentration (g L^{-1} or g m^{-2})
Y _{xEobs}	biomass yield on light supply ($\text{g mol photons}^{-1}$)

Abbreviation

ANOVA	one-way analysis of variance
BF ₃	boron trifluoride
BHT	butylated hydroxytoluene
DIC	dissolved inorganic carbon
DMSO	dimethyl sulfoxide
FAMES	fatty acid methyl esters
FAS	fatty acid synthase
FFA	free fatty acids
GF-FID	gas chromatography coupled to a flame ionization detector
GF-MS	gas chromatography coupled to a mass spectrometer
HC	hydrocarbon
LED	light emitting diode
IL	intracellular lipid
PAR	photosynthetic active radiations
PBR	photobioreactor
PS II	photosystem II
PUFA	polyunsaturated fatty acids
TL	total lipid
TLC	thin layer chromatography

List of figures

Figure 1-1: Types of hydrocarbons produced by four races of <i>B. braunii</i>	19
Figure 1-2: Principle of saturation pulse quenching analysis.....	37
Figure 1-3: Structure of chlorophylls and carotenoids.....	40
Figure 1-4: Main biosynthetic pathway of hydrocarbon of race B.....	47
Figure 2-1: <i>B. braunii</i> race B strain BOT-22.....	52
Figure 2-2: Schematic of PBR.....	55
Figure 2-3: Pictures of the two PBRs system.....	56
Figure 2-4: Curve of the gas hold up of the PBR.....	58
Figure 2-5: Graph of the (OD ₇₅₀) and dry cell weight.....	59
Figure 2-6: Light response curve (P/I).....	62
Figure 2-7: Calibration curve of the dissolved inorganic carbon concentration measurement.....	63
Figure 2-8: Total lipid extraction.....	66
Figure 2-9: Hydrocarbon extraction.....	67
Figure 2-10: <i>B. braunii</i> BOT-22.....	70
Figure 3-1: Total hydrocarbon and intracellular lipids content percentage on dry cell weight (% total HC and % IL) of <i>B. braunii</i> race B strain BOT-22 at 2 incident PFD 50 and 500 $\mu\text{mol photons m}^{-2} \text{s}^{-1}$	82
Figure 3-2: Total hydrocarbon and intracellular lipids content percentage on dry cell weight (% total HC and % IL) of <i>B. braunii</i> race B strain BOT-22 at 2 incident dilution rates 0.178 and 0.357 d^{-1}	83
Figure 3-3: Total hydrocarbon and intracellular lipids content percentage on dry cell weight (% total HC and % IL) of <i>B. braunii</i> race B strain BOT-22 under continuous light and light and dark cycle (8 hours of light and 16 hours of dark) with 21% dissolved oxygen concentration.....	85
Figure 3-4: Total hydrocarbon and intracellular lipids content percentage on dry cell weight (% total HC and %IL) of <i>B. braunii</i> race B strain BOT-22 under continuous light with 4% and 21% of dissolved oxygen concentration.....	86
Figure 3-5: Total hydrocarbon and intracellular lipids content percentage on dry cell weight (% total HC and %IL) of <i>B. braunii</i> race B strain BOT-22 under continuous light and light and dark cycle (8 hours of light and 16 hours of dark) with 4% dissolved oxygen concentration.....	87
Figure 3-6: Total hydrocarbon and intracellular lipids content percentage on dry cell weight (% total HC and %IL) of <i>B. braunii</i> race B strain BOT-22 under light and dark cycle (8 hours of light and 16 hours of dark) with 4 %, 21 % and 400 % of dissolved oxygen concentration.....	88
Figure 3-7: Fatty acids profile of <i>B. braunii</i> race B strain BOT-22.....	89
Figure 3-8: Comparison of main fatty acids compositions of <i>B. braunii</i> race B strain BOT-22 at two different light intensities (50 and 500 $\mu\text{mol photons m}^{-2} \text{s}^{-1}$). Other common parameters were: continuous light, dilution rate of 0.178 d^{-1} and 21 % dissolved oxygen concentration.....	93
Figure 3-9: Comparison of main fatty acids compositions of <i>B. braunii</i> race B strain BOT-22 at two different light periods (continuous light and end of dark period. Other common parameters were: light intensity 500 $\mu\text{mol photons m}^{-2} \text{s}^{-1}$, dilution rate of 0.357 d^{-1} and 21 % dissolved oxygen concentration.....	94
Figure 3-10: Comparison of main fatty acids compositions of <i>B. braunii</i> race B strain BOT-22 at two different dissolved oxygen concentrations (4 % and 21 %). Other common parameters were: continuous light, light intensity 500 $\mu\text{mol photons m}^{-2} \text{s}^{-1}$ and dilution rate of 0.357 d^{-1}	95

Figure 3-11: Photosynthetic factors (Fv/Fm, α and ETRm) of <i>B. braunii</i> race B strain BOT-22 at two incident PFDs 50 and 500 $\mu\text{mol photons m}^{-2} \text{s}^{-1}$	96
Figure 3-12: Photosynthetic factors (Fv/Fm, α and ETRm) of <i>B. braunii</i> race B strain BOT-22 at two incident dilution rates 0.178 and 0.357 d^{-1}	97
Figure 3-13: Photosynthetic factors (Fv/Fm, α and ETRm) of <i>B. braunii</i> race B strain BOT-22 under continuous light and light and at the end of a dark period with 21 % dissolved oxygen concentration	97
Figure 3-14: Photosynthetic factors (Fv/Fm, α and ETRm) of <i>B. braunii</i> race B strain BOT-22 under continuous light and at the end of a 16h dark period with 4 % dissolved oxygen concentration	98
Figure 3-15: Photosynthetic factors (Fv/Fm, α and ETRm) of <i>B. braunii</i> race B strain BOT 22 under continuous light with 4 % and 21 % of dissolved oxygen concentration	99
Figure 3-16: Photosynthetic factors (Fv/Fm, α and ETRm) of <i>B. braunii</i> race B strain BOT-22 under light and after a 16h dark incubation with 4 %, 21 % and 400 % of dissolved oxygen concentration	100
Figure 3-17: Pigment analysis (chlorophyll <i>a</i> , <i>b</i> and carotenoid) and ratio of carotenoid over total chlorophyll of <i>B. braunii</i> race B strain BOT-22 at 2 incident PFD 50 and 500 $\mu\text{mol photons m}^{-2} \text{s}^{-1}$	101
Figure 3-18: Pigment analysis (chlorophyll <i>a</i> , <i>b</i> and carotenoid) and ratio of carotenoid over total chlorophyll of <i>B. braunii</i> race B strain BOT-22 at 2 incident dilution rate 0.178 and 0.357 d^{-1}	105
Figure 3-19: Pigment analysis (chlorophyll <i>a</i> , <i>b</i> and carotenoids) and ratio of carotenoids over total chlorophylls of <i>B. braunii</i> race B strain BOT-22 under continuous light and light and after a 16 h dark incubation with 21 % dissolved oxygen concentration	103
Figure 3-20: Pigment analysis (chlorophyll <i>a</i> , <i>b</i> and carotenoid) and ratio of carotenoid over total chlorophyll of <i>B. braunii</i> race B strain BOT-22 at 2 incident dilution rate 0.178 and 0.357 d^{-1}	104
Figure 3-21: Pigment analysis (chlorophyll <i>a</i> , <i>b</i> and carotenoids) and ratio of carotenoids over total chlorophylls of <i>B. braunii</i> race B strain BOT-22 under continuous light with 4 % and 21 % of dissolved oxygen concentration	105
Figure 3-22: Pigment analysis (chlorophyll <i>a</i> , <i>b</i> and carotenoid) and ratio of carotenoids over total chlorophylls of <i>B. braunii</i> race B strain BOT-22 at the end of a 16 h dark period with 4%, 21% and 400% of dissolved oxygen concentration	106
Figure 4-1: Evolution of r_{EX} (specific light supply rate) and biomass productivity of a <i>B. braunii</i> culture after changing the incident PFD on surface of the photobioreactor, from 50 to 500 $\mu\text{mol photons m}^{-2} \text{s}^{-1}$ and the dilution rate from 0.178 d^{-1} to 0.357 d^{-1}	108
Figure 4-2: Biomass productivity of <i>B. braunii</i> in continuous cultures as a function of the r_{EX} (specific light supply rate) value in continuous cultures	109
Figure 4-3: Evolution of r_{EX} (specific light supply rate) and photosynthetic pigment composition: ratio of Chl <i>a</i> over Chl <i>b</i> (w:w) of <i>B. braunii</i> race culture after changing the incident PFD on surface of the photobioreactor, from 50 to 500 $\mu\text{mol photons m}^{-2} \text{s}^{-1}$ and the dilution rate from 0.178 d^{-1} to 0.357 d^{-1}	111
Figure 4-4: Evolution of r_{EX} (specific light supply rate) and photosynthetic pigment composition: ratio of carotenoids over total chlorophylls (w:w) of <i>B. braunii</i> race culture after changing the incident PFD on surface of the photobioreactor, from 50 to 500 $\mu\text{mol photons m}^{-2} \text{s}^{-1}$ and the dilution rate from 0.178 d^{-1} to 0.357 d^{-1}	111

Figure 4-5: Evolution of r_{EX} (specific light supply rate) and photosynthetic activities (Fv/Fm) of <i>B. braunii</i> BOT-22 culture after changing the incident PFD on surface of the photobioreactor, from 50 to 500 $\mu\text{mol photons m}^{-2} \text{s}^{-1}$ and the dilution rate from 0.178 d^{-1} to 0.357 d^{-1}	113
Figure 4-6: Photosynthetic characteristics of a <i>B. braunii</i> culture as a function of the r_{EX} (specific light supply rate) value in the continuous cultures.....	114
Figure 4-7: r_{EX} (specific light supply rate) and residual inorganic carbon concentration (mg L^{-1}) inside the PBR for cultivating <i>B. braunii</i> race B strain BOT-22 at two incidents PFD 50 and 500 $\mu\text{mol photons m}^{-2} \text{s}^{-1}$	115
Figure 4-8: r_{EX} (specific light supply rate) and residual nitrate concentration (mg L^{-1}) inside the PBR for cultivating <i>B. braunii</i> race B strain BOT-22 at two incidents PFD 50 and 500 $\mu\text{mol photons m}^{-2} \text{s}^{-1}$	116
Figure 4-9: r_{EX} (specific light supply rate) and residual phosphate concentration (mg L^{-1}) inside the PBR for cultivating <i>B. braunii</i> race B strain BOT-22 at two incidents PFD 50 and 500 $\mu\text{mol photons m}^{-2} \text{s}^{-1}$	116

List of tables

Table 1-1: CO ₂ concentration for growing <i>B. braunii</i> race B and specific growth rate in different studies.....	26
Table 1-2: PAR, photoperiod and light source for <i>B. braunii</i> races in different studies.....	30
Table 1-3: Chl <i>a</i> / Chl <i>b</i> , total carotenoids, Car/ Chl for <i>B. braunii</i> in different studies.....	41
Table 1-4: Cultivation system, cell density and biomass productivity for <i>B. braunii</i> and some other strains in different studies.....	45
Table 1-5: Hydrocarbon contents (%) and hydrocarbon culture concentration of identified <i>B. braunii</i> species.....	48
Table 1-6: Major hydrocarbons detected from isolated strains of <i>B. braunii</i>	49
Table 2-1: Final concentrations of modified AF6 mineral medium.....	53
Table 3-1: Biomass concentration and productivity (volumetric and surface), in steady state cultures of <i>Botryococcus braunii</i> BOT-22 race B strain at two incident light intensities on the photobioreactor surface (50 and 500 μmol photons m ⁻² s ⁻¹) and two dilution rates 0.178 and 0.357 d ⁻¹	73
Table 3-2: The maximum values of biomass concentration and productivity obtained in cultures of different <i>Botryococcus braunii</i> race B. strains.....	74
Table 3-3: Biomass concentration and productivity (volumetric and surface) of <i>B. braunii</i> BOT-22 race B strain at 500 μ mole photons m ⁻² s ⁻¹ and 0.357 d ⁻¹ dilution rates under continuous light and light and dark cycle with 21 % of dissolved oxygen concentration.....	76
Table 3-4: Biomass concentration and productivity (volumetric and surface) of <i>B. braunii</i> BOT-22 race B strain at 500 μmol photons m ⁻² s ⁻¹ and 0.357 d ⁻¹ dilution rates under continuous light and light and dark cycle with 4 % of dissolved oxygen concentration.....	77
Table 3-5: Biomass concentration and productivity (volumetric and surface) of <i>B. braunii</i> BOT-22 race B strain at 500 μmol photons m ⁻² s ⁻¹ and 0.357 d ⁻¹ dilution rates under continuous light and with 4 % and 21 % of dissolved oxygen concentration.....	78
Table 3-6: Hydrocarbon concentration, hydrocarbon productivity (volumetric and surface) and hydrocarbon content in steady state cultures of <i>Botryococcus braunii</i> BOT-22 race B strain at two incident light intensities on the photobioreactor surface (50 and 500 μmol photons m ⁻² s ⁻¹) and two dilution rates 0.178 and 0.357 d ⁻¹	80
Table 3-7: The maximum values of hydrocarbon contents (%) and hydrocarbon concentration obtained in cultures of different <i>Botryococcus braunii</i> race B. strains.....	81
Table 3-8: Biomass concentration (g L ⁻¹), PUFAs content (%), C16-C18 content (%), hydrocarbon and intracellular content (%) on DCW of <i>Botryococcus braunii</i> BOT 22 race B strain at two incident light intensities (50 and 500 μmol photons m ⁻² s ⁻¹) on the photobioreactor surface, two dilution rates (0.178 and 0.357 d ⁻¹), two light periods (continuous light and light and dark cycle) and different dissolved oxygen concentrations (4%, 21 % and 400 %).....	90
Table 3-19: Biomass concentration (g L ⁻¹), C16-C18 content (%), hydrocarbon and intracellular content (%) on DCW obtained in cultures of different <i>Botryococcus braunii</i> strains in the literature and in this study.....	91

References

- Aaronson, S., Bemer¹, T., Gold, K., Kushner, L., Patni, N.J., Repak, A., Rubin, D. (1983) Some observations on the green planktonic alga, *Botryococcus braunii* and its bloom form. J. Plankton Res. 5, 693–700.
- Abinandan, S., Shanthakumar, S. (2015) Challenges and opportunities in application of microalgae (*Chlorophyta*) for wastewater treatment: A review. Renew. Sustain. Energy Rev. 52, 123–132.
- Achitouv, E., Metzger, P., Rager, M.-N., Largeau, C. (2004) C₃₁–C₃₄ methylated squalenes from a Bolivian strain of *Botryococcus braunii*. Phytochemistry 65, 3159–3165.
- Akkerman, I., Janssen, M., Rocha, J., Wijffels, R.H. (2002) Photobiological hydrogen production: photochemical efficiency and bioreactor design. Int. J. Hydrogen Energy 27, 1195–1208.
- Al-Hothaly, K. A., Adetutu, E. M., Taha, M., Fabbri, D., Lorenzetti, C., Conti, R., May, B. H., Shar, S. S., Bayoumi, R. A., Ball, A. S. (2015) Bio-harvesting and pyrolysis of the microalgae *Botryococcus braunii*. Bioresour. Technol. 191, 117–123.
- An, J.Y., Sim, S.J., Lee, J.S., Kim, B.W. (2003) Hydrocarbon production from secondarily treated piggy wastewater by the green alga *Botryococcus braunii*. J. Appl. Phycol. 15 (2–3), 185–191.
- Asada, K. (2006) Production and scavenging of reactive oxygen species in chloroplasts and their functions. Plant Physiol. 141(2), 391–396.
- Asada, K. (1999) The water-water cycle in chloroplasts: scavenging of active oxygens and dissipation of excess photons. Annu. Rev. Plant Physiol. Plant Mol. Biol. 50(1), 601–639.
- Ashokkumar, V., Rengasamy, R. (2012) Mass culture of *Botryococcus braunii* Kutz. under open raceway pond for biofuel production. Bioresour. Technol. 104, 394–399.
- Ashokkumar, V., Agila, E., Sivakumar, P., Salam, Z., Rengasamy, R., Nasir Ani, F. (2014) Optimization and characterization of biodiesel production from microalgae *Botryococcus* grown at semi-continuous system. Energy Convers. Mgmt. 88, 936–946.
- Baba, M., Kikuta, F., Suzuki, I., Watanabe, M.M., Shiraiwa, Y. (2012) Wavelength specificity of growth, photosynthesis, and hydrocarbon production in the oil-producing green alga *Botryococcus braunii*. Bioresour. Technol. 109, 266–270.
- Babcock, R.W., Malda, J., Radway, J.C. (2002) Hydrodynamics and mass transfer in a tubular airlift photobioreactor. J. Appl. Phycol. 14, 169–184.

- Baldwin, D.S., Whittington, J., Oliver, R. (2003) Temporal variability of dissolved P speciation in a eutrophic reservoir- implications for predicating algal growth. *Water Res.* 37, 4595–4598.
- Ball, S., Colleoni, C., Cenci, U., Raj, J.N., Tirtiaux, C. (2011) The evolution of glycogen and starch metabolism in eukaryotes gives molecular clues to understand the establishment of plastid endosymbiosis. *J. Exper. Bot.* 62, 1775–1801.
- Banerjee, A., Sharma, R., Chisti, Y., Banerjee, U.C. (2002) *Botryococcus braunii*: a renewable source of hydrocarbons and other chemicals. *Crit. Rev. Biotechnol.* 22, 245–279.
- Barber, J. (1994) Molecular basis of the vulnerability of photosystem II to damage by light. *Aust. J. Plant Physiol.* 22, 201–208.
- Barbosa, M.J., Janssen, M., Ham, N., Tramper, J., Wijffels, R.H. (2003) Microalgae cultivation in air-lift reactors: modeling biomass yield and growth rate as a function of mixing frequency. *Biotechnol. Bioeng.* 82, 170–179.
- Becker, E.W. (1994) *Microalgae*. Cambridge: Cambridge University Press.
- Becker, E.W. (2007) Micro-algae as a source of protein. *Biotechnol. Adv.* 25, 207–210.
- Behrenfeld, M., Práasil, O., Kolber, Z., Babin, M., Falkowski, P. (1998) Compensatory changes in photosystem II electron turnover rates protect photosynthesis from photoinhibition. *Photosynth. Res.* 58, 259–268.
- Ben-Amotz, A., Tomabene, T.G., Thomas, W.H. (1985) Chemical profile of selected species of microalgae with emphasis on lipids. *J. Phycol.* 21, 72–81.
- Berkaloff, C, Casadevall, E., Largeau, C., Metzger, P., Peracca, S., Virlet, J. (1983) The resistant polymer of the walls of the hydrocarbon rich alga *Botryococcus braunii*. *Phytochemistry* 22, 389–397.
- Berkaloff, C., Rousseau, B., Couté, A., Casadevall, E., Metzger, P., Chirac, C. (1984) Variability of cell wall structure and hydrocarbon type in different strains of *Botryococcus braunii*. *J. Phycol.* 20, 377–389.
- Bjorkman, O., Demmig, B. (1987) Photon yield of O₂ evolution and chlorophyll fluorescence characteristics at 77-K among vascular plants of diverse origins. *Planta* 170, 489–504.
- Bolton, J.R., Hall, D.O. (1991) The maximum efficiency of photosynthesis. *Photochem. Photobiol.* 53, 545–548.
- Borowitzka, M.A., Borowitzka, L.J. (1988) *Dunaliella*. In: *Microalgal Biotechnology* (eds M.A. Borowitzka & L.J. Borowitzka), Cambridge University Press, Cambridge, UK. 27–58.

- Borowitzka, M. (1997) Microalgae for aquaculture: opportunities and constraints. *J. Appl. Phycol.* 9(5), 393–401.
- Borowitzka, M.A. (1999 a) Pharmaceuticals and agrochemicals from microalgae. In: Cohen Z, editor. *Chemicals from microalgae*. Taylor & Francis 313–352.
- Borowitzka, M.A. (1999 b) Commercial production of microalgae: ponds, tanks, tubes and fermenters. *J. Biotechnol.* 70(1–3), 313–321.
- Brenckmann, F., Largeau, C., Casadevall, E., Berkaloff, C. (1985) Influence de la nutrition azotée sur la croissance et la production d'hydrocarbures de l'algue *Botryococcus braunii*. In: Palz W, Coombs J, Hall DO (eds) *Energy from biomass*. Elsevier, London, 717–721.
- Brennan, L., Owende, P. (2010) Biofuels from microalgae—A review of technologies for production, processing, and extractions of biofuels and co-products. *Renew. Sustain. Energy Rev.* 14, 557–577.
- Brown, A.C., Knights, B.A., Conway, E. (1969) Hydrocarbon content and its relationship to physiological state in the green alga *Botryococcus braunii*. *Phytochemistry* 8, 543–547.
- Burner, T., Dubinsky Z., Wyman, K., Falkowski, P.G. (1989) Photoadaptation and the package effect in *Dunaliella tertiolecta* (Chlorophyceae). *J. Phycol.* 25, 70–78.
- Camacho Rubio, F., García Camacho, F., Fernández Sevilla, J.M., Chisti, Y., Molina Grima, E. (2003) A mechanistic model of photosynthesis in microalgae. *Biotechnol. Bioeng.* 81, 459–473.
- Cardozo, K.H.M., Guaratini, T., Barros, M.P., Falcão, V.R., Tonona, A.P., Lopes, N.P., Campos, S., Torres, M.A., Souza, A.O., Colepicolo, P., Pinto, E. (2007) Metabolites from algae with economical impact. *Comp. Biochem. Phys. C* 146, 60–78.
- Carvalho, A.P., Silva, S.O., Baptista, J.M., Malcata, F.X. (2011) Light requirements in microalgal photobioreactors: An overview of biophotonic aspects. *Appl. Microbiol. Biotechnol.* 89, 1275–1288.
- Casadevall, E., Dif, D., Largeau, C., Gudín, C., Chaumont, D., Desanti, O. (1985) Studies on batch and continuous cultures of *Botryococcus braunii*: hydrocarbon production in relation to physiological state, cell ultrastructure, and phosphate nutrition. *Biotechnol. Bioeng.* 27, 286–295.
- Casper-Lindley, C., Bjorkman, O. (1998) Fluorescence quenching in four unicellular algae with different light-harvesting and xanthophyll-cycle pigments. *Photosynth. Res.* 56, 277–289.

- Catarina Guedes, A., Meireles, L., Amaro, H., Malcata, X. (2010) Changes in lipid class and fatty acid composition of cultures of *Pavlova lutheri*, in response to light intensity. *J. Am. Oil Chem. Soc.* 87, 791–801.
- Cheirsilp, B., Torpee, S. (2012) Enhanced growth and lipid production of microalgae under mixotrophic culture condition: Effect of light intensity, glucose concentration and fed-batch cultivation. *Bioresour. Technol.* 110, 510–516.
- Chen, H-B., Wu, J-Y., Wang, C-F., Fu, C-C., Shieh, C-J., Chen, C-I., Wang, C-Y., Liu, Y-C. (2010) Modeling on chlorophyll a and phycocyanin production by *Spirulina platensis* under various light-emitting diodes. *Biochem. Eng. J.* 53, 52–56.
- Cheng, P., Ji, B., Gao, L., Zhang, W., Wang, J., Tianzhong, L. (2013) The growth, lipid and hydrocarbon production of *Botryococcus braunii* with attached cultivation. *Bioresour. Technol.* 138, 95–100.
- Chiang, I.Z., Huang, W.Y., Wu, J.T. (2004) Allelochemicals of *Botryococcus braunii* (Chlorophyceae). *J. Phycol.* 40, 474–480.
- Chisti, Y. (2007) Biodiesel from microalgae. *Biotechnol. Adv.* 25 (3), 294–306.
- Chisti, Y. (2008 a) Biodiesel from microalgae beats bioethanol. *Trends Biotechnol.* 26 (3), 126–131.
- Chisti, Y. (2008 b) Response to Reijnders: do biofuels from microalgae beat biofuels from terrestrial plants? *Trends Biotechnol.* 26 (7), 351–352.
- Cho, D.H., Ramanan, R., Heo, J., Shin, D.S., Oh, H.M., Kim, H.S. (2016) Influence of limiting factors on biomass and lipid productivities of axenic *Chlorella vulgaris* in photobioreactor under chemostat cultivation. *Bioresour. Technol.* 211, 367–373.
- Converti, A., Casazza, A.A., Ortiz, E.Y., Perego, P., Del Borghi, M. (2009) Effect of temperature and nitrogen concentration on the growth and lipid content of *Nannochloropsis oculata* and *Chlorella vulgaris* for biodiesel production. *Chem. Eng. Process.* 48, 1146–1151.
- Cornet, J.F., Dussap, C.G. (2009) A simple and reliable formula for assessment of maximum volumetric productivities in photobioreactors. *Biotechnol. Prog.* 25, 424–435.
- Cosgrove, J., Borowitzka, M. (2006) Applying pulse amplitude modulation (PAM) fluorometry to microalgae suspensions: stirring potentially impacts fluorescence. *Photosynth. Res.* 88, 343–350.
- Cournac, L., Latouche, G., Cerovic, Z., Redding, K., Ravenel, J., Peltier, G. (2002) In Vivo Interactions between photosynthesis, mitorespiration, and chlororespiration in *Chlamydomonas reinhardtii*. *Plant. Physiol.* 129, 1921–1928.

- Cuaresma, M., Janssen, M., Vilchez, C., Wijffels, R.H. (2009) Productivity of *Chlorella sorokiniana* in a short-path (SLP) panel photobioreactor under high irradiance. *Biotechnol. Bioeng.* 104, 352–359.
- Dayananda, C., Sarada, R., Shamala, T.R., Ravishankar, G.A. (2006) Influence of nitrogen sources on growth, hydrocarbon and fatty acid production by *Botryococcus braunii*. *Asian J. Plant Sci.* 5, 799–804.
- Dayananda, C., Sarada, R., Usha, Rani M., Shamala, T.R., Ravishankar, G.A. (2007 a) Autotrophic cultivation of *Botryococcus braunii* for the production of hydrocarbons and exopolysaccharides in various media. *Biom. Bioe.* 31, 87–93.
- Dayananda, C., Sarada, R., Kumar, V., Ravishankar, G.A. (2007 b) Isolation and characterization of hydrocarbon producing green alga *Botryococcus braunii* from Indian freshwater bodies. *Electron. J. Biotechnol.* 10, 78–91.
- Degen, J., Uebele, A., Retze, A., Schmid-Staiger, U., Trosch, W. (2001) A novel airlift photobioreactor with baffles for improved light utilisation through the flashing light effect. *J. Biotechnol.* 92, 89–94.
- Demmig-Adames, B., Adams, W.W., Logan, B.A., Verhoeven, A.S. (1995) Xanthophyll-cycle dependent energy dissipation and flexible photosystem II efficiency in plants acclimated to light stress. *Aust. J. Plant Physiol.* 22, 249–260.
- Dennis, M.W., Kolattukudy, P.E. (1991) Alkane biosynthesis by decarbonylation of aldehyde catalyzed by a microsomal preparation from *Botryococcus braunii*. *Arch. Biochem. Biophys.* 287, 268–275.
- Dennis, M., Kolattukudy, P.E. (1992) A cobalt-porphyrin enzyme converts a fatty aldehyde to a hydrocarbon and CO. *Proc. Natl. Acad. Sci. U. S. A.* 89, 5306–5310.
- Derenne, S., Largeau, C., Casadevall, E., Sellier, N. (1990) Direct relationship between the resistant biopolymer and tetraterpenic hydrocarbon in the lycopadiene- race of *Botryococcus braunii*. *Phytochemistry* 29, 2187–2192.
- Dote, Y., Sawayama, S., Inoue, S., Minowa, T., Yokoyama, S. (1994) Recovery of liquid fuel from hydrocarbon-rich microalgae by thermochemical liquefaction. *Fuel* 73, 1855–1857.
- Doucha, J., Livansky K. (2006) Productivity, CO₂/O₂ exchange and hydraulics in outdoor open high density microalgal (*Chlorella* sp.) photobioreactors operated in a Middle and Southern European climate. *J. Appl. Phycol.* 18, 811–826.
- Dubinsky, Z., Matsukawa, R., Karube, I. (1995) Photobiological aspects of algal mass culture. *J. Mar. Biotechnol.* 2, 61–65.

- Edge, R., McGarvey, D.J., Truscott, T.G. (1997) The carotenoids as anti-oxidants –a review. *J. Photoch. Photobio. B.* 41, 189–200.
- Endo, T., Asada, K. (2008) Photosystem I and photoprotection: cyclic electron flow and water-water cycle. In: *Photoprotection, Photoinhibition, Gene Regulation, and Environment*, (Eds) B. Demmig-Adams, W.W. Adams, A.K. Matoo, Springer. Dordrecht, 21, 205–221.
- Eriksen, N.T., Geest, T., Iversen, J.J.L. (1996) Phototrophic growth in the lumostat: a photobioreactor with on-line optimization of light intensity. *J. Appl. Phycol.* 8, 345–352.
- Eriksen, N. (2008) The technology of microalgal culturing. *Biotechnol. Lett.* 30(9), 1525–1536.
- Eroglu, E., Melis, A. (2010) Extracellular terpenoid hydrocarbon extraction and quantitation from the green microalgae *Botryococcus braunii* var. Showa. *Bioresour. Technol.* 101, 2359–2366.
- Eroglu, E., Okada, S., Melis, A. (2011) Hydrocarbon productivities in different *Botryococcus* strains: comparative methods in product quantification. *J. Appl. Phycol.* 23, 763–775.
- Escoubas, J., Lomas, M., LaRoche, J., Falkowski, P. G. (1995) Light intensity regulation of cab gene transcription is signaled by the redox state of the plastoquinone pool. *Proc. Natl. Acad. Sci. USA* 92, 10237–10241.
- Falkowski, P. G., LaRoche, J. (1991) Acclimation to spectral irradiance in algae. *J. Phycol.* 27, 8–14.
- Falkowski, P. G. (1992) Molecular ecology of phytoplankton photosynthesis. In Falkowski, P. G., Woodhead, A. D. [Eds.] *Primary Productivity and Biogeochemical Cycles in the Sea*. Plenum Press, New York, 47–67.
- Faramarzi, M.A., Forootanfar, H., Shakibaei, M. (2010) *Microalgal Biotechnology*, Tehran University of Medical Sciences.
- Fernandes, B.D., Dragoner, G.M., Teixeira, J.A., Vicente, A.A. (2010) Light regime characterization in an airlift. Photobioreactor for production of microalgae with high starch content. *Appl. Biochem. Biotechnol.* 161, 218–226.
- Fernandes, B.D., Mota, A., Teixeira, J.A., Vicente, A.A. (2015) Continuous cultivation of photosynthetic microorganisms: Approaches, applications and future trends. *Biotechnol. Adv.* 33(6), 1228–1245.
- Fredrickson, A.G., Tsuchiya, H.M. (1970) Utilization of the Effects of Intermittent Illumination on Photosynthetic microorganisms. Center for Agricultural Publication and Documentation, Wageningen, The Netherlands.

- Fu, W., Guðmundsson, Ó., Paglia, G., Herjólfsson, G., Andrésón, Ó.S., Pálsson, B., Brynjólfsson, S. (2013) Enhancement of carotenoid biosynthesis in the green microalga *Dunaliella salina* with light-emitting diodes and adaptive laboratory evolution. *Appl. Microbiol. Biotechnol.* 97, 2395–2403.
- García-Malea López, M.C., Del Río Sánchez, E., Casas López, J.L., Acién Fernández, F.G., Fernández Sevilla, J.M., Rivas, J., Guerrero, M.G., Molina Grima, E. (2006) Comparative analysis of the outdoor culture of *Haematococcus pluviialis* in tubular and bubble column photobioreactors. *J. Biotechnol.* 123, 329–342.
- Ge, Y., Lu, J., Tian, G. (2011) Growth characteristics of *Botryococcus braunii* 765 under high CO₂ concentration in photobioreactor. *Bioresour. Technol.* 102, 130–134.
- Genty, B., Briantais, J.M., Baker, N.R. (1989) The relationship between the quantum yield of photosynthetic electron transport and quenching of chlorophyll fluorescence. *Biochim. Biophys. Acta* 990, 87–92.
- Ghirardi, M.L., Zhang, J.P., Lee, J.W., Flynn, T., Seibert, M., Greenbaum, E., Melis, A. (2000) Microalgae: a green source of renewable H₂. *Trends Biotechnol.* 18, 506–511.
- Gilmore, A.M. (1997) Mechanistic aspects of xanthophyll-cycle dependent photoprotection in higher plant chloroplasts and leaves. *Physiol. Plantarum* 99, 197–209.
- Gołębiowski, M., Boguś, M.I., Paszkiewicz, M., Stepnowski, P. (2011) Cuticular lipids of insects as potential biofungicides: methods of lipid composition analysis. *Anal. Bioanal. Chem.* 399, 3177–3191.
- Gomes, S.M.D.S., Lima, V.L.A.D., Souza, A.P. D., Nascimento, J. J. V. R. D., Nascimento, E. S. D. (2014) Chloroplast pigments as indicators of lead stress. *Eng. Agríc. Jaboticabal*, 34, 5, 877–884.
- Gordon, J. M., Polle, J. E. (2007) Ultrahigh bioproductivity from algae. *Appl. Microbiol. Biotechnol.* 76, 969–975.
- Griehl, C. C., Kleinert, C., Griehl, C. C., Bieler, S. (2014) Design of a continuous milking bioreactor for non-destructive hydrocarbon extraction from *Botryococcus braunii*. *J. Appl. Phycol.* 27 (5), 1833–1843.
- Guschina, I.A., Harwood, J.L. (2006) Lipids and lipid metabolism in eukaryotic algae. *Lipid Res.* 45, 160–186.
- Gutierrez-Wing, M.T., Silaban, a., Barnett, J., Rusch, K.A. (2014) Light irradiance and spectral distribution effects on microalgal bioreactors. *Eng. Life Sci.* 14, 574–580.

- Hadj-Romdhane, F., Zheng, X., Jaouen, P., Pruvost, J., Grizeau, D., Croué, J.P., Bourseau, P. (2013) The culture of *Chlorella vulgaris* in a recycled supernatant: effects on biomass production and medium quality. *Bioresour. Technol.* 132, 285–292.
- Hall, D.O., Acien Fernandez, F.G., Guerrero, E.C., Rao, K.K., Molina Grima, E. (2003) Outdoor helical tubular photobioreactors for microalgal production: modeling of fluid-dynamics and mass transfer and assessment of biomass productivity. *Biotechnol. Bioeng.* 82, 62–73.
- Hifney, A.F., Abdel-Basset, R. (2014) Photosynthesis, respiration and carotenoid contents in the green alga *Botryococcus braunii* at elevated nutrient levels. *J. Biol. Earth Sci.* 4, B191–B198.
- Hillen, L.W., Pollard, G., Wake, L.V., White, N. (1982) Hydrocracking of the oils of *Botryococcus braunii* to transport fuels. *Biotechnol. Bioeng.* 24, 193–205.
- Hoek, C. van den, Mann, D.G., Jahns, H.M. (1995) *Algae: An Introduction to Phycology*. Cambridge University Press, Cambridge, 623.
- Hu, Q. (2013) Environmental effects on cell composition. In: Richmond, A. (Ed.), *Handbook of Microalgal Culture: Biotechnology and Applied Phycology*. Blackwell Science, Victoria, 114–122.
- Hu, Q., Richmond, A. (1996) Productivity and photosynthetic efficiency of *Spirulina platensis* as affected by light intensity, algal density and rate of mixing in a flat plate photobioreactor. *J. Appl. Phycol.* 8 (2), 139–145.
- Hu, Q., Guterman, H., Richmond, A. (1996) A flat inclined modular photobioreactor for outdoor mass cultivation of photoautotrophs. *Biotechnol. Bioeng.* 51, 51–60.
- Hu, Q., Sommerfeld, M., Jarvis, E., Ghirardi, M., Posewitz, M., Seibert, M., Darzins, A. (2008) Microalgal triacylglycerols as feedstocks for biofuel production: perspectives and advances. *Plant J.* 54, 621–639.
- Huang, Z., Poulter, C.D. (1989 a) Tetramethylsqualene, a triterpene from *Botryococcus braunii* var. Showa. *Phytochemistry* 28, 1467–1470.
- Huang, Z., Poulter, C.D. (1989 b) Stereochemical studies of botryococcene biosynthesis: analogies between 1'-1 and 1'-3 condensations in isoprenoid pathway. *J. Am Chem. Soc.* 111, 2713–2715.
- Huang, X., Wang, C., Zhang, J., Wiesenberg, G.L.B., Zhang, Z., Xie, S. (2011) Comparison of free lipid compositions between roots and leaves of plants in the Dajiuhu Peatland, Central China. *Geochem. J.* 45, 365–373.

- Huertas, E., Montero, O., Lubián, L.M. (2000) Effects of dissolved inorganic carbon availability on growth, nutrient uptake and chlorophyll fluorescence of two species of marine microalgae. *Aqua. Eng.* 22, 181–197.
- Huntley, M., Redalje, D. (2007) CO₂ mitigation and renewable oil from photosynthetic microbes: a new appraisal. *Mitig. Adapt. Strat. Glob. Change* 12, 573–608.
- Iqbal, M., Grey, D., Stepan-Sarkissian, F., Fowler, M.W. (1993) A flat-sided photobioreactor for culturing microalgae. *Aqua. Eng.* 12, 183–190.
- Ishimatsu, A., Matsuura, H., Sano, T., Kaya, K., Watanabe, M.M. (2012) Biosynthesis of isoprene units in the C34 Botryococcene molecule produced by *Botryococcus braunii* strain Bot-22. *Proc. Environ. Sci.* 15, 56–65.
- Iwamoto, H., Sato, S. (1986) Production of EPA by freshwater unicellular algae. *J. Am. Oil Chem. Soc.* 63, 434.
- Jin, J., Dupré C., Legrand, J., Grizeau, D. (2016 a) Extracellular hydrocarbon and intracellular lipid accumulation are related to nutrient-sufficient conditions in pH-controlled chemostat cultures of the microalga *Botryococcus braunii* SAG 30.81. *Algal Res.* 17, 244–252.
- Jin J., Dupré C., Yoneda K., Watanabe M.M., Legrand J., Grizeau D. (2016 b) Characteristics of extracellular hydrocarbon-rich microalga *Botryococcus braunii* for biofuels production: Recent advances and opportunities. *Proc. Biochem.* 51, 1866–1875.
- Jiménez, C., Cossío, B.R., Labella, D., Xavier, Niell, F. (2003) The feasibility of industrial production of *Spirulina (Arthrospira)* in southern Spain. *Aquaculture* 217(1–4), 179–190.
- Jones, J.G. (1969) Studies on lipids of soil microorganisms with particular reference to hydrocarbons. *J. Gen. Microbiol.* 59, 145–152.
- Kalacheva, G.S., Zhila, N.O., Volova, T.G., Gladyshev, M.I. (2000) The effect of temperature on the lipid composition of the green alga *Botryococcus*. *Microbiol.* 71, 286–293.
- Kasai, F., Kawachi, M., Erata, M., Watanabe, M.M. (2004) NIES-Collection List of Strains: Microalgae and Protozoa, 7th edn. National Institute for Environmental Studies, Tsukuba, Japan, 49.
- Kalacheva, G.S., Zhila, N.O., Volova, T.G. (2002) Lipid and hydrocarbon compositions of a collection strain and a wild sample of the green microalga *Botryococcus*. *Aquat. Ecol.* 36, 317–330.
- Kanz, T., Bold, H.C. (1969) In: *Physiological Studies, Morphological and Taxonomical Investigation of Nostoc and Anabaena in Culture*. Austin, TX: University of Texas, Publication No. 6924.

- Karimi Alavijeh, M., Yaghmaei, S. (2016) Biochemical production of bioenergy from agricultural crops and residue in Iran. *Waste Management* 52, 375–394.
- Katsuda, T., Lababpour, A., Shimahara, K., Katoh, S. (2004) Astaxanthin production by *Haematococcus pluvialis* under illumination with LEDs. *Enzyme Microb. Technol.* 35, 81–86.
- Kawachi, M., Inouye, I., Honda, D., O’Kelly, C.J., Bailey, J.C., Bidigare, R.R., Andersen, R.A. (2002) The Pinguiphyceae classis nova, a new class of chromophyte algae whose members produce large amounts of omega-3 fatty acids. *Phycol. Res.* 50, 31–47.
- Kawachi, M., Tanoi, T., Demura, M., Kaya, K., Watanabe, M.M. (2012) Relationship between hydrocarbons and molecular phylogeny of *Botryococcus braunii*. *Algal Res.* 1, 114–119.
- Kay, R.A. (1991) Microalgae as food and supplement. *Crit. Rev. Food Sci. Nutr.* 30, 555–573.
- Kaya, K., Nakazawa, A., Matsuura, H., Honda, D., Inouye, I., Watanabe, M.M. (2011) Thraustochytrid Aurantiochytrium sp. 18W-13a accumulates high amounts of squalene. *Biosci. Biotechnol. Biochem.* 75, 2246–2248.
- Kenny, C., Bayona, D., Garcés, L.A. (2014) Effect of different media on exopolysaccharide and biomass production by the green microalga *Botryococcus braunii*. *J. Appl. Phycol.* 26(5), 2087–2095.
- Khatri, W., Hendrix, R., Niehaus, T., Chappell, J., Curtis, W.R. (2014) Hydrocarbon Production in High Density *Botryococcus braunii* Race B Continuous Culture. *Biotechnol. Bioeng.* 111, 493–503.
- Khozin-Goldberg, I., Bigogno, C., Shreshta, P., Cohen, Z. (2002) Nitrogen starvation induces the accumulation of arachidonic acid in the freshwater green microalga *Parrietochloris incise* (Trebouxiophyceae). *J. Phycol.* 38, 991–994.
- Khozin-Goldberg, I., Iskandarov, U. (2011) LC-PUFA from photosynthetic microalgae: occurrence, biosynthesis, and prospects in biotechnology. *App. Microbiol. Biotechnol.* 91, 905–915.
- Kim, N.J., Lee, Ch.G. (2001) A Theoretical Consideration on Oxygen Production Rate in Microalgal Cultures. *Biotechnol. Bioproc. Eng.* 6, 352–358.
- Kliphuis, A.M.J., Martens, D.E., Janssen, M., Wijffels, R.H. (2011) Effect of O₂ : CO₂ Ratio on the primary metabolism of *Chlamydomonas reinhardtii*. *Biotechnol. Bioeng.* 108(10), 2390–2402.
- Knights, B.A., Brown, A.C., Conway, E., Middleditch, B.S. (1970) Hydrocarbons from the green form of the freshwater alga *Botryococcus braunii*. *Phytochemistry* 9, 1317–1324.

- Kojima, E., Zhang, K. (1999) Growth and hydrocarbon production by microalga *Botryococcus braunii* in bubble column photobioreactor. *J. Biosci. Bioeng.* 87, 811–815.
- Kok, B. (1953) Experiments on photosynthesis by *Chlorella* in flashing light. In: J. S. Burlew (ed.). *Algal Culture from Laboratory to Pilot Plant*. Carnegie Institution of Washington Publication, Washington, DC, USA, 63–75.
- Kok, B. (1956) Photosynthesis in flashing light. *Biochim. Biophys. Acta* 21, 245–258.
- Kunst, L., Samuels, L. (2009) Plant cuticles shine: advances in wax biosynthesis and export. *Curr. Opin. Plant Biol.* 12, 721–727.
- Kumar, A., Ergas, S., Yuan, X., Sahu, A., Zhang, Q.O., Dewulf, J., Xavier Malcata, F., Van Langenhove, H. (2010) Enhanced CO₂ fixation and biofuel production via microalgae: recent developments and future directions. *Trends Biotechnol.* 28, 371–380.
- Ladygina, N., Dedyukhina, E.G., Vainshtein, M.B. (2006) A review on microbial synthesis of hydrocarbons. *Proc. Biochem.* 41, 1001–1014.
- Lam, M. K., Lee, K. T. (2015) Bioethanol Production from Microalgae. *Handbook of Marine Microalgae. Biotechnol. Adv.* Elsevier Inc 197–208.
- Largeau, C., Casadevall, E., Berkaloff, C., Dhamelinourt, P. (1980) Sites of accumulation and composition of hydrocarbons in *Botryococcus braunii*. *Phytochemistry* 19, 1043–1051.
- Laureillard, J., Largeau, C., Casadevall, E. (1988) Oleic acid in the biosynthesis of the resistant biopolymers of *Botryococcus braunii*. *Phytochemistry* 27, 2095–2098.
- Laws, E.A., Taguchi, S., Hirata, J., Pang, L. (1986) Continued studies of high algal productivities in a shallow flume. *Biomass* 11, 39–50.
- Lee, C.G., Palsson, B.O. (1994) High-density algal photobioreactors using light-emitting-diodes. *Biotechnol. Bioeng.* 44, 1161–1167.
- Lee, C.G. (1999) Calculation of light penetration depth in photobioreactors. *Biotechnol. Bioproc. Eng.* 4, 78–81.
- Lee, Y.K. (2001) Microalgal mass culture systems and methods: Their limitation and potential. *J. Appl. Phycol.* 13(4), 307–315.
- Lee, E., Pruvost, J., He, X., Munipalli, R., Pilon, L. (2014) Design tool and guidelines for outdoor photobioreactors. *Chem. Eng. Sci.* 106, 18–29.
- Ley, A.C., Mauzerall, D. (1982) Absolute absorption cross-section of photosystem-II and the minimum quantum requirement for photosynthesis in *Chlorella vulgaris*. *Biochim. Biophys. Acta* 680, 95–106.
- Li, Y., Qin, J.G. (2005) Comparison of growth and lipid content in three *Botryococcus braunii* strains. *J. Appl. Phycol.* 17, 551–556.

- Lichtenthaler, H.K., Wellburn, A.R. (1983) Determination of total carotenoids and chlorophyllaandbof leaf extracts in different solvents. *Biochem. Soc. Trans.* 603, 591– 592.
- Lichtenthaler, H.K., Buschmann, C. (2001) Chlorophylls and Carotenoids: Measurement and Characterization by UV–VIS Spectroscopy, *Curr. Protoc. Food Anal. Chem.* John Wiley & Sons, Inc., In, 2001.
- Liu, T., Wang, J., Hu, Q., Cheng, P., Ji, B., Liu, J., Chen, Y., Zhang, W., Chen, X., Chen, L., Gao, L., Ji, C., Wang, H. (2013) Attached cultivation technology of microalgae for cost-affordable biomass feedstock production. *Bioresour. Technol.* 127, 216–222.
- Lorenz, R.T., Cysewski, G.R. (2003) Commercial potential for *Haematococcus* microalga as a natural source of astaxanthin. *Trends Biotechnol.* 18, 160–167.
- Lu, N., Wei, D., Jiang, X., Chen, F., Yang, S. (2012) Regulation of lipid metabolism in the snow alga *Chlamydomonas nivalis* response to NaCl stress: an integrated analysis by cytomic and lipidomic approaches. *Proc. Biochem.* 47, 1017–1206.
- Lupi, F.M., Fernandes, H.M.L., Sa-Correia, I., Navalis, J.M. (1991) Temperature profiles of cellular growth and exopolysaccharide synthesis by *Botryococcus braunii* Kutz UC58. *J. Appl. Phycol.* 3, 35–42.
- Lupi, F.M., Fernandes, HML., Tomme, M.M., SaCorreia, I., Novais, J.M. (1994) Influence of nitrogen source and photoperiod on exopolysaccharide synthesis by the microalga *Botryococcus braunii*. *Enzyme Microb. Technol.* 16, 546–550.
- Marquez, F.J., Sasaki, K., Nishio, S. (1995) Inhibitory effect of oxygen accumulation on the growth of *Spirulina platensis*. *Biotechnol. Lett.* 17(2), 225–228.
- Mashayekhi, M., Sarrafzadeh, M.H., Tavakoli, O., Soltani, N., Faramarzi, M.A. (2017) Potential for biodiesel production and carbon capturing from *Synechococcus elongatus*: An isolation and evaluation study. *Biocatal. Agric. Biotechnol.* 9, 230–235.
- Masojidek, J., Torzillo, G., Koblizek, M., Kopecky, J., Bernardini, P., Saachi, A., Komenda, J. (1999) Photoadaptation of two members of the Chlorophyta (*Scendesmus* and *Chlorella*) in laboratory and outdoor cultures: changes in chlorophyll fluorescence quenching and xanthophyll cycle. *Planta* 209, 126–135.
- Masojidek, J., Torzillo, G., Kopecky, J., Koblizek, M., Nidiaci, L., Komenda, J., Lukavska, A., Saachi, A. (2000) changes in chlorophyll fluorescence quenching and pigment composition in the green alga *Chlorococcum* sp. grown under nitrogen deficiency and salinity stress. *J. Appl. Phycol.* 12, 417–426.

- Masojidek, J., Koblizek, M., Torzillo, G. (2007) Chapter 2. Photosynthesis in Microalgae, in: Richmond, A., Hu, Q., (Eds.), Handbook of Microalgal Culture. Blackwell Publishing Ltd 20–39.
- Masojidek, J., Torzillo, G. (2008) Mass cultivation of fresh water microalgae. Ecol. Eng. 2226–2235.
- Masojidek, J., Torzillo G., Koblizek, M. (2013) Handbook of Microalgal Culture: Applied Phycology and Biotechnology, Second Edition. Edited by Amos Richmond and Qiang Hu. John Wiley & Sons, Ltd. Published 2013 by Blackwell Publishing Ltd.
- Massie, T.M., Ryabov, A., Blasius, B., Weithoff, G., Gaedke, U. (2013) Complex transient dynamics of stage-structured populations in response to environmental changes. Am. Nat. 182, 103–119.
- Mata, T.M., Martins, A.A., Caetano, N.S. (2010) Microalgae for biodiesel production and other applications: a review. Renew. Sust. Energy Rev. 14, 217–232.
- Matsushima, D., Jenke-Kodama, H., Sato, Y., Fukunaga, Y., Sumimoto, K., Kuzuyama, T., Matsunaga, S., Okada, S. (2012) The single cellular green microalga *Botryococcus braunii*, race B possesses three distinct 1-deoxy-D- xylulose 5-phosphate synthases. Plant Sci. 185–186, 309–320.
- Maxwell, J.R., Douglas, A.G., Eglinton, G., McCormick, A. (1968) The botryococcenes—hydrocarbons of novel structure from the alga *Botryococcus braunii* Kützing. Phytochemistry 7, 2157–2171.
- Melis, A. (2002) Green alga hydrogen production: progress, challenges and prospects. Int. J. Hydrogen Energy 27, 1217–1228.
- Melis, A. (2009) Solar energy conversion efficiencies in photosynthesis: minimizing the chlorophyll Antennae to maximize efficiency. Plant Sci. 177, 272–280.
- Metting, B., Pyne, J.W. (1986) Biologically-active compounds from microalgae. Enzyme Microb. Technol. 8, 386–394.
- Metzger, P., Casadevall, E. (1983) Structure de trois nouveaux botryococcènes synthétisés par une souche de *Botryococcus braunii* cultivée en laboratoire. Tetrahedron Lett. 24, 4013–4016.
- Metzger, P., Berkaloff, C., Casadevall, E., Coute, A. (1985) Alkadiene- and botryococcene-producing races of wild strains of *Botryococcus braunii*. Phytochemistry 24, 2305–2312.
- Metzger, P., David, M., Casadevall, E. (1987) Biosynthesis of triterpenoid hydrocarbons in the B-race of the green alga *Botryococcus braunii*. Sites of production and nature of the methylating agent. Phytochemistry 26, 129–134.

- Metzger, P., Casadevall, E. (1987) Lycopadiene, a tetraterpenoid hydrocarbon from new strains of the green alga *Botryococcus braunii*. *Tetrahedron Lett.* 28, 3931–3934.
- Metzger, P., Villareal-Rosales, E., Casadevall, E., Couté, A. (1989) Hydrocarbons, aldehydes and triacylglycerols in some strains of the race A of the green alga *Botryococcus braunii*. *Phytochemistry* 28, 2349–2353.
- Metzger, P., Allard, B., Casadevall, E., Berkaloff, C., Couté, A. (1990) Structure and chemistry of a new chemical race of *Botryococcus braunii* (Chlorophyceae) that produces lycopadiene, a tetraterpenoid hydrocarbon. *J. Phycol.* 26, 258–266.
- Metzger, P., Pouet, Y., Summons, R. (1997) Chemotaxonomic evidence for the similarity between *Botryococcus braunii* L race and *Botryococcus neglectus*. *Phytochemistry* 44, 1071–1075.
- Metzger, P., Largeau, C. (1999) Chemicals of *Botryococcus braunii*. In: Cohen Z (ed) *Chemicals from microalgae*. Taylor & Francis, London, 205–260.
- Metzger, P., Largeau, C. (2005) *Botryococcus braunii*: a rich source for hydrocarbons and related ether lipids. *Appl. Microbiol. Biotechnol.* 66, 486–496.
- Moheimani, N. R., Matsuura, H., Watanabe, M. M., Borowitzka, M. A. (2014) Non-destructive hydrocarbon extraction from *Botryococcus braunii* BOT-22 (race B). *J. Appl. Phycol.* 26 (3), 1453–1463.
- Mohsenpour, S.F., Richards, B., Willoughby, N. (2012) Spectral conversion of light for enhanced microalgae growth rates and photosynthetic pigment production. *Bioresour. Technol.* 125, 75–81.
- Molina Grima, E., Camacho, F.G., Perez, J.A.S., Sevilla, J.M.F., Fernandez, F.G.A., Gomez, A.C. (1994) A Mathematical model of microalgal growth in light-limited chemostat culture. *J. Chem. Technol. Biotechnol.* 61, 167–173.
- Molina Grima, E., Garcia Camacho, F., Acien Fernandez, F.G. (1999) Production of EPA from *Phaeodactylum tricorutum*. In: *Chemicals from Microalgae* (ed. Z. Cohen), Taylor & Francis, London, 57–92.
- Molina Grima, E., Fernandez, J., Acien, f.g., Chisti, Y. (2001) Tubular photobioreactor design for algal culture. *J. Biotechnol.* 92, 113–131.
- Moreno, J., Ángeles, Vargas, M., Rodríguez, H., Rivas, J., Guerrero, M.G. (2003) Outdoor cultivation of a nitrogen-fixing marine cyanobacterium, *Anabaena* sp. ATCC 33047. *Biomol. Eng.* 20, 191–197.

- Moustafa, A., Beszteri, B., Maier, U.G., Bowler, C., Valentin, K., Bhattacharya, D. (2009) Genomic footprints of a cryptic plastid endosymbiosis in diatoms. *Science* 324 (5935), 1724–1726.
- Munoz, R., Guieysse, B. (2006) Algal-bacterial processes for the treatment of hazardous contaminants: a review. *Water Res.* 40, 2799–2815.
- Muntean, E., Muntean, N., Dragoş, N., Bercea, V. (2008) Carotenoids as biomarkers in *Botryococcus braunii* algae. *Lucr. Şt. Fac. Agric., Timișoara*, 40, 3, 49–53.
- Murakami, M., Ikenouchi, M. (1997) The biological CO₂ fixation and utilization project by RITE (2): screening and breeding of microalgae with high capability in fixing CO₂. *Energy Convers. Mgmt.* 38(Suppl. 1), S493–S497.
- Murata, N., Takahashi, S., Nishiyama, Y., Allakhverdiev, S.I. (2007) Photoinhibition of photosystem II under environmental stress. *Biophysica et Biophysica Acta (BBA) – Bioenergetics* 1767 (6), 414–421.
- Nakazawa, A., Matsuura, H., Kose, R., Kato, S., Honda, D., Inouye, I., Kaya, K., Watanabe, M.M. (2012) Optimization of culture conditions of the thraustochytrid *Aurantiochytrium* sp. Strain 18W-13a for squalene production. *Bioresour. Technol.* 109, 287–291.
- Netto, A. T., Campostrini, E., De Oliveira, J. G., Bressan-Smith, R. E. (2005) Photosynthetic pigments, nitrogen, chlorophyll *a* fluorescence and SPAD-502 readings in coffee leaves. *Scientia Horticulturae*, 104 (2), 199–209.
- Nguyen, B. T., Rittmann, B. E. (2015) Predicting dissolved inorganic carbon in photoautotrophic microalgae culture via the nitrogen source. *Environ. Sci. Technol.* 49 (16), 9826–9831.
- Niehaus, T.D., Okada, S., Devarenne, T.P., Watt, D.S., Sviripa, V., Chappell, J. (2011) Identification of unique mechanisms for triterpene biosynthesis in *Botryococcus braunii*. *Proc. Natl. Acad. Sci. U. S. A.* 108, 12260–12265.
- Niyogi, K.K., Bjorkman, O., Grossman, A.R. (1997) The roles of specific xanthophylls in photoprotection. *Proc. Natl. Acad. Sci. (USA)*, 94, 14162–14167.
- Ogbonna, J.C., Yada, H., Tanaka, H. (1995) Light supply coefficient: A new engineering parameter for photobioreactor design. *J. Ferm. Bioeng.* 80, 4, 369–376.
- Ogbonna, J.C., Tanaka, H. (2000) Light requirement and photosynthetic cell cultivation – Development of processes for efficient light utilization in photobioreactors. *J. Appl. Phycol.* 12, 207–218.
- Okada, S., Murakami, M., Yamaguchi, K. (1995) Hydrocarbon composition of newly isolated strains of the green microalga *Botryococcus braunii*. *J. Appl. Phycol.* 7, 555–559.

- Okada, S., Murakami, M., Yamaguchi, K. (1997) Hydrocarbon production by the Yayoi, a new strain of the green microalga *Botryococcus braunii*. Appl. Biochem. Biotechnol. 67, 79–86.
- Okada, S., Devarenne, T.P., Chappell, J. (2000) Molecular characterization of squalene synthase from the green microalga *Botryococcus braunii*, race B. Arch. Biochem. Biophys. 373, 307–317.
- Okada, S., Devarenne, T.P., Murakami, M., Abe, H., Chappell, J. (2004) Characterization of botryococcene synthase enzyme activity, a squalene synthase-like activity from the green microalga *Botryococcus braunii*, race B. Arch. Biochem. Biophys. 422, 110–118.
- Oncel, S., Sukan, V.F. (2008) Comparison of two different pneumatically mixed column photobioreactors for the cultivation of *Arthrospira platensis* (*Spirulina platensis*). Bioresour. Technol. 99, 4755–4760.
- Oncel, S. S. (2015) Biohydrogen from Microalgae, Uniting Energy, Life, and Green Future. Handbook of Marine Microalgae. Biotechnol. Adv. Elsevier Inc 159–196.
- Ono, E., Cuello, J.L. (2007) Carbon dioxide mitigation using thermophilic *Cyanobacteria*. Biosyst. Eng. 96, 129–134.
- Pal, D., Khozin-Golberg, I., Cohen, Z., Boussiba, S. (2011) The effect of light, salinity, and nitrogen availability on lipid production by *Nannochloropsis* sp. Appl. Microbiol. Biotechnol. 90, 1429–1441.
- Paniagua-Michel, J., Olmos-Soto, J., Ruiz, M. A. (2012) Pathways of Carotenoid Biosynthesis in Bacteria and Microalgae. in Barredo, J.-L. (ed.) Microbial Carotenoids from Bacteria and Microalgae: Methods and Protocols. Totowa, NJ: Humana Press, 1–12.
- Park, K.H., Kim, D.I., Lee, C.G. (2000) Effect of flashing light on oxygen production rates in high-density algal cultures. J. Microbiol. Biotechnol. 10, 817–822.
- Park, K.H., Lee, C.G. (2000) Optimization of algal photobioreactors using flashing lights. Biotechnol. Bioproc. Eng. 5, 186–190.
- Pérez-Mora, L.S., Matsudo, M.C., Cezare-Gomes, E.A., Carvalho, J.C.M. (2016) An investigation into producing *Botryococcus braunii* in a tubular photobioreactor. J. Chem. Technol. Biotechnol. DOI 10.1002/jctb.4934.
- Phillips, J.N., Myers, J. (1954) Growth rate of *Chlorella* in flashing light. Plant Physiol. 29, 152–161.
- Pirt, S.J., Lee, Y.K., Richmond, A., Pirt, M.W. (1980) The photosynthetic efficiency of *Chlorella* biomass growth with reference to solar energy utilization. J. Chem. Biotechnol. 30, 25–34.

- Platt, T., Gallegos, C., Harrison, W. (1980) Photoinhibition of photosynthesis in natural assemblages of marine phytoplankton. *J. Mar. Res.* 38, 687–701.
- Posten, C., Schaub, G. (2009) Microalgae and terrestrial biomass as source for fuels – A process view. *J. Biotechnol.* 142 (1), 64–69.
- Pour Hosseini, S.R., Tavakoli, O., Sarrafzadeh, M.H. (2017) Experimental optimization of SC-CO₂ extraction of carotenoids from *Dunaliella salina*. *J. Sup. Flui.* 121, 89–95.
- Prabandono, K., Amin, S. (2015) Biofuel Production from Microalgae. *Handbook of Marine Microalgae. Biotechnol. Adv. Elsevier Inc* 145–158.
- Pulz, O., Gross, W. (2004) Valuable products from biotechnology of microalgae. *Appl. Microbiol. Biot.* 65, 635–648.
- Pushparaj, B., Pelosi, E., Tredici, M.R., Pinzani, E., Materassi, R. (1997) As integrated culture system for outdoor production of microalgae and *cyanobacteria*. *J. Appl. Phycol.* 9(2), 113–119.
- Qiang, H., Zarmi, Y., Richmond, A. (1998) Combined effects of light intensity, light-path and culture density on output rate of *Spirulina platensis* (*Cyanobacteria*). *European J. Phycol.* 33,165–171.
- Qin, J. (2005) Bio-hydrocarbons from algae: Impacts of temperature, light and salinity on algae growth. A Report for the Rural Industries Research and Development Corporation, Australian Government. RIRDC Publication No 05/025 and RIRDC Project No SQC-1A. pp. 18.
- Qin, J.G., Li, Y. (2006) Optimization of the growth environment of *Botryococcus braunii* strain CHN 357. *J. Freshwater Ecol.* 21, 169–176.
- Rabinowitch, E.I. (1945) *Chemistry of Photosynthesis, Chemosynthesis and Related Processes in Vitro and in Vivo.* Interscience Publishers, New York, NY, USA.
- Ramaraj, R., Kawaree, R., Unpaprom, Y. (2016) Direct Transesterification of Microalga *Botryococcus braunii* Biomass for Biodiesel Production. *Emer. Life Sci. Res.* 2(2), 1–7.
- Ramos de Ortega, A., Roux, J.C. (1986) Production of *Chlorella* biomass in different types of flat bioreactors in temperate zones. *Biomass* 10, 141–156.
- Ranga Rao, A., Sarada, R., Baskaran, V., Ravishankar, G.A. (2006) Antioxidant activity of *Botryococcus braunii* extract elucidated in vitro models. *J. Agr. Food Chem.* 54, 4593–4599.
- Ranga Rao, A., Dayananda, C., Sarada, R., Shamala, T.R., Ravishankar, G.A. (2007 a) Effect of salinity on growth of green alga *Botryococcus braunii* and its constituents. *Bioresour. Technol.* 98, 560–564.

- Ranga Rao, A., Sarada, R., Ravishankar, G.A. (2007 b) Influence of CO₂ on growth and hydrocarbon production in *Botryococcus braunii*. J. Microbiol. Biotechnol. 17, 414–419.
- Ravelonandro, P.H., Ratianarivo, D.H., Joannis-Cassan, C., Isambert, A., Raherimandimby M. (2008) Influence of light quality and intensity in the cultivation of *Spirulina platensis* from Toliara (Madagascar) in a closed system. J. Chem. Technol. Biotechnol. 83, 842–848.
- Redfield, A.C., Ketchum, B.H., Richards, F.A. (1963) The influence of organisms on the composition of sea-water. In: Hill MN (ed) The sea: ideas and observations on progress in the study of the seas. Wiley, New York, 26–77.
- Richardson, K., Beardall, J., Raven, J.A. (1983) Adaptation of unicellular algae to irradiance: An analysis of strategies. New Phytol. 93, 157–191.
- Richmond, A. (1986) In: CRC Handbook of Microalgal Mass Culture. Boca Raton, FL: CRC Press, p. 127 printed in United States.
- Richmond, A. (1996) Efficient utilization of high irradiance for production of photoautotrophic cell mass: a survey. J. Appl. Phycol. 8(4–5), 381–387.
- Richmond, A. (1999) Physiological principles and modes of cultivation in mass production of photoautotrophic microalgae. In: Cohen Z, ed. Chemical from Microalgae. Philadelphia: Taylor and Francis, 353–386.
- Richmond, A. (2000) Microalgal biotechnology at the turn of the millennium: a personal view. J. Appl. Phycol. 12 (3–5), 441–451.
- Richmond, A. (2004) Biological principles of mass cultivation. In: Richmond A, ed. Microalgal culture. Oxford: Blackwell Science Ltd 125–177.
- Richmond, A. (2013) Biological principles of mass cultivation of photoautotrophic microalgae. Handbook of Microalgal Culture: Appl. Phycol. Biotechnol. Second Edition, 169–204.
- Richmond, A., Boussiba, S., Vonshak, A., Kopel, R. (1993) A new tubular reactor for mass production of microalgae outdoors. J. Appl. Phycol. 5, 327–332.
- Richmond, A., Cheng-Wu, Z., Zarmi, Y. (2003) Efficient use of strong light for high photosynthetic productivity: interrelationships between the optical path, the population density and the cell growth inhibition. Biomol. Eng. 20, 229–236.
- Rivas, M. O., Vargas, P., Riquelme, C. E. (2010) Interactions of *Botryococcus braunii* Cultures with Bacterial Biofilms. Microb. Ecol. 60, 628–635.

- Rochatte, V., Dauchet, J., Cornet, J-F. (2016) Experimental validation and modelling of a photobioreactor operating with diluted and controlled light flux. *J. Physics: Conf. Series* 676, 012021, doi:10.1088/1742-6596/676/1/012021.
- Rodolfi, L., Zittelli, G.C., Bassi, N., Padovani, G., Biondi, N., Bonini, G., Tredici, M.R. (2008) Microalgae for oil: strain selection, induction of lipid synthesis and outdoor mass cultivation in a low-cost photobioreactor. *Biotechnol. Bioeng.* 102(1), 100–112.
- Rosenberg, J.N., Oyler, G.A., Wilkinson, L., Betenbaugh, M.J. (2008) A green light for engineered algae: redirecting metabolism to fuel a biotechnology revolution. *Curr. Opin. Biotech.* 19 (5), 430–436.
- Ruangsomboon, S. (2012) Effect of light, nutrient, cultivation time and salinity on lipid production of newly isolated strain of the green microalga, *Botryococcus braunii* KMITL 2. *Bioresour. Technol.* 109, 261–265.
- Sakamoto, K., Baba, M., Suzuki, I., Watanabe, M.M., Shiraiwa, Y. (2012) Optimization of light for growth, photosynthesis, and hydrocarbon production by the colonial microalga *Botryococcus braunii* BOT-22. *Bioresour. Technol.* 110, 474–479.
- Samorì, C., Torri, C., Samorì, G., Fabbri, D., Galletti, P., Guerrini, F., Pistocchi, R., Tagliavini, E. (2010) Extraction of hydrocarbons from microalga *Botryococcus braunii* with switchable solvents. *Bioresour. Technol.* 101, 3274–3279.
- Sanchez Miron, A., Contreras Gomez, A., Garca Camacho, F., Molina Grima, E., Chisti, Y. (1999) Comparative evaluation of compact photobioreactors for large-scale monoculture of microalgae. *J. Biotechnol.* 70(1–3), 249–270.
- Sanchez Miron, A., Ceron Garcia, M-C., Garcia Camacho, F., Molina Grima, E., Chisti, Y. (2002) Growth and biochemical characterization of microalgal biomass produced in bubble column and airlift photobioreactors: studies in fed-batch culture. *Enzyme and Microbial Technology* 31(7), 1015–1023.
- Sarrafzadeh, M.H., La, H.J., Seo, S.H., Asgharnejad, H., Oh, H.M. (2015) Evaluation of various techniques for microalgal biomass quantification. *J. Biotechnol.* 216(20), 90–97.
- Schindler, D.W. (1977) Evolution of phosphorus limitation in lakes. *Science* 195, 260–262.
- Schwartz, R.E. (1990) Pharmaceuticals from cultured algae. *J. Ind Microbiol.* 5, 113–123.
- Scott, S.A., Davey, M.P., Dennis, J.S., Horst, I., Howe, C.J., Lea-Smith, D.J., Smith, A.G. (2010) Biodiesel from algae: challenges and prospects. *Curr. Opin. Biotechnol.* 21, 277–286.

- Senousy, H.H., Beakes, G.W., Hack, E. (2004) Phylogenetic placement of *Botryococcus braunii* (Trebouxiophyceae) and *Botryococcus sudeticus* isolate UTEX 2629 (Chlorophyceae). *J. Phycol.* 40, 412–423.
- Setlik, I., Sust, V., Malek, I. (1970) Dual purpose open circulation units for large scale culture of algae in temperature zone. 1. Basic design considerations and scheme of pilot plant. *Algol. Stud. (Trebouxiophyceae)*, 1, 111–164.
- Setlik, I., Allakhverdiev, S.I., Nedbal, L., Setlikov´ a, E., Klimov V.V. (1990) Three types of photosystem II photoinactivation. 1. Damaging processes on the acceptor side. *Photosynth. Res.* 23, 39–48.
- Sforza, E., Calvaruso, C., Meneghesso, A., Morosinotto, T., Bertucco, A. (2015) Effect of specific light supply rate on photosynthetic efficiency of *Nannochloropsis salina* in a continuous flat plate photobioreactor. *Appl. Microbiol. Biotechnol.* 99(19), 8309–8318.
- Sheehan, J., Dunahay, T., Benemann, J., Roessler, P. (1998) A look back at the U.S. Department of Energy’s aquatic species program—biodiesel from algae. Close-Out Report, NREL/TP-580-24190.
- Shen, Y., Yuan, W., Pei, Z., Mao, E. (2008) Culture of microalga *Botryococcus* in livestock wastewater. *T. ASABE.* 51 (4), 1395–1400.
- Shiho, M., Kawachi, M., Horioka, K., Nishita, Y., Ohashi, K., Kaya, K., Watanabe, M. M. (2012) Business Evaluation of a Green Microalgae *Botryococcus Braunii* Oil Production System. *Proc. Environ. Sci.* 15, 90–109.
- Shimamura, R., Watanabe, S., Sakakura, Y., Shiho, M., Kaya, K., Watanabe, M.M. (2012) Development of *Botryococcus* Seed Culture System for Future Mass Culture. *Proc. Environ. Sci.* 15, 80–89.
- Shimizu, Y. (1996) Microalgal metabolites: a new perspective. *Annu. Rev. Microbiol.* 50, 431–465.
- Shimizu, Y. (2003) Microalgal metabolites. *Curr. Opin. Microbiol.* 6, 236–243.
- Singh, Y., Kumar, H.D. (1991) Lipid and hydrocarbon production by *Botryococcus* sp. under nitrogen limitation and anaerobiosis. *World J. Microbiol. Biotechnol.* 8, 121–124.
- Singh, S., Kate, B.N., Banerjee, U.C. (2005) Bioactive compounds from *cyanobacteria* and microalgae: an overview. *Crit. Rev. Biotechnol.* 25, 73–95.
- Singh, A., Smyth, B.M., Murphy, J.D. (2010) A biofuel strategy for Ireland with an emphasis on production of biomethane and minimization of land-take. *Renew. Sustain. Energy Rev.* 14, 277–288.

- Sirakov, I., Velichkova, K., Beev, G., Staykov, Y. (2013) The influence of organic carbon on bioremediation process of wastewater originate from aquaculture with use of microalgae from genera *Botryococcus* and *Scenedesmus*. *Agric. Sci. Technol.* 5 (4), 443–447.
- Solovchenko, A.E., Khozin-Goldberg, I., Didi-Cohen, S., Cohen, Z., Merzlyak, M.N. (2008) Effects of light intensity and nitrogen starvation on growth, total fatty acids and arachidonic acid in the green microalga *Parietochloris incisa*. *J. Appl. Phycol.* 20, 245–251.
- Sousa, C., Winter de, L., Janssen, M., Vermue, M.H., Wijffels, R.H. (2011) Growth of the microalga *Neochloris oleoabundans* at high oxygen partial pressure and sub-saturating light intensities. *Bioresour. Technol.* 212, 104, 656–670.
- Spolaore, P., Joannis-Cassan, C., Duran, E., Isambert, A. (2006) Commercial applications of microalgae. *J. Biosci. Bioeng.* 101, 87–96.
- Suh, I.S., Lee, S.B. (2003) A light distribution model for an internally radiating photobioreactor. *Biotechnol. Bioeng.* 82, 180–189.
- Sukenik, A., Carmeli, Y., Berner, T. (1989) Regulation of fatty acid composition by irradiance level in the eustigmatophyte *Nannochloropsis* sp. *J. Phycol.* 25, 686–692.
- Sukenik, A.; Zmora, O.; Carmeli, Y. (1993) Biochemical quality of marine unicellular algae with special emphasis on lipid composition. II. *Nannochloropsis* sp. *Aquaculture* 117, 313–326.
- Suzuki, R., Ito, N., Uno, Y., Nishii, I., Kagiwada, S., Okada, S., Noguchi, T. (2013) Transformation of lipid bodies related to hydrocarbon accumulation in a green alga, *Botryococcus braunii* (race B). *PLOS ONE*, 8 (12).
- Takagi, M., Karseno, Toshida, T. (2006) Effect of salt concentration on intracellular accumulation of lipids and triacylglyceride in marine microalgae *Dunaliella* cells. *J. Biosci. Bioeng.* 101, 223–226.
- Talukdar, J., Kalita, M. C., Goswami, B. C. (2012) Influence of dissolved inorganic carbon and nitrogen sources on growth, total lipid content and calorific value of the freshwater oleaginous microalgae *Ankistrodesmus falcatus* (Corda) Ralfs. *Environ. Res. Eng. Mgmt.* 3(61), 14–25.
- Talukdar, J., Kalita, M. C., Goswami, B. C., Hong, D. D., Das, H. C. (2014) Liquid hydrocarbon production potential of a novel strain of the microalga *botryococcus braunii*: Assessing the reliability of in situ hydrocarbon recovery by wet process solvent extraction. *Energy Fuels*.s 28 (6), 3747–3758.

- Tanabe, Y., Kato, S., Matsuura, H., Watanabe, M. M. (2012) A *Botryococcus* strain with bacterial ectosymbionts grows fast and produces high amount of hydrocarbons. *Proc. Environ. Sci.* 15, 22–26.
- Tanabe, Y., Ioki, M., Watanabe, M.M. (2014) The fast-growing strain of hydrocarbon-rich green alga *Botryococcus braunii* BOT-22, is a vitamin B₁₂ autotroph. *J. Appl. Phycol.* 26, 9–13.
- Tanabe, Y., Okazaki, Y., Yoshida, M., Matsuura, H., Kai, A., Shiratori, T., Ishida, K., Nakano, S., Watanabe, M. M. (2015) A novel alphaproteobacterial ectosymbiont promotes the growth of the hydrocarbon-rich green alga *Botryococcus braunii*. *Nature.* (3), 1424–1440.
- Tang, D., Han, W., Li, P., Miao, X., Zhong, J. (2011) CO₂ biofixation and fatty acid composition of *Scenedesmus obliquus* and *Chlorella pyrenoidosa* in response to different CO₂ levels. *Bioresour. Technol.* 102(3), 3071–3076.
- Tanoi, T., Kawachi, M., Watanabe, M.M. (2011) Effects of carbon source on growth and morphology of *Botryococcus braunii*. *J. Appl. Phycol.* 23, 25–33.
- Tedesco, M.A., Duerr, E.O. (2006) Light, temperature and nitrogen starvation effects on the total lipid and fatty acid content and composition of *Spirulina platensis* UTEX 1928. *J. Appl. Phycol.* 1(3), 201–209.
- Templier, J., Diesendorf, C., Largeau, C., Casadevall, E. (1992) Metabolism of n-alkadienes in the a race of *Botryococcus braunii*. *Phytochemistry* 31, 113–120.
- Terry, K.L., Raymond, L.P. (1985) System design for the autotrophic production of microalgae. *Enzyme Microb. Technol.* 7, 474–487.
- Thomas, W.H., Tornabene, T.G., Weissman, J. (1984) Screening for Lipid Yielding Microalgae: Activities for 1983. Final Subcontract Report. Solar Energy Research Institute, USA.
- Townsend, S.A. (2001) Perennial domination of phytoplankton by *Botryococcus* and *Peridinium* in a discontinuously polymictic reservoir (tropical Australia). *Arch. Hydrobiol.* 151, 529–548.
- Tredici, M.R., Zittelli, G.C. (1998) Efficiency of sunlight utilization: tubular versus flat photobioreactors. *Biotechnol. Bioeng.* 57 (2), 187–197.
- Tredici, M.R. (2009) Photobiology of microalgae mass cultures: understanding the tools for the next green revolution. *Biofuels* 1 (1), 143–162.

- Triantaphylides, C., Krischke, M., Hoebrechts, F.A., Ksas, B., Gresser, G., Havaux, M., Van Breusegem, F., Mueller, M.J. (2008) Singlet oxygen is the major reactive oxygen species involved in photooxidative damage to plants. *Plant Physiol.* 148(2), 960–968.
- Tschiersch, H., Ohmann, E. (1993) Photoinhibition in *Euglena gracilis*: involvement of reactive oxygen species. *Planta* 191, 316–323.
- Ugwu, C.U., Ogbonna, J., Tanaka, H. (2002) Improvement of mass transfer characteristics and productivities of inclined tubular photobioreactors by installation of internal static mixers. *Appl. Microbiol. Biotechnol.* 58(5), 600–607.
- Ugwu, C., Aoyagi, H., Uchiyama, H. (2007) Influence of irradiance, dissolved oxygen concentration, and temperature on the growth of *Chlorella sorokinian*. *Photosynthetic* 45(2), 309–311.
- Ugwu, C.U., Aoyagi, H., Uchiyama, H. (2008) Photobioreactors for mass cultivation of algae. *Bioresour. Technol.* 99, 4021–4028.
- Vacha, F. (1995) The role of oxygen in photosynthesis. *Photosynthetica* 31, 321–334.
- Vázquez-Duhalt, R., Arredondo-Vega, B.Q. (1991) Haloadaptation of the green alga *Botryococcus braunii* (Race A). *Phytochemistry* 30, 2919–2925.
- Vejrazka, C., Janssen, M., Streefland, M., Wijffels, R.H. (2011) Photosynthetic efficiency of *Chlamydomonas reinhardtii* in flashing light. *Biotechnol. Bioeng.* 108(12), 2905–2913.
- Vejrazka, C., Janssen, M., Benvenuti, G., Streefland, M., Wijffels, R.H. (2013) Photosynthetic efficiency and oxygen evolution of *Chlamydomonas reinhardtii* under continuous and flashing light. *Appl. Microbiol. Biotechnol.* 97, 1523–1532.
- Venkatesan, S., Swamy, M. S., Jayavel, D., Senthil, C. (2013) Effects of nitrate and phosphate on total lipid content and pigment production in *Botryococcus braunii* Kutzing KM-104. *J. acad. Indus. Res.* 1, 820–824.
- Villarreal-Rosales, E., Metzger, P., Casadevall, E. (1992) Ether lipid production in relation to growth in *Botryococcus braunii*. *Phytochemistry* 31, 3021–3027.
- Viola, R., Nyvall, P. & Pedersén, M. (2001) The unique features of starch metabolism in red algae. *Proc. R. Soc. Lond. B.* 268, 1417–1422.
- Vonshak, A., Torzillo, G., Tomaseli, L. (1994) Use of chlorophyll fluorescence to estimate the effect of photoinhibition in outdoor cultures of *Spirulina platensis*. *J. Appl. Phycol.* 6, 31–34.
- Vonshak, A., Chanawongse, L., Bunnag, B., Tanticharoen, M. (1996 a) Light acclimation in three *Spirulina platensis* (cyanobacteria) isolates. *J. Appl. Phycol.* 8, 35–40.

- Vonshak, A., Torzillo, G., Accolla, P., Tomaselli, L. (1996 b) Light and oxygen stress in *Spirulina platensis* (cyanobacteria) grown outdoors in tubular reactors. *Physiol. Plant.* 97, 175–179.
- Vunjak-Novakovic, G., Kim, Y., Wu, X., Berzin, I., Merchuk, J. (2005) Air-lift bioreactors for algal growth on flue gas: mathematical modeling and pilot plant studies. *Ind. Eng. Chem. Res.* 44, 6154–6163.
- Wagenen, J.V., Miller, T.W., Hobbs, S., Hook, P., Crowe, B., Huesemann, M. (2012) Effects of Light and Temperature on Fatty Acid Production in *Nannochloropsis Salina*. *Energies* 5, 731–740.
- Wake, L.V., Hillen, L.W. (1980) Study of a “Bloom” of the oil-rich alga *Botryococcus braunii* in the Darwin River Reservoir. *Biotechnol. Bioeng.* 22, 1637–1656.
- Wang, B., Li, Y., Wu, N., Lan, C.Q. (2008) CO₂ bio-mitigation using microalgae. *Appl. Microbiol. Biotechnol.* 79, 707–718.
- Wang, J.Y., Zhu, S.G., Xu, C.F. (2003) Photosynthesis. In: Wang JY, Zhu SG, Xu CF, editors. *Biochem.* 2.3 ed. Beijing: Higher Education Express, 197–229.
- Wang, S.K., Wang, F., Stiles, A.R., Guo, C., Liu, C.Z. (2014) *Botryococcus braunii* cells: Ultrasound-intensified outdoor cultivation integrated with in situ magnetic separation. *Bioresour. Technol.* 167, 376–382.
- Wang, X., Kolattukudy, P.E. (1995) Solubilization and purification of aldehyde-generating fatty acyl-CoA reductase from green alga *Botryococcus braunii*. *FEBS Lett.* 370, 15–18.
- Wang, Z.T., Ullrich, N., Joo, S., Waffenschmidt, S., Goodenough, U. (2009) Algal lipid bodies: stress induction, purification and biochemical characterization in wild-type and starchless *Chlamydomonas reinhardtii*. *Eukaryot. Cell* 8, 1856–1868.
- Watanabe, Y., Saiki, H. (1997) Development of a photobioreactor incorporating *Chlorella* sp. for removal of CO₂ in stack gas. *Energy Convers. Mgmt.* 38 (Suppl. 1), S499–S503.
- Watanabe, M.M., Tanabe, Y. (2013) Biology and Industrial Potential of *Botryococcus braunii*, *Handbook of Microalgal Culture: Appl. Phycol. Biotechnol.* Second Edition. Edited by Amos Richmond and Qiang Hu., chapter 19, John Wiley & Sons, Ltd. Published 2013, 369–387.
- Watanabe, H., Li, D., Nakagawa, Y., Tomishige, K., Watanabe, M. M. (2015) Catalytic gasification of oil-extracted residue biomass of *Botryococcus braunii*. *Bioresour. Technol.* 191, 452–459.
- Weetall, H.H. (1985) Studies on the nutritional requirements of the oil-producing alga *Botryococcus braunii*. *Appl. Biochem. Biotech.* 11, 377–391.

- Weiss, T.L., Johnston, J.S., Fujisawa, K., Sumimoto, K., Okada, S., Chappell, J., Devarenne, T.P. (2010) Phylogenetic placement, genome size, and GC content of the liquid-hydrocarbon-producing green microalga *Botryococcus braunii* strain Berkeley (Showa) (Chlorophyta). *J. Phycol.* 46, 534–540.
- Weiss, T. L., Roth, R., Goodson, C., Vitha, S., Black, I., Azadi, P., Rusch, J., Holzenburg, A., Devarenne, T. P., Goodenough, U. (2012) Colony organization in the green alga *Botryococcus braunii* (Race B) is specified by a complex extracellular matrix. *Eukaryot. Cell* 11 (12), 1424–1440.
- Weller, S., Franck, J. (1941) Photosynthesis in flashing light. *J. Phys. Chem.* 45, 1359–1373.
- Williams, P.J.L. (2007) Biofuel: microalgae cut the social and ecological costs. *Nature* 450, 478.
- Wolf, F.R., Nonomura, A.M., Bassham, A. (1985 a) Growth and branched hydrocarbon production in a strain of *Botryococcus braunii* (Chlorophyta). *J. Phycol.* 21, 388–396.
- Wolf, F.R., Nemethy, E.K., Blanding, J.H., Bassham, J.A. (1985 b) Biosynthesis of unusual acyclic isoprenoids in the green alga *Botryococcus braunii*. *Phytochemistry* 24, 733–737.
- Wood, J.B. (1984) Fatty acids and saponifiable lipids. In: *Algal Physiol. Biochem.* (ed. W.D.P. Stewart), University of California Press, Berkeley, CA 236–265.
- Xu, H., Miao, X., Wu, Q. (2006) High quality biodiesel production from microalga *Chlorella protothecoides* by heterotrophic growth in fermenters. *J. Biotechnol.* 126, 499–507.
- Xu, L., Liu, R., Wang, F., Liu, C.Z. (2012 a) Development of a draft-tube airlift bioreactor for *Botryococcus braunii* with an optimized inner structure using computational fluid dynamics. *Bioresour. Technol.* 119, 300–305.
- Xu, L., Wang, F., Guo, C., Liu, C.Z. (2012 b) Improved algal oil production from *Botryococcus braunii* by feeding nitrate and phosphate in an airlift bioreactor. *Eng. Life Sci.* 12, 171–177.
- Xue, S., Su, Z., Cong, W. (2011) Growth of *Spirulina platensis* enhanced under intermittent illumination. *J. Biotechnol.* 151(3), 271–277.
- Yamaguchi, K., Nakano, H., Murakami, M., Konosu, S., Nakayama, O., Kanda, M., Nakamura, A., Iwamoto, H. (1987) Lipid composition of a green alga, *Botryococcus braunii*. *Agric. Biol. Chem.* 51 (2), 493–498.
- Yang, S., Wang, J., Cong, W., Cai, Z., Ouyang, F. (2004) Utilization of nitrite as a nitrogen source by *Botryococcus braunii*. *Biotechnol. Lett.* 26, 239–243.

- Yeesang, C., Cheirsilp, B. (2011) Effect of nitrogen, salt, and iron content in the growth medium and light intensity on lipid production by microalgae isolated from freshwater sources in Thailand. *Bioresour. Technol.* 102, 3034–3040.
- Yeh, N., Chung, J-P. (2009) High-brightness LEDs—Energy efficient lighting sources and their potential in indoor plant cultivation. *Renew. Sust. Energ. Rev.* 13, 2175–2180.
- Yeh, K.L., Chang, J.Sh., Chen, W.M. (2010) Effect of light supply and carbon source on cell growth and cellular composition of a newly isolated microalga *Chlorella vulgaris* ESP-31. *Eng. Life Sci.* 10(3), 201–208.
- Yen, H.W., Hu, I.C., Chen, C.Y., Ho, S.H., Lee, D.J., Chang, J.S. (2013) Microalgaebased biorefinery from biofuels to natural products. *Bioresour. Technol.* 135,166–174.
- Yoshimura, T., Okada, S., Honda, M. (2013) Culture of the hydrocarbon producing microalga *Botryococcus braunii* strain Showa: Optimal CO₂, salinity, temperature, and irradiance conditions. *Bioresour. Technol.* 133, 232–239.
- Yoo, C., Jun, S.Y., Lee, J.Y., Ahn, C.Y., Oh, H.M. (2010) Selection of microalgae for lipid production under high levels carbon dioxide. *Bioresour. Technol.* 101, 71–74.
- Zemke, P.E., Wood, B.D., Dye, D.J. (2010) Considerations for the maximum production rates of triacylglycerol from microalgae. *Biom. Bioe.* 34, 145–151.
- Zhang, K., Kojima, E. (1998) Effect of light intensity on colony size of microalga *Botryococcus braunii* in bubble column photobioreactors. *J. Ferment. Bioeng.* 86, 573–576.
- Zhang, H., Wang, W., Li, Y., Yang, W., Shen, G. (2011) Mixotrophic cultivation of *Botryococcus braunii*. *Biom. Bioe.* 35(5), 1710–1715.
- Zijffers, J.W.F., Schippers, K.J., Zheng, K., Janssen, M., Tramper, J., Wijffels, R.H. (2010) Maximum photosynthetic yield of green microalgae in photobioreactors. *Mar. Biotechnol.* 12, 708–718.
- Zeng, X., Danquah, M.K., Chen, X.D., Lu, Y. (2011) Microalgae bioengineering: From CO₂ fixation to biofuel production. *Renew. Sustain. Energy Rev.* 15, 3252– 3260.
- Zhila, N.O., Kalacheva, G.S., Volova, T.G. (2011) Effect of salinity on the biochemical composition of the alga *Botryococcus braunii* Kutz IPPAS H-252. *J. Appl. Phycol.* 23, 47–52.